Copyright

by

Chinemerem Clement Okezie

2024

The Thesis Committee for Chinemerem Clement Okezie
Certifies that this is the approved version of the following Thesis:

Calibrating Performance Predictions for Large-Scale Injection

APPROVED BY
SUPERVISING COMMITTEE:

_____
Alexander P. Bump, Co-Supervisor

_____
Susan D. Hovorka, Co-Supervisor

_____
Hailun Ni, Reader

Calibrating Performance Predictions for Large-Scale Injection

by

Chinemerem Clement Okezie

Thesis

Presented to the Faculty of the Graduate School of

The University of Texas at Austin

in Partial Fulfillment

of the Requirements

for the Degree of

Master of Science in Energy and Earth Resources

The University of Texas at Austin

August 2024

Dedication

I would like to dedicate this thesis to my mom and dad for their continued love and support. Special dedication to Frank and every selfless person doing the good work of making the lives of others better.

Acknowledgements

First, I want to give all glory to God for making all things possible in due season.

Second, I want to thank my advisor, Dr. Alex Bump, for allowing me to learn from him and become a better version of myself. Time has yet again proven to be the most elusive concept in the universe, as I'm not quite sure where it has gone. I still remember our first meeting and deeply appreciate the hundreds that followed, along with the great research discussions that accompanied them. Thank you for your guidance over the past couple of years, for asking for more, and for exploring ideas with me.

Third, I want to thank Dr. Susan Hovorka for her support and guidance and for giving me the amazing opportunity to be a part of the Gulf Coast Carbon Center. It has been a wonderful experience for me to work with and learn from brilliant individuals, and I want her to know that I am leaving better than I arrived.

I also want to thank Dr. Hailun Ni for being part of my committee and providing essential guidance where necessary. Thank you to Dr. Seyyed Hosseini for always making time to discuss parts of my research and for making the brine version of EasiTool available. I want to acknowledge Dr. Charlie Zheng for sharing his time and knowledge as I explored the Edwards Group and Michael Wang for always being willing to provide IT support and all the raster logs he could get his hands on.

Thanks to Director Richard Chuchla for his support and guidance over the past few years. I have enjoyed every part of the Energy and Earth Resources program, met great individuals, and made some friends along the way.

To all members of the Gulf Coast Carbon Center and the EER graduating class of 2024, thank you, and see you soon!

Abstract

Calibrating Performance Predictions for Large-Scale Injection

Chinemerem Clement Okezie, M.S.E.E.R.

The University of Texas at Austin, 2024

Co-Supervisors: Alexander P. Bump and Susan D. Hovorka

Current Carbon Capture and Storage (CCS) projects build on over 50 years of experience with CO_2 injection. However, the planned injection rates of projects currently under development are as much as an order of magnitude larger than anything previously attempted in saline aquifers.

In the United States, about half of these large-scale projects under development are mostly concentrated in the Gulf Coast region. That is mainly due to the region's young, thick, and permeable sandstones and its proximity to large emission sources.

To calibrate predictions for large-scale injection in this region, historic saltwater injection into non-producing reservoirs in the Texas Gulf Coast is used as an industrial analog. The Texas Gulf Coast was chosen for its long history of large-volume saltwater injection. Data from over 8,000 saltwater disposal (SWD) wells were analyzed in this study. Injection pressure, rate, and volume data come from the Texas Railroad Commission (RRC) reports via B3 Insights but need significant Quality Checks (QC) to be usable. Of the >8000 Saltwater Disposal Wells in the database, only 5,105 Saltwater Disposal wells have monthly injection data.

Results from the regional study show that 4,805 wells injected ~20.3 billion stock tank barrels (stb) of saltwater into the onshore Texas Gulf of Mexico from 1990 to 2020, the period for which

digital records are available. That is volumetrically equivalent to ~2.3 Gt CO_2 at reservoir conditions. More than 15 billion stb (~1.7 Gt CO_2 Eq.) of the total volume were injected below 800 m, the depth at which CO_2 attains its supercritical state. The bulk of this injection has targeted Oligocene, Miocene, Woodbine, Wilcox, and Lower Cretaceous formations.

The injectivity results obtained for 592 wells with reliable pressure data showed a wide distribution of well injectivity indexes with a P90 of 1892 stb/year/psi, P50 of 355.5 stb/year/psi, and a P10 of 51.55 stb/year/psi. The injectivity results obtained for saltwater were translated into CO_2 equivalents, considering only single perforation wells injecting below 800 m, with the distribution resulting in a P90 of 0.713 Mt/year/1000 psi, P50 of 0.125 Mt/year/1000 psi, and a P10 of 0.0118 Mt/year/1000 psi. Further regional study, shows the Miocene, Woodbine, and Oligocene to have the best injectivities and potentials for CO_2 injection in the Texas Gulf Coast.

The wide distribution of injectivity observed in the regional study shows that large-scale injection is possible in the onshore Texas Gulf Coast, with some wells injecting up to 1 Megaton of CO_2 equivalent per year. However, some wells have low injectivity indexes, and this can be largely attributed to the issue of intermittency observed to be common with saltwater injection as a majority of the wells operated below their maximum permitted monthly volume and pressure, which means that for most cases, the injectivity values only provide a minimal indication of reservoir performance.

A detailed case study of a local well cluster that cut across Caldwell and Guadalupe Counties shows the target injection unit, the Edwards Group, to be heterogenous and volumetrically the biggest target in the Lower Cretaceous. A few shallow wells in this unit, mostly with open-hole completions and possibly intersecting fracture sets, account for most of the high volumes going into the unit, possibly the low bottomhole pressures reported for the cluster, and the high

injectivities observed in the cluster. The injectivity range estimated for wells in this cluster injecting below 800 m in this study is questionable for large-scale CO2 injection and further studies will be required to confirm that trends of highly injectivity zones are also present below 800 m in the Edwards, as this could potentially be a huge storage resource in the up-dip Texas Gulf Coast. The detailed case study of a local well cluster in Refugio County analyzes the high pressures reported for the cluster to assess the possible impact of heterogeneity on pressure buildup in the Miocene.

Furthermore, the observed local variations in injectivity among wells in the same formation are possibly due to intermittency and variations in reservoir properties.

The results and insights from this study show the valuable experience saltwater injection provides to de-risk CCS, the potential of multiple target formations for large-scale CCS, that injectivities and volumes estimated in this study only provide a minimum indication of performance due to the issue of intermittency associated with saltwater injection, and the potential impact of heterogeneities. There is also a suggestion of well interference with a few wells sharing similar injectivity profiles. There is not enough evidence of compartmentalization based on the data available and the analysis carried out in this study.

Table of Contents

List of Tables……..... 12

List of Figures……..... 13

Chapter 1: Introduction……..... 16

1.1 Background of Study…….. 16

1.2 Problem Statement……... 21

1.3 Scope of Study……..... 22

1.4 Geological Setting……... 23

Chapter 2: Literature Review……..... 30

2.1 Class II Wells……... 30

2.2 Class VI Wells……..... 33

2.3 Previous Work on using Class II Saltwater Disposal Wells as an Analog…..... 35

2.4 Key Performance Indicators……..... 37

Chapter 3: Methodology……..... 38

3.1 Data Gathering and Sources……. 38

3.2 Quality Check and Data Adjustment…… 41

3.3 Volume Analysis…….. 46

3.4 Rate Analysis……47

3.5 Injection Target (Formation) Assignment…… 47

3.6 Injectivity Analysis…….. 51

3.7 Petrophysical Analysis……..... 58

3.8 Geological Characterization……..... 59

3.9 Software……..... 59
3.9.1 Enhanced Analytical Simulation Tool (EASiTool)……... 59
3.9.1.1 Calibrated Forward Modeling with EASiTool……... 61
3.9.2 Petra…….. 68
3.9.3 NeuraLog Digitizing and Quality Control……..... 68
3.9.4 Petrel E&P Software Platform…….. 68
3.9.5 Python……... 68
3.9.6 ArcMap……. 70
Chapter 4: Results – Regional Assessment…… 71
4.1 Volume……. 71
4.2 Injectivity Index……..... 74
4.3 Normalized Injectivity Index…….…….. 79
Chapter 5: Results – Case Study I: Edwards Injection Trend…… 84
5.1 Background……. 84
5.2 Calibrated Forward Modeling of the Edwards Trend Injection…… 85
Chapter 6: Results – Case Study II: Catahoula Injection Trend……..... 87
6.1 Background……. 87
6.2 Calibrated Forward Modeling of the Catahoula Trend Injection……. 88
Chapter 7: Discussion……... 90
7.1 Summary of Regional and Detailed Case Studies……..... 90
7.2 Observed Local Variations in Injectivity…….. 91
7.3 Policy Recommendations for Class VI Projects……..... 98
7.4 Sources of Uncertainty……..... 99

Chapter 8: Conclusion……..... 101

Chapter 9: Future Work……..... 103

Appendix A…….……..... 104

Appendix B……..... 217

Appendix C……..... 226

References ……..... 235

List of Tables

Table 3.1: Key Primary Data Types……..... 38

Table 3.2: Formations Merged into Injection Intervals…….. 48

Table 3.3: Injection Formation Status for Wells in the Texas Gulf Coast……... 50

Table 5.1: Parameter Values for Edwards Case Study……..... 85

Table 6.1: Parameter Values for Catahoula Case Study…….. 88

Table 7.1: Injectivity Summary for Five Wells Injecting into the Catahoula Formation..... 93

Table 7.2: Injectivity Summary for Seven Wells Injecting into the Edwards Formation..... 94

List of Figures

Figure 1.1: Changes in Atmospheric Carbon Dioxide Concentration over the Past 800 Years and Post-Industrial Revolution Global Temperatures (Lindsey, 2024; NASA Earth Observatory, n.d.; NASA GISS, 2023) 17

Figure 1.2: Capacity of Commercial Facility Pipeline (Global CCS Institute, 2023) 19

Figure 1.3: Saltwater Injection Trend in the Texas Gulf Coast from 1990 to 2020..... 20

Figure 1.4: Large-Scale Projects along the Gulf Coast (Bump and Hovorka, 2024) 22

Figure 1.5: The Geological Cross-Section of the Gulf Coast (Bump et al., 2021) 24

Figure 1.6: Large Faults in the Gulf Coast (United States Geological Survey, 2021) 24

Figure 1.7: Modified Stratigraphic Section showing the Edwards Formation (Cook, 1979) .. 26

Figure 1.8: Geological Overview of the Edwards Trend (Ewing et al., 1990; Phelps et al., 2014; Schultz,1993) 27

Figure 1.9: Geological Overview of the Catahoula Trend (Ewing et al., 1990) 29

Figure 2.1: Class II Wells (EPA, 2024) 32

Figure 2.2: Class VI Wells (EPA, 2024) 34

Figure 2.3: Class VI Permit Tracker (EPA, 2024) 35

Figure 3.1: Texas Gulf Coast Saltwater Disposal Wells 40

Figure 3.2: Sample Well Log Data from IHS 41

Figure 3.3: Volume (stb) versus year 43

Figure 3.4: Rate (stb/day) versus year 43

Figure 3.5: Random Forest Classifier Summary 49

Figure 3.6: Disposal Wells by Injection Target 51

Figure 3.7: The Moody Diagram 54

Figure 3.8: CO_2-Brine Density and Viscosity Ratio 58

Figure 3.9: Well Cross-Section for the Edwards Injection Trend 63

Figure 3.10: Well Cross-Section for the Catahoula Injection Trend 66

Figure 3.11: Basin Area for the Oligo-Miocene Trend 67

Figure 4.1: Saltwater Disposal Wells in the Texas Gulf Coast colored by their Total Injection Volume 71

Figure 4.2: Total Injected Volume by Injection Interval 73

Figure 4.3: Saltwater Injectivity Index Distribution in stb/year/psi 74

Figure 4.4: CO_2 Injectivity Index in megatons per year per 1000 psi 75

Figure 4.5: CO_2 Injectivity Index (Mt/year/1000 psi) Distribution on an Interval-by-Interval basis..... 77

Figure 4.6: CO_2 Injectivity Index (Mt/year/1000 psi) by Injection Interval..... 78

Figure 4.7: Saltwater Normalized Injectivity Index (stb/year/psi/ft) Distribution..... 79

Figure 4.8: CO_2 Normalized Injectivity Index (Mt/year/1000 psi/ft) Distribution..... 80

Figure 4.9: CO_2 Normalized Injectivity Index (Mt/year/1000 psi/ft) Distribution on an Interval by Interval basis..... 82

Figure 4.10: CO_2 Normalized Injectivity Index (Mt/year/1000 psi/ft) Distribution on an Interval-by-Interval basis 83

Figure 5.1: Volume Map showing the Edwards Injection Trend..... 84

Figure 5.2: Simulation Results for the Edwards Case Study..... 86

Figure 6.1: Volume Map showing the Catahoula Injection Trend..... 87

Figure 6.2: Simulation Results for the Catahoula Case Study..... 89

Figure 7.1: Injectivity Index (stb/day/psi) versus volume (stb)..... 95

Figure 7.2: Injection Pressure, Maximum Monthly Pressure, Permitted Pressure, and Rate versus Time for wells injecting into the Catahoula Formation……... 96

Figure 7.3: Injection Pressure, Maximum Monthly Pressure, Permitted Pressure, and Rate versus Time for wells injecting into the Edwards Formation……. 97

1. Introduction

1.1 Background of Study

Since the Industrial Revolution, human activities such as burning fossil fuel, deforestation, and urbanization have caused an increase in the concentration of greenhouse gases, especially carbon dioxide (CO_2), in the atmosphere. The global average atmospheric carbon dioxide is 417.06 ppm (Figure 1.1), almost double the pre-industrial levels (Lindsey, 2024). Increased atmospheric CO_2 leads to a positive radiative forcing (i.e., net energy gain) in the climate system, which causes global warming. According to the IPCC (2007), the global average temperature due to human activities has surpassed 1ºC above pre-industrial levels (Figure 1.1). It is on track to surpass the 1.5ºC limit set in the 2015 Paris Agreement by 2040 if the current rate of warming continues. Hence, this calls for urgent actions to get to net-zero emissions and avoid the catastrophic events that could result from such an increase in temperature. To get to net-zero emissions, different solutions have been proposed, such as a transition towards renewable energy sources like wind and solar, improvement of energy efficiency in energy systems, afforestation, reforestation, Carbon Capture and Storage (CCS), etc. While every solution is important and needed to achieve the net-zero goal, the Intergovernmental Panel on Climate Change (IPCC) in their fifth assessment report, projected that the cost of climate change mitigation will increase by 138% in 2100 if CCS technologies are not adopted (IPCC, 2014) and in their 2018 1.5ºC special report, listed CCS as one of the three mandatory emission reduction technologies in the four key emission reduction technology pathways (IPCC, 2018)

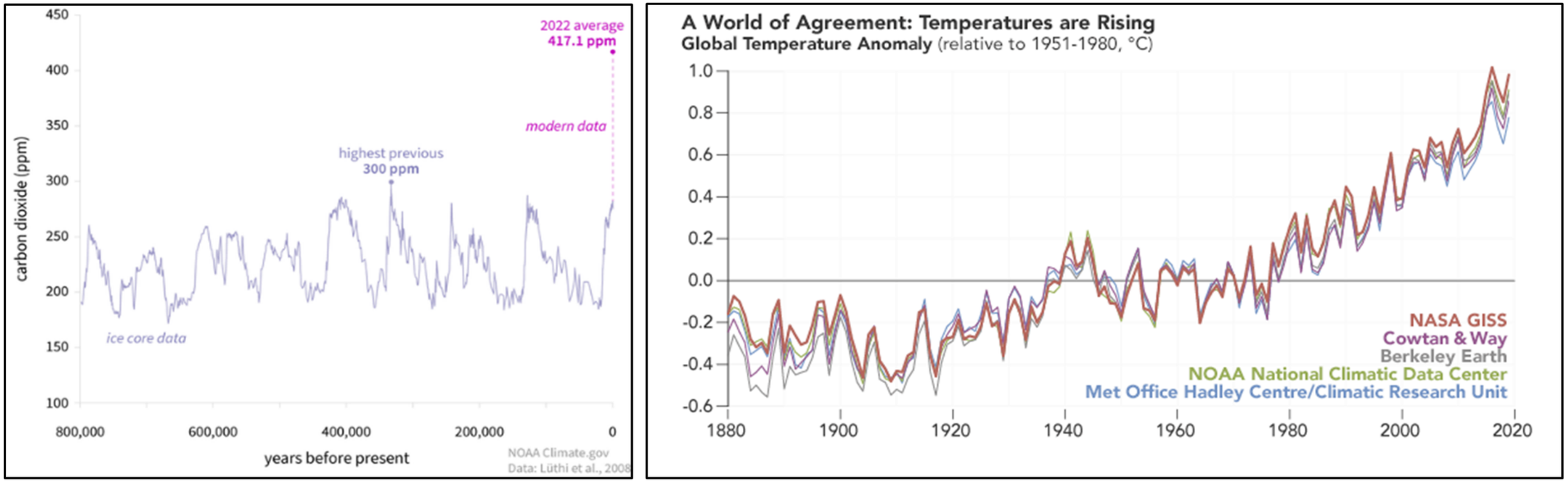

Figure 1.1 The figure on the left from Lindsey (2024) shows the atmospheric carbon dioxide concentration over the past 800 years, with a sudden spike in recent times. The figure on the right (NASA Earth Observatory, n.d.) has the red line from NASA GISS (2023), which shows that global temperature has surpassed 1 degree Celsius since the Industrial Revolution.

Carbon Capture and Storage involves the prevention of CO_2 from being emitted into the atmosphere by capturing it, usually from a point source, and sequestering it in a subsurface geologic formation. While the concept of permanent CO_2 storage in saline aquifers is relatively new, the process of capturing CO_2 from a source and injecting it into subsurface formations has been around since 1972 when CO_2 was captured from the Terrell natural gas processing facility for Enhanced Oil Recovery (EOR) in oil fields in West Texas Permian Basin (National Petroleum Council, 2019). The process has proved successful so far having seen millions of tons of CO_2 injected into oil fields in the United States and around the world for EOR (IEAGHG, 2013; IEA, 2016).

With the growing need for large-scale geologic sequestration of CO_2 in saline aquifers and recent policy reforms around the world, especially in the United States, many industry stakeholders have begun to show keen interest in the CCS technology, leading to an exponential growth (Figure 1.2) in the number of commercial CCS facilities in the United States and around the world since 2017 (Global CCS Institute, 2023). These commercial facilities, especially the ones in the United States have set very high storage targets. The scale of some of these projects under review is orders of magnitude higher than that of past projects like the Decatur project, with some of these projects targeting to design wells injecting approximately 2-4 megatons of CO_2 per annum (Mtpa) (Bump and Hovorka, 2024; Clean Air Task Force, 2024).

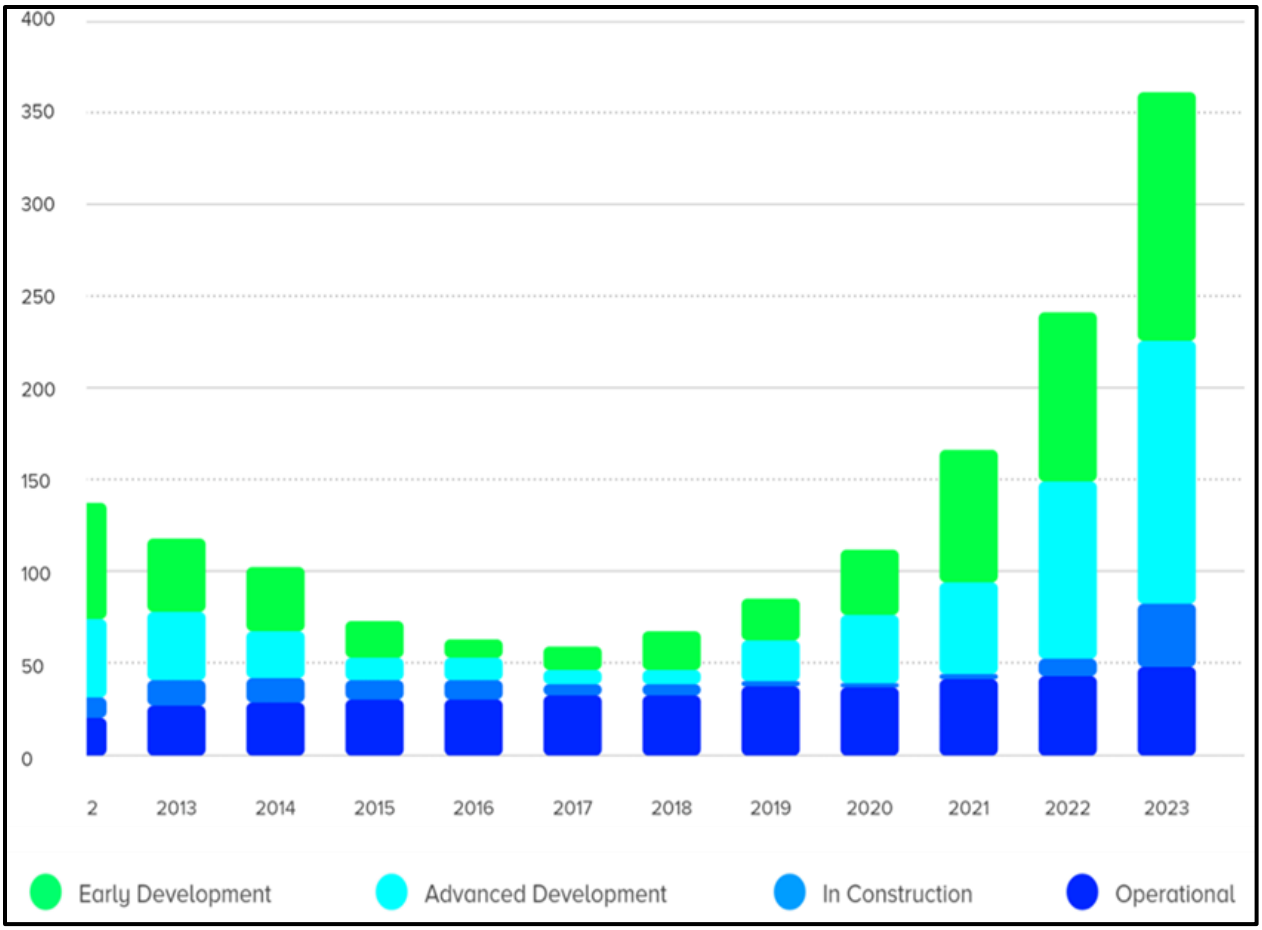

Figure 1.2 Exponential growth in the capacity of commercial facility pipeline since 2017 (Global CCS Institute, 2023)

Generally, fluid injection in the United States can be traced back to the 1930s when the petroleum industry in the United States started the injection of liquids into underground formations as a means of disposing of saltwater (sometimes referred to as brine in this study) that was produced alongside crude oil and in some cases were used to enhance oil recovery from subsurface formations (Clark et al., 2005; McCurdy, 2011; Environmental Protection Agency, 2024). The wells designed to inject saltwater associated with hydrocarbon production are classified as Class II wells under the 1974 Safe Water Drinking Act (SWDA).

Since the first Class II well was drilled in the Texas Gulf Coast, over 20 billion barrels of saltwater have been permanently disposed into non-producing formations in the region. When restricted to only volumes injected below 800 m (the depth at which CO_2 attains its supercritical state) the injection volume is more than 15 billion barrels. When this volume is approximately translated into CO_2 equivalents at reservoir conditions, by assuming a CO_2 density of 700 kg/m^3, it results in 2.3 Gt. Saltwater injection demonstrates that the region's geology is capable of accepting large volumes of fluid. With over 30 years of injection history (Figure 1.3) and a large dataset available from Class II wells in the Texas Gulf Coast, there are many lessons that CCS projects can learn from these saltwater disposal wells to help address the concerns shared by many CCS stakeholders on the technical and economic feasibility of large-scale CCS projects in the Texas Gulf Coast region.

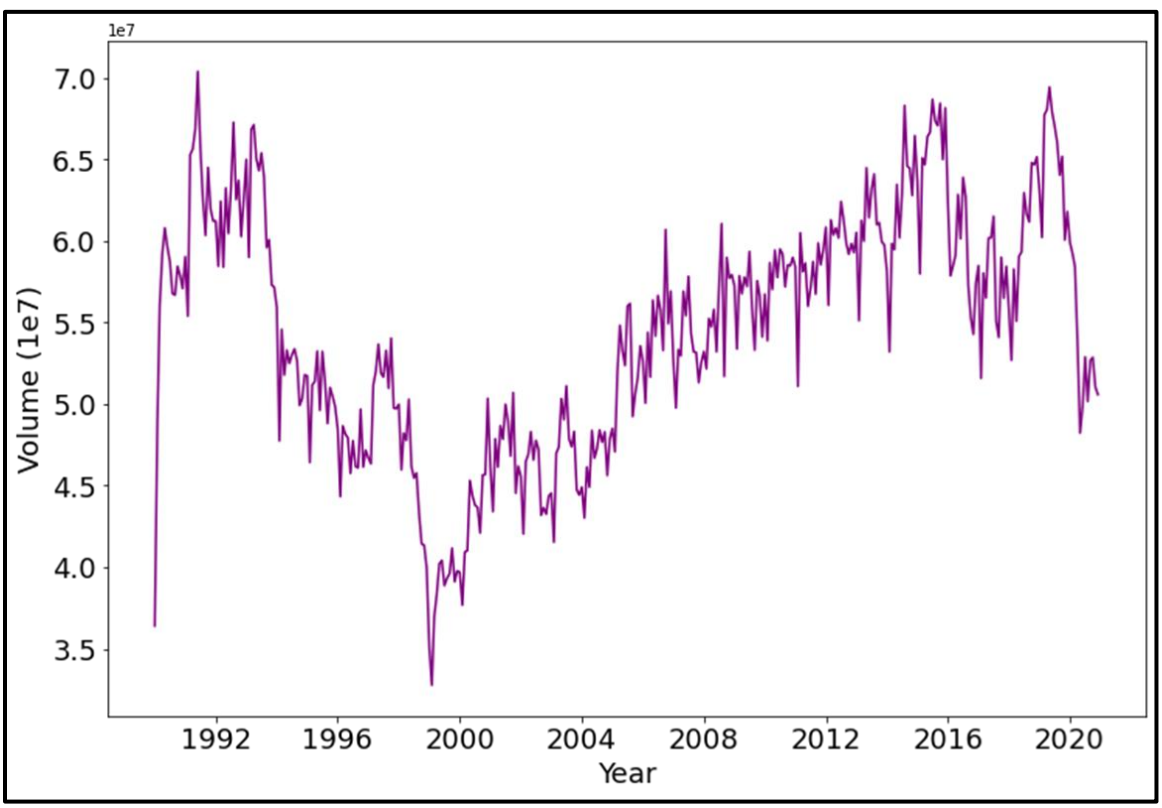

Figure 1.3 Saltwater injection trend in the Texas Gulf Coast from 1990 to 2020

1.2 Problem Statement

The Carbon Capture and Storage industry is looking to build on many years of experience with CO_2 injection into the subsurface either for Enhanced Oil Recovery (EOR) or demonstration purposes. However, with projects currently under development targeting rates that are orders of magnitude higher than what has been previously attempted for CO_2 injection into saline aquifers (Figure 1.4), there is a need to calibrate predictions for large-scale injection, to assess the technical feasibility and potential risks associated with the projects of such large scales. Also, as the growth of CCS continues, there is a key question relating to how pressure buildup and well interference will affect projects of such magnitudes.

Ni et al. (2021) leveraged data from saltwater disposal wells to estimate the volume of CO_2 that can be stored in the Gulf Coast region. The authors achieved this by developing multiple cases through multiple assumptions. These include a direct conversion of injected saltwater volume to CO_2 assuming the same injection rate, assuming no injection intermittency with wells injecting at their highest historical injection rates, and assuming continuous injection at the maximum permitted injection rate.

This study builds on the work of Ni et al. (2021), using saltwater injection as an analog for large-scale CO_2 injection due to the time and scale of injection, to calibrate performance predictions made for large-scale injection projects in the Texas Gulf Coast region.

This study not only assesses capacity, but also injection performance across different wells and formations, considering the key factors driving or limiting performance across different formations, such as pressure buildup, heterogeneity, intermittency, compartmentalization, well interference, and the potential challenges or opportunities they present to large-scale CCS projects

in the region. Thereby suggesting ways potential risks can be minimized to help quell some of the concerns shared by the CCS stakeholders.

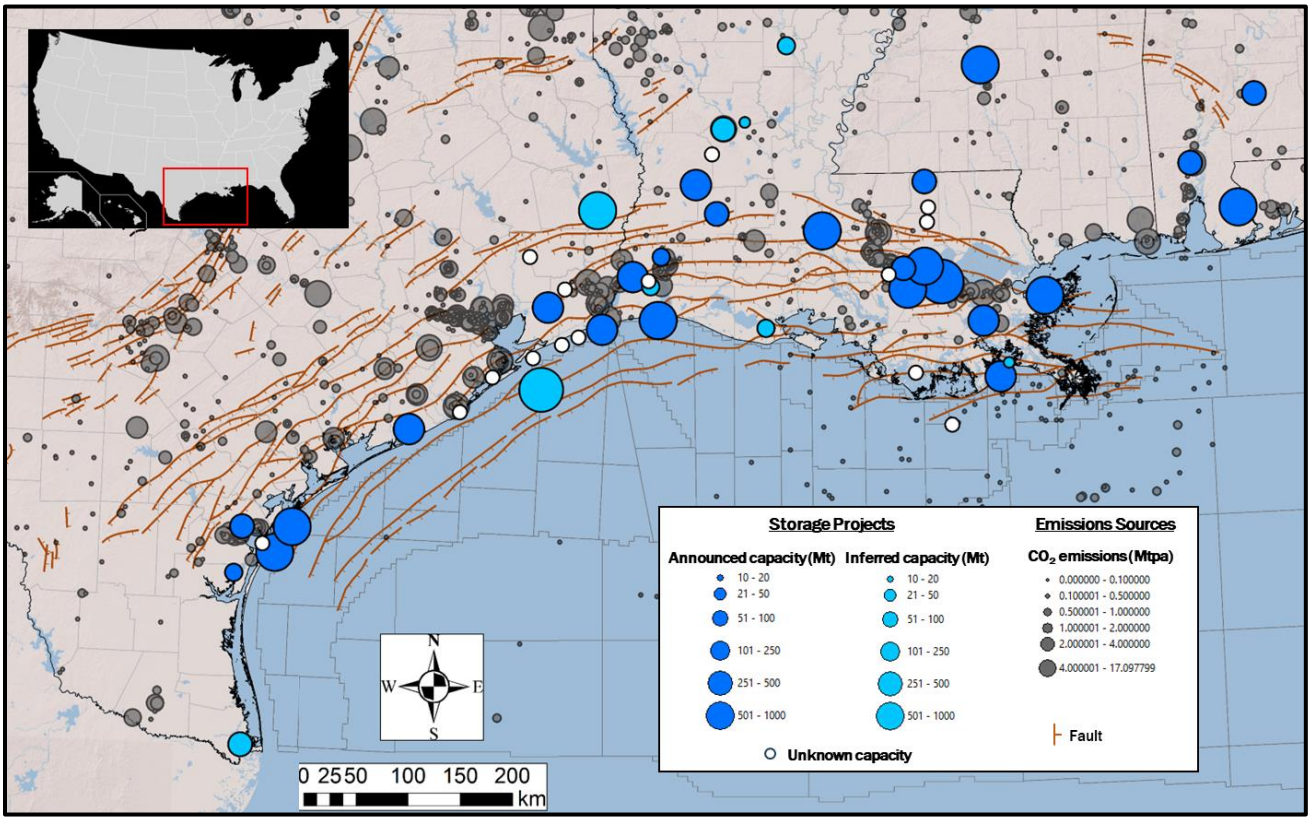

Figure 1.4 Large-Scale CCS Projects along the Gulf Coast (Bump and Hovorka, 2024). The blue bubbles represent announced capacity, the sky-blue bubbles represent inferred capacity, and the grey bubbles represent CO_2 emission sources.

1.3 Scope of Study

This study focuses on the Texas Gulf Coast, with saltwater injection data from 1990 to 2020. This period has been selected because it represents the period in which the Railroad Commission has digital records of injection data that are consistent and reliable enough to carry out this study. Specific assessments of injection into the Edwards Group and Catahoula Formation

were carried out to assess the potential of the Edwards for CCS and understand the contributing factors to the injection performances observed in these two units.

1.4 Geological Setting

The United States Onshore Gulf Coast, north of the Gulf of Mexico, is a great coastal plain slightly tilted towards the coast (Figure 1.5), with the land surface falling about 5 feet per mile before giving way to coastal swamps and open water. Most of the sediments below the region are Tertiary and Quaternary in age and thicken and dip toward the coastline (Carsey, 1950). The Gulf Coast accumulated large volumes of hydrocarbons, with Fault and salt structures and top seals playing an important role (Figure 1.6).

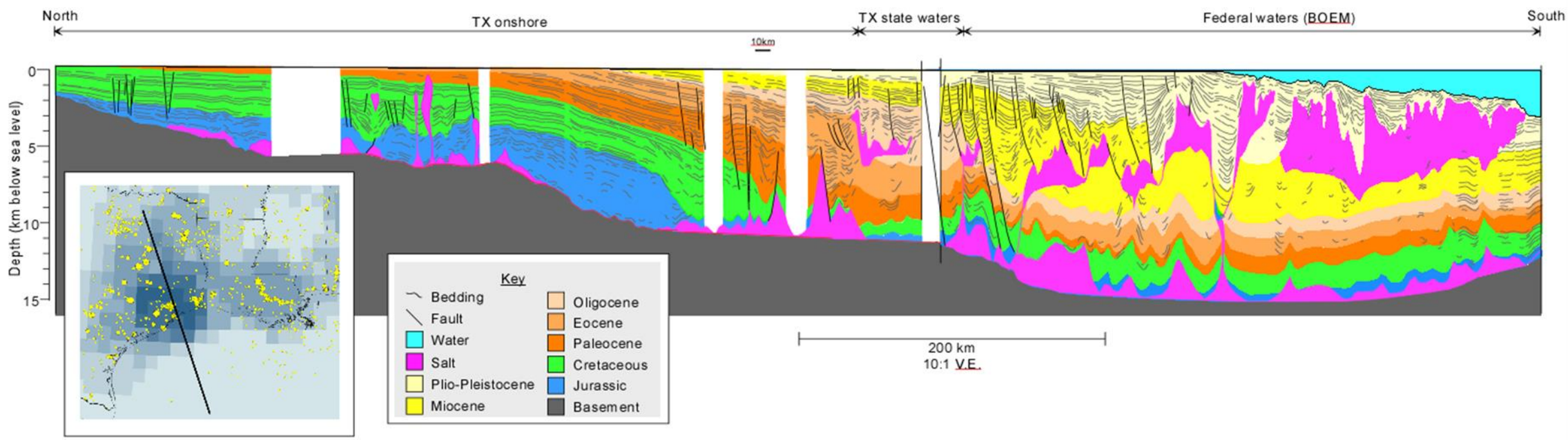

Figure 1.5 The Geological Cross-Section of the Gulf Coast with formations prograding coastward and the older Jurassic on the left and younger Plio-Pleistocene on the right (Bump et al., 2021)

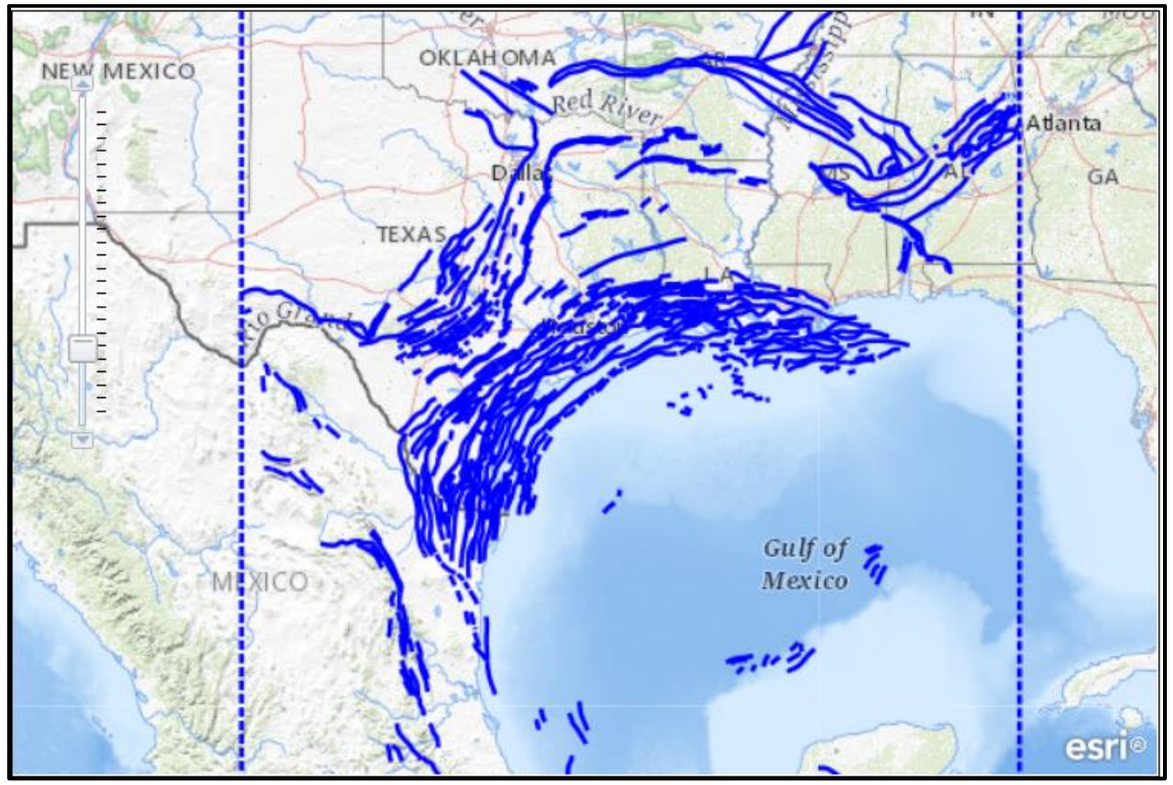

Figure 1.6 Large Faults in the Gulf Coast (United States Geological Survey, 2021)

The Edwards Group in the Luling-Branyon Field is a leached, porous dolomite and dolomitic limestone deposited in tidal-flat and shallow-marine environments (Cook, 1979; Swanson et al., 2017). It is found at an average depth of 2,130 ft from the surface (Davis and Goode, 1957). The complex diagenetic history of the limestone and the occurrence of hard chert lentils make the reservoir quality variable (Cook, 1979; Swanson et al., 2017). According to Hovorka et al. (1998), the amount and distribution of dolomitized facies correspond to the intervals that have increased hydraulic conductivity. Along the Northern margin of the Comanche Platform, the Edwards Group has a thin edge. The unit's thickness increases southwards, with sections up to 450 ft thick present in the subsurface of South Texas a few miles west of the eastern platform edge (Fisher and Rodda, 1969). Farther south and towards Northern Mexico, the Edwards unit has a thickness of as much as 600 ft (Fisher and Rodda, 1969) and up to 1000 ft in the southwest near the Maverick Basin (Rose, 1972). Overlying the Edwards Group is a thin sequence of approximately time-equivalent open-marine marl and nodular carbonate mudstone containing oxytropidoceroid ammonites (Fisher and Rodda, 1969) and Rose, 1972 described these overlying formations as the Georgetown, Del Rio, and Buda Formations. Below the Edwards is the Glen Rose Formation (Rose, 1972). The Edwards Group (Figure 1.7) comprises the Kainer Formation, a massive dolomitic micrite, and the Person Formation, described as limestone and dolomite collapse breccias (Swanson et al., 2017). According to Cook (1979), the upper 50 ft of Edwards is the primary reservoir, possessing good porosity and permeability, with production from Edwards extending just below approximately 2100 ft. Chenault and Lambert (2005) suggested that the Edwards Group extends throughout both the Fredericksburg and Washita Divisions in the San Marcos platform area. With the focus area of this study along the San Marcos arch (Figure 1.8), this study takes Chenault and Lambert (2005) and Geomap (2009) approaches by placing the Edwards Group in both the Washita and Fredericksburg Divisions, with the upper Edwards, which is largely the injection target, under the Washita Division.

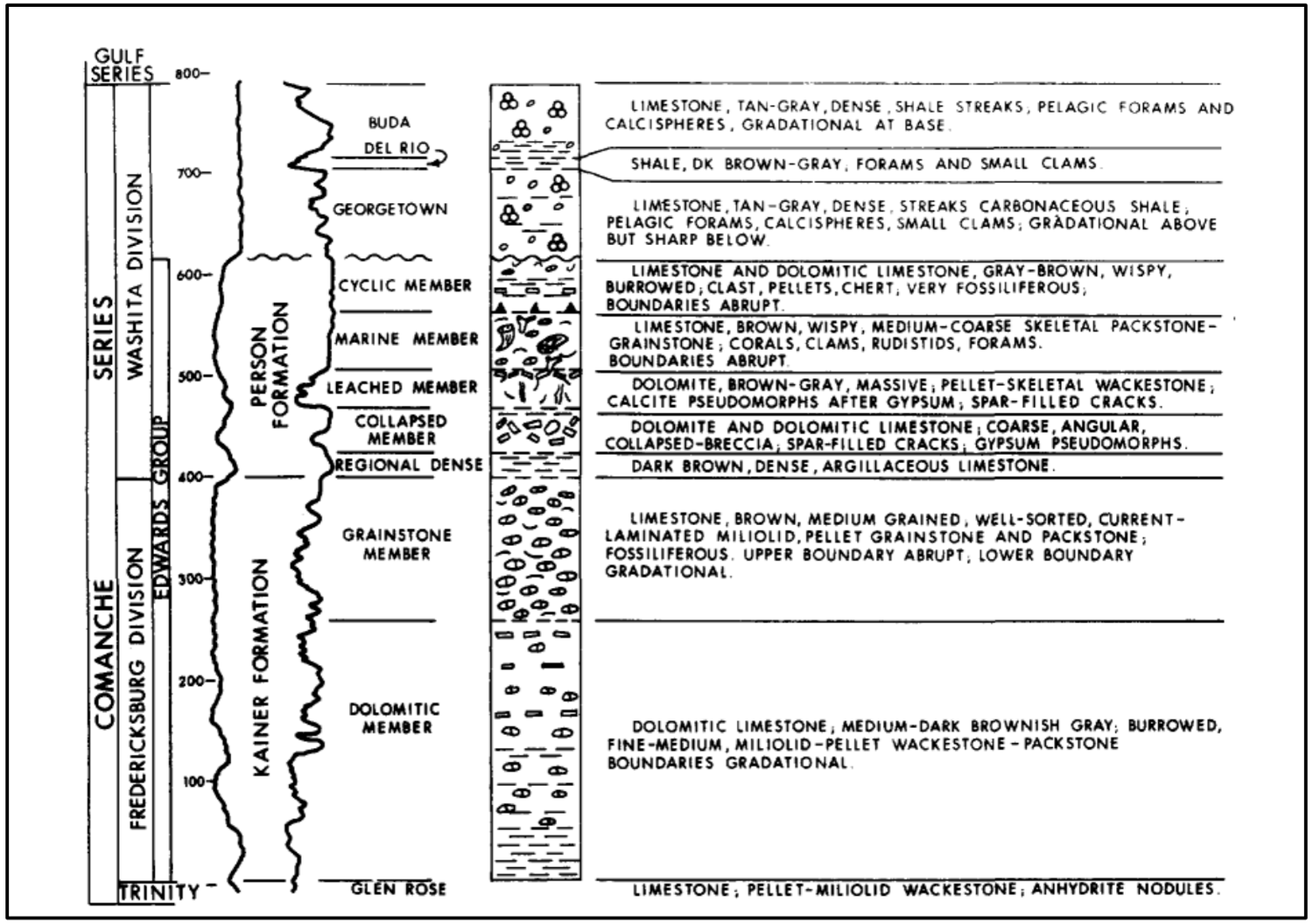

Figure 1.7 Modified Stratigraphic Section from Rose, 1972 showing the Edwards Group (Cook, 1979)

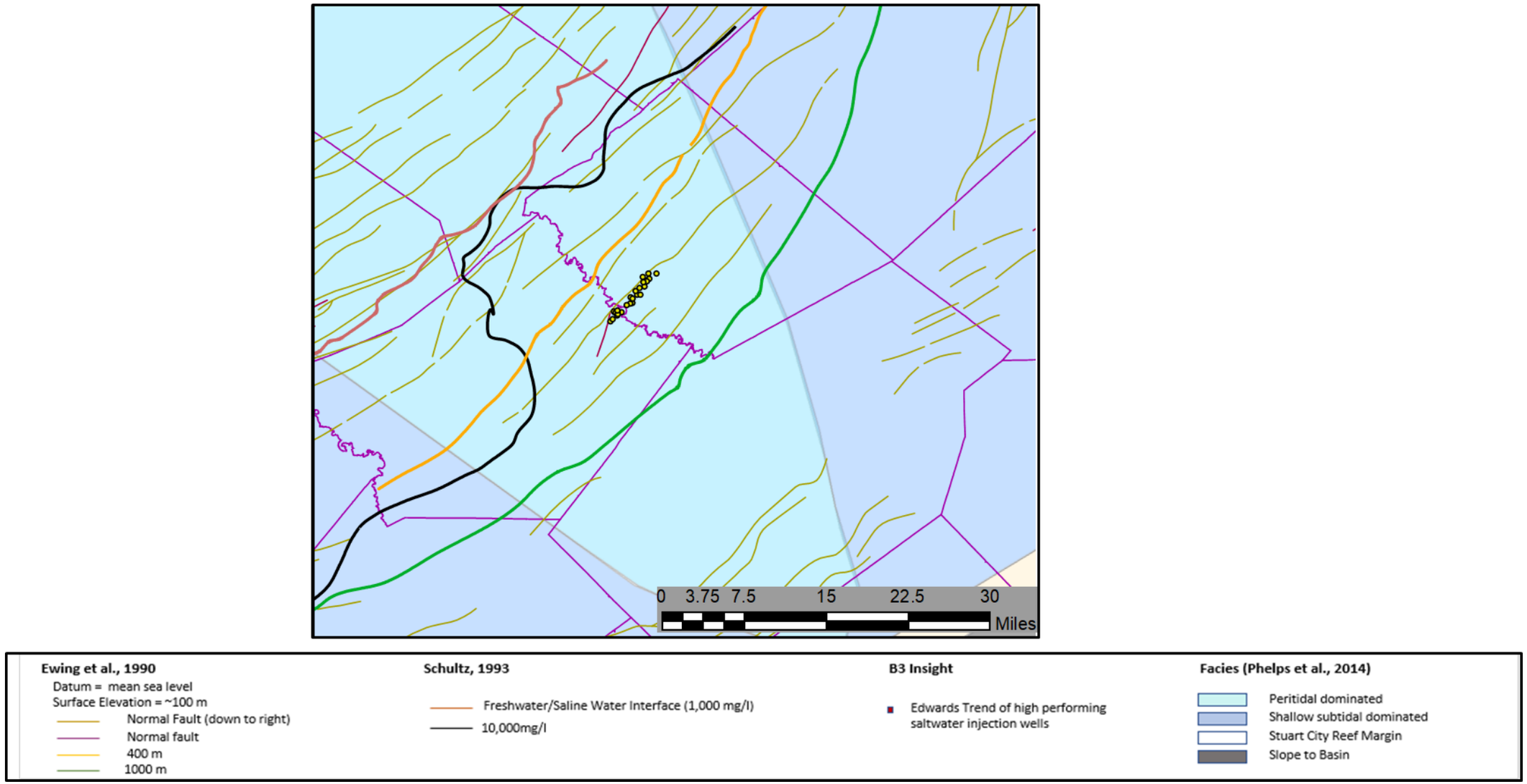

Figure 1.8 Geological Overview of a local well cluster near the Luling-Branyon Field (Ewing et al., 1990; Phelps et al., 2014; Schultz, 1993). The red and black lines represent the 1,000 mg/l and the 10,000 mg/l lines respectively. The gold and pink lines show normal Faults, the yellow line is the 400-meter line, and the green line is the 1,000-meter line. The red dots show the cluster of wells injecting into the Edwards. The throw for the normal Faults in yellow is down in the SW direction. The different colors represent facies type.

The Catahoula Formation in the Tom O'Connor field (Refugio County, Southern Texas) consists of non-marine sands, clays, and volcano-clastic deposits interbedded with fluvial sediments. (Chowdhury et al., 2006; Galloway and Kaiser, 1980). Around the Tom O'Connor Field, the formation consists of 40% to 60% of sand (Corpus Christi Geological Society, 1968). The average formation thickness increases basinward, however, growth fault belts disrupt sedimentary patterns, with the formation's average thickness ranging from 150 ft to 200 ft in central Texas, 200 ft to 600 ft in East Texas, and about 800 ft to 1000 ft in South Texas (Chowdhury et al., 2006; Galloway, 1977). The Catahoula sands have excellent reservoir properties with an average porosity of 29% and permeability of 1400 md in the major fields in Refugio County, such as the Tom O'Connor Field. Growth faults initiated by early deltaic propagation extend up to the Catahoula and deeply influence the trends of the fluvial sand units (Galloway, 1977). The Catahoula Formation is placed in the Miocene Epoch, with the upper part of the formation overlaying the thick Anahuac marine shale, which overlays the Frio Formation (Chowdhury et al., 2006; Corpus Christi Geological Society, 1968; Wilmarth, 1938). The Catahoula trend near the Tom O'Connor Field (Figure 1.9) has wells located on either side of a fault. This fault is non-sealing because the fault's throw is minimal, with a similar geology on either side of the fault. Also, the pressure response observed from wells on both sides of the fault is almost the same.

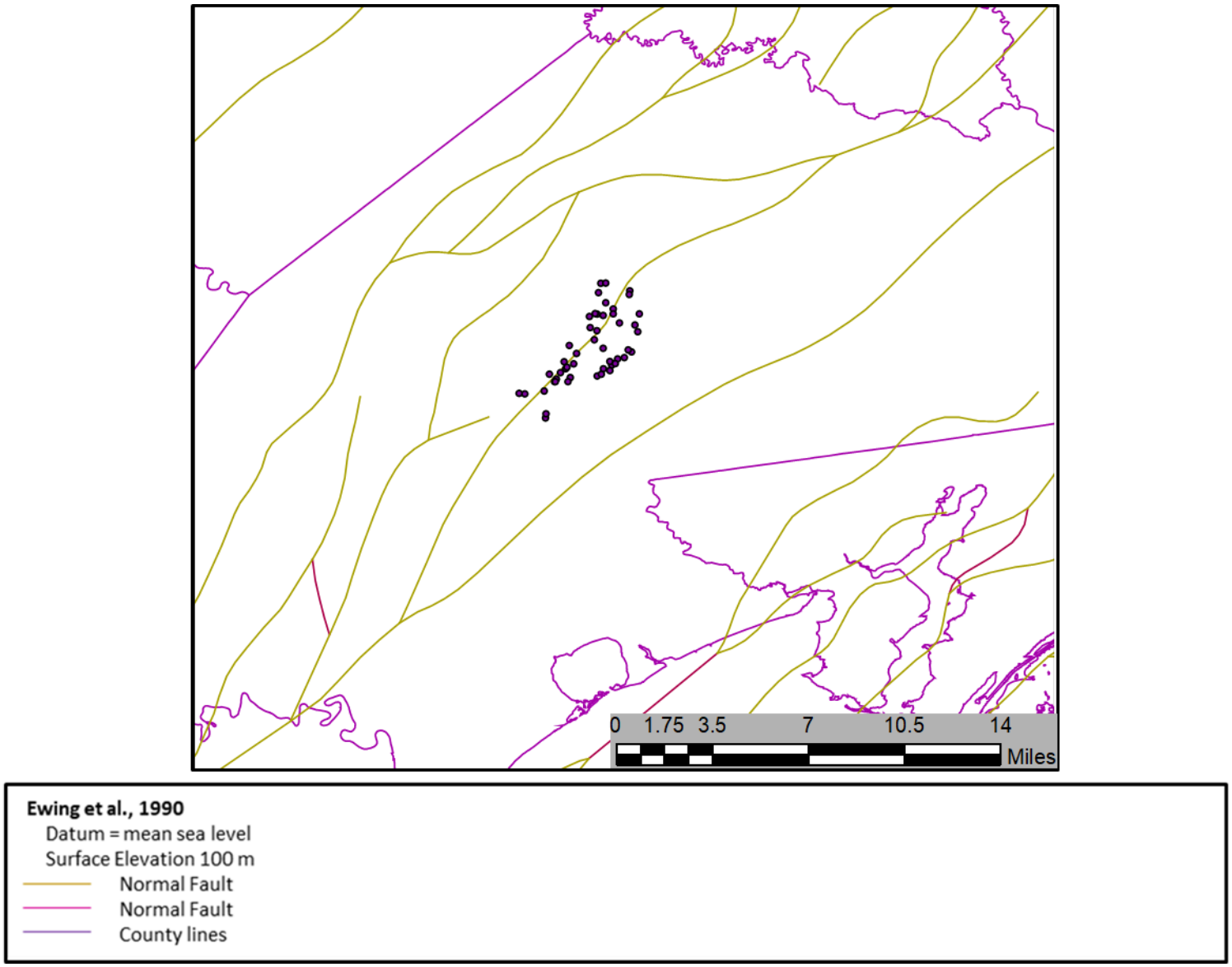

Figure 1.9 Geological Overview of the Catahoula Trend near the Tom O'Connor Field (Ewing et al., 1990;) The gold lines represent faults, the purple lines are county lines, and the dots show the wells in the cluster.

2. Literature Review

2.1 Class II Wells

Brine associated with oil and gas production has been injected into underground formations by the petroleum industry in the United States since the 1930s (Brasier and Kobelski, 1996). In addition, industrial waste fluid can also be deep-well injected. The first deep industrial waste injection well was drilled in Texas by Dupont in 1949 (Clark et al., 2005). By 1961, Texas became the first state to adopt regulations regarding industrial injection wells (Warner and Orcutt, 1973). However, regulations at the state level were not uniform in terms of protecting water quality levels for potentially usable groundwater (Clark et al., 2005). Following documented cases of groundwater contamination due to underground waste injection such as the case of a waste injection well at the Hammermill Paper Company in Erie, Pennsylvania, the United States Congress passed the Safe Water Drinking Act which allowed the Environmental Protection Agency (EPA) to establish the Underground Injection Control Program (UIC) in 1974 (McCurdy, 2011). Following these regulations, the EPA established a national standard for current and potential drinking water sources as <10,000 mg/L total dissolved solids (TDS) (EPA, 1980). Under this program, Class II was established for injecting fluids associated with oil and gas production, which includes large amounts of saltwater (brine). The number of injection wells in the United States has increased over the years from 30 in the early 1960s (Smith, 1996) to approximately 180,000 Class II wells currently in operation (EPA, 2024). Every day, over 2 billion gallons of fluids are injected in the United States, with most of the injection wells in Texas, California, Louisiana, and Kansas (EPA, 2024). The EPA divides Class II wells (Figure 2.1) into three categories:

a. *Disposal Wells*: These wells are used to inject brines associated with oil and gas production or wastewater from hydraulic fracturing activities into the same or similar underground formation for disposal and they represent 20% of Class II wells (EPA, 2024).

b. *Enhanced Recovery Wells*: These wells, representing 80% of Class II wells, are used to inject fluids consisting of brine, fresh water, steam, polymers, or carbon dioxide into oil-bearing formations to recover residual oil and in limited applications, natural gas (EPA, 2024).

c. *Hydrocarbon Storage Wells*: These wells are used to inject liquid hydrocarbons into underground formations, such as salt caverns, for storage as part of the U.S. Strategic Petroleum Reserve, and there are over 100 of these wells in operation in the United States (EPA, 2024).

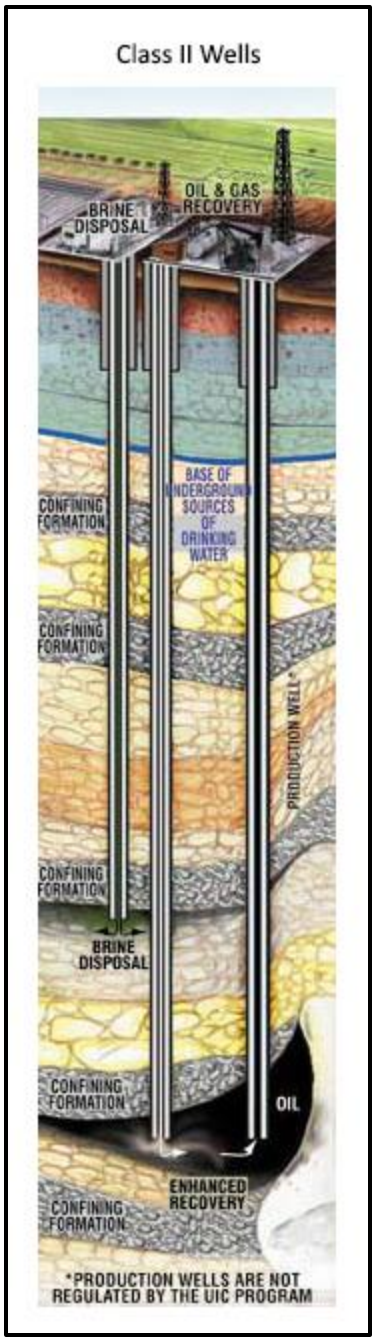

Figure 2.1 Class II Wells (EPA, 2024). The base of underground sources of drinking water is marked by a thick blue line. The left well is used for saltwater disposal while the other two wells are used for enhanced oil recovery, with the producing well on the right and the injection well in the middle.

Class II wells can make an industrial analog for wells used for CO_2 injection due to the scale of injection and its long history. Studying Class II wells can help provide some insights into how large-scale fluid injection performance can evolve with time and how existing regulations can be improved to ensure the potential challenges and risks associated with large-scale Class VI wells can be mitigated.

2.2 Class VI Wells

Class VI wells are used to inject carbon dioxide (CO_2) into deep rock formations for geologic sequestration (IEAGHG, 2018; EPA, 2024). This well class (Figure 2.2) was established by EPA in 2010. However, the implementation has been initially slow, with only six well permits issued prior to 2022 (Lau, 2022). Three states now have Primacy (i.e. state, territory, or tribal responsibilities associated with implementing EPA-approved UIC programs) for Class VI wells (Lau, 2022; EPA, 2024) and active Class VI wells are increasing. Currently, there are about 64 Class VI projects under review at the EPA (Figure 2.3), with about 30 of these projects located in the Gulf Coast region (EPA, 2024). To help reduce the long wait times associated with Class VI permits, other states such as Texas have announced their intention to seek Primacy over Class VI wells.

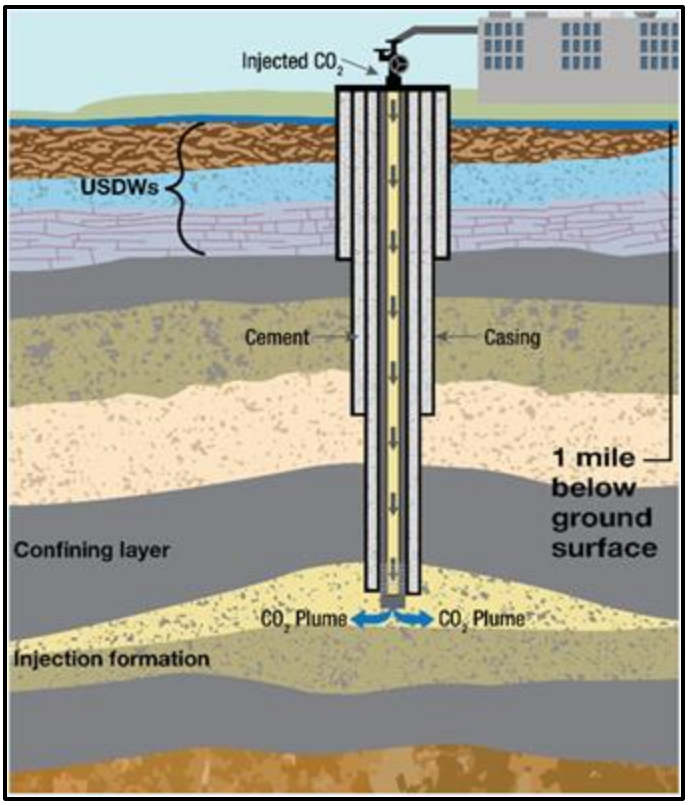

Figure 2.2 Class VI Well (EPA, 2024)

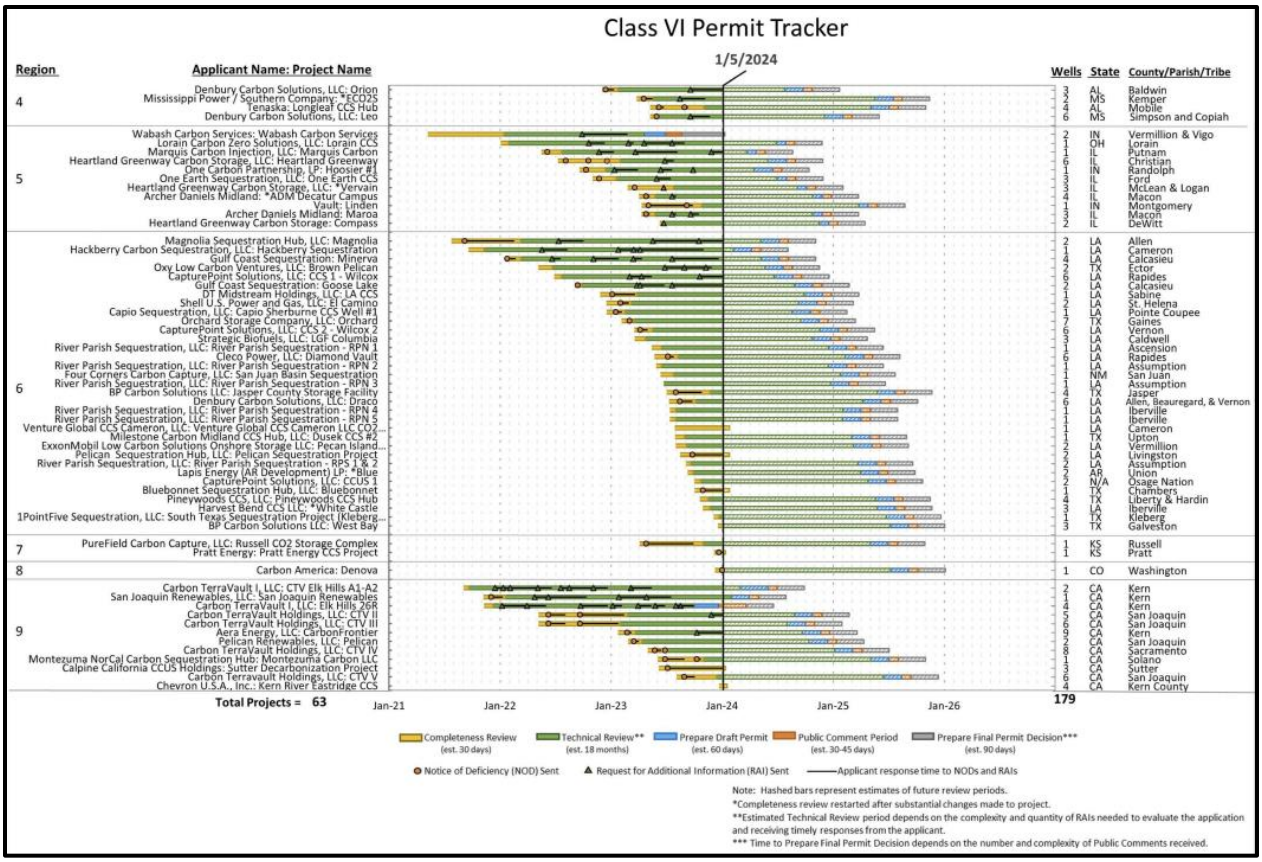

Figure 2.3 Class VI Permit Tracker (EPA, 2024)

2.3 Previous Work on Using Class II Saltwater Disposal Wells as an Analog

Ni et al. (2021) evaluated the technical feasibility of gigatons of CO_2 storage in the U.S. Gulf Coast using data from saltwater disposal wells in the region and assessed the best formations for disposal. Most of the saltwater injection data used by Ni et al. were obtained from B3 insight and IHS Enerdeq. Ni et al. considered injection data from 1983 to 2017 for the Texas Gulf Coast and assumed 3000 ft to be the depth below which CO_2 is supercritical and selected only wells injecting below this depth. Ni et al. focused their analysis on both the Texas and Louisiana Gulf Coast. They leveraged parameters such as total injection volume, rate per well, capacity per well, injection pressure, pressure buildup, and injectivity index proxy to assess performance. For the Texas Gulf Coast, Ni et al. selected wells marked as injecting into non-producing formations to

reflect permanent disposal. Their study also used three scenarios to evaluate the CO_2 injection capacity of the U.S. Gulf Coast, converting saltwater volume to an equivalent mass of CO_2 assuming a supercritical CO_2 density of 700 kg/m3. The first scenario, designated as the lowest-estimate scenario, computes capacity by simply adding up the actual disposal volume for the active wells. The second scenario regarded as the second-estimate scenario, computes capacity by assuming no injection intermittency and that the active wells used are injecting at their highest historical injection rate. The third scenario dubbed the highest-estimate scenario, takes advantage of the linear relationship between pressure and injection rate by assuming constant injectivity and constant injection at maximum authorized pressure values. Their results showed that the 1 gigaton per year goal can only be achieved with the highest estimate scenario, and it would typically require 1500 wells injecting at 20,000 bbl/day to achieve this goal. Their results also showed that low-rate wells are more common in the region and suggested that this is likely because the wells available are sufficient for the amount of saltwater trucked for injection and that the Miocene and Frio are the highest injectivity formations.

Several aspects of the analysis were not undertaken by Ni et al. Injectivity index calculations in their study assumed no friction loss when converting wellhead pressure to bottomhole pressure for pressure buildup assessment. Their study also did not account for two-phase flow in their rate calculations, did not assess other potential factors contributing to limited injection performance, did not account for the huge variations in performance seen both regionally and locally, and did not translate injectivity results obtained for saltwater disposal wells to CCS terms in Mt CO_2/day/psi.

2.4 Key Performance Indicators

Storage capacity is a key performance indicator, and it involves the estimation of the amount of CO_2 that can be stored in geologic formations (Fang et al., 2010). The process of estimating the CO_2 storage capacity of a geologic formation is complex (Bradshaw et al., 2007; van der Meer and Yavuz, 2009), especially due to the various types of traps and trapping mechanisms possible, the different rates at which each trapping becomes effective, and the different physical states in which CO_2 might occur (Bradshaw et al., 2007). In the past, static assessment of the efficiency of CO_2 pore volume occupancy has been used to determine storage capacity, ignoring the impact of pressure buildup and compressibility of materials in the storage space (van der Meer and Yavuz, 2009). However, it is important to also consider injectivity as it takes the effect of pressure buildup and compressibility into consideration, providing a better evaluation of the storage potential of a location.

Injectivity is another key performance indicator, and it involves the measure of a geologic formation's ability to accept fluid injected into it. Injectivity is a function of the rate at which CO_2 can be injected and the ability of CO_2 to migrate from the injection well (Fang et al., 2010; De Silva and Ranjith, 2012). Different geologic formations have different flow properties and different boundary conditions, which can influence the ability of injected CO_2 to migrate away from the injection point. Formations with low porosity and permeability values with a closed boundary condition will most likely have more difficulties accepting fluid, as pressure buildup is more likely to be high in these formations due to limited space to dissipate pressure, ultimately leading to low injectivity, while formations with high porosity and permeability values with an open boundary condition will most likely experience the opposite. The injectivity index (J) is the ratio of a well volumetric flow rate (q) to the corresponding pressure differential (Δp) (Fang et al., 2010).

$$J = \frac{q}{\Delta p}$$ Equation 2.1

3. Methodology

3.1 Data Gathering and Sources

The primary data used in this study was obtained from saltwater disposal wells in the Texas Gulf Coast. These data are usually self-reported by industry operators every month as required by the Rail Road Commission (RRC). Access to the primary data from 8,348 wells in the Texas Gulf Coast region was possible thanks to B3 Insight, which acquires the data from the RRC and makes it easily accessible via spreadsheet and available for sale to the public. Each well is typically assigned a well ID by B3 Insight, which makes it easier to track compared to the API number, which has more digits. Each well also contains other data types such as county name, field name, injection start date, injection status, completion date, operator name, injection type, etc. Table 3.1 summarizes the other primary data types used in this study, and Figure 3.1 shows the location of the wells from which these primary data were obtained.

The secondary data used in this study, such as the well logs (Figure 3.2) and the Texas tectonic map, were obtained from IHS and Ewing et al., 1990 respectively.

Table 3.1 Key Primary Data Types

Serial Number	Primary Data Type
1	Well ID
2	API Number
3	Volume
4	Rate

5	Pressure
6	Completion interval
7	Injection target (formation)
8	Latitude
7	Longitude

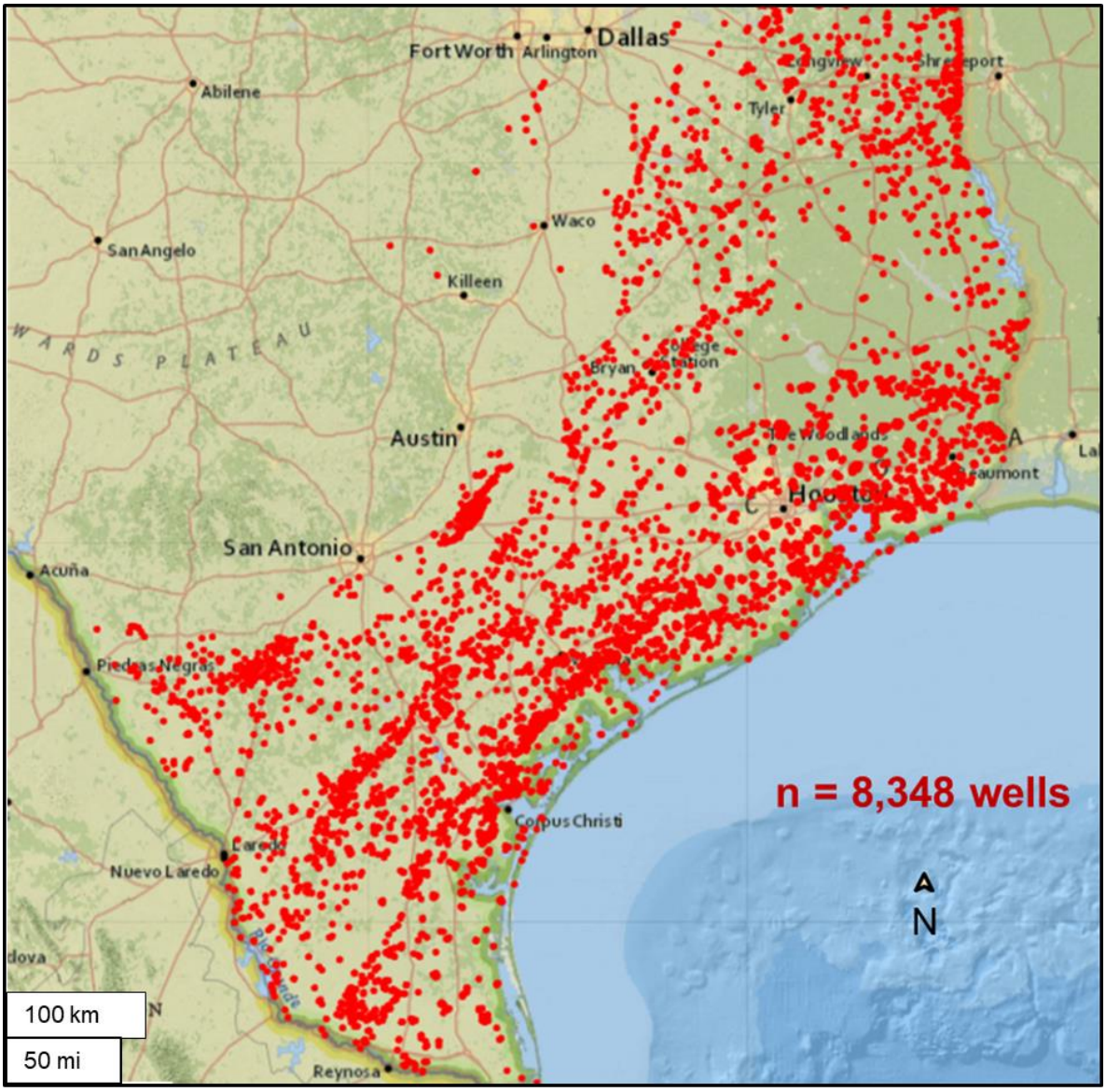

Figure 3.1 – Texas Gulf Coast Saltwater Disposal Wells. This includes only wells injecting into non-productive zones.

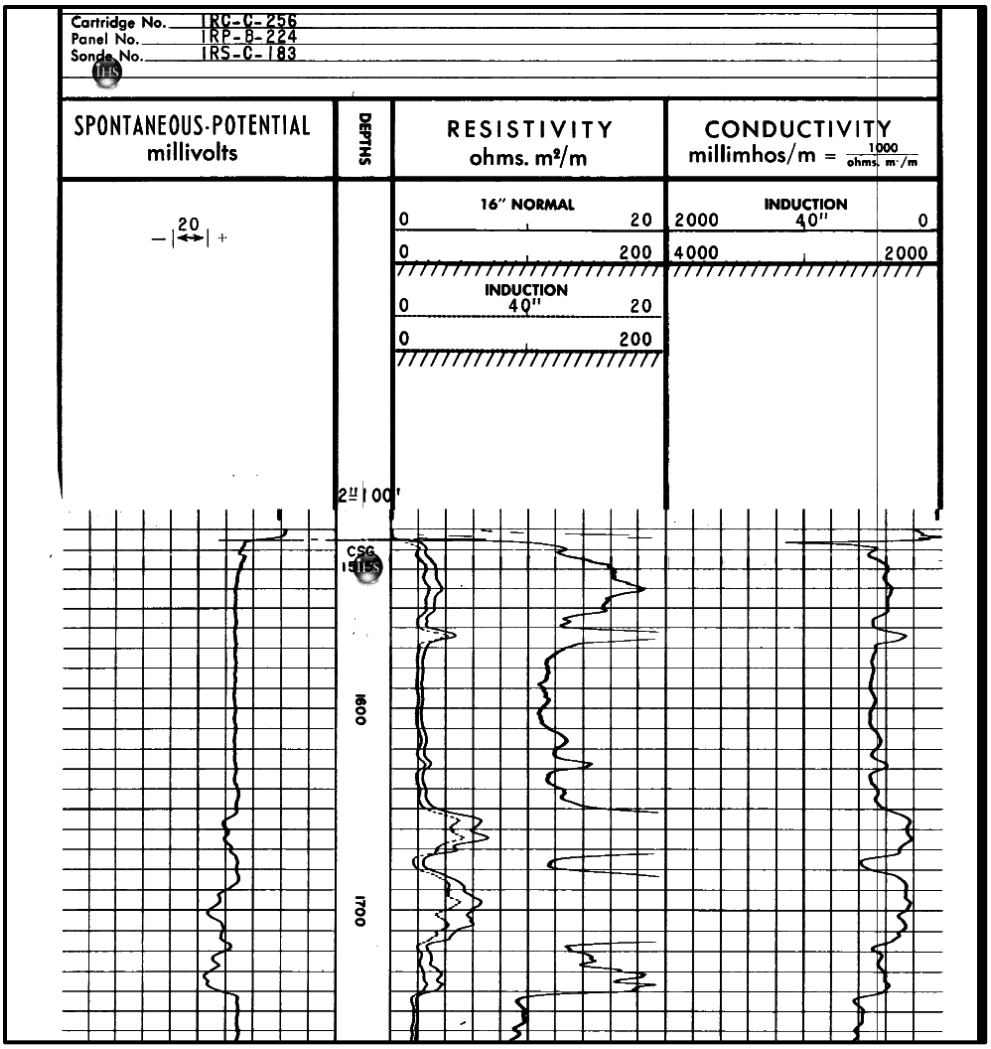

Figure 3.2 – Sample Well Log Data from IHS. The logs are mostly available as raster files and require digitization to be more useful.

3.2 Quality Check and Data Adjustment

These 8,348 wells have their injecting type marked as *injecting into a non-productive zone*. The different data types reported for these wells are inconsistent due to poor quality control, with lots of outliers in the volume, rate, and pressure data, and there were many inconsistencies between the rate and pressure data. The data from these wells were checked to ensure quality. The following paragraphs summarize the processes applied to the different data types to ensure good data quality.

The volume data for each well was plotted against time to ensure consistency in the data and avoid any outliers that could impact the data quality. Wells with zero volume records and those with inconsistent data (Figure 3.3 – left side) were excluded from the list, while wells like the one shown on the right side of Figure 3.3 were moved to the next level of quality check. Most of the data for these selected wells were largely consistent. However, several wells with spikes in their data (similar to what is shown on the left side of Figure 3.4) had those spikes eliminated by replacing the high values causing the spikes with the average value estimated using other data points, resulting in more consistent data. To further ensure quality, only injection data from 01/01/1990 to 12/31/2020 were used for volume analysis, as data outside of this period were inconsistent and reduced the data quality. Also, according to the Railroad Commission, digital records of these data only became available in the late 1980s. Out of 8,348 wells, only 5,105 wells have their monthly injection data reported, and following a quality check, only 4,805 wells were deemed to have good enough data for volume analysis.

The rate data for each well was also plotted against time to ensure consistency and eliminate outliers. This data is the monthly volume divided by the number of days in each month. There was no need to remove any well due to their rate data. The only issue was the data spike in some wells (Figure 3.4 – left side). A similar approach of replacing the high values with an average value of other data points for each well was used to ensure consistency in the rate data (Figure 3.4 – right side). This adjustment was applied to only 17 wells.

It is important to note that the volume and rate data recorded for each well is dependent on the injection schedule, which may be intermittent in response to the produced water delivered for disposal.

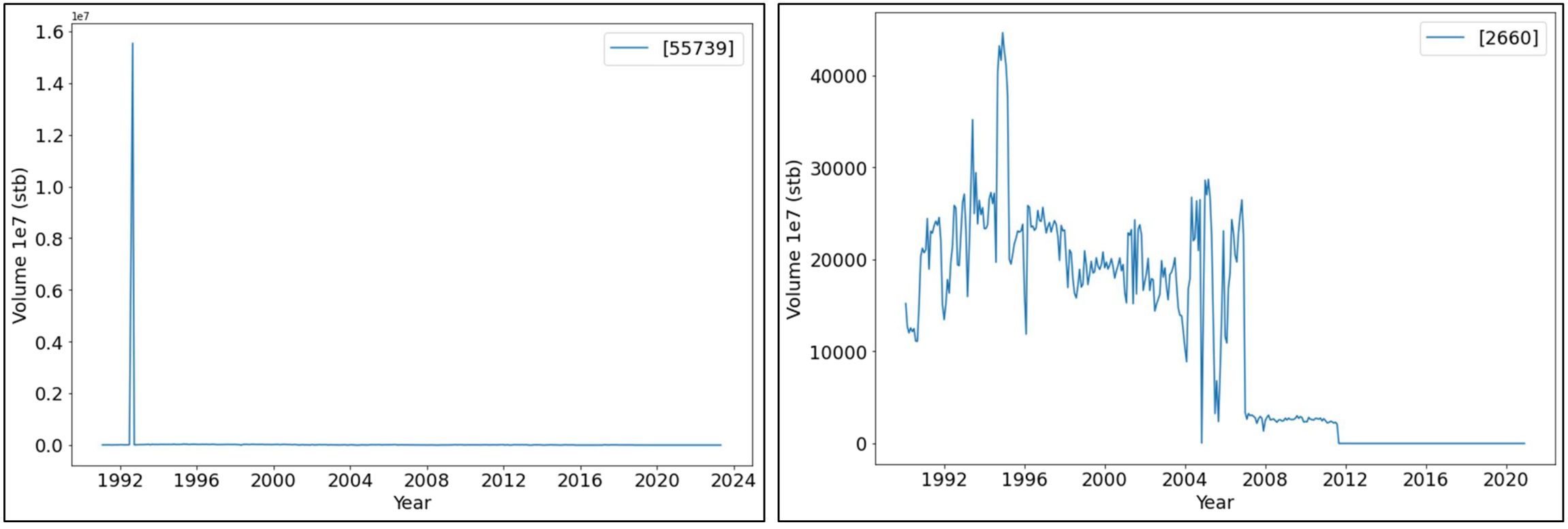

Figure 3.3 Volume (STB) versus year plot. The figure on the left shows a sample well with zero volume record, while the figure on the right shows what the volume record for a sample selected well looks like.

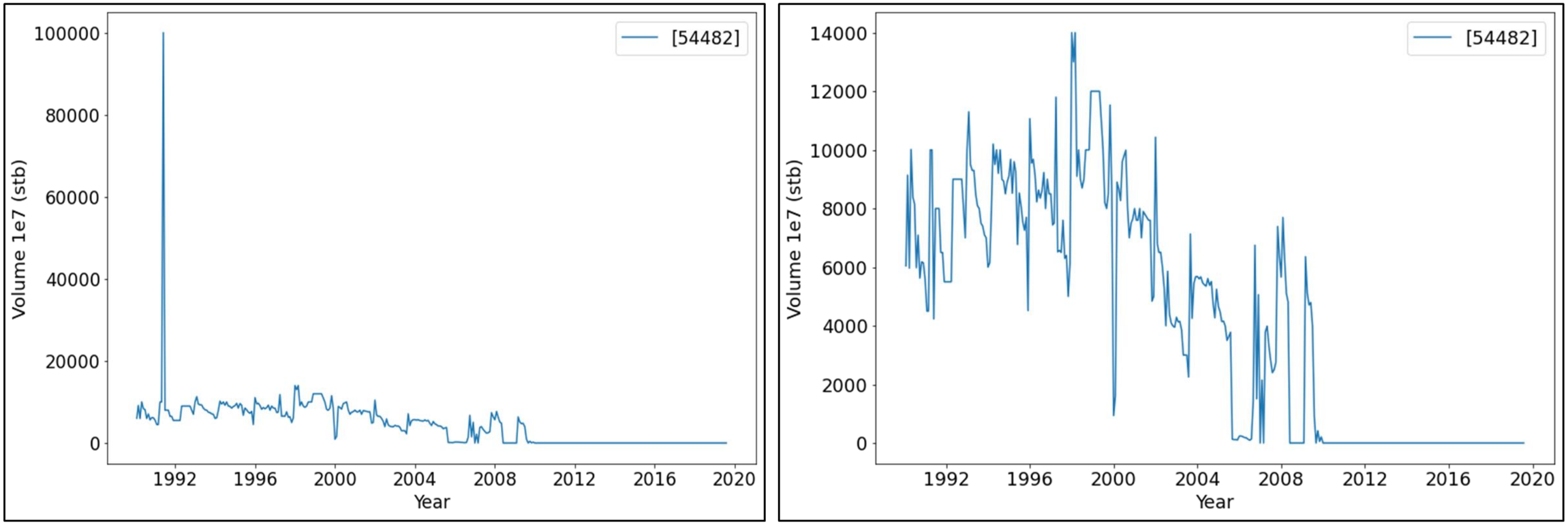

Figure 3.4 Rate (STB/day) versus year. The figure on the left shows a sample well with a spike in the rate data, while the figure on the right shows rate data for the same well, following data adjustment

To utilize the wellhead pressure data for injectivity calculations, the following steps were used to select wells with good enough pressure data:

i. Eliminate wells with 0 as their most occurring monthly rate and pressure values over the lifetime of the well.

ii. Eliminate wells with less than 12 months' worth of pressure data.

iii. Eliminate wells with negative pressure and rate correlation.

Having applied these steps, it was noticed that some wells had constant pressure data for two consecutive months with changing rates. Hence, for every well, if the pressure reported is constant across two consecutive months, the data for the most recent month is removed from the data frame. This ensures better data quality as injection pressure is expected to change with the rate. Out of the 4002 wells with injection formations, only 600 wells met the criteria provided above. Hence, these wells were used for further analysis involving pressure.

The completion data provides information on the top and bottom of perforation for every well. However, the low resolution of this data makes it difficult to use. While most of the wells have perforation intervals of 300 ft or below, which, based on field experience, is understood to be possible and has been observed for saltwater disposal wells, some wells have perforation intervals up to 6,000 ft, which is likely inaccurate. So far, these large perforations can be attributed to the wells having multiple perforations within the reported intervals or having open-hole completions. Some of these large perforation-length wells have been marked in the report to have open-hole completions, and this can lead to easily assuming that all wells with large perforation lengths have open completions. Unfortunately, this assumption is not entirely correct due to the inconsistencies in the reported data. For example, a few wells with only a few feet of perforation length were

assigned to have open-hole completions, and a few others with large perforation lengths were marked as not open holes. There are 15 wells marked to have open-hole completions, with 7 of those wells injecting into the Lower Cretaceous and 5 of them accounting for the large percentage of the volumes going into the Lower Cretaceous. 1 of the 5 wells is responsible for the significantly high, outlying injectivity index discussed later in this chapter. The Miocene, Oligocene, and Wilcox have 2 wells each marked to have open completions, while the Wilcox and Claiborne have one well each with open perforations. While there is a high possibility that the large perforation length wells have open completions, there is also another possibility of those wells having multiple perforations within the reported large intervals, making the normalized injectivity index estimated for such wells less accurate.

Hence, for the calculation of normalized injectivity index (i.e., simply the injectivity index divided by perforation length), only wells with single perforation were used to eliminate the uncertainty associated with wells with multiple completions as it is unclear how each of those intervals contributes to the general performance of the wells. However, this doesn't eliminate all the uncertainties as there are still wells (66) with single perforation lengths above 300 ft, making it unclear if those wells have multiple perforations with the reported intervals or they have open-hole completions and adding some uncertainties to the normalized injectivity index results. These uncertainties prompted the introduction of two cases in the normalized injectivity index calculations, with one of the cases including the wells with large perforations and the other not including those wells.

3.3 Volume Analysis

Following the selection of 4,805 wells with good volume data, the following plots were made to get a better understanding of how injection volume changed over time and how injection volumes are distributed across the entire Texas Gulf Coast:

i. *Volume with time:* this plot shows how injection volume across the Texas Gulf Coast changed from 1990 to 2020.

ii. *Injection Volume Map*: This map shows the distribution of wells across the Texas Gulf Coast colored by their injection volume, allowing us to identify focus areas for further analysis. These focus areas could be areas with large-volume wells, low-volume wells, or both. Wells with total injection volume greater than 20,000,000 stb are colored red, wells with total injection volume greater than 1,000,000 stb but less than 20,000,000 stb are colored blue, and wells with less than 1,000,000 stb are colored yellow.

iii. *Injection Volume versus Injection Target (Unit)*: This bar chart shows different injection intervals and the total volume they've received from 1990 to 2020. The height of each bar represents the total volume associated with the unit. Also, this plot was made using the 4002 wells with a formation assigned to them.

For the purpose of this study, I assumed a simple reservoir volume equivalence to convert saltwater volume to mass of CO_2 equivalent at reservoir conditions. Equation 3.1 was used to achieve that, assuming a CO_2 density of 700 kg/m3 and formation volume factor of 1.02 rbbl/stb for brine at reservoir conditions.

$$CO_2 mass(Gt) = V_{brine}(STB) \times B_{brine}\left(\frac{rbbL}{STB}\right) \times 5.615\left(\frac{rcf}{rbbl}\right) \times 0.0283\left(\frac{rcm}{rcf}\right) \times \rho_{co_2}\left(\frac{kg}{rcm}\right) \times 0.001\left(\frac{ton}{kg}\right) \times \frac{1}{1{,}000{,}000{,}000}\left(\frac{Gt}{\text{ton}}\right)$$

Equation 3.1

Where V_{brine} represents the volume of brine, and B_{brine} represents the formation volume factor for brine.

3.4 Rate Analysis

The rate data for each well is simply the total volume injected in any given month divided by the total number of days in the month. Hence, there is a high correlation between rate and volume. There is some uncertainty associated with the rate data, especially due to intermittency, as it is unknown how frequently wells inject fluids every month. This uncertainty could lead to an underestimation of the average monthly rate. For example, if a well injects X stb of water for only 5 days in Month A with 30 days, the average monthly rate will be reported as X/30. If more water was available for that month (Y stb), perhaps the well could have injected (X+Y)/30.

3.5 Injection Target (Formation) Assignment

Some wells have their injection target reported, while others have no injection target reported. For the wells with reported injection targets, most of the names reported are uncommon, field-specific, or obsolete. Hence, they were assigned to more common formation names in current chronostratigraphy (see Appendix A). For example, Dexter was assigned to Woodbine, and Yegua was assigned to Claiborne. Following this, some of these common formation names were merged into different injection intervals, and Table 3.2 summarizes these mergers.

Table 3.2 Formations merged into injection intervals.

Injection Interval	**Other Associated Formation**
Miocene	Fleming, Goliad, Catahoula

Oligocene	Vicksburg, Frio
Lower Cretaceous	Washita, Rodessa, Fredericksburg, Trinity,
Pleistocene	Bentley, Chicot
Austin	Clarksville
Navarro	Escondido

These wells were tagged "*wells with formation*." Some of the reported injection targets following assignment to conventional formation names were found to not exist in the Texas Gulf Coast. These injection targets include Barnett, Louann Salt, Guadalupian, Ellenberger, and Rustler. Hence, wells assigned to these injection targets were excluded from further analysis. Also, some injection target names reported for some wells were not found in the literature and could not be assigned to any conventional formation names. Such wells were tagged "*wells with unidentified formations*." Wells without any injection target reported were tagged "*wells without formation*." To assign injection targets to wells with unidentified formations and wells without formation, a machine learning (ML) model was trained using the latitude, longitude, and top-depth data from the wells with formation. Some wells that fall into these two categories could not be assigned any formation because their top depths were not reported. For wells in the categories with multiple top depth data, an average top depth is used because most times, these multiple perforations are in the same injection target. Below is the summary of the ML model.

Machine Learning Model – Random Forest Classifier

```
from sklearn.ensemble import RandomForestClassifier
from sklearn.preprocessing import LabelEncoder

Group_le = LabelEncoder()

ver_grouped_wells["Group_Encoded"] = Group_le.fit_transform(ver_grouped_wells["Group"])

features = ["TopDepthFt", "SurfaceHoleLatitude", "SurfaceHoleLongitude"]
target = ["Group_Encoded"]

X = ver_grouped_wells[features]
Y = ver_grouped_wells[target]

X_train, X_test, Y_train, Y_test = train_test_split(X, Y, test_size=0.2, random_state=42)

classifier = RandomForestClassifier(n_estimators=100, random_state=42)
classifier.fit(X_train, Y_train)

Y_pred = classifier.predict(X_test)
```

Figure 3.5 Random Forest Classifier Summary

It is important to note that different classifiers, such as KNeighborsClassifier and SupportVectorMachine were also used for this task. The RandomForestClassifer (Figure 3.5) proved to be the best for this task, with a prediction accuracy of 74.5%. While this model does not produce a perfect prediction and adds a bit of uncertainty to the results, it does a good job of assigning wells to an injection target (Figure 3.6) with wells injecting into shallower intervals such as the Miocene and Oligocene located closer to the coast following the trend that can be seen in Figure 1.5. Hence, this provides a good enough pass for further regional analysis. For specific analysis of injection trends of interest, injection targets for wells in those trends are reconfirmed using well logs.

Out of the 8,348 wells in the Texas Gulf Coast, Table 3.3 summarizes how these wells were assigned their formations. The 722 wells include only wells without multiple injection targets reported for them as the volume data does not indicate where any particular volume is going, and doing this appeared to not solve all the problems of multiple perforations as even some wells with multiple perforations at different intervals have only a single formation reported.

Table 3.3 Injection formation status for wells in the Texas Gulf Coast

Type	**Count**
Wells with reported formations verified to be in the Texas Gulf Coast	722
Wells with Predicted formations	5606
Wells without reported or predicted formations	2020

Out of the 4,805 wells used for volume analysis, only 4002 wells have a formation assigned to them (either reported or predicted). These wells were used to generate Figure 3.6, which shows injection volume by injection target. The rest have no top depth reported for them. Hence, could not be assigned to any injection target.

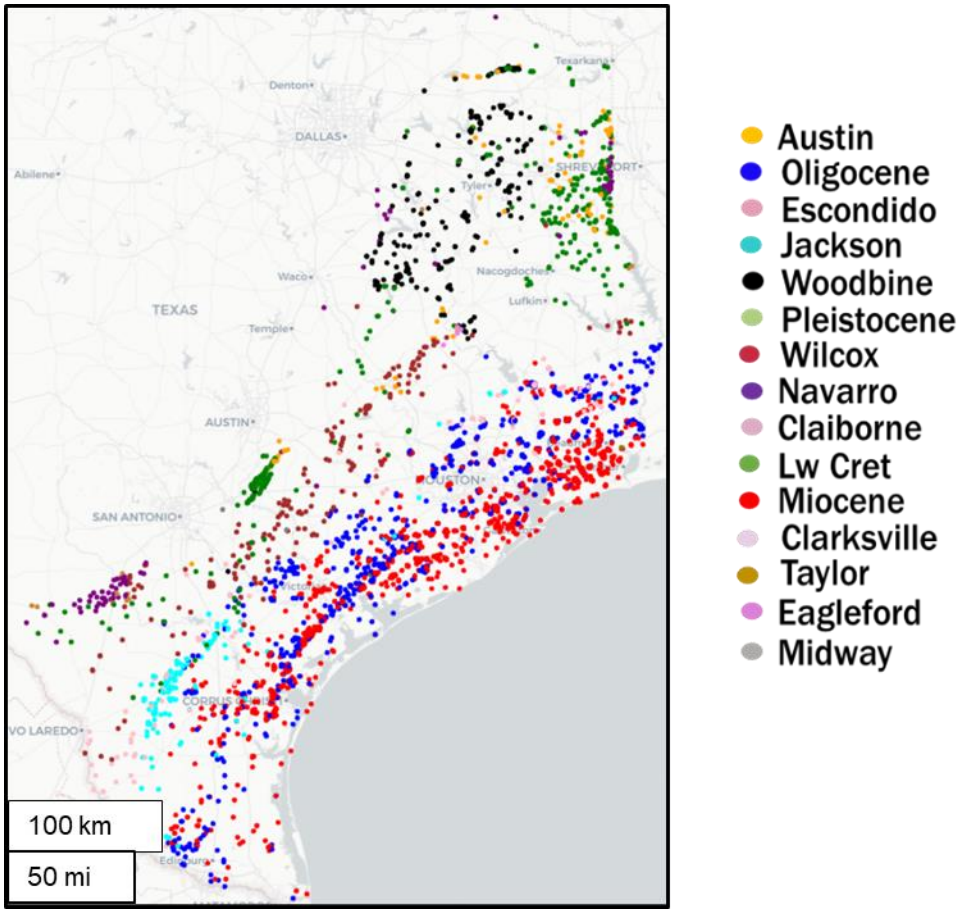

Figure 3.6 Disposal wells by injection target. Wells injecting into younger intervals, such as the Miocene and Oligocene, can be seen closer to the coastline.

3.6 Injectivity Analysis

While the volume analysis provides some insights into performance, the injectivity index provides a better indicator of a well's performance. The formula below was used to calculate the injectivity index.

$$J = \left|\frac{q}{(P_f - P_{BH})}\right| = \frac{kh}{141.2\mu B\left(\ln\frac{r_e}{r_w} - \frac{3}{4} + s\right)}$$

Equation 3.2

Where J represents the injectivity index (stb/day/psi), q represents the average injection rate (stb/day), P_{BH} represents the bottom-hole flowing pressure (psi), P_f represents the reference formation pressure (psi), k represents permeability (md), h represents thickness (ft), μ represents viscosity (cp), B represents formation volume factor, r_e represents drainage radius (ft), r_w represents wellbore radius (ft), and s represents skin. P_f is assumed to be hydrostatic, and a regional hydrostatic gradient of 0.465 psi/ft combined with the reported bottom depth of perforation for each well, was used to calculate the hydrostatic pressure of the formation each well is injecting into. Out of the 600 wells with good pressure data, only 599 wells had completion data reported. Out of these 599 wells, only 593 wells had an internal diameter of the completion material reported (i.e., values <> zero or NaN). These 593 wells were then used for injectivity analysis as flow type in these other wells could not be estimated without the internal diameter data. To calculate the injectivity index, the reported wellhead pressure had to be converted to bottomhole flowing pressure (P_{BH}) using the Darcy-Weisbach equation shown below:

$$q = 411 \cdot 147 E_{eff} D_{\mathrm{ID}}^{2.5} \left(\frac{g_c}{F_{Dw} \rho \Delta L} \left[(p_1 - p_2) + \frac{g\rho}{144 g_c} (z_1 - z_2) \right] \right)^{0.5} \quad \text{Equation 3.3}$$

Where:

q = Flow rate through tubing (STB/day)

E_{eff} = Efficiency (tuning) factor for the tubing (~1.0)

D_{ID} = Inner tubing diameter (In)

g/gc = ~1.0

F_{DW} = Darcy-Weisbach friction factor (dimensionless)

ρ = Fluid density (lb_m/ft^3)

ΔL = tubing length (ft)

p1, p2 = pressures at two points in a section of tubing (psi)

z1, z2 = Elevations at two points in a tubing section (ft)

411.147 = Equation constant

144 = Unit conversion (In^2/ft^2)

To determine the Darcy-Weisbach friction factor, the type of flow along the pipe had to be determined, and this was achieved using the Reynolds equation shown below:

$$N_{RE} = \frac{1.4775q}{\mu D_{\mathrm{ID}}} \qquad \text{Equation 3.4}$$

Where q is the flow rate, D_{ID} is the inner tubing diameter (in), and μ is the dynamic viscosity (cp). The Reynolds number is the ratio of inertial forces to viscous forces. The inertia forces represent flow velocity and geometry, and for this analysis, the dynamic viscosity is approximated to 1cp.

Having computed the Reynolds number, the following equations were used to estimate the dimensionless frictional factor:

For Re < 2000 (laminar flow):

$$f = 64/\mathrm{Re}$$

For Re 2000 < Re < 4000 (transition flow):

$f = 0.045$ (Estimated using the Moddy Diagram (Figure 3.7), assuming a relative roughness of 0.001)

For Re > 4000 (turbulent flow):

$$f = \frac{0.25}{\left[\log\left(\frac{\varepsilon/D}{3 \cdot 7} + \frac{5.74}{\mathrm{Re}^{0.9}}\right)\right]^2}$$

Equation 3.5

(Swamee-Jain Equation, assuming a relative roughness to be 0.001)

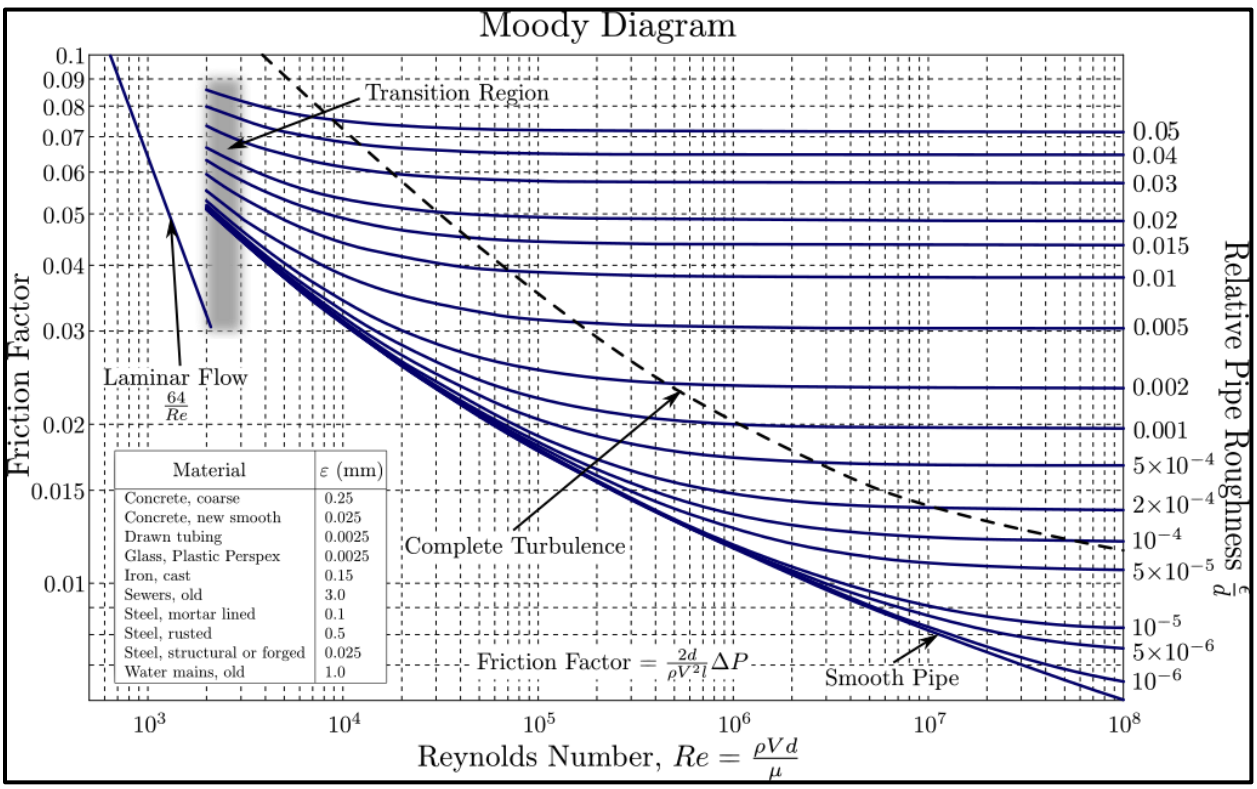

Figure 3.7 The Moody Diagram (Wikipedia)

For the injectivity index analysis, the raw injectivity index results obtained for saltwater injection are first summarized in stock tank barrels per year per psi before they are translated into CO_2 equivalents in megatons per year per 1000 psi of allowable pressure differential. The Injectivity

index is also considered on an injection interval-by-injection interval basis in this study, with only the top five wells based on volume considered. These intervals include the Miocene, Oligocene, Woodbine, Lower Cretaceous, and Wilcox.

Having estimated the injectivity index for each of the 593 wells, one could argue that wells with higher injectivity indexes could be wells with higher perforation intervals and higher injection rates, leading to further scrutiny to better represent the ability of different formations to accept fluids by calculating the normalized injectivity index and eliminating the impact of completions. The normalized injectivity index is simply the ratio of the injectivity index to the perforation interval for each well. This parameter eliminates, to a large extent, the impact of perforation intervals. However, as pointed out earlier, the uncertainties associated with the normalized injectivity index calculation due to the low resolution of the completion data provided for some wells led to the normalized injectivity index computed for only wells with single perforation, with multiple cases developed depending on perforation length. The normalized injectivity index is measured in stb/day/psi/ft and is given by the equation below:

$$\frac{J}{h} = \left|\frac{q}{(P_f - P_{BH})}\right| = \frac{k}{141.2\mu B\left(\ln\frac{r_e}{r_w} - \frac{3}{4} + s\right)} \qquad \text{Equation 3.6}$$

Multiple scenarios are developed when computing normalized injectivity indexes using the injectivity index results translated for CO_2. First, only wells with single perforations less than 300 ft and injecting below 800 m are considered. The 300 ft cutoff is used because this is believed to be the maximum perforation length that has been observed in the field for saltwater disposal wells. The second scenario involves including 39 single perforation wells with perforation lengths greater than 300 ft and also injecting below 800 m, understanding the uncertainty associated with the large

perforation lengths. The normalized injectivity index is also considered on an injection interval-by-interval basis in this study, with only the top five wells based on volume considered. These intervals include the Miocene, Oligocene, Woodbine, Lower Cretaceous, and Wilcox.

To understand what the injectivity results mean for CCS, the results obtained for single-phase (brine) flow were converted to two-phase (brine-CO_2) flow by considering viscosity and relative permeability. Only single-perforation wells injecting below 800 m (169 wells), the depth at which CO_2 is supercritical, were considered here. Only wells with single perforation were considered for this case because it eliminates the uncertainty that arises with averaging the top depth data for wells with multiple perforation intervals, as some of the intervals might be above 800 m, and it is not clear how each interval contributes to the general performance of such wells. For a single-phase system that involves the injection of brine into a system that already has brine in it, the equation below can be used to represent the injectivity index of the system.

$$II_{brine} = \frac{kh}{141.2\mu_{brine}B_{brine}\left(\ln\frac{r_e}{r_w} - \frac{3}{4} + s\right)}$$

Equation 3.7

For a two-phase system that involves the injection of CO_2 into a system that already has brine in it, the equation below can be used to represent the injectivity index of the system, leveraging a similar logic in Hosseini and Nicot (2012).

$$II_{co_2} = \frac{kk_{rco_2}h}{141.2\mu_{co_2}B_{co_2}\left(\ln\frac{r_e}{r_w} - \frac{3}{4} + s\right)}$$

Equation 3.8

The combination of equations 3.7 and 3.8 results in equation 3.9 below, which was used to calculate the injectivity index of a two-phase system where CO_2 is being injected into a brine-saturated system.

$$II_{co_2} = II_{brine}\left(\frac{k_{rco_2}\mu_{brine}B_{brine}}{\mu_{co_2}B_{co_2}}\right)$$

Equation 3.9

To estimate the relative permeability of sandstones and carbonates, I referred to Burnside and Naylor (2014) with published experimental values for the relative permeability of sandstones and carbonates to CO_2. For all the formations considered in this study except the Lower Cretaceous and Austin, which are both carbonates, I used the measurements of Berea sandstone from Krevor et al. (2012) with an average porosity of 22.1% and permeability of 914 md. At maximum CO_2 saturation of 0.55, the end-point relative permeability of CO_2 is 0.38. For carbonates of the Lower Cretaceous and Austin Chalk, I used the measurements of the Nisku Formation, from Bennion and Bachu (2010) with an average porosity of 10.9% and a permeability of 74.4 md. At a maximum CO_2 saturation of 0.603, the end-point relative permeability of CO_2 is 0.1078. The ratio of CO_2 to brine viscosity is approximated to be 0.12 (Figure 3.8), assuming the average injection depth is less than 2 km (Tsar et al., 2013).

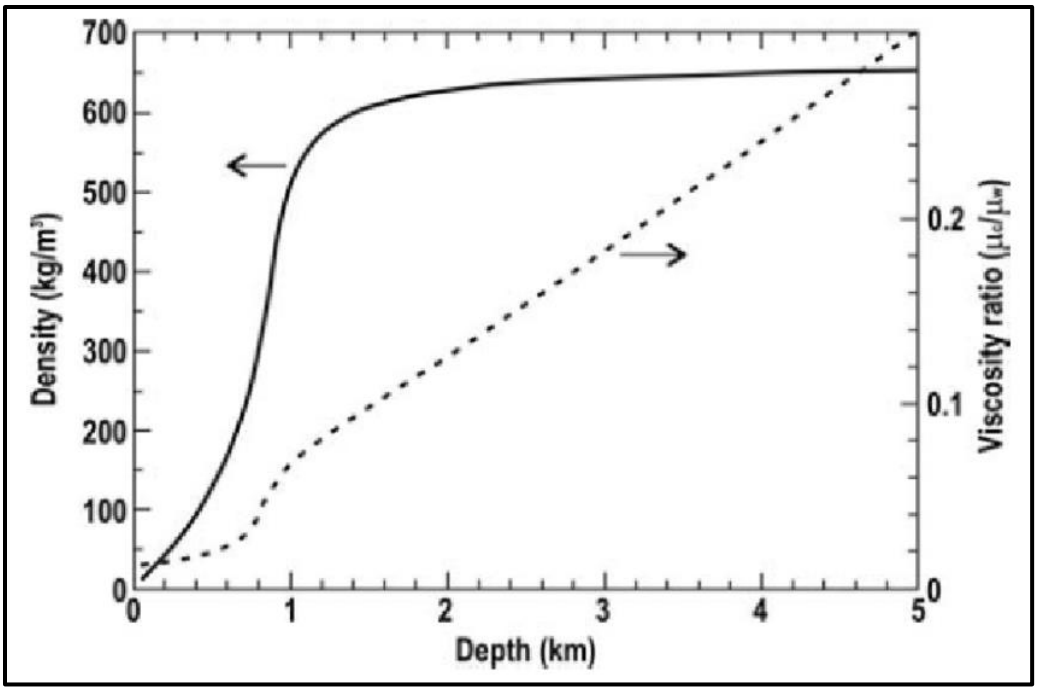

Figure 3.8 CO_2*-Brine Density and Viscosity ratio (Tsar et al., 2013)*

One of the wells (API 4218730407) was removed from the injectivity analysis due to its very high injectivity index value, to remove the outlier effect from the injectivity analysis, leaving only 592 wells for further analysis. Based on observation and having probed this well, there seems to be nothing abnormal with this well, so it is logical to consider it separately. The well is connected to the Edwards formation, had significantly higher rates reported for it, and its completion type was reported as open-hole completion.

3.7 Petrophysical Analysis

This is done for the local assessment of specific well clusters of interest. The goals here are to understand how performance varies locally within an injection target or even within a specific injection interval and the factors influencing this variability in performance across wells injecting in the same unit. A well cross-section is created using the available gamma-ray or normalized spontaneous potential logs of wells in these clusters of interest or nearby wells. For a particular

well cluster of interest, the target formation is determined using the perforation data to gain insights into geological changes across wells. Following the identification of the target formation, the average thickness of the formation is estimated, and the average porosity of the formation is estimated using the density porosity or neutron porosity logs (if available). For clusters without any nearby well with density or neutron log, the porosity is determined from the literature.

3.8 Geological Characterization

To better understand the specific areas of interest, it was critical to identify the location of structures such as Faults. It was also important to understand if the Edwards well cluster falls below the 10,000 mg/l line (bad water line), the depth with high salinity, below which CCS projects are not prohibited by law. Ewing et al. (1990) Tectonic map of Texas was used to identify fault locations and extract depth and surface elevation data. For the Edwards Group in the Luling field, Schultz (1993) provided the bad-water line data, and Phelps et al. (2014) provided some information on facies.

3.9 Software

3.9.1 Enhanced Analytical Simulation Tool (EASiTool)

The EASiTool is an in-house simulation model at the Gulf Coast Carbon Center. There are two versions available. The version used in this study is the brine version, which models saltwater disposal into saline aquifers. The brine version is only available internally. For both versions, the model assumes the formation to be homogenous, isotropic, Isothermal, and horizontal with constant thickness (Hosseini et al., 2018). Fluid injection is done through fully penetrating vertical wells at a constant rate (Hosseini et al., 2018). This analytical model predicts the impact of pressure on fluid (CO_2 or brine) injectivity and storage capacity of reservoirs (Ganjdanesh and Hosseini, 2017). Different equations are used to estimate the normalized bottomhole pressure of a reference

well injecting in a reservoir with either an open boundary condition (assumes basin to be infinite) or a closed boundary condition (refer to Hosseini et al., 2018 for more details on these equations and how pressure buildup is distributed in a multi-well scenario).

EasiTool requires input for multiple parameters, and some of these parameters were estimated using the following methods:

a. Compressibility

Compressibility refers to the measure of the change in volume resulting from the external pressure applied to the surface of an object (Fanchi, 2002). It is usually expressed in 1/psi. To estimate the rock compressibility for our EasiTool simulation, we refer to the following correlations below:

For limestones with porosities ranging from 0.02 to 0.33, Newman (1973) as shown in Tiab and Donaldson (2012),

$$C_f = \frac{0.8535}{1 + 2.367 \times 10^6 \phi^{0.93023}}$$

Equation 3.10

For unconsolidated sandstones with porosities greater than 0.25 (Ganat et al., 2024)

$$C_f = (-65.462\phi + 31.194)10^{-6}$$

Equation 3.11

b. Pressure

To estimate the average reservoir pressure, the bottom depth for each well is multiplied by a regional pressure gradient of 0.465 psi/ft, and the average of these values resulted in the average reservoir pressure.

c. Temperature

To estimate the average reservoir temperature, the bottom depth reported for each well in feet was multiplied by a regional temperature gradient of 0.00762, and the resulting values were added to the atmospheric temperature of 20 degrees Celsius.

d. Salinity

Assuming a salinity of 10,000 mg/l and solute to be NaCl, Equation 3.12 was used to convert salinity to mol/kg

$$Salinity(\frac{mol}{kg}) = \frac{10{,}000\ mg/L}{1000\ mg/g\ \times\ 58.44\ g/Mol\ \times 1.025\ kg/L} \qquad \text{Equation 3.12}$$

3.9.1.1 Calibrated Forward Modeling with EasiTool

For each formation involved, this involves simulating a base case that uses a combination of the average formation properties either calculated from the well logs or pulled from literature for the field and the reported values for other parameters and tuning the necessary parameters to match the bottomhole pressure calculated by the simulator to the reported bottomhole pressure if the calculated bottomhole pressure is above the reported bottomhole pressure.

For the Edwards injection trend, three different cases were simulated. These include Base Case, Case B, and Case C. The Base Case sets the boundary condition to closed, Case B sets the boundary condition to open and is subdivided into two to reflect the uncertainty in formation thickness, and Case C maintains the boundary conditions as open and tunes the permeability parameter for the two subcases. For all cases, average reservoir porosity remains the same at 0.28 and was estimated using the DPHI and NPHI log. This porosity value coincidentally matches the value provided for the field by Galloway et al. (1983). The permeability of 200 md used in the

Base Case, Case B_1, and Case C_1 is the average permeability of Edwards in the Luling field and was obtained from Galloway et al. (1983). Simulation time refers to the maximum injection time in the trend. The average thickness value of 55 m used in the Base Case, Case B_1, and Case C_1 is the difference between the Perf Zone 2 below Horizon 14 and the top of the formation marked by Horizon 2 (Figure 3.9). One well has no perforation below Horizon 14 and is not included in the calculation. The average thickness value of 101 m used in Case B_2 and Case C_2 is the difference between the Perf Zone 3 and the top of the formation marked by Horizon 2 (Figure 3.9). For wells with no perforations below Perf Zone 2, the bottom of the gamma-ray log is used. To run the simulation, the maximum injection pressure (bottomhole pressure) is required for each well. In the Edwards injection trend, only 8 wells have this data available as they are the wells with good pressure data. The average of the maximum injection pressure from these 8 wells is assigned to the other 20 to run the simulation. The average Injection well radius of 0.11 m used for the simulation is the average of the hole sizes reported for the 8 wells with the data available.

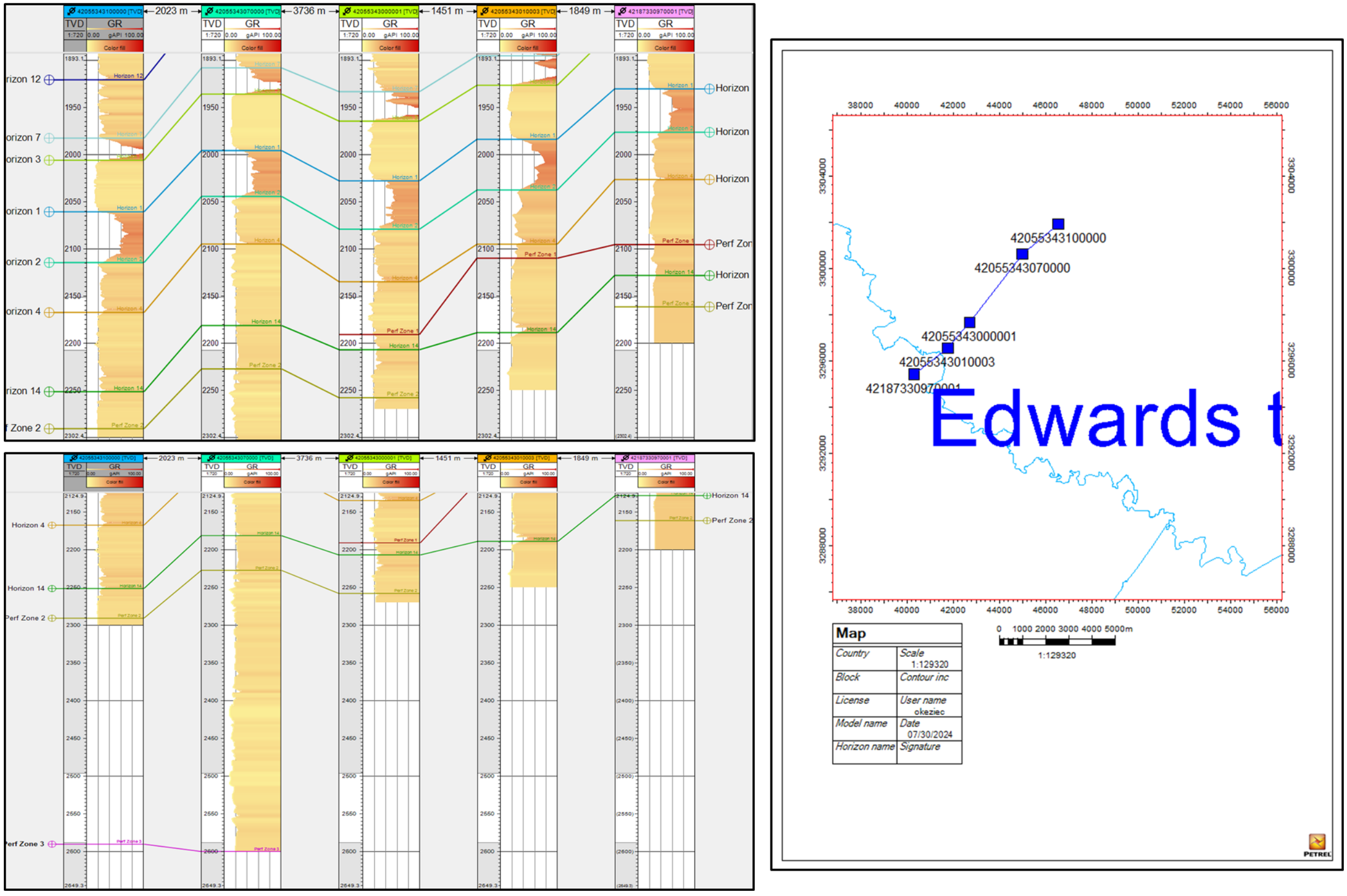

Figure 3.9 Well cross section for the Edwards injection trend (Georgetown is merged into the Edwards for this study). The cross-section was created using the gamma-ray logs for these wells. The top figure includes the shallower intervals where most of the gamma-ray logs cover. The bottom figure is a continuation and includes the deeper interval, and as observed, most of the gamma-ray logs do not cover the deeper intervals, raising some uncertainty on how deep the Edwards extend in this location. This uncertainty is accounted for during the forward modeling. The map on the right provides an overview of the direction of this cross-section (NE-SW) (Selected Horizons here were quality checked by Charlie Zheng).

For the Catahoula injection trend, three different cases were also simulated. These include Base_Case_R, Case_B_R, and Case_C_R. The Base_Case_R is simulated using a combination of approximated average reservoir properties (porosity and permeability) and reported values for the other parameters. The approximated values of 0.29 for porosity and 500 md for permeability are somewhat conservative compared to the average reported by Corpus Christi Geological Society (1968) for the Catahoula sands in the Tom O'Connor field. The Base_Case_R involves 9 wells with single or multiple perforations within the interval, and their injection pressure (bottomhole) data is available and deemed good enough. Case_B_R combines the 9 wells used in Base_Case_R with another 13 wells injecting into the same interval but without injection pressure available or deemed bad. Hence, the maximum permitted pressures for these wells were used instead. One of the 13 wells had its permitted pressure reported as zero, and this value was replaced with the average of the pressures for the other 21 wells. Another one of the 13 wells had no volume reported for the period considered and was not included in the simulation. Therefore, Case_B_R involves 21 wells. Case_C_R combines the 21 wells used in Case_B_R with another 27 wells with multiple perforations, with at least one of those perforations in the interval being considered. The assumption for Case_C_R is that most of the volume injected through these 27 wells is going into the interval being considered, hence relevant for expanded evaluation. Four of the 27 wells have their injection pressure (bottomhole) data reported. The maximum permitted injection pressure was also used for the other 23 wells introduced without their injection pressure available. Two of these 27 wells have no injection for the period considered and are excluded from the simulation. Hence, we have a total of 46 wells for Case_C_R. Another 1 of the 27 wells has no permitted injection pressure reported for it and had the average of the pressures for the other 45 wells assigned to it. For all cases here, the boundary condition is first set to closed, an average porosity

of 0.29, an average permeability of 500 md, an average thickness of 128.9 m calculated by substituting the depth of Horizon 4 from that of Horizon 3 Figure 3.10), and an approximate Basin area of 25 km x 35 km (Figure 3.11) was used. Simulation time refers to the maximum injection time in the trend. The average Injection well radius of 0.24 was used for the Base Case, 0.24 m was used for Case_B_R, and 0.23 m was used for Case_C_R. For each case, the average injection well radius represents the average hole size of all the wells used.

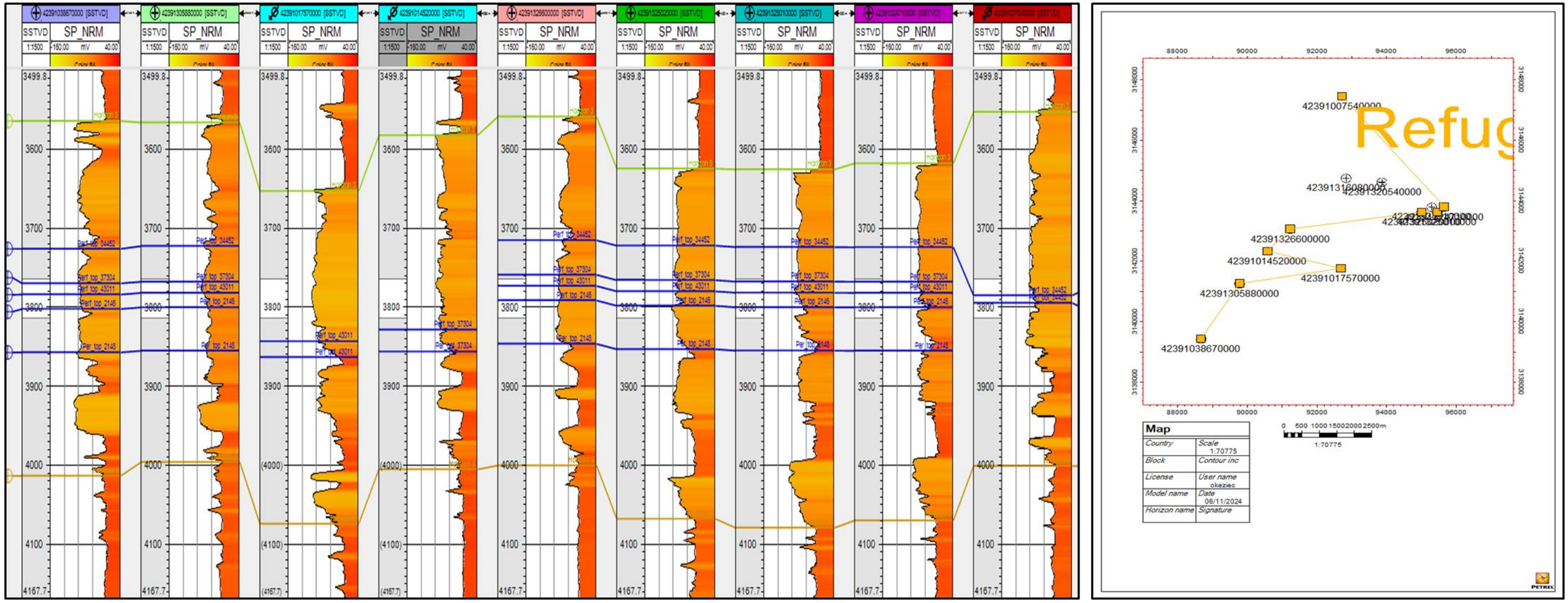

Figure 3.10 Well cross section for the Catahoula injection trend with the perforation tops and in a few cases, perforation bottom marked with blue lines. The cross-section was made using the normalized spontaneous potential logs for injection wells in the trend and other neighboring non-injection wells. It runs in the SW-NE direction, as seen in the map on the right. The wells (3) with only two blue lines showing the top and bottom of perforations are the only saltwater disposal wells in this cross-section. The interval of interest here is between Horizon 3 and 4, marked by the green and yellow lines respectively.

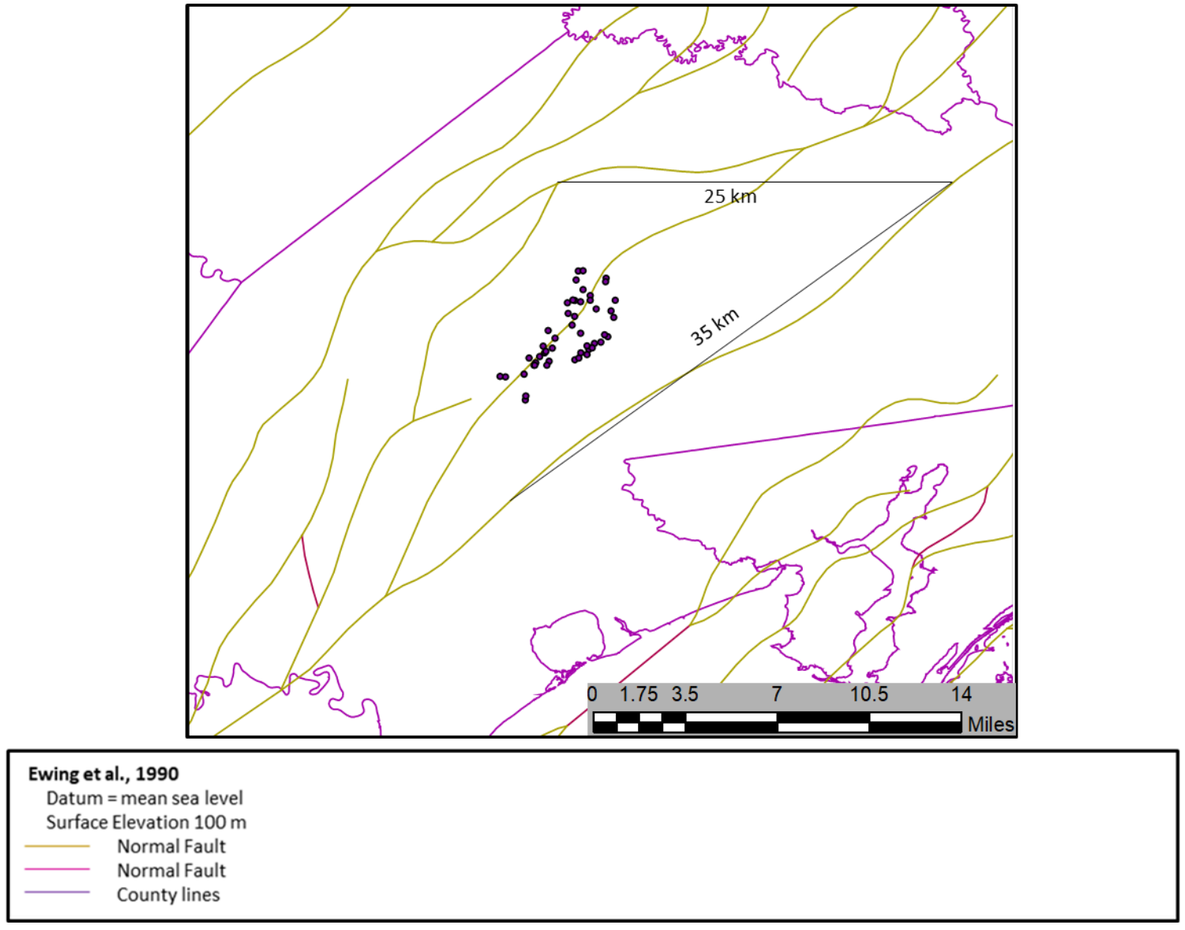

Figure 3.11 Approximate Basin Area for the Oligo-Miocene Trend. The gold lines represent faults, while the purple lines are county lines.

3.9.2 Petra

This software is provided by IHS Markit, which is part of S&P Global. It is an integrated solution for data management, manipulation, visualization, and integration of geological, geophysical, and engineering data (IHS Markit, 2021). This study leveraged Petra mainly for the management and initial assessment/quality check of well logs before they are digitized using Neuralog.

3.9.3 NeuraLog Digitizing and Quality Control

This software is provided by Neuralog and allows for semi-automated digitizing of well logs. Most of the well logs used in this study are available only in raster (.tif) format (i.e., scanned images). Hence, they had to be converted into a digital (.las) format for further analysis in Petrel.

3.9.4 Petrel E&P Software Platform

This software is provided by SLB. It provides access to features that allow for the execution of tasks such as interpreting seismic data, building geological models, creating well cross-sections, etc. For this study, Petrel was used for creating well cross-sections of wells in areas of interest and petrophysical analysis.

3.9.5 Python

This is a general-purpose programming language used in this study, mainly for data analysis, data visualization, task automation, and developing machine learning models. The following libraries and modules were used in this study:

- *NumPy*: This is a community-developed, open-source library that provides array-aware functions to operate on multi-dimensional Python arrays (Harris et al., 2020).
- *Pandas*: this is an open-source library that makes it easier to work with datasets in Python.

- *Matplotlib*: This open-source library enables the creation of high-quality plots in Python.
- *SciPy*: This is an open-source library used in Python for modeling and solving scientific problems (*Virtanen et al., 20220*).
- *Scikit-Learn*: This library integrates a wide range of state-of-the-art machine-learning algorithms for supervised and unsupervised problems (Pedregosa et al., 2012).
- *Seaborn*: This library is based on matplotlib, and it provides a high-level interface for producing beautiful graphics (Gupta, 2018).
- *Folium*: This library allows the creation of powerful leaflet maps in Python.
- *Cartopy*: This library is used in Python for creating beautiful maps that are used for data analysis.
- *Geopandas*: This library is used in Python to easily carry out operations on geospatial data.
- *PyProj*: This library provides functions used for transforming coordinates.
- *Datetime*: This module is used in Python for manipulating dates and times.
- *Statistics*: This module provides access to more advanced mathematical functions in Python.
- *OS*: This module provides functions for interacting with the operating system.
- *Math*: This module provides access to mathematical functions for performing different mathematical operations.
- *Warnings*: This module allows for the management of warnings encountered while programming.

3.9.6 ArcMap

This software is one of the two primary desktop GIS applications provided by Esri in the ArcGIS desktop suite (Esri, n.d.). It has been mainly leveraged in this study for creating, editing, and analyzing geospatial data.

4. Results – Regional Assessment

4.1 Volume

There is no clear geospatial trend of high-volume or low-volume wells in the region, making it difficult to point to where to target for optimum performance. The map below (Figure 4.1) shows the 4,805 saltwater disposal wells in the Texas Gulf Coast colored by their total injection volume.

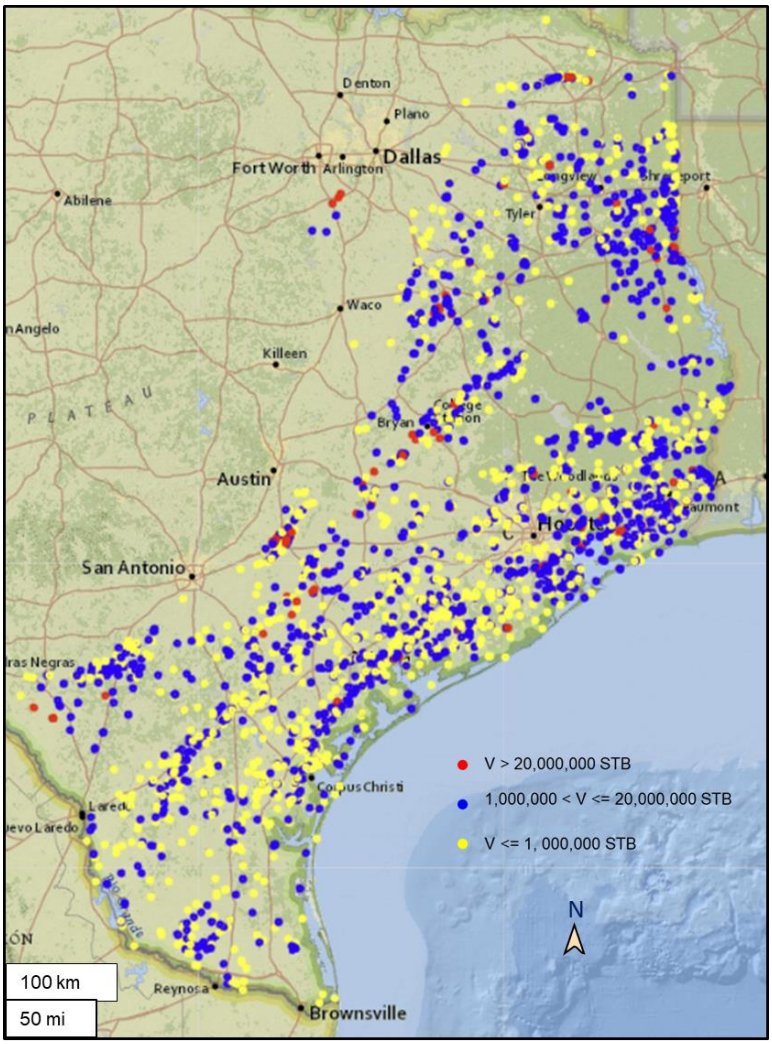

Figure 4.1: Saltwater Disposal wells in the Texas Gulf Coast, colored by their total injection volume.

The volume of saltwater injected into non-producing formations in the Texas Gulf Coast region has varied since 1990, with the volume of saltwater available for injection largely dependent on oil and gas production activities in the region. Hence, intermittency is a major issue for most of the saltwater disposal wells, as most of the wells are operating below their maximum permitted volumes. More than 75% of the over 20 billion barrels of saltwater has been injected below 800 m. That is over 15 billion barrels of saltwater.

Multiple intervals have been targeted for saltwater injection in the Texas Gulf Coast, but a majority of the injected volume has gone into 13 units (Figure 4.2). When all 4002 wells with injection targets assigned to them are considered, the Miocene, the Lower Cretaceous, Oligocene, and Woodbine account for 86.5% of the total injected volume. When only wells injecting below 800 m are considered, the Miocene, Oligocene, Woodbine, and Lower Cretaceous are still responsible for most of the total injected volume (85%). However, about half of the volume injected into the Lower Cretaceous was injected above 800 m. The Wilcox and Claiborne intervals lead the rest of the injection intervals for both scenarios.

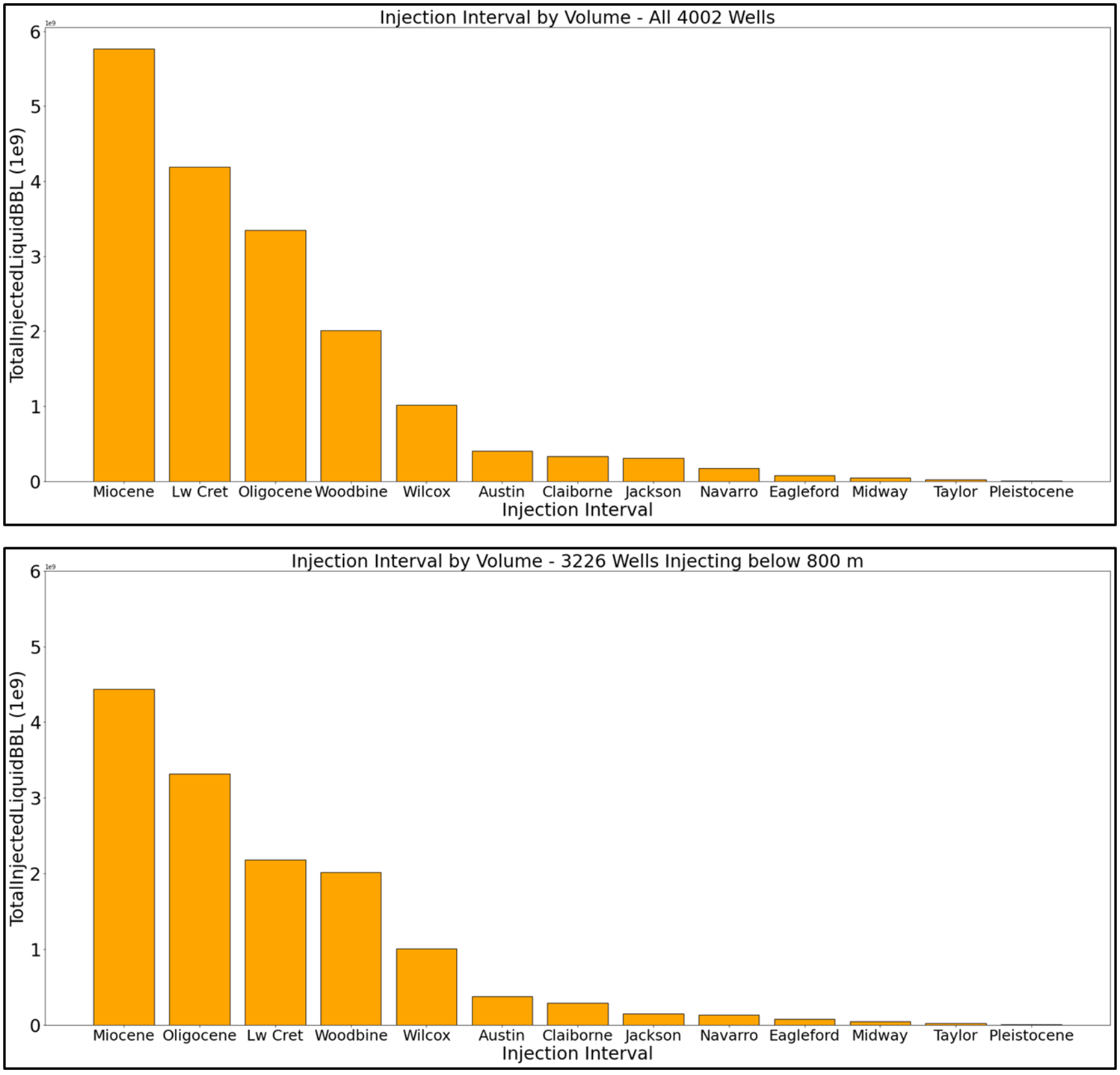

Figure 4.2 Total injected volume by injection interval. The top figure includes all 4002 wells, while the bottom figure includes only wells injecting below 800 m. The y-axis is in billion barrels (1e9).

4.2 Injectivity Index

The injectivity indexes for the 592 wells with reliable pressure data are summarized in Figure 4.3. They range from 2 STB/year/psi to over 21,000 STB/year/psi, with a P10 of 51.55 STB/year/psi, a P50 of 355.5 STB/year/psi, and a P90 of 1,892 STB/year/psi. From the figure, it can be seen that a large proportion of the wells are concentrated on the left side of the plot, and the number of wells reduces exponentially as the injectivity index increases towards the right side of the plot. This suggests that high injectivity index wells are obtainable in the Texas Gulf Coast, even though low injectivity index wells are more common. These low injectivity indexes are mostly due to intermittency, as a majority of the wells are injecting below the maximum permitted pressures and volumes. The issue of intermittency is further discussed in Section 7.4

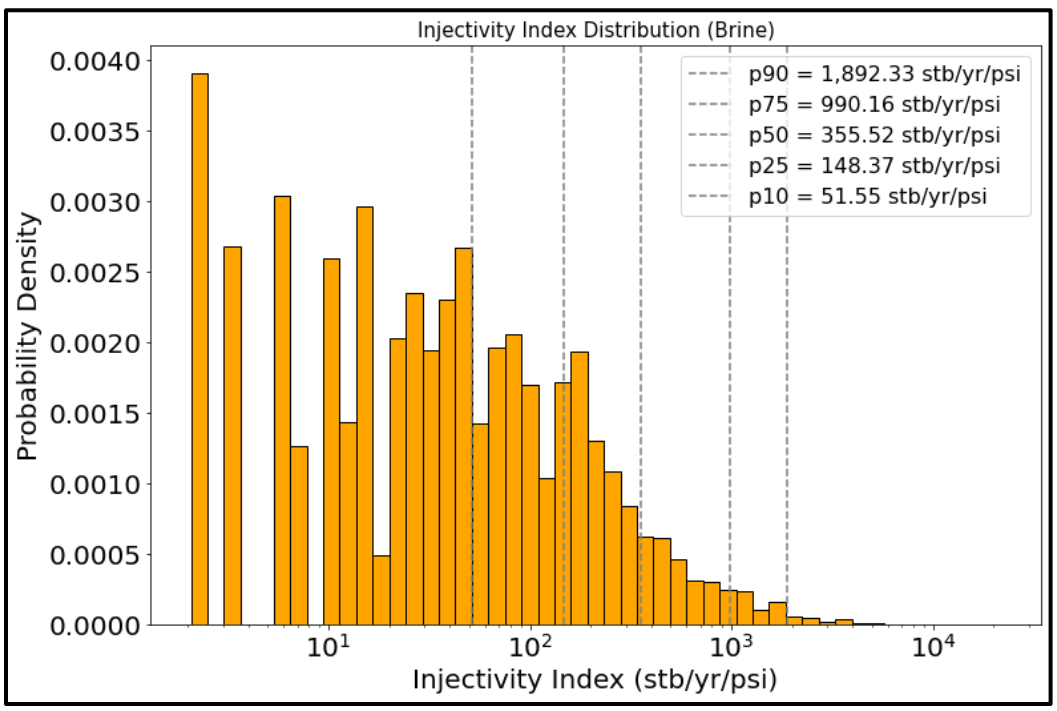

Figure 4.3 Saltwater Injectivity Index Distribution in STB/year/psi. This includes all 592 wells. The y-axis represents the probability density (i.e., relative likelihood), while the x-axis represents the apparent injectivity index value and is plotted in a logarithmic scale.

The injectivity index values obtained for saltwater are then translated into CO_2 equivalents for the 169 single-perforation wells injecting below 800m, using the methods described in this study (Figure 4.4). None of these wells actually inject CO_2. The estimated values provide only a minimum indication of performance as they follow the saltwater disposal schedule, which is prone to intermittency.

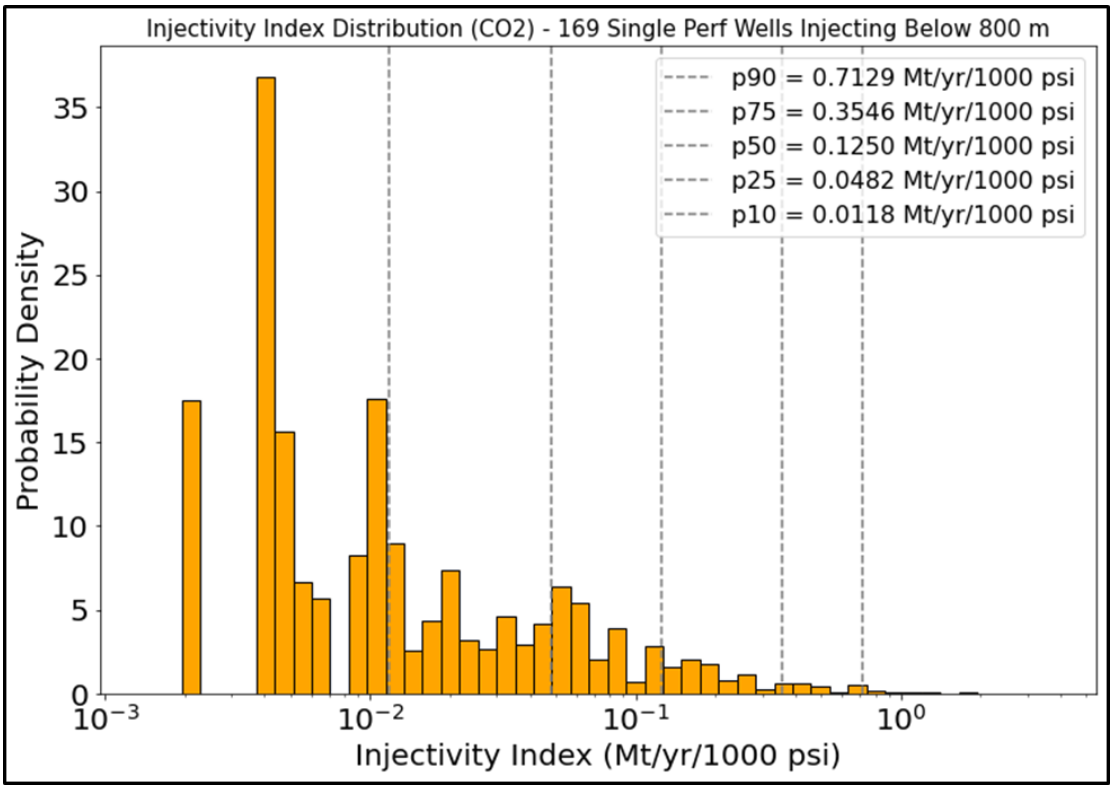

Figure 4.4 CO_2 Injectivity Index converted to megatons per year per 1000 psi. The figure shows the injectivity index distribution for 169 single perforation wells with the top of perforation below 800 m. The y-axis represents probability density (i.e., relative likelihood) while the x-axis represents the apparent injectivity index and is in logarithmic scale.

Figure 4.5 shows the Injectivity index in Mt/year/1000 psi subdivided by injection interval. The Miocene interval is observed to have on average, the highest injectivity index (i.e., the minimum injectivity index achieved by 50% percent of the wells), followed by the Woodbine,

Oligocene, Wilcox, and Lower Cretaceous intervals. The Miocene also has the highest P90 value (i.e., the minimum injectivity index achieved by the top 10% of the wells), followed by the Woodbine, Wilcox, Oligocene, and Lower Cretaceous.

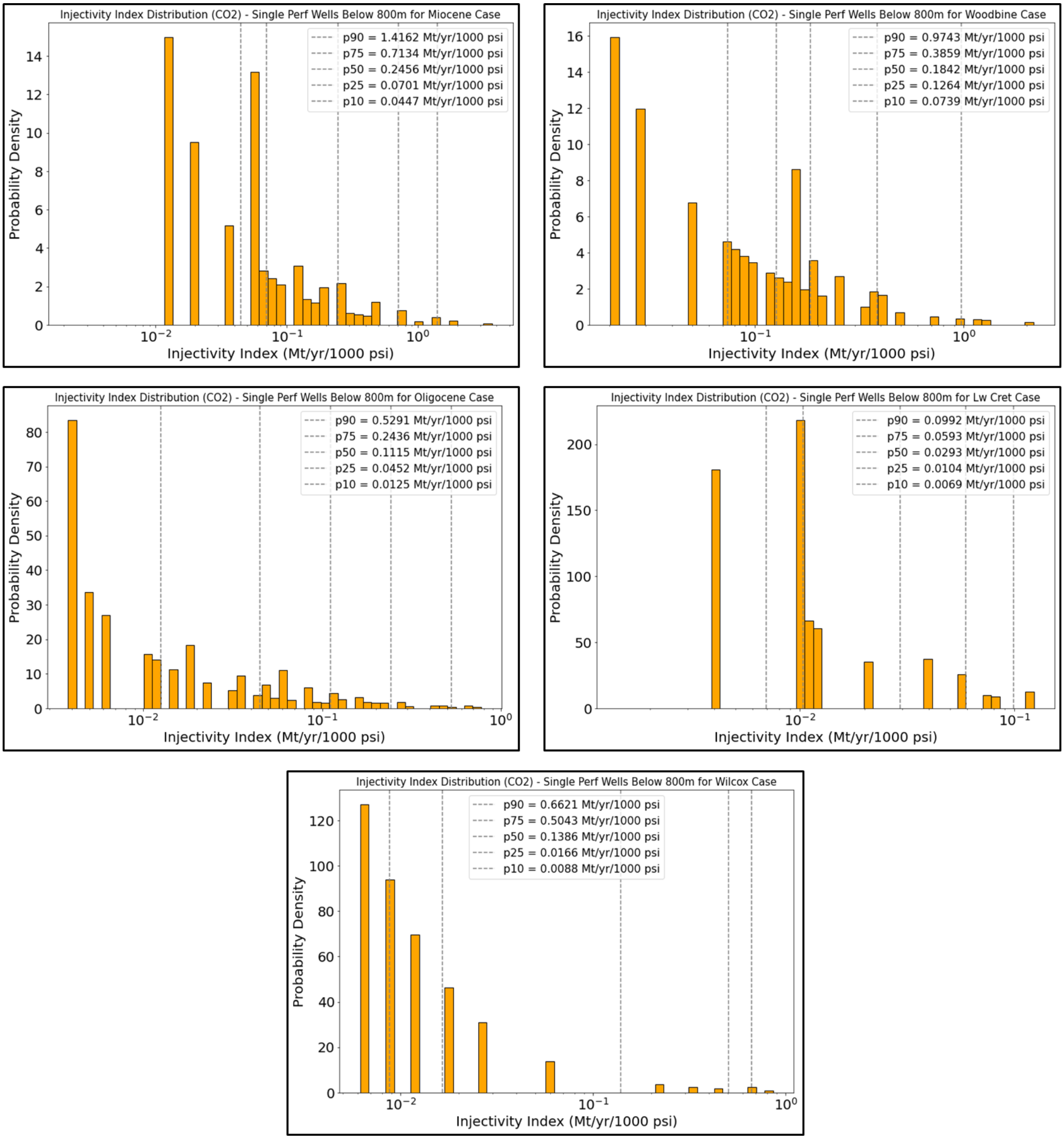

Figure 4.5 CO_2 Injectivity Index (Mt/year/1000 psi) distribution on an interval-by-interval basis. Only single perforation wells injecting below 800 m in each of these intervals are included in creating these figures.

The box and swarm plots below (Figure 4.6) summarize the performance of all the injection intervals in terms of the injectivity index.

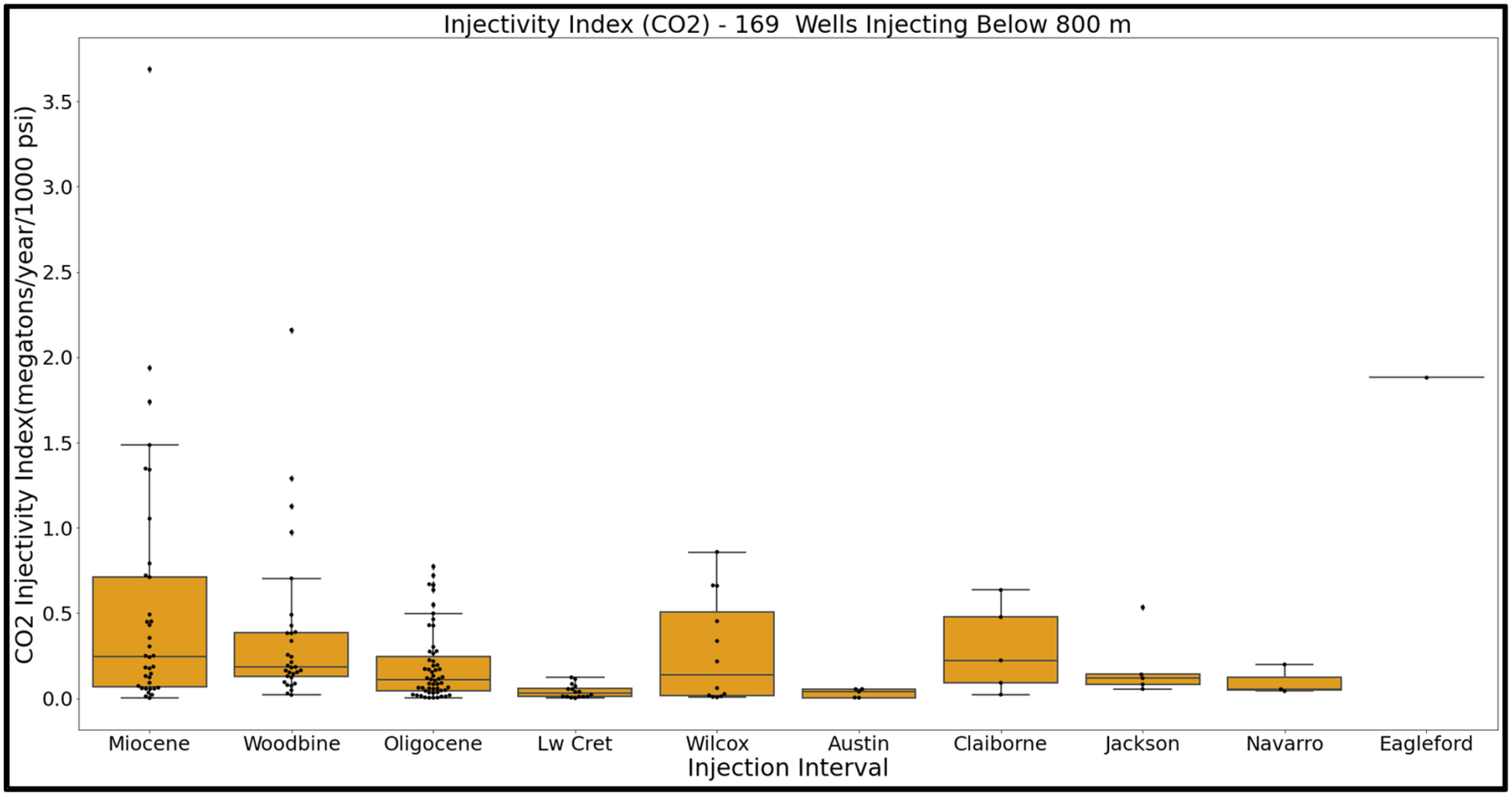

Figure 4.6 CO_2 Injectivity Index (Mt/year/1000 psi) by Injection Interval. The black dots represent the number of wells injecting into each interval. Caution should be taken when looking at these plots as injection intervals with a smaller number of wells may look as good as they are not, and this can be seen with Eagleford and Claiborne. The Miocene, Woodbine, and Oligocene intervals represent the top three when considering only intervals with at least 30 wells injecting below 800 m. The Wilcox and Jackson intervals lead the rest with less than 30 wells injecting below 800 m.

4.3 Normalized Injectivity Index

To remove the effects of different completions, the injectivity index distributions obtained for both brine and CO_2 equivalent are normalized using the reported perforation length for each well. However, uncertainties surrounding the completion data, especially for wells with large perforation lengths, mean the normalized injectivity index values estimated could be hugely underestimated. Figures 4.7 and 4.8 show the normalized injectivity index distributions for brine and CO_2 respectively.

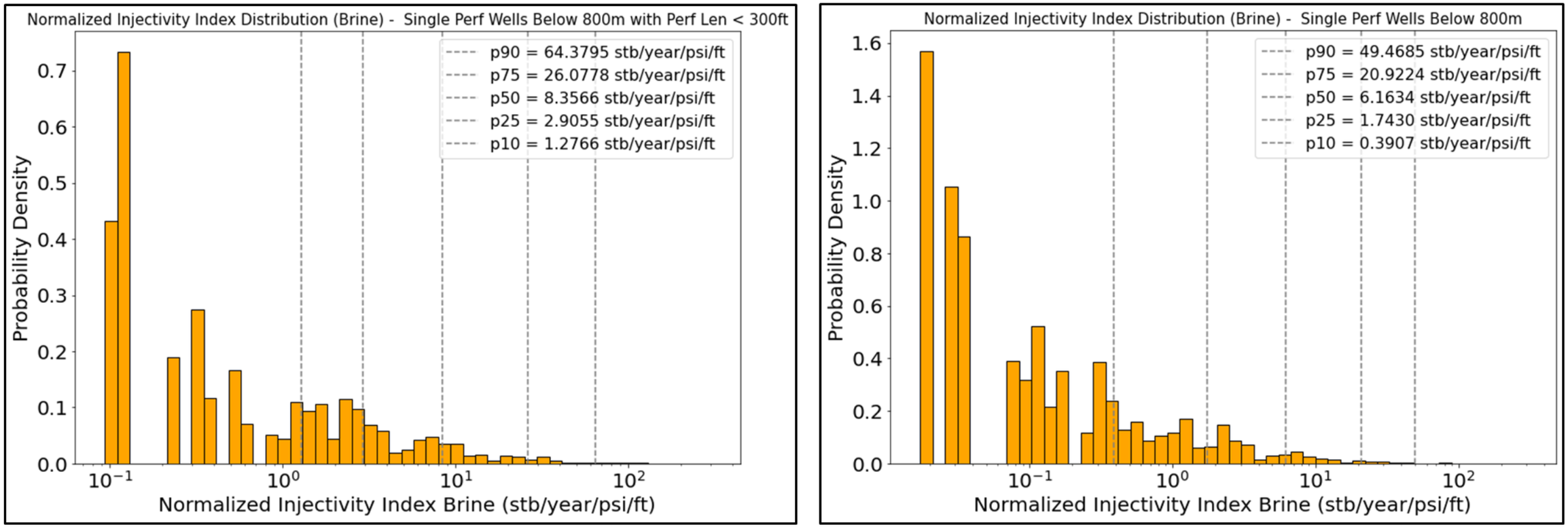

Figure 4.7 Saltwater Normalized injectivity indexes (stb/year/psi/ft) for single perforation wells divided into two. Both figures only include wells injecting below 800 m. The figure on the left includes only wells with perforation lengths less than 300 ft, while the figure on the right includes wells with perforation lengths larger than 300 ft. The y-axis represents probability density (i.e., relative likelihood), while the x-axis represents normalized injectivity index and is in logarithmic scale

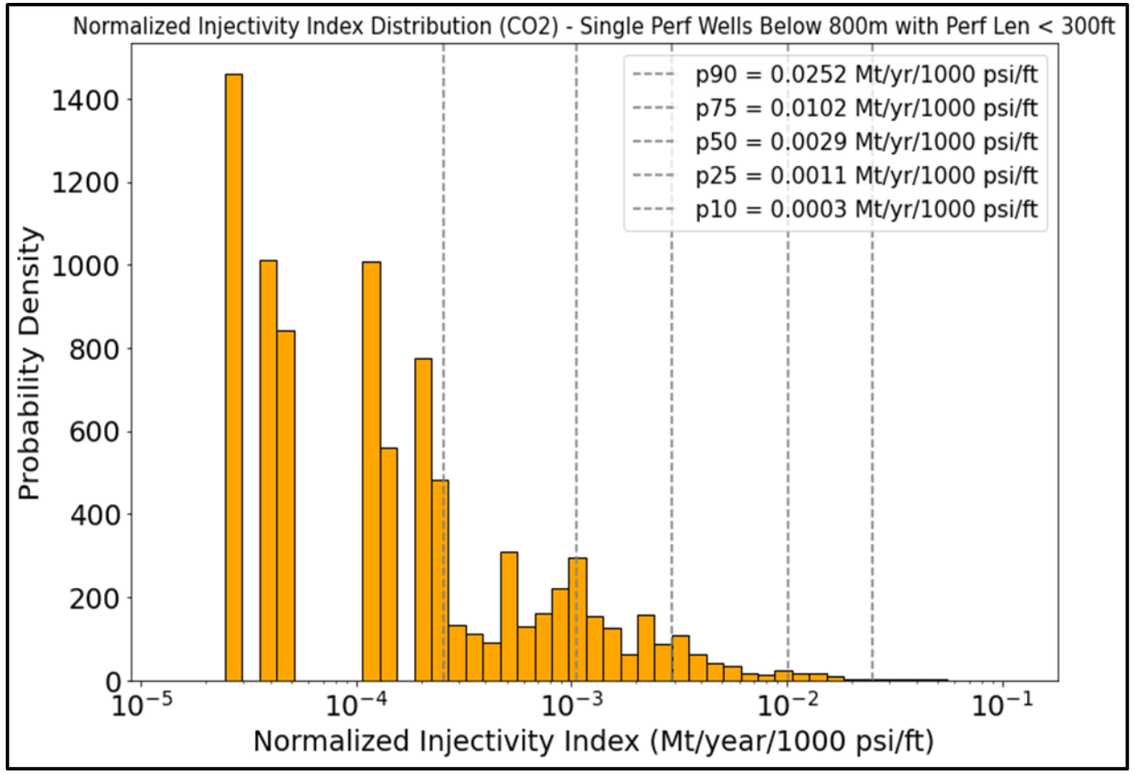

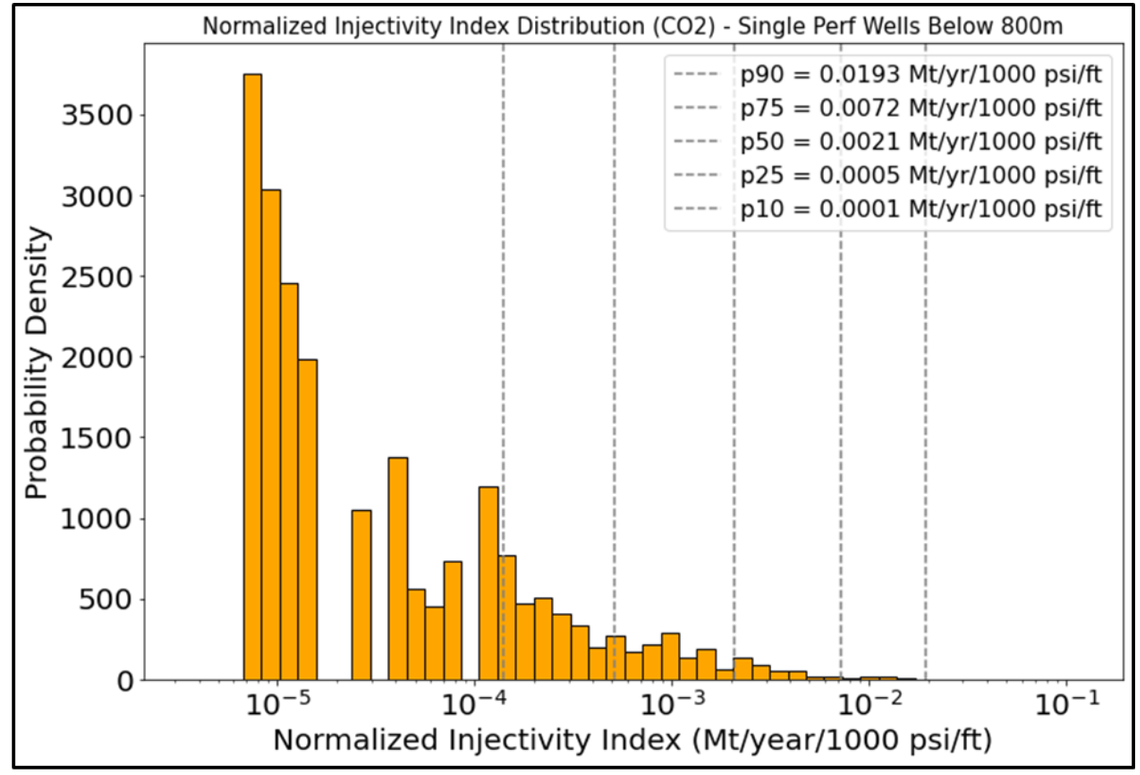

Figure 4.8 CO_2 Normalized injectivity indexes (Mt/year/1000 psi/ft) for single perforation wells divided into two. Both figures only include wells injecting below 800 m. The figure on the left includes only wells with perforation lengths less than 300 ft, while the figure on the right includes wells with perforation lengths larger than 300 ft. As expected, including the larger perforation shifts the distribution left, although in this case only slightly. The y-axis represents probability density (i.e., relative likelihood) while the x-axis represents normalized injectivity index and is in logarithmic scale.

Figure 4.9 shows the Normalized Injectivity index in Mt/year/1000 psi/ft subdivided by injection interval. The Miocene interval is also observed to have on average, the highest normalized injectivity index (i.e., the minimum normalized injectivity index achieved by 50% percent of the wells), followed by the Woodbine, Oligocene, Wilcox, and Lower Cretaceous intervals. This order is also true when the P90 is considered for all five injection intervals, suggesting the Miocene to also have the highest minimum normalized injectivity index achieved by the top 10% of its wells.

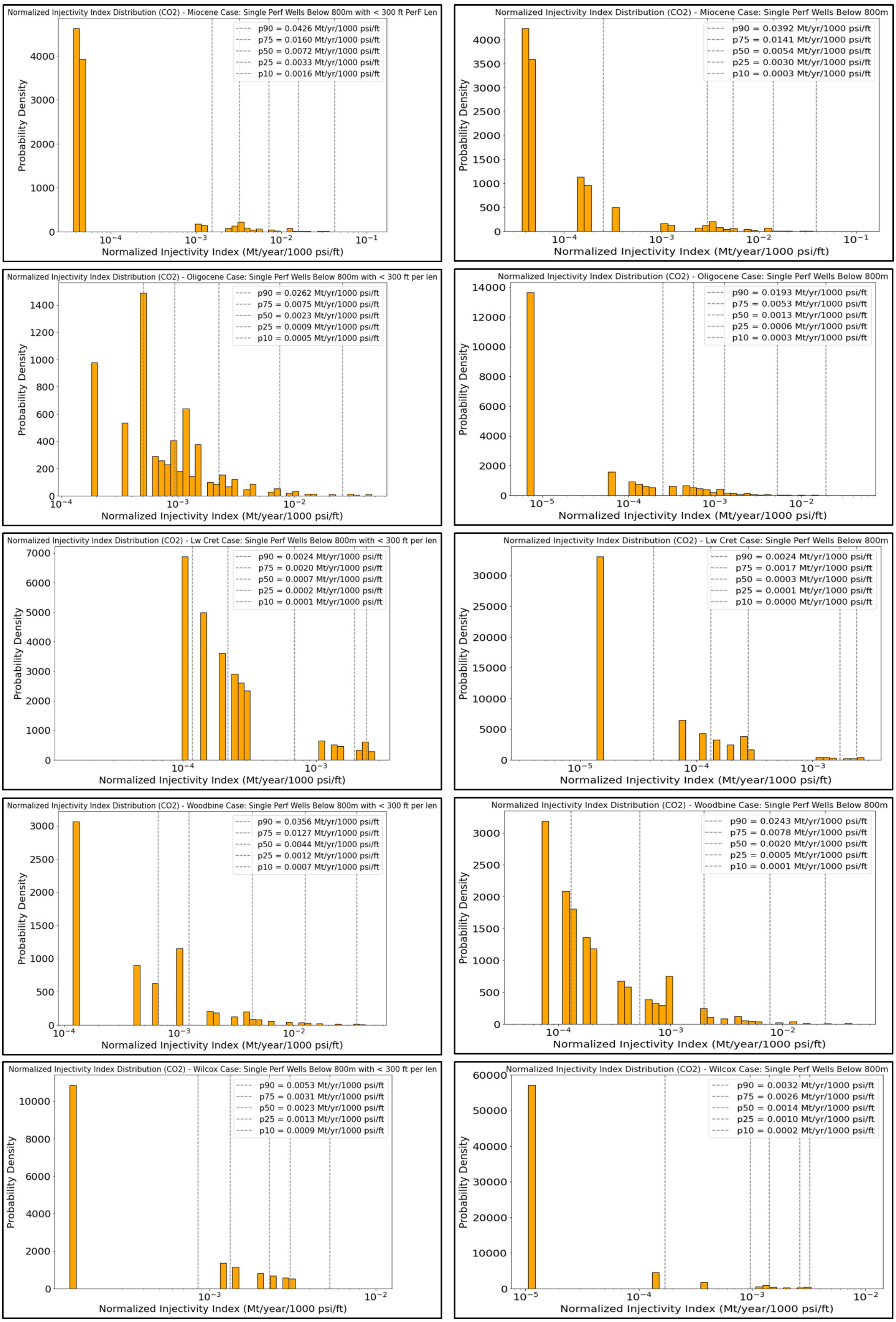

Figure 4.9 CO_2 Normalized *Injectivity Index (Mt/year/1000 psi/ft) for single perforation wells injecting below 800 m. The left column represents wells with perforation lengths less than 300 ft, while the right column includes wells. Each row represents a different injection interval.*

The box and swarm plots below (Figure 4.10) summarize the normalized injectivity index for all injection intervals.

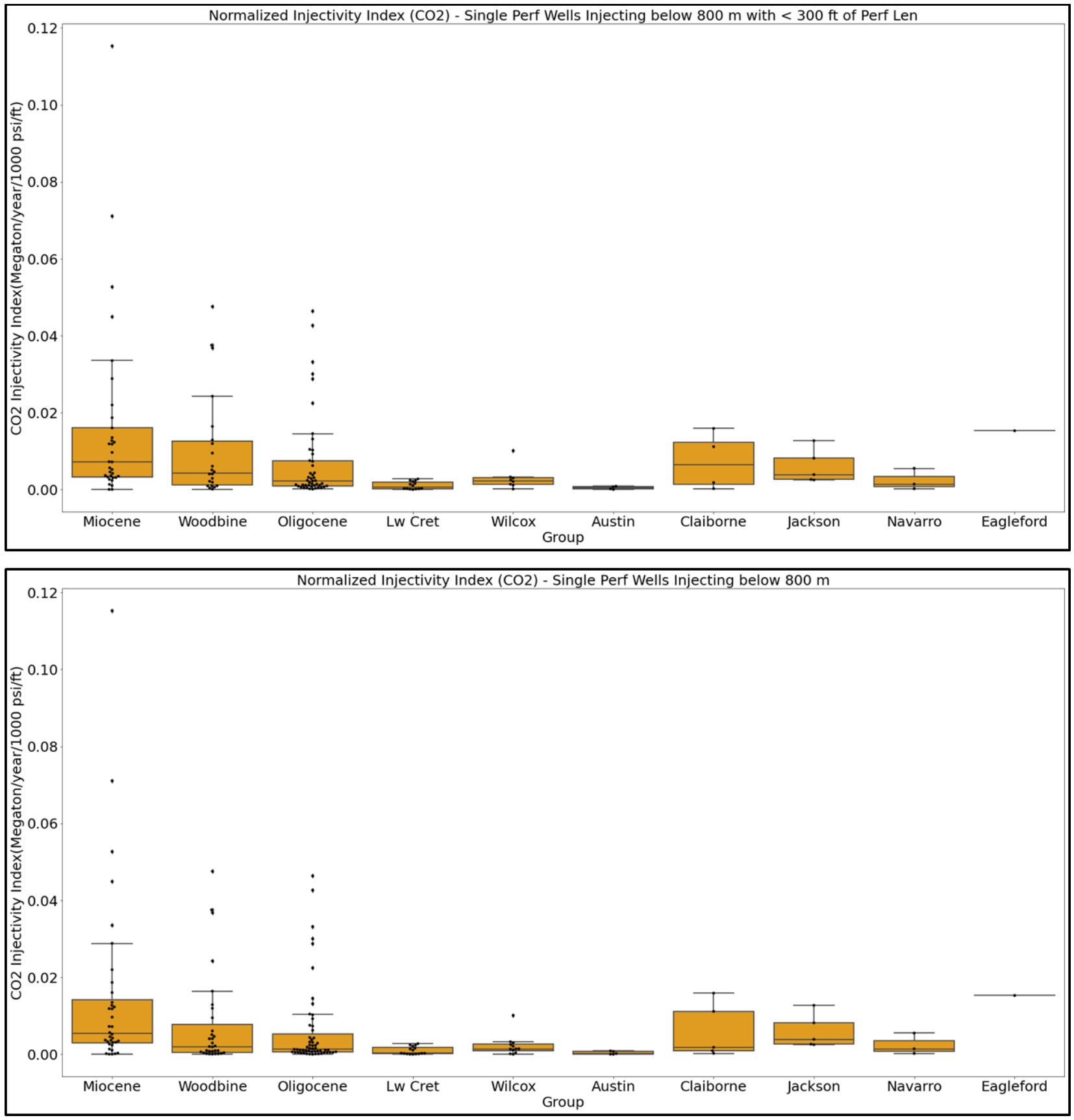

Figure 4.10 CO_2 Normalized Injectivity Index (Mt/year/1000 psi/ft) by injection interval. Both figures include wells injecting below 800 m. The top figure includes only single perforation wells with less than 300 ft of perforation length, while the bottom figures include wells with larger perforations above 300 ft. For both cases considered, Miocene, Woodbine, and Oligocene appear to be the top three injection intervals, especially when only intervals with at least 30 single perforation length wells are considered. Jackson can be observed to lead the rest of the injection intervals with less than 30 single perforation length wells.

5. Results – Case Study I: Edwards Injection Trend

5.1 Background

The Edwards injection trend (Figure 5.1) is a cluster of mostly high-volume injection wells injecting into the Edwards Group and are located near the Luling Field in Caldwell and Guadalupe counties of Texas. The high volumes associated with wells in this cluster prompted the in-depth assessment of this trend to assess the potential of the Edwards Group for storage as part of CCS projects in this area near urban and cement plant sources, which had not been documented in previous studies of storage resources. 43% of the wells in the trend have each injected a total volume of over 20 million stock tank barrels, 46% of the wells have each injected above 1 million stock tank barrels but less than or equal to 20 million stock tank barrels, and only 11% of the wells in this trend have injected less than or equal to 1 million stock tank barrels (Figure 5.1). To put this into context, a few of these wells are in the top 10. Only 4% of the 4,805 wells in the Texas Gulf Coast have volumes above 20 million stock tank barrels, and only 43% have volumes above 1 million stock tank barrels, making the Edwards trend very interesting.

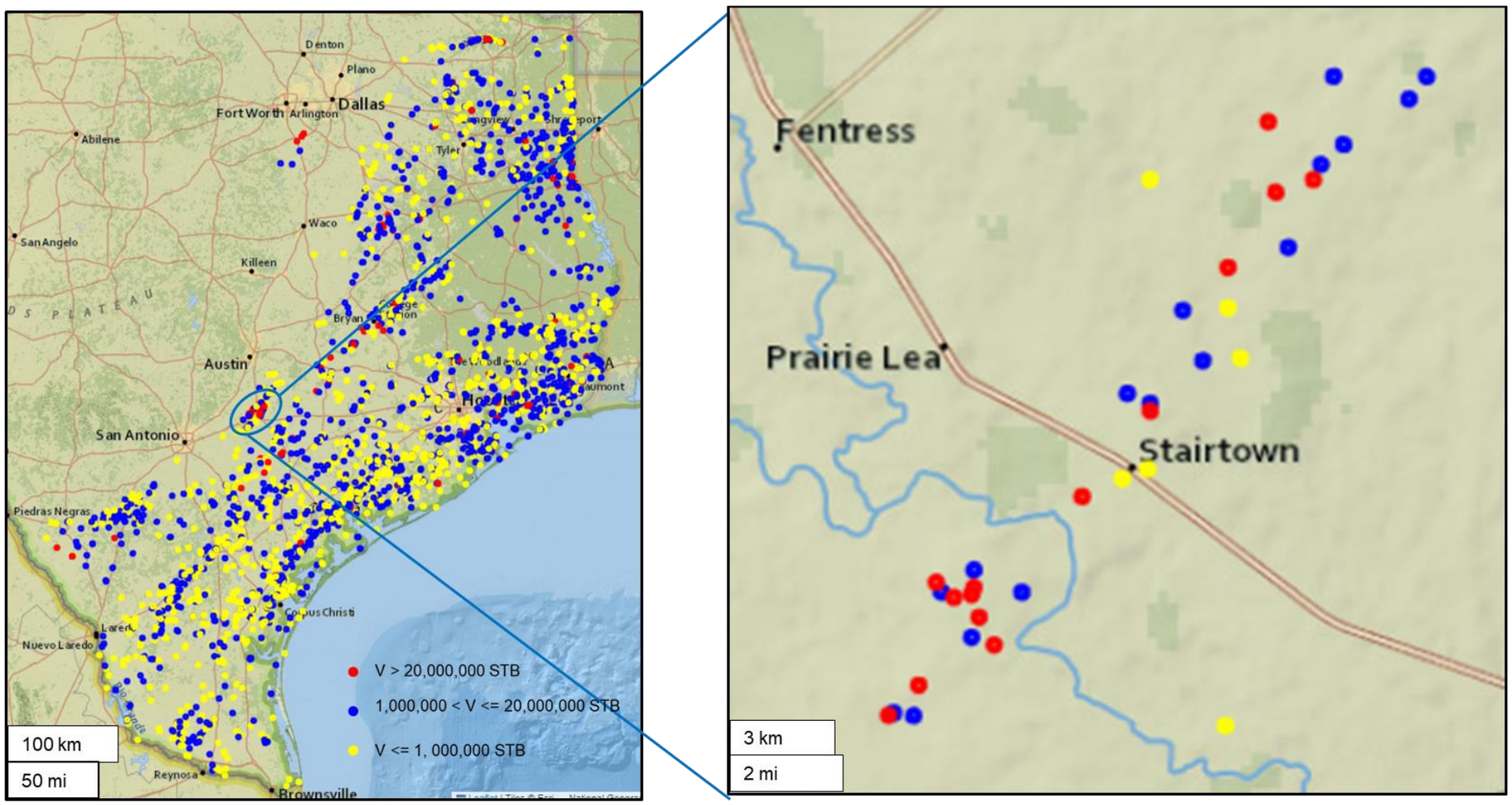

Figure 5.1 – Volume Map Highlighting the Edwards Injection Trend. The colors indicate the total volume disposed of by a well.

5.2 Calibrated Forward Modeling of the Edwards Trend Injection

The base case involved a closed boundary condition, with the boundaries defined by the nearest faults, extracted from Ewing et al. (1990). The base case produced no result as the simulation could not run due to the high volume being injected and the boundary condition being closed, and this led to the opening of the boundary conditions for the following cases. The key takeaway is that permeability had to be tuned up for the following cases to get the bottomhole pressure calculated by the model to match the maximum reported bottomhole pressure of 12.4 MPa for this trend.

Table 5.1 – Parameter values for all cases considered. Case B is divided into two subgroups with different values of thickness to account for uncertainty in thickness for this trend. For the base case, the boundary size used makes no difference in the simulation result.

Parameter	**Base Case**	**Case B_1**	**Case C_1**	**Case B_2**	**Case C_2**
Pressure (Mpa)	8.1	8.1	8.1	8.1	8.1
Temperature (C)	38.7	38.7	38.7	38.7	38.7
Thickness (m)	55	55	55	101	101
Salinity (mol/kg)	0.17	0.17	0.17	0.17	0.17
Porosity	0.28	0.28	0.28	0.28	0.28
Permeability (mD)	200	200	1320	200	690
Rock Compressibility (1/Pa)	1.71e-10	1.71e-10	1.71e-10	1.71e-10	1.71e-10
Boundary Condition	Closed	Open	Open	Open	Open
Simulation Time (months)	372	372	372	372	372
Injection Well Radius (m)	0.22	0.22	0.22	0.22	0.22

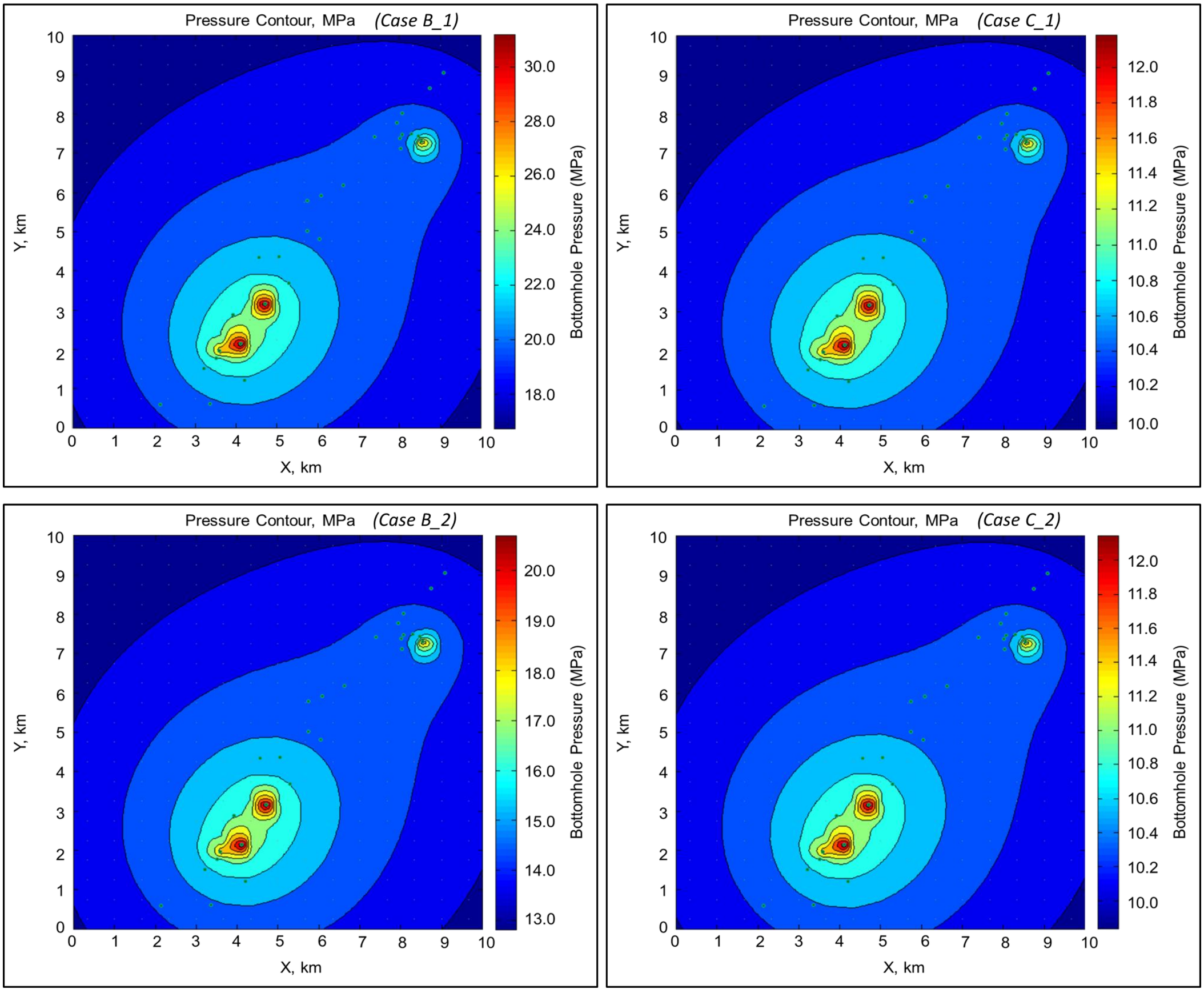

Figure 5.2 Simulation results for all the cases considered for the Edwards trend. Each box represents the results for each case considered. The color bar shows the bottomhole pressure. The x and y axes, which show dimension, are virtually irrelevant in these cases as boundary conditions were set to open. The key thing that differentiates the top row from the bottom row is their average formation thickness. The top row sets the average formation thickness to 55 m, while the bottom row sets it to 101 m. For the top row, permeability had to be tuned up to 1320 md for the maximum bottomhole pressure calculated by the model to match the maximum reported bottomhole pressure of 12.4 MPa while for the bottom row, permeability had to be tuned up to 690 mD for the maximum bottomhole pressure calculated by the model to match the maximum reported bottomhole pressure of 12.4 MPa.

6. Results – Case Study II: Catahoula Injection Trend

6.1 Background

This Catahoula injection trend (Figure 6.1) is a cluster of injection wells injecting into the Catahoula formation and are located along the Tom O'Connor field in the Refugio County of Texas. The large interest in the Miocene by many CCS projects in the region prompted the in-depth analysis to get a better understanding of the unit. The specific section being considered in this study is just above the Anahuac Shale, and it has multiple wells injecting into it. For comparison, almost all the wells considered in this cluster have injected more than 1 million stock tank barrels, also making this cluster interesting.

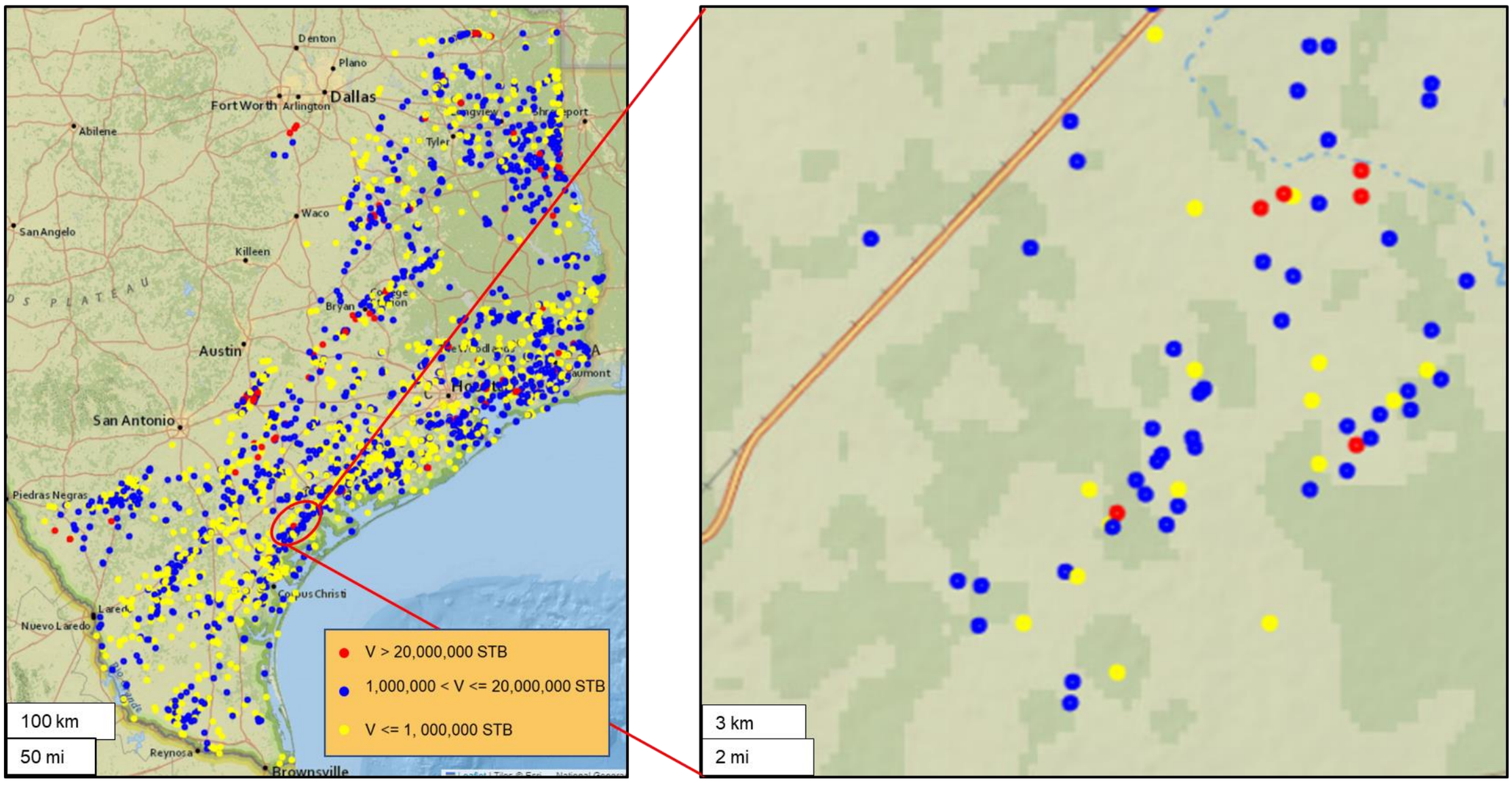

Figure 6.1 Volume Map Highlighting the Catahoula Injection Trend. The colors indicate the total volume disposed of by a well.

6.2 Calibrated Forward Modeling of the Catahoula Trend Injection

This is done to gain insights into how different factors influence injection performance in the Catahoula Formation. The key takeaway here is that moving from Base_Case_R to Case_C_R, the addition of more wells known to be injecting into the interval of interest did not get the maximum bottomhole pressure calculated by the model to match the maximum reported bottomhole pressure of 19.7 MPa.

Table 6.1 – Parameter values for all cases considered. The key difference for all the cases is the number of wells used for each case.

Parameter	**Base_Case_R**	**Case_B_R**	**Case_C_R**
Pressure (Mpa)	12.8	12.8	12.8
Temperature (C)	49.6	49.6	49.6
Thickness (m)	128.9	128.9	128.9
Salinity (mol/kg)	0.17	0.17	0.17
Porosity	0.29	0.29	0.29
Permeability (mD)	500	500	500
Rock Compressibility (1/Pa)	1.77e-9	1.77e-9	1.77e-9
Boundary Condition	Closed	Closed	Closed
Basin Area (km2)	875	875	875
Simulation Time (months)	346	372	372
Injection Well Radius (m)	0.24	0.24	0.23
Number of Wells	9	21	46
Total Volume Injected (Mton)	16.83	42.14 (13.73)	86.58 (14.36)

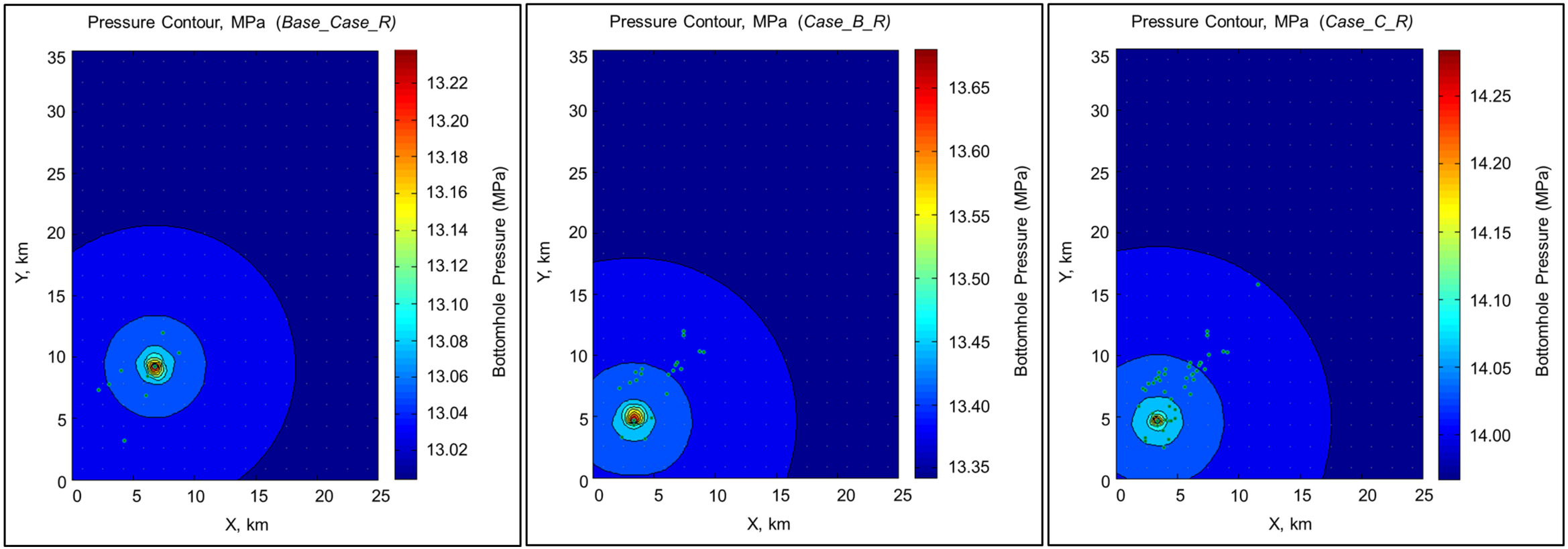

Figure 6.2 Simulation results for the Catahoula trend. The Base_Case_R (left figure) involves only 9 wells with their pressure data reported, and the maximum bottomhole pressure calculated by the model is below the maximum reported bottomhole pressure of 19.7 MPa. The Case_B_R (middle figure) involves 21 wells, with the additional 12 wells either having their injection pressure unavailable or had multiple perforations within the same interval or both, and the maximum bottomhole pressure calculated by the model remains below the maximum reported bottomhole pressure of 19.7 MPa for the initial 9 wells. The Case_C_R (right figure) involves a total of 46 wells, with the additional 25 wells having multiple perforations and at least one of those perforations within the interval being considered, assuming a majority of the volumes from these wells are going into the interval being considered. The maximum bottomhole pressure calculated by the model for this case remains below the maximum reported bottomhole pressure of 19.7 MPa for the initial 9 wells.

7. Discussion

7.1 Summary of Regional and Detailed Case Studies

Based on the Injectivity and Volume analysis, considering only wells injecting below 800m, the Miocene, Oligocene, and Woodbine appear to be the best options for CO_2 injection in the Texas Gulf Coast. Despite the large volumes initially observed to be going into the Lower Cretaceous, further study is required to determine if trends of high injectivity zones exist in the deeper subsurface (>800 m) and its potential for CO_2 storage, as the high injectivity and volumes observed for the Lower cretaceous in this study are associated with wells injecting into shallow units (<800 m).

The large volumes going into the Edwards Group were observed to only be possible with the model boundary being set to open and permeability set to values higher than the average permeability reported for the unit, as the maximum bottomhole pressure calculated by the model with the formation's average properties was significantly higher than maximum reported bottomhole pressure for the cluster of wells injecting into this formation. This does not in any way represent what the Edwards system is like. The analytical isotropic model used in this study assumes that properties are the same everywhere, which is not the case for the highly heterogeneous Edwards formation as pointed out by Cook (1979) and Swanson et al. (2007). Hovorka et al. (1998) pointed out that some samples from the unit have permeability above 1 Darcy due to microfractures and suggest that wells with high hydraulic conductivity intersect fracture sets that dominate conduit development and conduit flow and overwhelm any stratigraphic effects. Therefore, it is likely that the shallower wells with high injectivities and responsible for the majority of the volumes going into this unit intersect similar fracture sets with better flow properties than the unit's average, which results in lower pressure buildup in these wells. Injecting

similar volumes with the average formation properties will likely result in higher pressure buildup, as can be seen in the result produced by the isotropic model.

Using the analytical model to simulate the volumes injected into the Catahoula formation with a closed boundary condition and the formation's average properties resulted in a bottomhole pressure less than the reported maximum bottomhole pressure for the well cluster. This also does not mean that the Catahoula is a single unit with closed boundaries. As pointed out by Chowdhury et al. (2006) and Galloway (1977), growth faults extend up to the Catahoula and Chowdhury et al. (2006) and Galloway and Kaiser (1980) mentioned that there are fluvial sediments in the unit suggesting the presence of channels and floodplains in the unit. These features combine to make the Catahoula formation a heterogeneous system with high-permeability and low-permeability zones. The wells in this cluster are observed to have different pressure profiles. Hence, it is likely that the wells with higher reported bottomhole pressures intersect zones with worse flow properties than the formation's average. Injecting similar volumes with the average formation properties as was done with the analytical model resulted in lower pressure buildup mainly due to the model's inability to account for such heterogeneity.

7.2 Observed Local Variations in Injectivity

Local variations in injectivity were observed across wells injecting into the same interval within the Edwards Group and Catahoula Formation, and this raises the question why? The analysis carried out here is not about pressure buildup as most wells are observed to be injecting below their maximum permitted pressures, rather it involves comparing the different rate and pressure profiles for each of the wells considered to understand why one well has a higher or lower injectivity index compared to another well. Tables 7.1 and 7.2 show the wells of these two units

and their injectivity indexes. Figure 7.1 shows the injectivity trends for wells injecting into both units. From Figure 7.1, three things can be established:

i. The V-shape observed in both figures suggests heterogeneity in these formations as different wells mostly follow their linear trend within the shape. The width of the shape can suggest the extent of heterogeneity, with the Edwards Group exhibiting more heterogeneity than the Catahoula Formation.

ii. The linear trend observed in each well suggests intermittency, with the injectivity index increasing as more volume is available to be injected.

iii. For both units, a few wells share a similar linear trend, suggesting reservoir connectedness and hence possible well interference.

Figures 7.2 and 7.3 show the reported pressures and rates with time for wells in both units. The following insights from these plots provide further evidence to back up the first two points established earlier in this section:

i. Well 43011 and well 34452 have injected large volumes even though well 34452 was active for a longer time. When both wells are compared in Table 7.1 and Figure 7.2, it can be observed that well 43011 has a higher injectivity index because it achieved higher rates at relatively high pressures while well 34452 achieved relatively lower rates at similar pressures. When well 373704 is compared to well 2146 in Table 7.1 and Figure 7.2, it can be observed that well 37304 injected more water, achieved both high and low rates, and was active for a longer time with pressures relatively low compared to well 2146, which achieved mostly high rates, injected less during the short time it was active with pressures significantly higher than what was observed in well 37304.

Well 2148 appears to have the lowest injectivity. This is most likely due to a lack of water to inject, as the pressures reported during its injection period fall within the range observed in other wells in the cluster.

ii. In Table 7.2, well 61997 has the highest injectivity index. When compared to well 62106, which has the lowest injectivity index, it can be observed that well 61997 likely had more water to inject, which enabled it to achieve higher rates with similar pressure levels, and at some points slightly below what is observed in well 62106 that achieved relatively lower rates. Well 78999 has a higher injectivity index than well 83844, and this can be observed from the plots to be possibly due to well 78999 achieving lower pressure even with higher rates. Similar trends can be seen when other wells injecting into this formation are compared.

As observed from these plots, all the wells are operating below capacity (i.e., below permitted pressure and volume), which means that they are capable of taking more water if available, making the injectivity indexes estimated for these wells a minimum indicator of performance.

Table 7.1 Injectivity summary for five wells injecting into the Catahoula formation.

S/N	Well ID	Injectivity Index (Mt/year/1000 psi)
1	34452	0.71
2	37304	0.45
3	43011	1.05
4	2146	0.43

5	2148	0.35

Table 7.2 Injectivity summary for 7 wells injecting into the Edwards formation.

S/N	Well ID	Injectivity Index (Mt/year/1000 psi)
1	41705	1.52
2	61997	2.40
3	62106	0.93
4	74329	1.66
5	75254	1.65
6	78999	1.89
7	83844	1.35

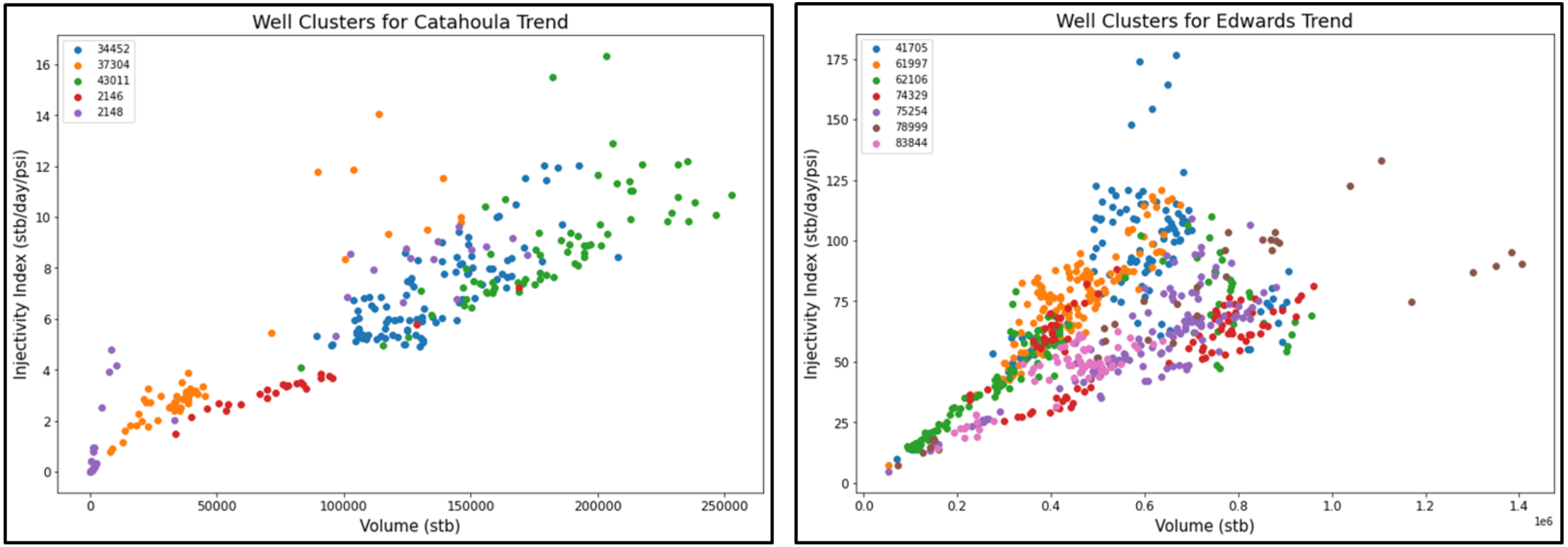

Figure 7.1 Injectivity index (stb/day/psi) versus volume (stb). The left figure shows the injectivity trend for wells injecting into the Catahoula Formation, while the right figure shows the injectivity trend for wells injecting into the Edwards Formation.

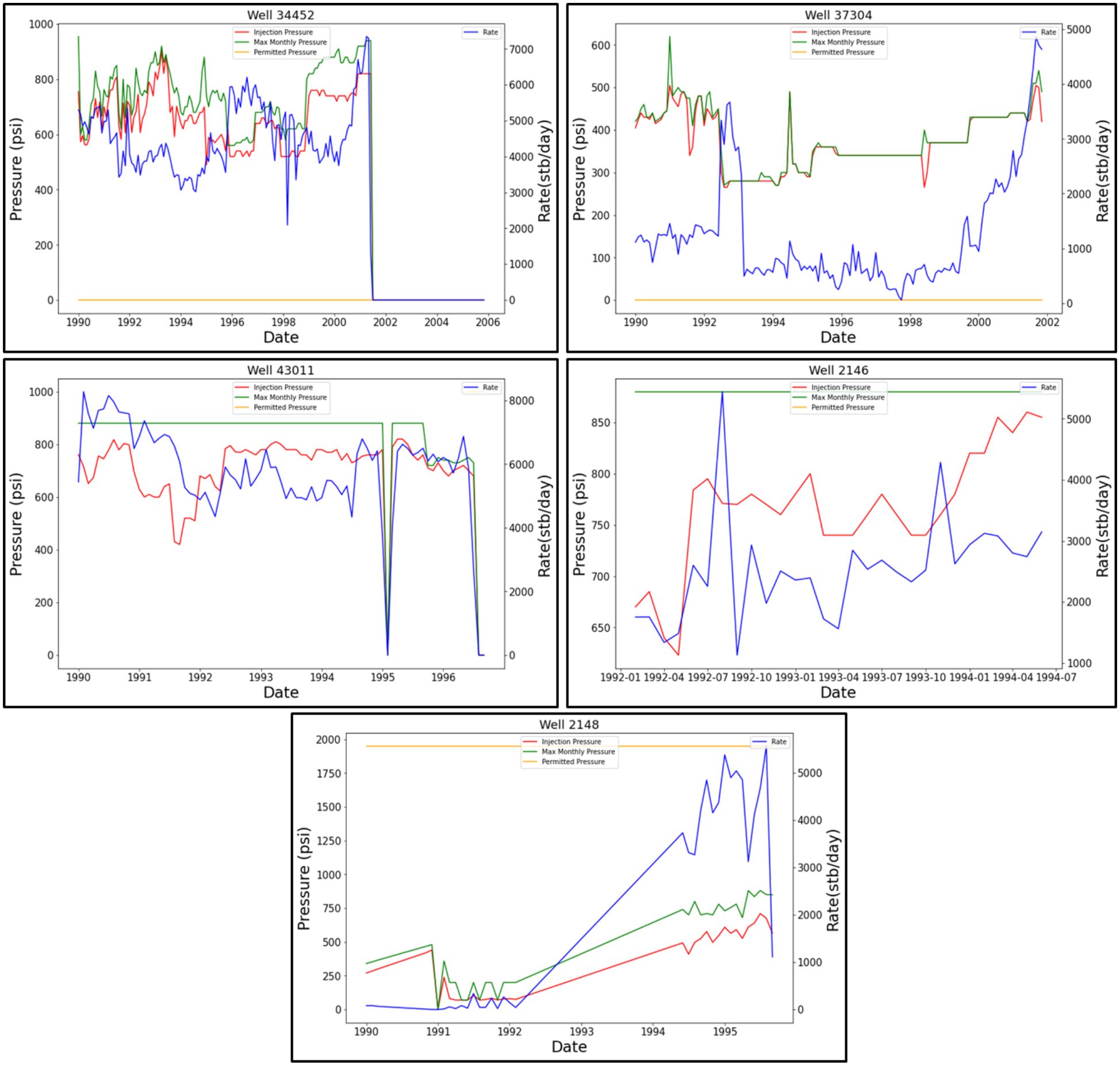

Figure 7.2 Injection pressure, maximum monthly pressure, permitted pressure, and rate versus time for wells injecting into the Catahoula Formation. The left y-axis includes different pressures in psi, and as can be seen, the permitted pressure is mostly erroneous or unavailable. The right y-axis shows the rate in stb/day, and the x-axis shows the date.

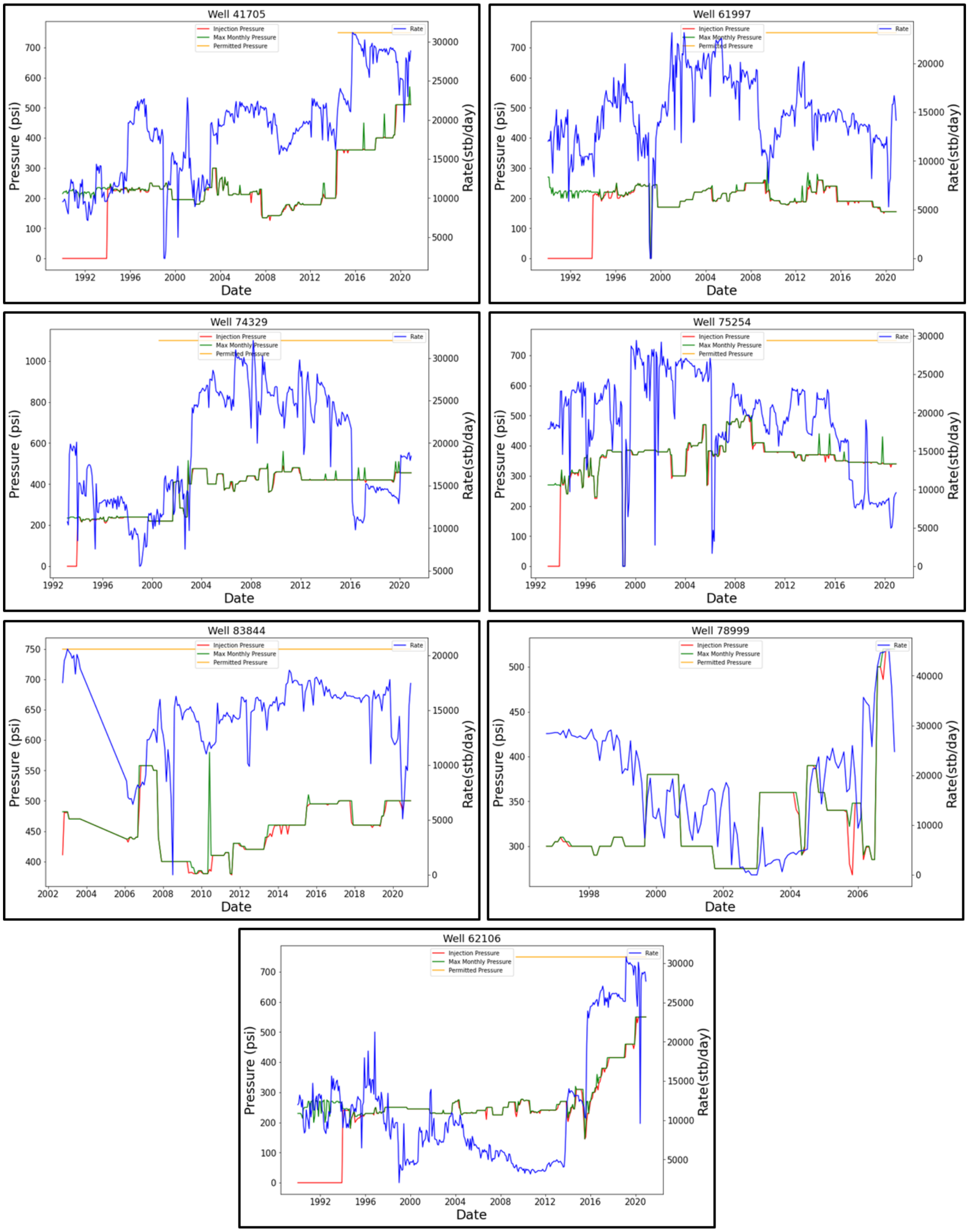

Figure 7.3 Injection pressure, maximum monthly pressure, permitted pressure, and rate versus time for wells injecting into the Edwards Group. The left y-axis includes different pressures in psi, and as can be seen, the permitted pressure is mostly erroneous or unavailable. The right y-axis shows the rate in stb/day, and the x-axis shows the date

7.3 Policy Recommendations for Class VI Projects

For regulators and policymakers, this study provides some key insights that should be considered to foster success for CCS in the Texas Gulf Coast. These cover technical feasibility, pressure buildup, data reporting, well interference, well monitoring, and intermittency.

With over 15 billion stock tank barrels (>1 Gt CO_2 Eq.) of saltwater injected into depths suitable for CO_2 injection and the observation of wells capable of disposing of more than 1 Mt of CO_2 equivalent annually in the Texas Gulf Coast, it is clear and reassuring to regulators and policymakers of the region's capability to be a key CCS hub in the United States.

As seen in this study, the resolution of the different data types is poor, the accuracy of pressure data provided for some wells, eliminated during QC in this study, by operators is questionable, and there is a piece of evidence suggesting well interference. The study also shows that most wells are injecting below their maximum pressures, although this is largely due to intermittency, which is unlikely to be present for CCS projects. Considering the nature of saltwater injection data, it is difficult to properly monitor pressure changes, potential well interference, and potential contamination of underground sources of drinking water (USDW). Hence, for Class VI projects, rules that require operators to provide data with better resolution and accuracy will be valuable. In particular, reports of the duration of injection in hours, results of fall-off tests, reports of wells with multiple completions, reports of the length and depth of all completions, and the use of a more conventional name when reporting injection targets would significantly improve data. Adopting some of these suggestions could go a long way to ensure pressure buildup is properly monitored, potential interference of a well by another well from a different project is detected, and USDWs are protected.

7.4 Sources of Uncertainty

From this study, it is clear that the scale of saltwater injection in the Texas Gulf Coast is comparable to the large scales planned for CCS projects in the region, making it a useful analog for large-scale CO_2 injection. That said, there are significant uncertainties in the saltwater injection data that limit its utility.

The majority of these uncertainties and limitations come from poor data resolution. For example, the volume, rate, and pressure data are reported monthly, with no indication of actual injection duration. In principle, a well might have injected the entire reported volume in only a few hours and stayed idle for the rest of the month, with the reported monthly pressure only reflecting the measurement made during these few hours. Perhaps the well could have injected a significantly larger volume in the month without a significant increase in pressure. Equally, another well might have injected continuously for an entire month to achieve the reported volume, with the pressure representing the average of multiple measurements in a month. However, as seen in Figures 7.1 and 7.2, the former is likely the case for a majority of these wells, as most of them are operating below their maximum permitted injection volume and pressure. Another example is the completion data in which only the top and bottom of perforations are reported. For large perforations (>300 ft), it makes it difficult to know if the large completions are indeed real or a combination of multiple perforations within the large interval. This also brings some uncertainties in the normalized injectivity index for the single-perforation wells with perforations larger than 300 ft, with their normalized injectivity index values possibly underestimated. Hence, the volume and injectivity results estimated in this study should be regarded to a large extent as a minimum indicator of what the majority of these wells are capable of.

The usage of machine learning models to assign formations to wells without any formation reported for them also draws some uncertainties as the accuracy is ~75%, which means it is not perfect, and it is important to acknowledge this even though the model does a good job as seen in Figure 3.6 and from the detailed case studies of the Edwards and Catahoula well clusters. The formations assigned to wells in each of these well clusters were verified to be correct through the well cross-section analysis.

8. Conclusion

With over 30 years of injection and more than 20 billion barrels of saltwater injected in the Texas Gulf Coast, saltwater injection has proven to be a useful analog for large-scale CO_2 injection in the region.

While the uncertainties in the saltwater injection data limit its utility, this study has been able to provide the following key insights that are beneficial to stakeholders:

i. Large-scale injection is technically feasible in the Texas Gulf Coast.

ii. Wells capable of disposing more than 1 megatons per annum are present.

iii. The volume and injectivity results only provide a minimum indication of reservoir performance, especially due to intermittency, as many wells with low injectivity were discovered to operate below their maximum permitted volume and pressure.

iv. The Miocene, Woodbine, and Oligocene formations present the best opportunities for large-scale injection in the Texas Gulf Coast.

v. The high injectivities and volumes observed in the Lower Cretaceous are mostly associated with wells injecting into shallow zones and further studies will be needed to confirm the existence of high-injectivity zones in the deeper subsurface (>800 m).

vi. Local variations in injectivity are mostly due to intermittency and formation heterogeneity.

vii. Reservoir connectedness, which can lead to well interference, is possible, with a few wells in the same unit sharing similar injectivity profiles.

viii. There is not enough evidence of compartmentalization from the analysis carried out.

ix. Better reporting by operators of Class VI wells could enable regulators and policymakers to effectively monitor pressure changes and potential contamination of USDW, and maintain the integrity of different projects close to each other.

9. Future Work

The next steps would involve reducing the uncertainties associated with the different data types used in this study. This may be achieved by collaborating with agencies such as the Railroad Commission and operators involved in saltwater injection to ensure better reporting. This may be needed to assess potential interference when CO_2 is injected into a formation that also receives saltwater and industrial waste fluids from Class II and Class I permits.

Replacing the analytical model used in this study with a more robust model will be another step to account for the different types of heterogeneities in different formations.

Appendix A – Well Assignment and Source

The reported names for most saltwater injection targets are uncommon, field-specific, or obsolete. Hence, they had to be assigned to be assigned to formation names that are more common in today's chronostratigraphy. The table below provides a summary of the reported names, their assigned names, and the sources that informed these assignments.

Reported Formations	**Key_Content**	**Assigned Group**	**Source**
EDWARDS	Edwards	Washita	Geomap (2009)
EDWARDS	Edwards	Washita	Geomap (2009)
EDWARDS LIME	Edwards	Washita	Geomap (2009)
SAN MIGUEL #1 SAND	San miguel	Taylor	Geomap (2009)
SAN MIGUEL #1 SAND	San miguel	Taylor	Geomap (2009)
EDWARDS B	Edwards	Washita	Geomap (2009)
VICKSBURG 1	Vicksburg	Vicksburg	Geomap (2009)
BURNELL (PETTUS)	Burnell	Claiborne	https://core.ac.uk/download/pdf/4268365.pdf
CATAHOULA	Catahoula	Catahoula	https://pubs.usgs.gov/of/1994/0461/report.pdf
MIOCENE	Miocene	Fleming	Geomap (2009)

MIOCENE	Miocene	Fleming	Geomap (2009)
CATAHOULA	Catahoula	Catahoula	https://pubs.usgs.gov/of/1994/0461/report.pdf
MCFADDIN 4400'	Mcfaddin	Frio	https://www.osti.gov/servlets/purl/140595
MIOCENE	Miocene	Fleming	Geomap (2009)
CATAHOULA	Catahoula	Catahoula	https://pubs.usgs.gov/of/1994/0461/report.pdf
CATAHOULA SAND	Catahoula	Catahoula	https://pubs.usgs.gov/of/1994/0461/report.pdf
CATAHOULA	Catahoula	Catahoula	https://pubs.usgs.gov/of/1994/0461/report.pdf
CATAHOULA	Catahoula	Catahoula	https://pubs.usgs.gov/of/1994/0461/report.pdf
YEGUA	Yegua	Claiborne	Geomap (2009)
CATAHOULA	Catahoula	Catahoula	https://pubs.usgs.gov/of/1994/0461/report.pdf
FRIO	Frio	Frio	https://pubs.usgs.gov/of/1994/0461/report.pdf
FRIO	Frio	Frio	https://pubs.usgs.gov/of/1994/0461/report.pdf
MIOCENE	Miocene	Fleming	Geomap (2009)
JACKSON	Jackson	Jackson	Geomap (2009)
MIOCENE	Miocene	Fleming	Geomap (2009)
FRIO 1	Frio	Frio	https://pubs.usgs.gov/of/1994/0461/report.pdf
LAGARTO	Lagarto	Fleming	Geomap (2009)
OAKVILLE	Oakeville	Fleming	Geomap (2009)

CATAHOULA	Catahoula	Catahoula	https://pubs.usgs.gov/of/1994/0461/report.pdf
VICKSBURG	Vicksburg	Vicksburg	Geomap (2009)
OAKVILLE	Oakeville	Fleming	Geomap (2009)
OAKVILLE	Oakeville	Fleming	Geomap (2009)
CATAHOULA	Catahoula	Catahoula	https://pubs.usgs.gov/of/1994/0461/report.pdf
CATAHOULA	Catahoula	Catahoula	https://pubs.usgs.gov/of/1994/0461/report.pdf
CATAHOULA	Catahoula	Catahoula	https://pubs.usgs.gov/of/1994/0461/report.pdf
MIOCENE	Miocene	Fleming	Geomap (2009)
FRIO	Frio	Frio	https://pubs.usgs.gov/of/1994/0461/report.pdf
MIOCENE	Miocene	Fleming	Geomap (2009)
MIOCENE	Miocene	Fleming	Geomap (2009)
TOP BASAL MIOCENE SAND/ANAHUAC	Miocene	Fleming	Geomap (2009)
M5	M	Fleming	Geomap (2009)
MIOCENE	Miocene	Fleming	Geomap (2009)
FRIO	Frio	Frio	https://pubs.usgs.gov/of/1994/0461/report.pdf
TOP OF FRIO	Frio	Frio	https://pubs.usgs.gov/of/1994/0461/report.pdf

MIOCENE MARKER 4	Miocene	Fleming	Geomap (2009)
MIOCENE MARKER 2	Miocene	Fleming	Geomap (2009)
BASE OF FRIO	Frio	Frio	https://pubs.usgs.gov/of/1994/0461/report.pdf
MIOCENE X Y Z CONS	Miocene	Fleming	Geomap (2009)
YEGUA	Yegua	Claiborne	Geomap (2009)
MIOCENE DISPOSAL	Miocene	Fleming	Geomap (2009)
FRIO - DISPOSAL	Frio	Frio	https://pubs.usgs.gov/of/1994/0461/report.pdf
JACKSON	Jackson	Jackson	Geomap (2009)
FRIO	Frio	Frio	https://pubs.usgs.gov/of/1994/0461/report.pdf
WILCOX	Wilcox	Wilcox	Geomap (2009)
FRIO 9	Frio	Frio	https://pubs.usgs.gov/of/1994/0461/report.pdf
FRIO F1A	Frio	Frio	https://pubs.usgs.gov/of/1994/0461/report.pdf
FRIO	Frio	Frio	https://pubs.usgs.gov/of/1994/0461/report.pdf
MIOCENE	Miocene	Fleming	Geomap (2009)
VICKSBURG - DISPOSAL	Vicksburg	Vicksburg	Geomap (2009)
MIOCENE - DISPOSAL	Miocene	Fleming	Geomap (2009)
MIOCENE	Miocene	Fleming	Geomap (2009)
HET LIME - DISPOSAL	Heterostegina	Catahoula	https://pubs.usgs.gov/of/1994/0461/report.pdf

COLE	Cole	Jackson	Geomap (2009)
JACKSON	Jackson	Jackson	Geomap (2009)
MIOCENE	Miocene	Fleming	Geomap (2009)
MIRANDO	Miranda	Jackson	https://repositories.lib.utexas.edu/bitstream/handle/2152/77978/txu-oclc-612464.pdf?sequence=1
TAFT	Taft	Frio	https://www.osti.gov/servlets/purl/140595
MIRANDO SAND	Miranda	Jackson	https://repositories.lib.utexas.edu/bitstream/handle/2152/77978/txu-oclc-612464.pdf?sequence=1
AUSTIN	Austin Chalk	Austin	Geomap (2009)
NACATOCH	Nacatoch	Navarro	https://repositories.lib.utexas.edu/bitstream/handle/2152/77501/txu-oclc-10367600.pdf?sequence=1
WOODBINE	Woodbine	Woodbine	Geomap (2009)
WOODBINE	Woodbine	Woodbine	Geomap (2009)
WOODBINE	Woodbine	Woodbine	Geomap (2009)
WOODBINE	Woodbine	Woodbine	Geomap (2009)
PALUXY SAND	Paluxy	Fredericksburg	Geomap (2009)
GEORGETOWN	Georgetown	Washita	Geomap (2009)
WOODBINE	Woodbine	Woodbine	Geomap (2009)
DEXTER	Dexter	Woodbine	https://www.gcags.org/Journal/2016.GCAGS.Journal/2016.GCAGS.Journal.v5.02.p25-46.Vallabhaneni.et.al.pdf

WOODBINE	Woodbine	Woodbine	Geomap (2009)
DEXTER	Dexter	Woodbine	https://www.gcags.org/Journal/2016.GCAGS.Journal/2016.GCAGS.Journal.v5.02.p25-46.Vallabhaneni.et.al.pdf
WOODBINE	Woodbine	Woodbine	Geomap (2009)
DEXTER	Dexter	Woodbine	https://www.gcags.org/Journal/2016.GCAGS.Journal/2016.GCAGS.Journal.v5.02.p25-46.Vallabhaneni.et.al.pdf
WOODBINE	Woodbine	Woodbine	Geomap (2009)
WOODBINE	Woodbine	Woodbine	Geomap (2009)
WOODBINE	Woodbine	Woodbine	Geomap (2009)
WOODBINE	Woodbine	Woodbine	Geomap (2009)
AUSTIN CHALK	Austin Chalk	Austin	Geomap (2009)
WOODBINE	Woodbine	Woodbine	Geomap (2009)
WOODBINE	Woodbine	Woodbine	Geomap (2009)
AUSTIN DENSE CHALK	Austin Chalk	Austin	Geomap (2009)
WOODBINE SAND & SHALE	Woodbine	Woodbine	Geomap (2009)
WOODBINE SAND	Woodbine	Woodbine	Geomap (2009)
WOODBINE SAND	Woodbine	Woodbine	Geomap (2009)
AUSTIN CHALK	Austin Chalk	Austin	Geomap (2009)

AUSTIN CHALK	Austin Chalk	Austin	Geomap (2009)
DEXTER A	Dexter	Woodbine	https://www.gcags.org/Journal/2016.GCAGS.Journal/2016.GCAGS.Journal.v5.02.p25-46.Vallabhaneni.et.al.pdf
WOODBINE	Woodbine	Woodbine	Geomap (2009)
BLOSSOM	Blossom	Austin	https://pubs.usgs.gov/of/1994/0461/report.pdf
BLOSSOM SAND	Blossom	Austin	https://pubs.usgs.gov/of/1994/0461/report.pdf
NACATOSH	Nacatoch	Navarro	https://repositories.lib.utexas.edu/bitstream/handle/2152/77501/txu-oclc-10367600.pdf?sequence=1
WOODBINE	Woodbine	Woodbine	Geomap (2009)
FRIO	Frio	Frio	Geomap (2009)
RUSTLER	Rustler	Rustler	https://pubs.usgs.gov/wri/wri91-4071/pdf/wri91-4071.pdf
CATAHOULA	Catahoula	Catahoula	https://pubs.usgs.gov/of/1994/0461/report.pdf
OAKVILLE	Oakeville	Fleming	Geomap (2009)
CATAHOULA	Catahoula	Catahoula	https://pubs.usgs.gov/of/1994/0461/report.pdf
CATAHOULA	Catahoula	Catahoula	https://pubs.usgs.gov/of/1994/0461/report.pdf
CATAHOULA	Catahoula	Catahoula	https://pubs.usgs.gov/of/1994/0461/report.pdf
FRIO	Frio	Frio	Geomap (2009)
DELAWARE	Delaware	Guadalupian	https://oaktrust.library.tamu.edu/bitstream/handle/1969.1/173304/GAO-THESIS-2018.pdf?sequence=1
GOVERNMENT WELLS	Government wells	Jackson	https://repositories.lib.utexas.edu/bitstream/handle/2152/77978/txu-oclc-612464.pdf?sequence=1

VICKSBURG	Vicksburg	Vicksburg	Geomap (2009)
WOODBINE	Woodbine	Woodbine	Geomap (2009)
CATAHOULA	Catahoula	Catahoula	https://pubs.usgs.gov/of/1994/0461/report.pdf
B. AUSTIN	Austin Chalk	Austin	Geomap (2009)
CATAHOULA	Catahoula	Catahoula	https://pubs.usgs.gov/of/1994/0461/report.pdf
CATAHOULA	Catahoula	Catahoula	https://pubs.usgs.gov/of/1994/0461/report.pdf
WOODBINE	Woodbine	Woodbine	Geomap (2009)
PALUXY	Paluxy	Fredericksburg	Geomap (2009)
WOODBINE	Woodbine	Woodbine	Geomap (2009)
WOODBINE	Woodbine	Woodbine	Geomap (2009)
COOK MOUNTAIN	Cook mountain	Claiborne	Geomap (2009)
FRIO	Frio	Frio	Geomap (2009)
GEORGETOWN	George town	Washita	Geomap (2009)
FRIO	Frio	Frio	Geomap (2009)
WOODBINE	Woodbine	Woodbine	Geomap (2009)
EDWARDS B	Edwards	Washita	Geomap (2009)

MIOCENE	Miocene	Fleming	Geomap (2009)
MIOCENE	Miocene	Fleming	Geomap (2009)
AUSTIN	Austin Chalk	Austin	Geomap (2009)
WOODBINE	Woodbine	Woodbine	Geomap (2009)
TOP WOODBINE	Woodbine	Woodbine	Geomap (2009)
LOWER TAYLOR SHALE	Taylor	Taylor	Geomap (2009)
EAGLEFORD	Eagleford	Eagleford	Geomap (2009)
JACKSON - INJECTION/ DISPOSAL; H2S	Jackson	Jackson	Geomap (2009)
WOODBINE	Woodbine	Woodbine	Geomap (2009)
CATAHOULA	Catahoula	Catahoula	https://pubs.usgs.gov/of/1994/0461/report.pdf
WOODBINE SAND	Woodbine	Woodbine	Geomap (2009)
CATAHOULA	Catahoula	Catahoula	https://pubs.usgs.gov/of/1994/0461/report.pdf
WASHITA	Washita	Washita	Geomap (2009)
WOODBINE SAND	Woodbine	Woodbine	Geomap (2009)
WOODBINE	Woodbine	Woodbine	Geomap (2009)

WOODBINE	Woodbine	Woodbine	Geomap (2009)
WOODBINE	Woodbine	Woodbine	Geomap (2009)
PECAN GAP	Pecan gap	Taylor	https://scholarworks.uark.edu/cgi/viewcontent.cgi?article=3849&context=etd
MIOCENE DISPOSAL	Miocene	Fleming	Geomap (2009)
OAKVILLE	Oakeville	Fleming	Geomap (2009)
MIOCENE	Miocene	Fleming	Geomap (2009)
WILCOX	Wilcox	Wilcox	Geomap (2009)
FRIO	Frio	Frio	Geomap (2009)
MIOCENE	Miocene	Fleming	Geomap (2009)
UPPER MIOCENE	Miocene	Fleming	Geomap (2009)
PALUXY	Paluxy	Fredericksburg	Geomap (2009)
GRETA	Greta	Frio	https://scholarworks.uark.edu/etd/2873/
UPPER GLEN ROSE	Glen rose	Trinity	Geomap (2009)
WOODBINE	Woodbine	Woodbine	Geomap (2009)
PETTIT	Pettet	Trinity	https://pubs.usgs.gov/of/1994/0461/report.pdf
WOODBINE	Woodbine	Woodbine	Geomap (2009)
MIOCENE 8	Miocene	Fleming	Geomap (2009)

PALUXY	Paluxy	Fredericksburg	Geomap (2009)
JACKSON	Jackson	Jackson	Geomap (2009)
FRIO	Frio	Frio	Geomap (2009)
MIOCENE SANDS - PRODUCED SALTWATER	Miocene	Fleming	Geomap (2009)
WILCOX	Wilcox	Wilcox	Geomap (2009)
FRIO	Frio	Frio	Geomap (2009)
WILCON	Wilcox	Wilcox	Geomap (2009)
MIOCENE	Miocene	Fleming	Geomap (2009)
WOODBINE	Woodbine	Woodbine	Geomap (2009)
TOP WOODBINE	Woodbine	Woodbine	Geomap (2009)
MIOCENE	Miocene	Fleming	Geomap (2009)
MIOCENE	Miocene	Fleming	Geomap (2009)
FRIO	Frio	Frio	Geomap (2009)
FRIO - DISPOSAL	Frio	Frio	Geomap (2009)
MASSIVE VICKSBURG	Vicksburg	Vicksburg	Geomap (2009)
WILCOX	Wilcox	Wilcox	Geomap (2009)

DOUGHERTY	Dougherty	Jackson	https://www.osti.gov/servlets/purl/140595
CATAHOULA	Catahoula	Catahoula	https://pubs.usgs.gov/of/1994/0461/report.pdf
JACKSON	Jackson	Jackson	Geomap (2009)
FRIO	Frio	Frio	Geomap (2009)
COLE SANDS	Cole	Jackson	Geomap (2009)
MIOCENE D-1B	Miocene	Fleming	Geomap (2009)
FRIO	Frio	Frio	Geomap (2009)
WOODBINE	Woodbine	Woodbine	Geomap (2009)
FRIO 6350 SAND	Frio	Frio	Geomap (2009)
FRIO 6500 SAND	Frio	Frio	Geomap (2009)
WOODBINE - EAST TEXAS FIELD (DISTRICT 6E)	Woodbine	Woodbine	Geomap (2009)
CATAHOULA	Catahoula	Catahoula	https://pubs.usgs.gov/of/1994/0461/report.pdf
FRIO	Frio	Frio	Geomap (2009)
MIOCENE A-7	Miocene	Fleming	Geomap (2009)
GRETTA	Greta	Frio	https://scholarworks.uark.edu/etd/2873/
JACKSON	Jackson	Jackson	Geomap (2009)

MIOCENE	Miocene	Fleming	Geomap (2009)
FRIO - DISPOSAL	Frio	Frio	Geomap (2009)
CATAHOULA	Catahoula	Catahoula	https://pubs.usgs.gov/of/1994/0461/report.pdf
NACATOSH	Nacatoch	Navarro	https://repositories.lib.utexas.edu/bitstream/handle/2152/77501/txu-oclc-10367600.pdf?sequence=1
FRIO	Frio	Frio	Geomap (2009)
AUSTIN CHALK	Austin Chalk	Austin	Geomap (2009)
SAN MIGUEL	San miguel	Taylor	Geomap (2009)
POTH A	Poth	Midway	https://www.beg.utexas.edu/files/publications/contract-reports/CR2013-Nicot-1.pdf
YEAGUA	Yegua	Claiborne	Geomap (2009)
WOODBINE	Woodbine	Woodbine	Geomap (2009)
CATAHOULA	Catahoula	Catahoula	https://pubs.usgs.gov/of/1994/0461/report.pdf
FRIO F1A	Frio	Frio	Geomap (2009)
MIOCENE	Miocene	Fleming	Geomap (2009)
M2	M	Fleming	Geomap (2009)
MIOCENE	Miocene	Fleming	Geomap (2009)
MIOCENE	Miocene	Fleming	Geomap (2009)
SAN MIGUEL #1 SAND	San miguel	Taylor	Geomap (2009)

GRETA	Greta	Frio	https://scholarworks.uark.edu/etd/2873/
OAKVILLE	Oakeville	Fleming	Geomap (2009)
KIAMICHI	Kiamichi	Fredericksburg	Geomap (2009)
WOODBINE (DEXTER)	Woodbine	Woodbine	Geomap (2009)
WOODBINE (LEWISVILLE)	Woodbine	Woodbine	Geomap (2009)
FRIO	Frio	Frio	Geomap (2009)
BUDA LIME	Buda	Washita	Geomap (2009)
WOODBINE	Woodbine	Woodbine	Geomap (2009)
M11	M	Fleming	Geomap (2009)
FRIO F1A	Frio	Frio	Geomap (2009)
BENTLEY	Bentley	Bentley	https://transboundary.tamu.edu/media/1169/1979_baker.pdf
M14	M	Fleming	Geomap (2009)
FRIO	Frio	Frio	Geomap (2009)
TOP OF WOODBINE SAND	Woodbine	Woodbine	Geomap (2009)
FRIO	Frio	Frio	Geomap (2009)
TOP OF WOODBINE	Woodbine	Woodbine	Geomap (2009)

BASE OF AUSTIN CHALK	Austin Chalk	Austin	Geomap (2009)
FRIO 2	Frio	Frio	Geomap (2009)
WILCOX	Wilcox	Wilcox	Geomap (2009)
FRIO F1A	Frio	Frio	Geomap (2009)
WOODBINE GROUP	Woodbine	Woodbine	Geomap (2009)
OAKVILLE	Oakeville	Fleming	Geomap (2009)
BASE MASSIVE ANHYDRITE	Anhydrite	Trinity	https://pubs.geoscienceworld.org/aapg/books/book/1484/chapter-abstract/107178760/Summary-of-Subsurface-Geology-of-Northeast-Texas?redirectedFrom=fulltext
BENTLEY	Bentley	Bentley	https://transboundary.tamu.edu/media/1169/1979_baker.pdf
UPPER VICKSBURG	Vicksburg	Vicksburg	Geomap (2009)
FRIO F1A	Frio	Frio	Geomap (2009)
FRIO 5	Frio	Frio	Geomap (2009)
VICKSBURG	Vicksburg	Vicksburg	Geomap (2009)
FRIO F1A	Frio	Frio	Geomap (2009)
M10	M	Fleming	Geomap (2009)
SUB-CLARKSVILLE	Clarksville	Clarksville	Geomap (2009)
ESCANDIDO	Escondido	Escondido	Geomap (2009)
BUDA	Buda	Washita	Geomap (2009)

MIOCNE	Miocene	Fleming	Geomap (2009)
MIOCENE M10	Miocene	Fleming	Geomap (2009)
MIOCENE	Miocene	Fleming	Geomap (2009)
ANAHUAC	Anahuac	Frio	Geomap (2009)
WOODBINE	Woodbine	Woodbine	Geomap (2009)
VICKSBURG	Vicksburg	Vicksburg	Geomap (2009)
FRIO	Frio	Frio	Geomap (2009)
WOODBINE SAND & SHALE	Woodbine	Woodbine	Geomap (2009)
PALUXY	Paluxy	Fredericksburg	Geomap (2009)
FRIO	Frio	Frio	Geomap (2009)
FRIO	Frio	Frio	Geomap (2009)
CATAHOULA	Catahoula	Catahoula	https://pubs.usgs.gov/of/1994/0461/report.pdf
GRETA	Greta	Frio	https://scholarworks.uark.edu/etd/2873/
GRETA	Greta	Frio	https://scholarworks.uark.edu/etd/2873/
WOODBINE	Woodbine	Woodbine	Geomap (2009)
MIOCENE	Miocene	Fleming	Geomap (2009)
MIOCENE - DISPOSAL	Miocene	Fleming	Geomap (2009)
LWR-MIOC.	Miocene	Fleming	Geomap (2009)

NACATOCH	Nacatoch	Navarro	https://repositories.lib.utexas.edu/bitstream/handle/2152/77501/txu-oclc-10367600.pdf?sequence=1
Y5	Yegua	Claiborne	Geomap (2009)
MIOCENE	Miocene	Fleming	Geomap (2009)
CATAHOULA	Catahoula	Catahoula	https://pubs.usgs.gov/of/1994/0461/report.pdf
LOWER PETTIT	Pettet	Trinity	https://pubs.usgs.gov/of/1994/0461/report.pdf
UPPER PETTIT	Pettet	Trinity	https://pubs.usgs.gov/of/1994/0461/report.pdf
CATAHAULA	Catahoula	Catahoula	https://pubs.usgs.gov/of/1994/0461/report.pdf
WOODBINE	Woodbine	Woodbine	Geomap (2009)
WOODBINE	Woodbine	Woodbine	Geomap (2009)
TOP WOODBINE	Woodbine	Woodbine	Geomap (2009)
TOP RODESSA	Rodessa	Rodessa	https://pubs.usgs.gov/of/2016/1026/ofr20161026.pdf
COLE SANDS	Cole	Jackson	Geomap (2009)
VICKSBURG	Vicksburg	Vicksburg	Geomap (2009)
YEGUA	Yegua	Claiborne	Geomap (2009)
MOODY'S RANCH	Moody branch	Jackson	Geomap (2009)
VICKSBURG	Vicksburg	Vicksburg	Geomap (2009)

WOODBINE	Woodbine	Woodbine	Geomap (2009)
AUSTIN CHALK	Austin Chalk	Austin	Geomap (2009)
TOP WOODBINE	Woodbine	Woodbine	Geomap (2009)
SAN MIGUEL	San miguel	Taylor	Geomap (2009)
EAGLE FORD	Eagleford	Eagleford	Geomap (2009)
DEXTER	Dexter	Woodbine	https://www.gcags.org/Journal/2016.GCAGS.Journal/2016.GCAGS.Journal.v5.02.p25-46.Vallabhaneni.et.al.pdf
MIOCENE M10	Miocene	Fleming	Geomap (2009)
TOP WOODBINE SAND	Woodbine	Woodbine	Geomap (2009)
ESCONDIDO	Escondido	Escondido	Geomap (2009)
MIOCENE	Miocene	Fleming	Geomap (2009)
FRIO	Frio	Frio	Geomap (2009)
MIOCENE/FRIO	Miocene	Fleming	Geomap (2009)
TOP FRIO	Frio	Frio	Geomap (2009)
MIDDLE YEGUA	Yegua	Claiborne	Geomap (2009)
CARRIZO	Carrizo	Wilcox	Geomap (2009)
MIOCENE	Miocene	Fleming	Geomap (2009)
MIOCENE	Miocene	Fleming	Geomap (2009)

EAGLEFORD SHALE	Eagleford	Eagleford	Geomap (2009)
MICENE	Miocene	Fleming	Geomap (2009)
FRIO F1A	Frio	Frio	Geomap (2009)
FRIO F11	Frio	Frio	Geomap (2009)
FRIO	Frio	Frio	Geomap (2009)
VICKSBURG	Vicksburg	Vicksburg	Geomap (2009)
FRIO	Frio	Frio	Geomap (2009)
MIOCENE - DISPOSAL	Miocene	Fleming	Geomap (2009)
COLE	Cole	Jackson	Geomap (2009)
WILCOX	Wilcox	Wilcox	Geomap (2009)
EDWARDS A	Edwards	Washita	Geomap (2009)
WOODBINE SAND	Woodbine	Woodbine	Geomap (2009)
FRIO	Frio	Frio	Geomap (2009)
CATAHOULA	Catahoula	Catahoula	https://pubs.usgs.gov/of/1994/0461/report.pdf
FRIO	Frio	Frio	Geomap (2009)
WILCOX	Wilcox	Wilcox	Geomap (2009)
SINTON	Sinton	Frio	https://scholarworks.uark.edu/cgi/viewcontent.cgi?article=4380&context=etd
WOODBINE SAND	Woodbine	Woodbine	Geomap (2009)
COCKFIELD	Cockfield	Claiborne	Geomap (2009)
MIOCENE - DISPOSAL	Miocene	Fleming	Geomap (2009)

MIRADO	Mirando	Jackson	https://repositories.lib.utexas.edu/bitstream/handle/2152/77978/txu-oclc-612464.pdf?sequence=1
YEGUA	Yegua	Claiborne	Geomap (2009)
OLMOS	Olmos	Navarro	https://pubs.usgs.gov/dds/dds-069/dds-069-h/REPORTS/69_H_CH_2.pdf
ANAHUAC	Anahuac	Frio	Geomap (2009)
MIOCENE M11	Miocene	Fleming	Geomap (2009)
AUSTIN CHALK	Austin Chalk	Austin	Geomap (2009)
COKER	Coker	EagleFord	https://pubs.usgs.gov/wri/1987/4112/report.pdf
FRIO	Frio	Frio	Geomap (2009)
GRETA	Greta	Frio	https://scholarworks.uark.edu/etd/2873/
SERPENTINE	Not real formation	Austin	https://www.baylor.edu/geosciences/doc.php/142586.pdf
CATAHOULA	Catahoula	Catahoula	https://pubs.usgs.gov/of/1994/0461/report.pdf
WOODBINE	Woodbine	Woodbine	Geomap (2009)
WOODBINE	Woodbine	Woodbine	Geomap (2009)
WILCOX	Wilcox	Wilcox	Geomap (2009)
COLE	Cole	Jackson	Geomap (2009)
MIOCENE	Miocene	Fleming	Geomap (2009)
T / AUSTIN CHALK	Austin Chalk	Austin	Geomap (2009)

5400 #3	5400	Frio	https://www.osti.gov/servlets/purl/140595
FRIO	Frio	Frio	Geomap (2009)
YEGUA SAND	Yegua	Claiborne	Geomap (2009)
GRETA	Greta	Frio	https://scholarworks.uark.edu/etd/2873/
WOODBINE	Woodbine	Woodbine	Geomap (2009)
FREDRICKSBURG	Fredericksburg	Fredericksburg	Geomap (2009)
BACON LIME	Bacon Lime	Trinity	https://pubs.geoscienceworld.org/aapg/books/book/1484/chapter-abstract/107178760/Summary-of-Subsurface-Geology-of-Northeast-Texas?redirectedFrom=fulltext
WILCOX	Wilcox	Wilcox	Geomap (2009)
CARRIZO	Carrizo	Wilcox	Geomap (2009)
RODESSA	Rodessa	Rodessa	https://pubs.usgs.gov/of/2016/1026/ofr20161026.pdf
JACKSON	Jackson	Jackson	Geomap (2009)
AUSTIN CHALK	Austin Chalk	Austin	Geomap (2009)
UPPER PETTIT	Pettet	Trinity	https://pubs.usgs.gov/of/1994/0461/report.pdf
WOODBINE	Woodbine	Woodbine	Geomap (2009)
GLEN ROSE	Glen rose	Trinity	Geomap (2009)
VICKSBURG	Vicksburg	Vicksburg	Geomap (2009)
AUSTIN CHALK	Austin Chalk	Austin	Geomap (2009)
QUEEN CITY	Queen city	Claiborne	Geomap (2009)

GRETA	Greta	Frio	https://scholarworks.uark.edu/etd/2873/
MIOCENE X Y Z CONS	Miocene	Fleming	Geomap (2009)
TRAVIS PEAK	Travis peak	Trinity	https://pubs.usgs.gov/bul/b2184-e/B2184E-508.pdf
FRIO	Frio	Frio	Geomap (2009)
SUB CLARKSVILLE	Clarksville	Clarksville	Geomap (2009)
TOP WOODBINE	Woodbine	Woodbine	Geomap (2009)
TOP SUBCLARKSVILLE	Clarksville	Clarksville	Geomap (2009)
OLMOS	Olmos	Navarro	https://pubs.usgs.gov/dds/dds-069/dds-069-h/REPORTS/69_H_CH_2.pdf
WILCOX	Wilcox	Wilcox	Geomap (2009)
T/MIOCENE	Miocene	Fleming	Geomap (2009)
FRIO	Frio	Frio	Geomap (2009)
FRIO - DISPOSAL	Frio	Frio	Geomap (2009)
FRIO	Frio	Frio	Geomap (2009)
CATAOULA - FRIO	Cataoula	Cataoula	https://pubs.usgs.gov/of/1994/0461/report.pdf
FRIO	Frio	Frio	Geomap (2009)
FRIO SANDS	Frio	Frio	Geomap (2009)
FRIO SANDS	Frio	Frio	Geomap (2009)
MIOCENE	Miocene	Fleming	Geomap (2009)

PECAN GAP	Pecan gap	Taylor	https://scholarworks.uark.edu/cgi/viewcontent.cgi?article=3849&context=etd
MIOCENE - DISPOSAL	Miocene	Fleming	Geomap (2009)
FRIO	Frio	Frio	Geomap (2009)
MIOCENE - DISPOSAL	Miocene	Fleming	Geomap (2009)
VICKSBURG - DISPOSAL	Vicksburg	Vicksburg	Geomap (2009)
MIOCENE	Miocene	Fleming	Geomap (2009)
MIOCENE	Miocene	Fleming	Geomap (2009)
MIOCENE	Miocene	Fleming	Geomap (2009)
FRIO	Frio	Frio	Geomap (2009)
FRIO	Frio	Frio	Geomap (2009)
WILCOX	Wilcox	Wilcox	Geomap (2009)
PECAN GAP	Pecan gap	Taylor	https://scholarworks.uark.edu/cgi/viewcontent.cgi?article=3849&context=etd
PETTIT	Pettet	Trinity	https://pubs.usgs.gov/of/1994/0461/report.pdf
M/ANHYDRITE	Anhydrite	Trinity	https://pubs.geoscienceworld.org/aapg/books/book/1484/chapter-abstract/107178760/Summary-of-Subsurface-Geology-of-Northeast-Texas?redirectedFrom=fulltext
WOODBINE	Woodbine	Woodbine	Geomap (2009)
LOWER PETTIT	Pettet	Trinity	https://pubs.usgs.gov/of/1994/0461/report.pdf
UPPER PETTIT	Pettet	Trinity	https://pubs.usgs.gov/of/1994/0461/report.pdf
LOWER PETTIT	Pettet	Trinity	https://pubs.usgs.gov/of/1994/0461/report.pdf

UPPER PETTIT	Pettet	Trinity	https://pubs.usgs.gov/of/1994/0461/report.pdf
WILCOX	Wilcox	Wilcox	Geomap (2009)
MIOCENE	Miocene	Fleming	Geomap (2009)
T. YEGUA	Yegua	Claiborne	Geomap (2009)
OLMOS	Olmos	Navarro	https://pubs.usgs.gov/dds/dds-069/dds-069-h/REPORTS/69_H_CH_2.pdf
AUSTIN CHALK	Austin Chalk	Austin	Geomap (2009)
YEGUA	Yegua	Claiborne	Geomap (2009)
MIOCENE	Miocene	Fleming	Geomap (2009)
CATAHOULA	Catahoula	Catahoula	https://pubs.usgs.gov/of/1994/0461/report.pdf
OAKVILLE-MIOCENE	Oakeville	Fleming	Geomap (2009)
SIMSBORO	Simsboro	Wilcox	https://pubs.usgs.gov/of/1994/0461/report.pdf
CATAHOULA	Catahoula	Catahoula	https://pubs.usgs.gov/of/1994/0461/report.pdf
GRETA	Greta	Frio	https://scholarworks.uark.edu/etd/2873/
MIOCENE	Miocene	Fleming	Geomap (2009)
TOP OF CATAHOULA	Catahoula	Catahoula	https://pubs.usgs.gov/of/1994/0461/report.pdf
WOODBINE - DISPOSAL	Woodbine	Woodbine	Geomap (2009)

BUDA - H2S	Buda	Washita	Geomap (2009)
AUSTIN CHALK - H2S	Austin Chalk	Austin	Geomap (2009)
CATAHOULA	Catahoula	Catahoula	https://pubs.usgs.gov/of/1994/0461/report.pdf
WOODBINE	Woodbine	Woodbine	Geomap (2009)
CATAHOULA	Catahoula	Catahoula	https://pubs.usgs.gov/of/1994/0461/report.pdf
MIOCENE	Miocene	Fleming	Geomap (2009)
MCFADDIN (4400)	Mcfaddin	Frio	https://www.osti.gov/servlets/purl/140595
CATAHOULA	Catahoula	Catahoula	https://pubs.usgs.gov/of/1994/0461/report.pdf
CATAHOULA	Catahoula	Catahoula	https://pubs.usgs.gov/of/1994/0461/report.pdf
CATAHOULA	Catahoula	Catahoula	https://pubs.usgs.gov/of/1994/0461/report.pdf
FRIO	Frio	Frio	Geomap (2009)
FRIO	Frio	Frio	Geomap (2009)
FRIO	Frio	Frio	Geomap (2009)
WOODBINE	Woodbine	Woodbine	Geomap (2009)
WOODBINE	Woodbine	Woodbine	Geomap (2009)
GOODLAND (LIME)	Goodland	Fredericksburg	https://pubs.usgs.gov/of/2016/1026/ofr20161026.pdf
AUSTIN CHALK	Austin Chalk	Austin	Geomap (2009)

WOODBINE	Woodbine	Woodbine	Geomap (2009)
POTH B IN MIDWAY	Poth	Midway	https://www.beg.utexas.edu/files/publications/contract-reports/CR2013-Nicot-1.pdf
AUSTIN CHALK	Austin Chalk	Austin	Geomap (2009)
AUSTIN CHALK	Austin Chalk	Austin	Geomap (2009)
FRIO SAND	Frio	Frio	Geomap (2009)
COLE	Cole	Jackson	Geomap (2009)
HILL	Not real formation	Rodessa	https://pubs.usgs.gov/of/2016/1026/ofr20161026.pdf
SERPENTINE	Not real formation	Austin	https://www.baylor.edu/geosciences/doc.php/142586.pdf
WOODBINE	Woodbine	Woodbine	Geomap (2009)
FRIO	Frio	Frio	Geomap (2009)
FRIO	Frio	Frio	Geomap (2009)
LOMA NOVIA	Loma novia	Jackson	https://repositories.lib.utexas.edu/bitstream/handle/2152/77978/txu-oclc-612464.pdf?sequence=1
FRIO	Frio	Frio	Geomap (2009)
PECAN GAP	Pecan gap	Taylor	https://scholarworks.uark.edu/cgi/viewcontent.cgi?article=3849&context=etd
WOODBINE	Woodbine	Woodbine	Geomap (2009)
EDWARDS	Edwards	Washita	Geomap (2009)

WOODBINE	Woodbine	Woodbine	Geomap (2009)
AUSTIN CHALK	Austin Chalk	Austin	Geomap (2009)
WOODBINE	Woodbine	Woodbine	Geomap (2009)
BUDA LIME	Buda	Washita	Geomap (2009)
VICKSBURG	Vicksburg	Vicksburg	Geomap (2009)
WASHITA	Washita	Washita	Geomap (2009)
ANAHUAC	Anahuac	Frio	Geomap (2009)
VICKSBURG	Vicksburg	Vicksburg	Geomap (2009)
MIOCENE	Miocene	Fleming	Geomap (2009)
YEGUA	Yegua	Claiborne	Geomap (2009)
FRIO	Frio	Frio	Geomap (2009)
CATAHOULLA	Catahoula	Catahoula	https://pubs.usgs.gov/of/1994/0461/report.pdf
CATAHOULA	Catahoula	Catahoula	https://pubs.usgs.gov/of/1994/0461/report.pdf
RODESSA	Rodessa	Rodessa	https://pubs.usgs.gov/of/2016/1026/ofr20161026.pdf
FRIO	Frio	Frio	Geomap (2009)
RODESSA	Rodessa	Rodessa	https://pubs.usgs.gov/of/2016/1026/ofr20161026.pdf
PETTIT	Pettet	Trinity	https://pubs.usgs.gov/of/1994/0461/report.pdf
WOODBINE	Woodbine	Woodbine	Geomap (2009)

WOODBINE	Woodbine	Woodbine	Geomap (2009)
MIOCENE	Miocene	Fleming	Geomap (2009)
OAKVILLE	Oakeville	Fleming	Geomap (2009)
GRETTA - DISPOSAL	Greta	Frio	https://scholarworks.uark.edu/etd/2873/
FRIO	Frio	Frio	Geomap (2009)
QUEEN CITY	Queen city	Claiborne	Geomap (2009)
MIOCENE	Miocene	Fleming	Geomap (2009)
GOLIAD - INJECTION/ DISPOSAL	Goliad	Goliad	https://citeseerx.ist.psu.edu/document?repid=rep1&type=pdf&doi=d91b2c88ce1ae6fadff51afd823dac7829777e29
FRIO	Frio	Frio	Geomap (2009)
WILCOX	Wilcox	Wilcox	Geomap (2009)
MIOCENE	Miocene	Fleming	Geomap (2009)
CATAHOULA	Catahoula	Catahoula	https://pubs.usgs.gov/of/1994/0461/report.pdf
COLE	Cole	Jackson	Geomap (2009)
GRETA	Greta	Frio	https://scholarworks.uark.edu/etd/2873/
FRIO - DISPOSAL	Frio	Frio	Geomap (2009)
YEGUA	Yegua	Claiborne	Geomap (2009)
MIOCENE 3300	Miocene	Fleming	Geomap (2009)
WILCOX	Wilcox	Wilcox	Geomap (2009)

QUEEN CITY	Queen city	Claiborne	Geomap (2009)
CARRIZO	Carrizo	Wilcox	Geomap (2009)
AUSTIN CHALK	Austin Chalk	Austin	Geomap (2009)
FRIO / MIOCENE	Frio	Frio	Geomap (2009)
FRIO	Frio	Frio	Geomap (2009)
AUSTIN CHALK	Austin Chalk	Austin	Geomap (2009)
BLOSSOM SAND	Blossom	Austin	https://pubs.usgs.gov/of/1994/0461/report.pdf
COLE SAND	Cole	Jackson	Geomap (2009)
LOWER PETTIT	Pettet	Trinity	https://pubs.usgs.gov/of/1994/0461/report.pdf
UPPER PETTIT	Pettet	Trinity	https://pubs.usgs.gov/of/1994/0461/report.pdf
WILCOX	Wilcox	Wilcox	Geomap (2009)
LOWER WILCOX	Wilcox	Wilcox	Geomap (2009)
PETTUS	Pettet	Trinity	https://pubs.usgs.gov/of/1994/0461/report.pdf
WILCOX	Wilcox	Wilcox	Geomap (2009)
CATAHOULA	Catahoula	Catahoula	https://pubs.usgs.gov/of/1994/0461/report.pdf
OLMOS	Olmos	Navarro	https://pubs.usgs.gov/dds/dds-069/dds-069-h/REPORTS/69_H_CH_2.pdf
MIDDLE HET	Heterostegina	Catahoula	https://pubs.usgs.gov/of/1994/0461/report.pdf
COLE	Cole	Jackson	Geomap (2009)

MIOCENE - DISPOSAL	Miocene	Fleming	Geomap (2009)
FRIO	Frio	Frio	Geomap (2009)
MIOCENE	Miocene	Fleming	Geomap (2009)
FRIO	Frio	Frio	Geomap (2009)
CATAHOULA	Catahoula	Catahoula	https://pubs.usgs.gov/of/1994/0461/report.pdf
FRIO	Frio	Frio	Geomap (2009)
WOODBINE	Woodbine	Woodbine	Geomap (2009)
DALE LIME	Dale Lime	Austin	https://pubs.usgs.gov/dds/dds-069/dds-069-h/REPORTS/69_H_CH_2.pdf
MIOCENE 22	Miocene	Fleming	Geomap (2009)
FRIO - DISPOSAL	Frio	Frio	Geomap (2009)
CATAHOULA	Catahoula	Catahoula	https://pubs.usgs.gov/of/1994/0461/report.pdf
WOODBINE	Woodbine	Woodbine	Geomap (2009)
CATAHOULA-FRIO - INJECTION/ DISPOSAL; H2S	Catahoula	Catahoula	https://pubs.usgs.gov/of/1994/0461/report.pdf
FRIO	Frio	Frio	Geomap (2009)
MOODYS BRANCH	Moody branch	Jackson	Geomap (2009)
WOODBINE	Woodbine	Woodbine	Geomap (2009)
RODESSA	Rodessa	Rodessa	https://pubs.usgs.gov/of/2016/1026/ofr20161026.pdf

WILCOX	Wilcox	Wilcox	Geomap (2009)
FRIO	Frio	Frio	Geomap (2009)
ANAHUAC	Anahuac	Frio	Geomap (2009)
CATAHOULA	Catahoula	Catahoula	https://pubs.usgs.gov/of/1994/0461/report.pdf
WOODBINE	Woodbine	Woodbine	Geomap (2009)
CATAHOULA - DISPOSAL	Catahoula	Catahoula	https://pubs.usgs.gov/of/1994/0461/report.pdf
FRIO - DISPOSAL	Frio	Frio	Geomap (2009)
WILCOX	Wilcox	Wilcox	Geomap (2009)
FRIO	Frio	Frio	Geomap (2009)
MIOCENE - DISPOSAL	Miocene	Fleming	Geomap (2009)
GRETA	Greta	Frio	https://scholarworks.uark.edu/etd/2873/
FRIO	Frio	Frio	Geomap (2009)
WILCOX	Wilcox	Wilcox	Geomap (2009)
CATAHOULA	Catahoula	Catahoula	https://pubs.usgs.gov/of/1994/0461/report.pdf
GRETA	Greta	Frio	https://scholarworks.uark.edu/etd/2873/
2ND UPPER COCKFIELD	Cockfield	Claiborne	Geomap (2009)
WILCOX - DISPOSAL	Wilcox	Wilcox	Geomap (2009)
FRIO	Frio	Frio	Geomap (2009)
JACKSON-YEGUA - DISPOSAL	Jackson	Jackson	Geomap (2009)

WOODBINE	Woodbine	Woodbine	Geomap (2009)
DEXTER A	Dexter	Woodbine	https://www.gcags.org/Journal/2016.GCAGS.Journal/2016.GCAGS.Journal.v5.02.p25-46.Vallabhaneni.et.al.pdf
EDWARDS	Edwards	Washita	Geomap (2009)
BUDA	Buda	Washita	Geomap (2009)
RODESSA	Rodessa	Rodessa	https://pubs.usgs.gov/of/2016/1026/ofr20161026.pdf
VICKSBURG	Vicksburg	Vicksburg	Geomap (2009)
BASE AUSTIN	Austin Chalk	Austin	Geomap (2009)
MIOCENE	Miocene	Fleming	Geomap (2009)
YEGUA	Yegua	Claiborne	Geomap (2009)
FRIO	Frio	Frio	Geomap (2009)
GOODLAND	Goodland	Fredericksburg	https://pubs.usgs.gov/of/2016/1026/ofr20161026.pdf
LOWER WILCOX	Wilcox	Wilcox	Geomap (2009)
CARRIZO	Carrizo	Wilcox	Geomap (2009)
TRAVIS PEAK	Travis peak	Trinity	https://pubs.usgs.gov/bul/b2184-e/B2184E-508.pdf
PETTIT	Pettet	Trinity	https://pubs.usgs.gov/of/1994/0461/report.pdf
WOODBINE	Woodbine	Woodbine	Geomap (2009)
FRIO	Frio	Frio	Geomap (2009)
CATAHOULA	Catahoula	Catahoula	https://pubs.usgs.gov/of/1994/0461/report.pdf

MIOCENE	Miocene	Fleming	Geomap (2009)
WOODBINE	Woodbine	Woodbine	Geomap (2009)
MIOCENE	Miocene	Fleming	Geomap (2009)
ANHYDRITE	Anhydrite	Trinity	https://pubs.geoscienceworld.org/aapg/books/book/1484/chapter-abstract/107178760/Summary-of-Subsurface-Geology-of-Northeast-Texas?redirectedFrom=fulltext
BASE AUSTIN CHALK	Austin Chalk	Austin	Geomap (2009)
PETTIT	Pettet	Trinity	https://pubs.usgs.gov/of/1994/0461/report.pdf
GOODLAND LIME	Goodland	Fredericksburg	https://pubs.usgs.gov/of/2016/1026/ofr20161026.pdf
OLMOS	Olmos	Navarro	https://pubs.usgs.gov/dds/dds-069/dds-069-h/REPORTS/69_H_CH_2.pdf
FRIO	Frio	Frio	Geomap (2009)
TOP JACKSON	Jackson	Jackson	Geomap (2009)
RODESSA	Rodessa	Rodessa	https://pubs.usgs.gov/of/2016/1026/ofr20161026.pdf
NAVARRO	Navarro	Navarro	Geomap (2009)
QUEEN CITY	Queen city	Claiborne	Geomap (2009)
YEGUA	Yegua	Claiborne	Geomap (2009)
EDWARDS	Edwards	Washita	Geomap (2009)
OAKVILLE	Oakeville	Fleming	Geomap (2009)

CATAHOULA	Catahoula	Catahoula	https://pubs.usgs.gov/of/1994/0461/report.pdf
CATAHOULA	Catahoula	Catahoula	https://pubs.usgs.gov/of/1994/0461/report.pdf
J SAND	Jackson	Jackson	Geomap (2009)
OAKVILLE	Oakeville	Fleming	Geomap (2009)
SAN MIGUEL 3	San miguel	Taylor	Geomap (2009)
SAN MIGUEL 1	San miguel	Taylor	Geomap (2009)
CATAHOULA	Catahoula	Catahoula	https://pubs.usgs.gov/of/1994/0461/report.pdf
WILCOX	Wilcox	Wilcox	Geomap (2009)
FREDERICKSBURG	Fredericksburg	Fredericksburg	Geomap (2009)
CATAHOULA	Catahoula	Catahoula	https://pubs.usgs.gov/of/1994/0461/report.pdf
FRIO (TOP)	Frio	Frio	Geomap (2009)
CATAHOULA	Catahoula	Catahoula	https://pubs.usgs.gov/of/1994/0461/report.pdf
OAKVILLE	Oakeville	Fleming	Geomap (2009)
CATAHOULA	Catahoula	Catahoula	https://pubs.usgs.gov/of/1994/0461/report.pdf
CATAHOULA	Catahoula	Catahoula	https://pubs.usgs.gov/of/1994/0461/report.pdf
DUCK CREEK	Duck creek	Washita	https://www.twdb.texas.gov/publications/reports/numbered_reports/doc/R314/Report%20314.pdf
MARGINULINA	Margulina	Fleming	Geomap (2009)

FRIO	Frio	Frio	Geomap (2009)
FRIO	Frio	Frio	Geomap (2009)
GRETA SAND	Greta	Frio	https://scholarworks.uark.edu/etd/2873/
FRIO	Frio	Frio	Geomap (2009)
MARG	Margulina	Fleming	Geomap (2009)
NACATOCH	Nacatoch	Navarro	https://repositories.lib.utexas.edu/bitstream/handle/2152/77501/txu-oclc-10367600.pdf?sequence=1
WOODBINE	Woodbine	Woodbine	Geomap (2009)
FRIO 25	Frio	Frio	Geomap (2009)
WOODBINE	Woodbine	Woodbine	Geomap (2009)
CARRIZO	Carrizo	Wilcox	Geomap (2009)
CARRIZO	Carrizo	Wilcox	Geomap (2009)
MASSIVE WILCOX	Wilcox	Wilcox	Geomap (2009)
WOODBINE	Woodbine	Woodbine	Geomap (2009)
NACATOCH	Nacatoch	Navarro	https://repositories.lib.utexas.edu/bitstream/handle/2152/77501/txu-oclc-10367600.pdf?sequence=1
FRIO	Frio	Frio	Geomap (2009)
PETTUS	Pettet	Trinity	https://pubs.usgs.gov/of/1994/0461/report.pdf
GOODLAND LIME	Goodland	Fredericksburg	https://pubs.usgs.gov/of/2016/1026/ofr20161026.pdf
HUSLEY(PALUXY)	Paluxy	Fredericksburg	Geomap (2009)

HUXLEY(6100)	Paluxy	Fredericksburg	Geomap (2009)
DUCK CREEK	Duck creek	Washita	https://www.twdb.texas.gov/publications/reports/numbered_reports/doc/R314/Report%20314.pdf
CATAHOULA	Catahoula	Catahoula	https://pubs.usgs.gov/of/1994/0461/report.pdf
WALES	Not real formation	Wilcox	https://www.gcags.org/Journal/2017.GCAGS.Journal/2017.GCAGS.Journal.v6.10.p150-160.Hamilton.and.Gottardi.pdf
MULA	Not real formation	La Mula	https://pubs.usgs.gov/circ/1985/0943/report.pdf
PETTUS	Pettet	Trinity	https://pubs.usgs.gov/of/1994/0461/report.pdf
SMACKOVER	Smack over	Smack over	Geomap (2009)
FRIO	Frio	Frio	Geomap (2009)
CATAHOULA	Catahoula	Catahoula	https://pubs.usgs.gov/of/1994/0461/report.pdf
MIOCENE	Miocene	Fleming	Geomap (2009)
CATAHOULA	Catahoula	Catahoula	https://pubs.usgs.gov/of/1994/0461/report.pdf
CATAHOUA	Catahoula	Catahoula	https://pubs.usgs.gov/of/1994/0461/report.pdf
ELLENBERGER	Ellenburger	Ellenberger	file:///C:/Users/okeziec.old/Downloads/Thesis-1988-A518d%20(2).pdf
BARNETT	Barnet	Barnett	file:///C:/Users/okeziec.old/Downloads/Thesis-1988-A518d%20(2).pdf
WOODBINE	Woodbine	Woodbine	Geomap (2009)

CATAHOULA	Catahoula	Catahoula	https://pubs.usgs.gov/of/1994/0461/report.pdf
RODESSA	Rodessa	Rodessa	https://pubs.usgs.gov/of/2016/1026/ofr20161026.pdf
MIOCENE	Miocene	Fleming	Geomap (2009)
RODESSA	Rodessa	Rodessa	https://pubs.usgs.gov/of/2016/1026/ofr20161026.pdf
OAKVILLE	Oakeville	Fleming	Geomap (2009)
CATAHOULA	Catahoula	Catahoula	https://pubs.usgs.gov/of/1994/0461/report.pdf
CATAHOULA	Catahoula	Catahoula	https://pubs.usgs.gov/of/1994/0461/report.pdf
AUSTIN CHALK	Austin Chalk	Austin	Geomap (2009)
DALE LIME	Dale Lime	Austin	https://pubs.usgs.gov/dds/dds-069/dds-069-h/REPORTS/69_H_CH_2.pdf
MARG	Margulina	Fleming	Geomap (2009)
FRIO	Frio	Frio	Geomap (2009)
MASSIVE	Anhydrite	Trinity	https://pubs.geoscienceworld.org/aapg/books/book/1484/chapter-abstract/107178760/Summary-of-Subsurface-Geology-of-Northeast-Texas?redirectedFrom=fulltext
WOLFE CITY	Wolfe city	Taylor	https://scholarworks.uark.edu/cgi/viewcontent.cgi?article=3849&context=etd
MIOCENE	Miocene	Fleming	Geomap (2009)
PETTIT	Pettet	Trinity	https://pubs.usgs.gov/of/1994/0461/report.pdf
FRIO	Frio	Frio	Geomap (2009)
WILCOX - DISPOSAL	Wilcox	Wilcox	Geomap (2009)

FLEMING	Fleming	Fleming	Geomap (2009)
MIOCENE M10	Miocene	Fleming	Geomap (2009)
ANAHUAC	Anahuac	Frio	Geomap (2009)
LOWER WILCOX	Wilcox	Wilcox	Geomap (2009)
MIOCENE 8	Miocene	Fleming	Geomap (2009)
CATAHOULA	Catahoula	Catahoula	https://pubs.usgs.gov/of/1994/0461/report.pdf
COCKFIELD R	Cockfield	Claiborne	Geomap (2009)
COCKFIELD S	Cockfield	Claiborne	Geomap (2009)
EDWARDS LIME	Edwards	Washita	Geomap (2009)
WHIT BAINS	Whiting basin	Louann Salt	https://scholarworks.sfasu.edu/cgi/viewcontent.cgi?article=1106&context=etds
FRIO-NOT LOGGED IN OPEN HOLE(BEHIND SURFACE CASING	Frio	Frio	Geomap (2009)
RODESSA	Rodessa	Rodessa	https://pubs.usgs.gov/of/2016/1026/ofr20161026.pdf
ELLENBURGER	Ellenburger	Ellenberger	file:///C:/Users/okeziec.old/Downloads/Thesis-1988-A518d%20(2).pdf
MIOCENE M10	Miocene	Fleming	Geomap (2009)

ELLENBURGER	Ellenburger	Ellenberger	file:///C:/Users/okeziec.old/Downloads/Thesis-1988-A518d%20(2).pdf
RODESSA	Rodessa	Rodessa	https://pubs.usgs.gov/of/2016/1026/ofr20161026.pdf
BASE MASSIVE	Anhydrite	Trinity	https://pubs.geoscienceworld.org/aapg/books/book/1484/chapter-abstract/107178760/Summary-of-Subsurface-Geology-of-Northeast-Texas?redirectedFrom=fulltext
PALUXY	Paluxy	Fredericksburg	Geomap (2009)
ANAHUAC	Anahuac	Frio	Geomap (2009)
EAGLEFORD	Eagleford	Eagleford	Geomap (2009)
PETTUS	Pettet	Trinity	https://pubs.usgs.gov/of/1994/0461/report.pdf
COLE SANDS	Cole	Jackson	Geomap (2009)
BLOSSOM SAND	Blossom	Austin	https://pubs.usgs.gov/of/1994/0461/report.pdf
COCKFIELD	Cockfield	Claiborne	Geomap (2009)
FRIO	Frio	Frio	Geomap (2009)
JETER	Not real formation	Rodessa	https://pubs.usgs.gov/of/2016/1026/ofr20161026.pdf
MIOCENE	Miocene	Fleming	Geomap (2009)
GRETA	Greta	Frio	https://scholarworks.uark.edu/etd/2873/
WASHITA	Washita	Washita	Geomap (2009)
MIOCENE	Miocene	Fleming	Geomap (2009)

VICKSBURG	Vicksburg	Vicksburg	Geomap (2009)
2ND UPPER COCKFIELD	Cockfield	Claiborne	Geomap (2009)
SECOND UPPER COCKFIELD	Cockfield	Claiborne	Geomap (2009)
MOODY'S BRANCH	Moody branch	Jackson	Geomap (2009)
TOP WOODBINE	Woodbine	Woodbine	Geomap (2009)
MIOCENE	Miocene	Fleming	Geomap (2009)
TRIO	Frio	Frio	Geomap (2009)
YEGUA	Yegua	Claiborne	Geomap (2009)
ANNONA	Annona	Taylor	https://pubs.usgs.gov/of/1994/0461/report.pdf
2ND UPPER COCKFIELD	Cockfield	Claiborne	Geomap (2009)
ANAHUAC - DISPOSAL	Anahuac	Frio	Geomap (2009)
FRIO 1	Frio	Frio	Geomap (2009)
PALUXY	Paluxy	Fredericksburg	Geomap (2009)
LOWER WILCOX SANDS	Wilcox	Wilcox	Geomap (2009)

RODESSA	Rodessa	Rodessa	https://pubs.usgs.gov/of/2016/1026/ofr20161026.pdf
RODESSA	Rodessa	Rodessa	https://pubs.usgs.gov/of/2016/1026/ofr20161026.pdf
BUDA	Buda	Washita	Geomap (2009)
GRETA	Greta	Frio	https://scholarworks.uark.edu/etd/2873/
WOODBINE	Woodbine	Woodbine	Geomap (2009)
YEGUA	Yegua	Claiborne	Geomap (2009)
CATAHULA	Catahoula	Catahoula	https://pubs.usgs.gov/of/1994/0461/report.pdf
MIOCENE C	Miocene	Fleming	Geomap (2009)
SERPENTINE	Not real formation	Austin	https://www.baylor.edu/geosciences/doc.php/142586.pdf
SERPENTINE	Not real formation	Austin	https://www.baylor.edu/geosciences/doc.php/142586.pdf
WOODBINE	Woodbine	Woodbine	Geomap (2009)
MASSIVE HOCKLEY	Hockley (Hockleyensis)	Jackson	https://www.twdb.texas.gov/groundwater/models/gam/ygjk/YGJK_Structure_Report.pdf
ATKINSON	Atkinson	Woodbine	http://ufdcimages.uflib.ufl.edu/UF/00/00/11/20/00001/UF00001120.pdf
WOODBINE	Woodbine	Woodbine	Geomap (2009)

SECOND UPPER COCKFIELD	Cockfield	Claiborne	Geomap (2009)
MAIN CONROE 1A	Hockley (Hockleyensis)	Jackson	https://www.twdb.texas.gov/groundwater/models/gam/ygjk/YGJK_Structure_Report.pdf
FIRST UPPER COCKFIELD	Cockfield	Claiborne	Geomap (2009)
MCFADDIN (3200)	Mcfaddin	Frio	https://www.osti.gov/servlets/purl/140595
FRIO - DISPOSAL	Frio	Frio	Geomap (2009)
AUSTIN CHALK	Austin Chalk	Austin	Geomap (2009)
WOODBINE	Woodbine	Woodbine	Geomap (2009)
VICKSBURG	Vicksburg	Vicksburg	Geomap (2009)
FRIO	Frio	Frio	Geomap (2009)
RODESSA	Rodessa	Rodessa	https://pubs.usgs.gov/of/2016/1026/ofr20161026.pdf
RODESSA	Rodessa	Rodessa	https://pubs.usgs.gov/of/2016/1026/ofr20161026.pdf
MASSIVE ANHYDRITE	Anhydrite	Trinity	https://pubs.geoscienceworld.org/aapg/books/book/1484/chapter-abstract/107178760/Summary-of-Subsurface-Geology-of-Northeast-Texas?redirectedFrom=fulltext
RODESSA	Rodessa	Rodessa	https://pubs.usgs.gov/of/2016/1026/ofr20161026.pdf
WOODBINE	Woodbine	Woodbine	Geomap (2009)

GRETA	Greta	Frio	https://scholarworks.uark.edu/etd/2873/
UNDIFFERENTIATED FRIO	Frio	Frio	Geomap (2009)
OAKEVILLE MEMBER-MIOCENE	Oakeville	Fleming	Geomap (2009)
MIOCENE FLEMING-OAKVILLE MBR.	Miocene	Fleming	Geomap (2009)
RODESSA	Rodessa	Rodessa	https://pubs.usgs.gov/of/2016/1026/ofr20161026.pdf
FRIO	Frio	Frio	Geomap (2009)
OAKVILLE MEMBER MIOCENE	Oakeville	Fleming	Geomap (2009)
OAKVILLE MEMBER MIOCENE SANDS	Oakeville	Fleming	Geomap (2009)
EVANGELINE	Evangeline	Goliad	https://citeseerx.ist.psu.edu/document?repid=rep1&type=pdf&doi=d91b2c88ce1ae6fadff51afd823dac7829777e29
FRIO 1A	Frio	Frio	Geomap (2009)
FRIO	Frio	Frio	Geomap (2009)
CATAHOULA	Catahoula	Catahoula	https://pubs.usgs.gov/of/1994/0461/report.pdf
OLMOS	Olmos	Navarro	https://pubs.usgs.gov/dds/dds-069/dds-069-h/REPORTS/69_H_CH_2.pdf
WOODBINE	Woodbine	Woodbine	Geomap (2009)
HOCKLEY	Hockley (Hockl	Jackson	https://www.twdb.texas.gov/groundwater/models/gam/ygjk/YGJK_Structure_Report.pdf

	eyensis)		
VICKSBURG	Vicksburg	Vicksburg	Geomap (2009)
ESCONDIDO	Escondido	Escondido	Geomap (2009)
MIOCENE	Miocene	Fleming	Geomap (2009)
FREDERICKSBURG	Fredericksburg	Fredericksburg	Geomap (2009)
FRIO	Frio	Frio	Geomap (2009)
BMA	Anhydrite	Trinity	https://pubs.geoscienceworld.org/aapg/books/book/1484/chapter-abstract/107178760/Summary-of-Subsurface-Geology-of-Northeast-Texas?redirectedFrom=fulltext
HACKBERRY	Hackberry	Frio	Geomap (2009)
NODOSARIA	Nodosaria	Frio	Geomap (2009)
MIOCENE	Miocene	Fleming	Geomap (2009)
RODESSA	Rodessa	Rodessa	https://pubs.usgs.gov/of/2016/1026/ofr20161026.pdf
OLMOS	Olmos	Navarro	https://pubs.usgs.gov/dds/dds-069/dds-069-h/REPORTS/69_H_CH_2.pdf
CATAHOULA	Catahoula	Catahoula	https://pubs.usgs.gov/of/1994/0461/report.pdf
WOODBINE	Woodbine	Woodbine	Geomap (2009)
MIOCENE B	Miocene	Fleming	Geomap (2009)
AUSTIN CHALK	Austin Chalk	Austin	Geomap (2009)

TRAVIS PEAK	Travis peak	Trinity	https://pubs.usgs.gov/bul/b2184-e/B2184E-508.pdf
WOODBINE B	Woodbine	Woodbine	Geomap (2009)
1ST QUEEN CITY	Queen city	Claiborne	Geomap (2009)
RODESSA	Rodessa	Rodessa	https://pubs.usgs.gov/of/2016/1026/ofr20161026.pdf
MIRANDO SAND	Mirando	Jackson	https://repositories.lib.utexas.edu/bitstream/handle/2152/77978/txu-oclc-612464.pdf?sequence=1
T/JACKSON	Jackson	Jackson	Geomap (2009)
FRIO	Frio	Frio	Geomap (2009)
YEGUA	Yegua	Claiborne	Geomap (2009)
PALUXY	Paluxy	Fredericksburg	Geomap (2009)
WILCOX	Wilcox	Wilcox	Geomap (2009)
MIOCENE	Miocene	Fleming	Geomap (2009)
HET	Heterostegina	Catahoula	https://pubs.usgs.gov/of/1994/0461/report.pdf
WOODBINE	Woodbine	Woodbine	Geomap (2009)
DUCK CREEK LIME	Duck creek	Washita	https://www.twdb.texas.gov/publications/reports/numbered_reports/doc/R314/Report%20314.pdf
MIOCENE - DISPOSAL	Miocene	Fleming	Geomap (2009)
MIOCENE	Miocene	Fleming	Geomap (2009)

WOODBINE	Woodbine	Woodbine	Geomap (2009)
KIAMICHI	Kiamichi	Fredericksburg	Geomap (2009)
LOWER EDWARDS	Edwards	Washita	Geomap (2009)
U. MIOCENE	Miocene	Fleming	Geomap (2009)
CATAHOULA	Catahoula	Catahoula	https://pubs.usgs.gov/of/1994/0461/report.pdf
AUSTIN CHALK	Austin Chalk	Austin	Geomap (2009)
WILCOX	Wilcox	Wilcox	Geomap (2009)
CARRIZO	Carrizo	Wilcox	Geomap (2009)
MIOCENE - DISPOSAL	Miocene	Fleming	Geomap (2009)
GRETA	Greta	Frio	https://scholarworks.uark.edu/etd/2873/
FRIO	Frio	Frio	Geomap (2009)
BAC	Austin Chalk	Austin	Geomap (2009)
LEWISVILLE B	Lewisville	Eagleford	https://carrresources.com/wp-content/uploads/2020/08/Regional-Woodbine.pdf
FRIO TOP	Frio	Frio	Geomap (2009)
COCKFIELD	Cockfield	Claiborne	Geomap (2009)
YEGUA 3800	Yegua	Claiborne	Geomap (2009)
BUCKNER	Buckner	Buckner	Geomap (2009)
VICKSBURG	Vicksburg	Vicksburg	Geomap (2009)

VICKSBURG	Vicksburg	Vicksburg	Geomap (2009)
MIOCENE 4900	Miocene	Fleming	Geomap (2009)
LOWER FRIO/UPPER VICKSBURG	Frio	Frio	Geomap (2009)
WILCOX	Wilcox	Wilcox	Geomap (2009)
LOWER EDWARDS	Edwards	Washita	Geomap (2009)
SAN MIGUEL #1 SAND	San miguel	Taylor	Geomap (2009)
GRETA	Greta	Frio	https://scholarworks.uark.edu/etd/2873/
FRIO TOP	Frio	Frio	Geomap (2009)
GRETA	Greta	Frio	https://scholarworks.uark.edu/etd/2873/
FRIO TOP	Frio	Frio	Geomap (2009)
LOWER EDWARDS	Edwards	Washita	Geomap (2009)
PALUXY	Paluxy	Fredericksburg	Geomap (2009)
AUSTIN CHALK	Austin Chalk	Austin	Geomap (2009)
PALUXY	Paluxy	Fredericksburg	Geomap (2009)
FREDERICKSBURG	Fredericksburg	Fredericksburg	Geomap (2009)
BAC (BASE AC)	Austin Chalk	Austin	Geomap (2009)

EAGLE FORD SH	Eagleford	Eagleford	Geomap (2009)
FRIO	Frio	Frio	Geomap (2009)
GLEN ROSE	Glen rose	Trinity	Geomap (2009)
TOP FRIO	Frio	Frio	Geomap (2009)
LOWER WILCOX	Wilcox	Wilcox	Geomap (2009)
AUSTIN CHALK	Austin Chalk	Austin	Geomap (2009)
GEORGETOWN	George town	Washita	Geomap (2009)
FRIO 5450	Frio	Frio	Geomap (2009)
FRIO A1	Frio	Frio	Geomap (2009)
QUEEN CITY	Queen city	Claiborne	Geomap (2009)
VICKSBURG 100	Vicksburg	Vicksburg	Geomap (2009)
WILCOX	Wilcox	Wilcox	Geomap (2009)
AUSTIN CHALK	Austin Chalk	Austin	Geomap (2009)
SERPENTINE	Not real formation	Austin	https://www.baylor.edu/geosciences/doc.php/142586.pdf
ANACACHO	Anacacho	Taylor	Geomap (2009)
QUEEN CITY	Queen city	Claiborne	Geomap (2009)
WOODBINE	Woodbine	Woodbine	Geomap (2009)
FRIO	Frio	Frio	Geomap (2009)

FRIO TOP	Frio	Frio	Geomap (2009)
QUEEN CITY	Queen city	Claiborne	Geomap (2009)
MASSIVE WX	Wilcox	Wilcox	Geomap (2009)
GRETA	Greta	Frio	https://scholarworks.uark.edu/etd/2873/
WOODBINE	Woodbine	Woodbine	Geomap (2009)
Y-2	Yegua	Claiborne	Geomap (2009)
WILCOX - DISPOSAL	Wilcox	Wilcox	Geomap (2009)
AUSTIN CHALK	Austin Chalk	Austin	Geomap (2009)
WOODBINE	Woodbine	Woodbine	Geomap (2009)
WILCOX	Wilcox	Wilcox	Geomap (2009)
MIOCENE - DISPOSAL	Miocene	Fleming	Geomap (2009)
OLMOS	Olmos	Navarro	https://pubs.usgs.gov/dds/dds-069/dds-069-h/REPORTS/69_H_CH_2.pdf
GLEN ROSE	Glen rose	Trinity	Geomap (2009)
MIDDLE FRIO	Frio	Frio	Geomap (2009)
WILCOX	Wilcox	Wilcox	Geomap (2009)
SAN MIGUEL	San miguel	Taylor	Geomap (2009)
QUEEN CITY	Queen city	Claiborne	Geomap (2009)
FRIO TOP	Frio	Frio	Geomap (2009)

TOP EDWARDS	Edwards	Washita	Geomap (2009)
FRIO TOP	Frio	Frio	Geomap (2009)
GRETA	Greta	Frio	https://scholarworks.uark.edu/etd/2873/
EDWARDS	Edwards	Washita	Geomap (2009)
3900 MICCENE	Miocene	Fleming	Geomap (2009)
OLMOS	Olmos	Navarro	https://pubs.usgs.gov/dds/dds-069/dds-069-h/REPORTS/69_H_CH_2.pdf
OLMOS	Olmos	Navarro	https://pubs.usgs.gov/dds/dds-069/dds-069-h/REPORTS/69_H_CH_2.pdf
WOODBINE	Woodbine	Woodbine	Geomap (2009)
HOCKLEY	Hockley (Hockleyensis)	Jackson	https://www.twdb.texas.gov/groundwater/models/gam/ygjk/YGJK_Structure_Report.pdf
TOP QUEEN CITY	Queen city	Claiborne	Geomap (2009)
CATAHOULA	Catahoula	Catahoula	https://pubs.usgs.gov/of/1994/0461/report.pdf
FRIO	Frio	Frio	Geomap (2009)
OLMOS	Olmos	Navarro	https://pubs.usgs.gov/dds/dds-069/dds-069-h/REPORTS/69_H_CH_2.pdf
LOW EDWARDS	Edwards	Washita	Geomap (2009)
MIRANDO SAND	Mirando	Jackson	https://repositories.lib.utexas.edu/bitstream/handle/2152/77978/txu-oclc-612464.pdf?sequence=1
HETEROSTEGINA	Heterostegina	Catahoula	https://pubs.usgs.gov/of/1994/0461/report.pdf

MARGINULINA 2	Marguline	Fleming	Geomap (2009)
POTH	Poth	Midway	https://www.beg.utexas.edu/files/publications/contract-reports/CR2013-Nicot-1.pdf
FRIO (F-1)	Frio	Frio	Geomap (2009)
WOODBINE	Woodbine	Woodbine	Geomap (2009)
FRIO	Frio	Frio	Geomap (2009)
WILCOX	Wilcox	Wilcox	Geomap (2009)
MARG A SAND	Marguline	Fleming	Geomap (2009)
AUSTIN CHALK	Austin Chalk	Austin	Geomap (2009)
WILCOX	Wilcox	Wilcox	Geomap (2009)
WILCOX	Wilcox	Wilcox	Geomap (2009)
KIAMICHI	Kiamichi	Fredericksburg	Geomap (2009)
LOWER EDWARDS	Edwards	Washita	Geomap (2009)
LOWER WOODBINE	Woodbine	Woodbine	Geomap (2009)
EDWARDS	Edwards	Washita	Geomap (2009)
EDWARDS	Edwards	Washita	Geomap (2009)
HOCKLEY C	Hockley (Hockleyensis)	Jackson	https://www.twdb.texas.gov/groundwater/models/gam/ygjk/YGJK_Structure_Report.pdf

EDWARDS	Edwards	Washita	Geomap (2009)
MIDWAY	Midway	Midway	https://pubs.usgs.gov/of/1994/0461/report.pdf
MIRANDO	Miranda	Jackson	https://repositories.lib.utexas.edu/bitstream/handle/2152/77978/txu-oclc-612464.pdf?sequence=1
CATAHOULA	Catahoula	Catahoula	https://pubs.usgs.gov/of/1994/0461/report.pdf
FRIO	Frio	Frio	Geomap (2009)
WILCOX (TOP OF LOGGED INTERVAL)	Wilcox	Wilcox	Geomap (2009)
WOODBINE	Woodbine	Woodbine	Geomap (2009)
WILCOX (TOP OF LOGGED INTERVAL)	Wilcox	Wilcox	Geomap (2009)
PETTIT	Pettet	Trinity	https://pubs.usgs.gov/of/1994/0461/report.pdf
GRETA	Greta	Frio	https://scholarworks.uark.edu/etd/2873/
NAVARRO	Navarro	Navarro	Geomap (2009)
NAVARRO	Navarro	Navarro	Geomap (2009)
NAVARRO	Navarro	Navarro	Geomap (2009)
NAVARRO	Navarro	Navarro	Geomap (2009)
NAVARRO	Navarro	Navarro	Geomap (2009)
NAVARRO	Navarro	Navarro	Geomap (2009)

NAVARRO	Navarro	Navarro	Geomap (2009)
NAVARRO	Navarro	Navarro	Geomap (2009)
NAVARRO	Navarro	Navarro	Geomap (2009)
NAVARRO	Navarro	Navarro	Geomap (2009)
FRIO TOP	Frio	Frio	Geomap (2009)
CHICOT	Chicot	Chicot	https://www.twdb.texas.gov/publications/reports/numbered_reports/doc/R236/R236.pdf
WOODBINE	Woodbine	Woodbine	Geomap (2009)
TOP OF GRETA	Greta	Frio	https://scholarworks.uark.edu/etd/2873/
FRIO	Frio	Frio	Geomap (2009)
WILCOX	Wilcox	Wilcox	Geomap (2009)
GRETA	Greta	Frio	https://scholarworks.uark.edu/etd/2873/
WILCOX	Wilcox	Wilcox	Geomap (2009)
OLMOS	Olmos	Navarro	https://pubs.usgs.gov/dds/dds-069/dds-069-h/REPORTS/69_H_CH_2.pdf
WILCOX	Wilcox	Wilcox	Geomap (2009)
SAN MIGUEL A	San miguel	Taylor	Geomap (2009)
FRIO	Frio	Frio	Geomap (2009)
TOP WOODBINE SAND	Woodbine	Woodbine	Geomap (2009)
FRIO	Frio	Frio	Geomap (2009)
GRETA	Greta	Frio	https://scholarworks.uark.edu/etd/2873/
BASE OF GRETA	Greta	Frio	https://scholarworks.uark.edu/etd/2873/

MIOCENE	Miocene	Fleming	Geomap (2009)
FRIO	Frio	Frio	Geomap (2009)
EDWARDS LIME	Edwards	Washita	Geomap (2009)
WILCOX	Wilcox	Wilcox	Geomap (2009)
OAKVILLE	Oakeville	Fleming	Geomap (2009)
WILCOX	Wilcox	Wilcox	Geomap (2009)
WILCOX	Wilcox	Wilcox	Geomap (2009)
CATAHOULA	Catahoula	Catahoula	https://pubs.usgs.gov/of/1994/0461/report.pdf
DEL RIO	Del rio	Washita	Geomap (2009)
MIOCENE	Miocene	Fleming	Geomap (2009)
CARRIZO	Carrizo	Wilcox	Geomap (2009)
L/WILCOX	Wilcox	Wilcox	Geomap (2009)
T. OF BUDA	Buda	Washita	Geomap (2009)
1ST MIRANDO	Mirando	Jackson	https://repositories.lib.utexas.edu/bitstream/handle/2152/77978/txu-oclc-612464.pdf?sequence=1
WILCOX - DISPOSAL	Wilcox	Wilcox	Geomap (2009)
WILCOX - DISPOSAL	Wilcox	Wilcox	Geomap (2009)
WILCOX - DISPOSAL	Wilcox	Wilcox	Geomap (2009)
MIOCENE MARKER 11	Miocene	Fleming	Geomap (2009)

MIOCENE MARKER 12	Miocene	Fleming	Geomap (2009)
FRIO	Frio	Frio	Geomap (2009)
CATAHOULA	Catahoula	Catahoula	https://pubs.usgs.gov/of/1994/0461/report.pdf
FRIO C	Frio	Frio	Geomap (2009)
WOODBINE	Woodbine	Woodbine	Geomap (2009)
EDWARDS TOP	Edwards	Washita	Geomap (2009)
WOODBINE	Woodbine	Woodbine	Geomap (2009)
PETTIT	Pettet	Trinity	https://pubs.usgs.gov/of/1994/0461/report.pdf
FRIO	Frio	Frio	Geomap (2009)
WILCOX	Wilcox	Wilcox	Geomap (2009)
EDWARDS	Edwards	Washita	Geomap (2009)
CARRIZO	Carrizo	Wilcox	Geomap (2009)
OAKVILLE SAND	Oakeville	Fleming	Geomap (2009)
RODESSA	Rodessa	Rodessa	https://pubs.usgs.gov/of/2016/1026/ofr20161026.pdf
BASE GRETA	Greta	Frio	https://scholarworks.uark.edu/etd/2873/
WILCOX	Wilcox	Wilcox	Geomap (2009)
MIDDLE MIOCENE	Miocene	Fleming	Geomap (2009)
AUSTIN CHALK	Austin Chalk	Austin	Geomap (2009)

TOP OF HACKBERRY	Hackberry	Frio	Geomap (2009)
OLMOS	Olmos	Navarro	https://pubs.usgs.gov/dds/dds-069/dds-069-h/REPORTS/69_H_CH_2.pdf
MIOCENE TOP	Miocene	Fleming	Geomap (2009)
GRETA SAND	Greta	Frio	https://scholarworks.uark.edu/etd/2873/
MIDDLE WILCOX	Wilcox	Wilcox	Geomap (2009)
TRAVIS PEAK	Travis peak	Trinity	https://pubs.usgs.gov/bul/b2184-e/B2184E-508.pdf
GRETA SAND	Greta	Frio	https://scholarworks.uark.edu/etd/2873/
MIRANDO SAND	Mirando	Jackson	https://repositories.lib.utexas.edu/bitstream/handle/2152/77978/txu-oclc-612464.pdf?sequence=1
EDWARDS	Edwards	Washita	Geomap (2009)
JACKSON	Jackson	Jackson	Geomap (2009)
WILCOX	Wilcox	Wilcox	Geomap (2009)
GRETA	Greta	Frio	https://scholarworks.uark.edu/etd/2873/
OLMOS	Olmos	Navarro	https://pubs.usgs.gov/dds/dds-069/dds-069-h/REPORTS/69_H_CH_2.pdf
YEGUA	Yegua	Claiborne	Geomap (2009)
GOVT. WELLS	Government wells	Jackson	https://repositories.lib.utexas.edu/bitstream/handle/2152/77978/txu-oclc-612464.pdf?sequence=1
1 ST MIRANDO	Mirando	Jackson	https://repositories.lib.utexas.edu/bitstream/handle/2152/77978/txu-oclc-612464.pdf?sequence=1

MIOCENE B	Miocene	Fleming	Geomap (2009)
VICKSBURG	Vicksburg	Vicksburg	Geomap (2009)
EDWARDS	Edwards	Washita	Geomap (2009)
AUSTIN CHALK	Austin Chalk	Austin	Geomap (2009)
EDWARDS - H2S	Edwards	Washita	Geomap (2009)
AUSTIN CHALK	Austin Chalk	Austin	Geomap (2009)
TRAVIS PEAK	Travis peak	Trinity	https://pubs.usgs.gov/bul/b2184-e/B2184E-508.pdf
WILCOX	Wilcox	Wilcox	Geomap (2009)
GLEN ROSE - DISPOSAL	Glen rose	Trinity	Geomap (2009)
WILCOX	Wilcox	Wilcox	Geomap (2009)
WILCOX	Wilcox	Wilcox	Geomap (2009)
CATAHOULA	Catahoula	Catahoula	https://pubs.usgs.gov/of/1994/0461/report.pdf
GRETA	Greta	Frio	https://scholarworks.uark.edu/etd/2873/
WOODBINE	Woodbine	Woodbine	Geomap (2009)
GRETTA - DISPOSAL	Greta	Frio	https://scholarworks.uark.edu/etd/2873/
RODESSA	Rodessa	Rodessa	https://pubs.usgs.gov/of/2016/1026/ofr20161026.pdf
GOODLAND LIME	Goodland	Fredericksburg	https://pubs.usgs.gov/of/2016/1026/ofr20161026.pdf
MIOCENE	Miocene	Fleming	Geomap (2009)

MIRANDO SAND	Mirando	Jackson	https://repositories.lib.utexas.edu/bitstream/handle/2152/77978/txu-oclc-612464.pdf?sequence=1
EDWARDS	Edwards	Washita	Geomap (2009)
BUDA	Buda	Washita	Geomap (2009)
MIOCENE B	Miocene	Fleming	Geomap (2009)
MIOCENE C	Miocene	Fleming	Geomap (2009)
FRIO	Frio	Frio	Geomap (2009)
TRAVIS PEAK	Travis peak	Trinity	https://pubs.usgs.gov/bul/b2184-e/B2184E-508.pdf
GLEN ROSE	Glen rose	Trinity	Geomap (2009)
EDWARDS	Edwards	Washita	Geomap (2009)
GEORGETOWN	George town	Washita	Geomap (2009)
COLE	Cole	Jackson	Geomap (2009)
EDWARDS	Edwards	Washita	Geomap (2009)
WILCOX	Wilcox	Wilcox	Geomap (2009)
WILCOX	Wilcox	Wilcox	Geomap (2009)
QUEEN CITY	Queen city	Claiborne	Geomap (2009)
WOODBINE	Woodbine	Woodbine	Geomap (2009)
DEXTER	Dexter	Woodbine	https://www.gcags.org/Journal/2016.GCAGS.Journal/2016.GCAGS.Journal.v5.02.p25-46.Vallabhaneni.et.al.pdf
MIDDLE MIOCENE	Miocene	Fleming	Geomap (2009)

TRAVIS PEAK	Travis peak	Trinity	https://pubs.usgs.gov/bul/b2184-e/B2184E-508.pdf
NAVARRO - DISPOSAL	Navarro	Navarro	Geomap (2009)
NAVARRO	Navarro	Navarro	Geomap (2009)
NAVARRO	Navarro	Navarro	Geomap (2009)
NAVARRO	Navarro	Navarro	Geomap (2009)
TOP LOWER WILCOX	Wilcox	Wilcox	Geomap (2009)
WOODBINE	Woodbine	Woodbine	Geomap (2009)
NAVARRO	Navarro	Navarro	Geomap (2009)
N	Navaro	Navarro	Geomap (2009)
NAVARRO	Navarro	Navarro	Geomap (2009)
WOODBINE	Woodbine	Woodbine	Geomap (2009)
EDWARDS	Edwards	Washita	Geomap (2009)
NAVRRO	Navarro	Navarro	Geomap (2009)
CATAHOULA	Catahoula	Catahoula	https://pubs.usgs.gov/of/1994/0461/report.pdf
WILCOX_LOWER	Wilcox	Wilcox	Geomap (2009)
NAVARRO - DISPOSAL	Navarro	Navarro	Geomap (2009)

NAVARRO	Navarro	Navarro	Geomap (2009)
TOP OF WILCOX	Wilcox	Wilcox	Geomap (2009)
NAVRRO	Navarro	Navarro	Geomap (2009)
NAVARRO	Navarro	Navarro	Geomap (2009)
EDWARDS	Edwards	Washita	Geomap (2009)
EDWARDS	Edwards	Washita	Geomap (2009)
NAVRRO	Navarro	Navarro	Geomap (2009)
CATAHOULA-ANAHUAC-INJECTION/DISPOSAL; H2S	Catahoula	Catahoula	https://pubs.usgs.gov/of/1994/0461/report.pdf
MIOCENE	Miocene	Fleming	Geomap (2009)
NAVARRO	Navarro	Navarro	Geomap (2009)
OLMOS	Olmos	Navarro	https://pubs.usgs.gov/dds/dds-069/dds-069-h/REPORTS/69_H_CH_2.pdf
NAVARRO	Navarro	Navarro	Geomap (2009)
OLMOS	Olmos	Navarro	https://pubs.usgs.gov/dds/dds-069/dds-069-h/REPORTS/69_H_CH_2.pdf
NAVARRO	Navarro	Navarro	Geomap (2009)

NAVARRO	Navarro	Navarro	Geomap (2009)
NAVARRO	Navarro	Navarro	Geomap (2009)
NAVARRO	Navarro	Navarro	Geomap (2009)
NAVARRO	Navarro	Navarro	Geomap (2009)
NAVARRO	Navarro	Navarro	Geomap (2009)
NAVARRO	Navarro	Navarro	Geomap (2009)
NAVARRO	Navarro	Navarro	Geomap (2009)
NAVARRO	Navarro	Navarro	Geomap (2009)
NAVARRO	Navarro	Navarro	Geomap (2009)
GRETA	Greta	Frio	https://scholarworks.uark.edu/etd/2873/
NAVARRO	Navarro	Navarro	Geomap (2009)
NAVARRO	Navarro	Navarro	Geomap (2009)
WILCOX	Wilcox	Wilcox	Geomap (2009)
EAGLE FORD	Eagleford	Eagleford	Geomap (2009)
PETTET	Pettet	Trinity	https://pubs.usgs.gov/of/1994/0461/report.pdf
WOODBINE	Woodbine	Woodbine	Geomap (2009)
PETTIT	Pettet	Trinity	https://pubs.usgs.gov/of/1994/0461/report.pdf
YEGUA	Yegua	Claiborne	Geomap (2009)

LOWER EDWARDS	Edwards	Washita	Geomap (2009)
UPPER EDWARDS	Edwards	Washita	Geomap (2009)
GLEN ROSE	Glen rose	Trinity	Geomap (2009)
BUDA	Buda	Washita	Geomap (2009)
OLMOS	Olmos	Navarro	https://pubs.usgs.gov/dds/dds-069/dds-069-h/REPORTS/69_H_CH_2.pdf
FRIO	Frio	Frio	Geomap (2009)
BASAL FRIO	Frio	Frio	Geomap (2009)
BUDA	Buda	Washita	Geomap (2009)
WOODBINE	Woodbine	Woodbine	Geomap (2009)
WOODBINE	Woodbine	Woodbine	Geomap (2009)
HET LIME - DISPOSAL	Heterostegina	Catahoula	https://pubs.usgs.gov/of/1994/0461/report.pdf
MARGULINA	Margulina	Fleming	Geomap (2009)
MIOCENE - DISPOSAL	Miocene	Fleming	Geomap (2009)
YEGUA (1ST)	Yegua	Claiborne	Geomap (2009)
MIRANDO SAND	Mirando	Jackson	https://repositories.lib.utexas.edu/bitstream/handle/2152/77978/txu-oclc-612464.pdf?sequence=1
BASE OF AUSTIN CHALK	Austin Chalk	Austin	Geomap (2009)

WOODBINE	Woodbine	Woodbine	Geomap (2009)
RODESSA	Rodessa	Rodessa	https://pubs.usgs.gov/of/2016/1026/ofr20161026.pdf
FRIO - DISPOSAL	Frio	Frio	Geomap (2009)
WILCOX	Wilcox	Wilcox	Geomap (2009)
NAVARRO	Navarro	Navarro	Geomap (2009)
CATAHOULA	Catahoula	Catahoula	https://pubs.usgs.gov/of/1994/0461/report.pdf
FRIO 1	Frio	Frio	Geomap (2009)
RODESSA	Rodessa	Rodessa	https://pubs.usgs.gov/of/2016/1026/ofr20161026.pdf
ESCONDIDE	Escondido	Escondido	Geomap (2009)
FRIO 1	Frio	Frio	Geomap (2009)
SUB CLARKSVILLE	Clarksville	Clarksville	Geomap (2009)
WILCOX	Wilcox	Wilcox	Geomap (2009)
M 13	M	Fleming	Geomap (2009)
CATAHOULA (TOP)	Catahoula	Catahoula	https://pubs.usgs.gov/of/1994/0461/report.pdf
VICKSBURG	Vicksburg	Vicksburg	Geomap (2009)
YEGUA	Yegua	Claiborne	Geomap (2009)
MIOCENE	Miocene	Fleming	Geomap (2009)
NAVARRO	Navarro	Navarro	Geomap (2009)

NAVARRO	Navarro	Navarro	Geomap (2009)
NAVARRO	Navarro	Navarro	Geomap (2009)
NAVARRO	Navarro	Navarro	Geomap (2009)
NAVARRO	Navarro	Navarro	Geomap (2009)
NAVARRO	Navarro	Navarro	Geomap (2009)
NAVARRO	Navarro	Navarro	Geomap (2009)
MEDICO (3080 YEGUA), JACKSON SERIES	Jackson	Jackson	Geomap (2009)
DUCK CREEK LIME	Duck creek	Washita	https://www.twdb.texas.gov/publications/reports/numbered_reports/doc/R314/Report%20314.pdf
FT WORTH LIME	Worth lime	Taylor	https://scholarworks.uark.edu/cgi/viewcontent.cgi?article=3849&context=etd
MIOCENE	Miocene	Fleming	Geomap (2009)
WOODBINE	Woodbine	Woodbine	Geomap (2009)
OLMOS SAND	Olmos	Navarro	https://pubs.usgs.gov/dds/dds-069/dds-069-h/REPORTS/69_H_CH_2.pdf
MIOCENE	Miocene	Fleming	Geomap (2009)
CATAHOULA-FRIO - INJECTION/ DISPOSAL	Catahoula	Catahoula	https://pubs.usgs.gov/of/1994/0461/report.pdf

FRIO	Frio	Frio	Geomap (2009)
WILCOX - DISPOSAL	Wilcox	Wilcox	Geomap (2009)
GLEN ROSE	Glen rose	Trinity	Geomap (2009)
VICKSBURG	Vicksburg	Vicksburg	Geomap (2009)
JACKSON	Jackson	Jackson	Geomap (2009)
CATAHOULA - DISPOSAL	Catahoula	Catahoula	https://pubs.usgs.gov/of/1994/0461/report.pdf
GRETA	Greta	Frio	https://scholarworks.uark.edu/etd/2873/
COCKFIELD UPPER	Cockfield	Claiborne	Geomap (2009)
MIOCENE	Miocene	Fleming	Geomap (2009)
NODOSARIA - DISPOSAL	Nodosaria	Frio	Geomap (2009)
LOWER WILCOX	Wilcox	Wilcox	Geomap (2009)
EDWARDS - H2S	Edwards	Washita	Geomap (2009)
ANAHUAC	Anahuac	Frio	Geomap (2009)
OLMOS	Olmos	Navarro	https://pubs.usgs.gov/dds/dds-069/dds-069-h/REPORTS/69_H_CH_2.pdf
MIRANDO	Mirando	Jackson	https://repositories.lib.utexas.edu/bitstream/handle/2152/77978/txu-oclc-612464.pdf?sequence=1
MIOCENE SAND	Miocene	Fleming	Geomap (2009)
WILCOX	Wilcox	Wilcox	Geomap (2009)

1ST MIRANDO	Mirando	Jackson	https://repositories.lib.utexas.edu/bitstream/handle/2152/77978/txu-oclc-612464.pdf?sequence=1
MIRANDO	Mirando	Jackson	https://repositories.lib.utexas.edu/bitstream/handle/2152/77978/txu-oclc-612464.pdf?sequence=1
1ST MIRANDO	Mirando	Jackson	https://repositories.lib.utexas.edu/bitstream/handle/2152/77978/txu-oclc-612464.pdf?sequence=1
1ST MIRANDO	Mirando	Jackson	https://repositories.lib.utexas.edu/bitstream/handle/2152/77978/txu-oclc-612464.pdf?sequence=1
MIRANDO	Mirando	Jackson	https://repositories.lib.utexas.edu/bitstream/handle/2152/77978/txu-oclc-612464.pdf?sequence=1
MIRANDO	Mirando	Jackson	https://repositories.lib.utexas.edu/bitstream/handle/2152/77978/txu-oclc-612464.pdf?sequence=1
TRAVIS PEAK	Travis peak	Trinity	https://pubs.usgs.gov/bul/b2184-e/B2184E-508.pdf
AUSTIN	Austin Chalk	Austin	Geomap (2009)
MIOCENE - DISPOSAL	Miocene	Fleming	Geomap (2009)
WOODBINE	Woodbine	Woodbine	Geomap (2009)
LOWER EDWARDS	Edwards	Washita	Geomap (2009)
FLEMING	Fleming	Fleming	Geomap (2009)
1ST MIRANDO	Mirando	Jackson	https://repositories.lib.utexas.edu/bitstream/handle/2152/77978/txu-oclc-612464.pdf?sequence=1
MIOCENE, LOWER-FRIO - DISPOSAL	Miocene	Fleming	Geomap (2009)
WILCOX	Wilcox	Wilcox	Geomap (2009)
EDWARDS - H2S	Edwards	Washita	Geomap (2009)

GEORGETOWN - H2S	George town	Washita	Geomap (2009)
EDWARDS	Edwards	Washita	Geomap (2009)
GEORGETOWN	George town	Washita	Geomap (2009)
NAVARRO - DISPOSAL	Navarro	Navarro	Geomap (2009)
NAVARRO	Navarro	Navarro	Geomap (2009)
LEWISVILLE - DISPOSAL	Lewisville	Eagleford	https://carrresources.com/wp-content/uploads/2020/08/Regional-Woodbine.pdf
NAVARRO	Navarro	Navarro	Geomap (2009)
NAVARRO	Navarro	Navarro	Geomap (2009)
NAVARRO	Navarro	Navarro	Geomap (2009)
CATAHOULA	Catahoula	Catahoula	https://pubs.usgs.gov/of/1994/0461/report.pdf
CATAHOULA	Catahoula	Catahoula	https://pubs.usgs.gov/of/1994/0461/report.pdf
QUEEN CITY	Queen city	Claiborne	Geomap (2009)
EAGLE FORD	Eagleford	Eagleford	Geomap (2009)
WOODBINE	Woodbine	Woodbine	Geomap (2009)
MIOCENE - DISPOSAL	Miocene	Fleming	Geomap (2009)
WOODBINE	Woodbine	Woodbine	Geomap (2009)

NACOTOCH	Nacatoch	Navarro	https://repositories.lib.utexas.edu/bitstream/handle/2152/77501/txu-oclc-10367600.pdf?sequence=1
CATAHOULA-FRIO - INJECTION/ DISPOSAL	Catahoula	Catahoula	https://pubs.usgs.gov/of/1994/0461/report.pdf
WILCOX	Wilcox	Wilcox	Geomap (2009)
LEWISVILLE	Lewisville	Eagleford	https://carrresources.com/wp-content/uploads/2020/08/Regional-Woodbine.pdf
WILCOX	Wilcox	Wilcox	Geomap (2009)
EDWARDS - H2S	Edwards	Washita	Geomap (2009)
EDWARDS - H2S, DISPOSAL	Edwards	Washita	Geomap (2009)
MIOCENE - DISPOSAL	Miocene	Fleming	Geomap (2009)
MCFADDIN (4400)	Mcfaddin	Frio	https://www.osti.gov/servlets/purl/140595
VICKSBURG	Vicksburg	Vicksburg	Geomap (2009)
WILCOX - DISPOSAL	Wilcox	Wilcox	Geomap (2009)
FRIO - DISPOSAL	Frio	Frio	Geomap (2009)
HET LIME - DISPOSAL	Heterostegina	Catahoula	https://pubs.usgs.gov/of/1994/0461/report.pdf
WILCOX - DISPOSAL	Wilcox	Wilcox	Geomap (2009)
WILCOX	Wilcox	Wilcox	Geomap (2009)
CATAHOULA-FRIO - INJECTION/ DISPOSAL;	Catahoula	Catahoula	https://pubs.usgs.gov/of/1994/0461/report.pdf

H2S; OVERPRES			
GLEN ROSE - DISPOSAL	Glen rose	Trinity	Geomap (2009)
EDWARDS - H2S	Edwards	Washita	Geomap (2009)
JACKSON	Jackson	Jackson	Geomap (2009)
WOODBINE	Woodbine	Woodbine	Geomap (2009)
1ST YEGUA SAND	Yegua	Claiborne	Geomap (2009)
GRETA	Greta	Frio	https://scholarworks.uark.edu/etd/2873/
NAVARRO A	Navarro	Navarro	Geomap (2009)
TRAVIS PEAK	Travis peak	Trinity	https://pubs.usgs.gov/bul/b2184-e/B2184E-508.pdf
FLEMING-CATAHOULA - DISPOSAL	Fleming	Fleming	Geomap (2009)
JACKSON - DISPOSAL	Jackson	Jackson	Geomap (2009)
TRAVIS PEAK	Travis peak	Trinity	https://pubs.usgs.gov/bul/b2184-e/B2184E-508.pdf
PITTSBURG	Pittsburg	Trinity	https://pubs.usgs.gov/of/1988/0450k/report.pdf
GLEN ROSE - DISPOSAL	Glen rose	Trinity	Geomap (2009)
EDWARDS - H2S	Edwards	Washita	Geomap (2009)
AUSTIN CHALK	Austin Chalk	Austin	Geomap (2009)

WOODBINE SAND	Woodbine	Woodbine	Geomap (2009)
JACKSON (COLE)	Jackson	Jackson	Geomap (2009)
OLMOS - INJECTION/ DISPOSAL	Olmos	Navarro	https://pubs.usgs.gov/dds/dds-069/dds-069-h/REPORTS/69_H_CH_2.pdf
FRIO	Frio	Frio	Geomap (2009)
GRETA (TOP)	Greta	Frio	https://scholarworks.uark.edu/etd/2873/
VICKSBURG	Vicksburg	Vicksburg	Geomap (2009)
WOODINE	Woodbine	Woodbine	Geomap (2009)
WHITSETT - DISPOSAL	Whitsett	Jackson	Geomap (2009)
LOWER PETTIT	Pettet	Trinity	https://pubs.usgs.gov/of/1994/0461/report.pdf
FRIO	Frio	Frio	Geomap (2009)
PETTET	Pettet	Trinity	https://pubs.usgs.gov/of/1994/0461/report.pdf
GLEN ROSE	Glen rose	Trinity	Geomap (2009)
EDWARDS - H2S	Edwards	Washita	Geomap (2009)
YEGUA - INJECTION/ DISPOSAL	Yegua	Claiborne	Geomap (2009)
WOODBINE	Woodbine	Woodbine	Geomap (2009)
CATAHOULA SANDSTONE	Catahoula	Catahoula	https://pubs.usgs.gov/of/1994/0461/report.pdf

CATAHOULA SANDSTONE	Catahoula	Catahoula	https://pubs.usgs.gov/of/1994/0461/report.pdf
CATAHOULA SANDSTONE	Catahoula	Catahoula	https://pubs.usgs.gov/of/1994/0461/report.pdf
JASPER	Jasper (under Oakville)	Fleming	https://www.twdb.texas.gov/publications/reports/numbered_reports/doc/R236/R236.pdf
CATAHOULA SANDSTONE	Catahoula	Catahoula	https://pubs.usgs.gov/of/1994/0461/report.pdf
NACATOCH	Nacatoch	Navarro	https://repositories.lib.utexas.edu/bitstream/handle/2152/77501/txu-oclc-10367600.pdf?sequence=1
WOODBINE - EAST TEXAS FIELD (DISTRICT 6E)	Woodbine	Woodbine	Geomap (2009)
CATAHOULA SANDSTONE	Catahoula	Catahoula	https://pubs.usgs.gov/of/1994/0461/report.pdf
CATAHOULA SANDSTONE	Catahoula	Catahoula	https://pubs.usgs.gov/of/1994/0461/report.pdf
PALUXY	Paluxy	Fredericksburg	Geomap (2009)
TRAVIS PEAK	Travis peak	Trinity	https://pubs.usgs.gov/bul/b2184-e/B2184E-508.pdf

CATAHOULA	Catahoula	Catahoula	https://pubs.usgs.gov/of/1994/0461/report.pdf
WOODBINE	Woodbine	Woodbine	Geomap (2009)
HET LIME - DISPOSAL	Heterostegina	Catahoula	https://pubs.usgs.gov/of/1994/0461/report.pdf
GLEN ROSE	Glen rose	Trinity	Geomap (2009)
COCKFIELD LOWER	Cockfield	Claiborne	Geomap (2009)
TOP OF WILCOX	Wilcox	Wilcox	Geomap (2009)
MIOCENE	Miocene	Fleming	Geomap (2009)
LOWER EDWARDS	Edwards	Washita	Geomap (2009)
CATAHOULA	Catahoula	Catahoula	https://pubs.usgs.gov/of/1994/0461/report.pdf
MIOCENE	Miocene	Fleming	Geomap (2009)
TRAVIS PEAK	Travis peak	Trinity	https://pubs.usgs.gov/bul/b2184-e/B2184E-508.pdf
CATAHOULA	Catahoula	Catahoula	https://pubs.usgs.gov/of/1994/0461/report.pdf
FRIO 1	Frio	Frio	Geomap (2009)
WOODBINE	Woodbine	Woodbine	Geomap (2009)
PALUXY	Paluxy	Fredericksburg	Geomap (2009)
PALUXY	Paluxy	Fredericksburg	Geomap (2009)

PALUXY	Paluxy	Fredericksburg	Geomap (2009)
WILCOX	Wilcox	Wilcox	Geomap (2009)
FRIO - DISPOSAL	Frio	Frio	Geomap (2009)
FRIO - DISPOSAL	Frio	Frio	Geomap (2009)
GOODLAND	Goodland	Fredericksburg	https://pubs.usgs.gov/of/2016/1026/ofr20161026.pdf
DYERSDALE, N. (Y-5)	Yegua	Claiborne	Geomap (2009)
CATAHOULA	Catahoula	Catahoula	https://pubs.usgs.gov/of/1994/0461/report.pdf
RODESSA	Rodessa	Rodessa	https://pubs.usgs.gov/of/2016/1026/ofr20161026.pdf
UPPER WOODBINE	Woodbine	Woodbine	Geomap (2009)
FRIO	Frio	Frio	Geomap (2009)
FRIO 4700'	Frio	Frio	Geomap (2009)
CATAHOULA	Catahoula	Catahoula	https://pubs.usgs.gov/of/1994/0461/report.pdf
NACATOCH	Nacatoch	Navarro	https://repositories.lib.utexas.edu/bitstream/handle/2152/77501/txu-oclc-10367600.pdf?sequence=1
BLOSSOM	Blossom	Austin	https://pubs.usgs.gov/of/1994/0461/report.pdf
CATAHOULA-FRIO - INJECTION/ DISPOSAL	Catahoula	Catahoula	https://pubs.usgs.gov/of/1994/0461/report.pdf
WOODBINE	Woodbine	Woodbine	Geomap (2009)

JACKSON - INJECTION/ DISPOSAL; H2S	Jackson	Jackson	Geomap (2009)
JACKSON - INJECTION/ DISPOSAL; H2S	Jackson	Jackson	Geomap (2009)
JACKSON - INJECTION/ DISPOSAL; H2S	Jackson	Jackson	Geomap (2009)
EDWARDS	Edwards	Washita	Geomap (2009)
FRIO - DISPOSAL	Frio	Frio	Geomap (2009)
CATAHOULA	Catahoula	Catahoula	https://pubs.usgs.gov/of/1994/0461/report.pdf
FRIO	Frio	Frio	Geomap (2009)
GRETA	Greta	Frio	https://scholarworks.uark.edu/etd/2873/
FRIO - DISPOSAL	Frio	Frio	Geomap (2009)
RODESSA	Rodessa	Rodessa	https://pubs.usgs.gov/of/2016/1026/ofr20161026.pdf
MIOCENE - DISPOSAL	Miocene	Fleming	Geomap (2009)
GLEN ROSE - DISPOSAL	Glen rose	Trinity	Geomap (2009)
CATAHOULA	Catahoula	Catahoula	https://pubs.usgs.gov/of/1994/0461/report.pdf
EDWARDS - H2S	Edwards	Washita	Geomap (2009)
FRIO - DISPOSAL	Frio	Frio	Geomap (2009)

FRIO	Frio	Frio	Geomap (2009)
FRIO	Frio	Frio	Geomap (2009)
WOODBINE	Woodbine	Woodbine	Geomap (2009)
VICKSBURG	Vicksburg	Vicksburg	Geomap (2009)
FRIO	Frio	Frio	Geomap (2009)
GLEN ROSE	Glen rose	Trinity	Geomap (2009)
EDWARDS - H2S	Edwards	Washita	Geomap (2009)
FRIO - DISPOSAL	Frio	Frio	Geomap (2009)
WILCOX - DISPOSAL	Wilcox	Wilcox	Geomap (2009)
GLEN ROSE - DISPOSAL	Glen rose	Trinity	Geomap (2009)
EDWARDS - H2S	Edwards	Washita	Geomap (2009)
JACKSON - INJECTION/ DISPOSAL; H2S	Jackson	Jackson	Geomap (2009)
ESCONDIDO - DISPOSAL	Escondido	Escondido	Geomap (2009)
WOODBINE	Woodbine	Woodbine	Geomap (2009)
GLEN ROSE - DISPOSAL	Glen rose	Trinity	Geomap (2009)
EDWARDS - H2S	Edwards	Washita	Geomap (2009)
CARRIZO	Carrizo	Wilcox	Geomap (2009)

MIOCENE	Miocene	Fleming	Geomap (2009)
FRIO F1A	Frio	Frio	Geomap (2009)
GLEN ROSE	Glen rose	Trinity	Geomap (2009)
EDWARDS - H2S	Edwards	Washita	Geomap (2009)
TOP OF YEGUA	Yegua	Claiborne	Geomap (2009)
YEGUA F	Yegua	Claiborne	Geomap (2009)
YEGUA B	Yegua	Claiborne	Geomap (2009)
CATAHOULA	Catahoula	Catahoula	https://pubs.usgs.gov/of/1994/0461/report.pdf
GLEN ROSE - DISPOSAL	Glen rose	Trinity	Geomap (2009)
RODESSA	Rodessa	Rodessa	https://pubs.usgs.gov/of/2016/1026/ofr20161026.pdf
BLOSSON/ TOKIO	Blossom	Austin	https://pubs.usgs.gov/of/1994/0461/report.pdf
GLEN ROSE - DISPOSAL	Glen rose	Trinity	Geomap (2009)
EDWARDS - H2S	Edwards	Washita	Geomap (2009)
EDWARDS - DISPOSAL	Edwards	Washita	Geomap (2009)
RODESSA	Rodessa	Rodessa	https://pubs.usgs.gov/of/2016/1026/ofr20161026.pdf
PETTET	Pettet	Trinity	https://pubs.usgs.gov/of/1994/0461/report.pdf
MIOCENE - DISPOSAL	Miocene	Fleming	Geomap (2009)

WILCOX CONSOLIDATED	Wilcox	Wilcox	Geomap (2009)
JACKSON - INJECTION/ DISPOSAL; H2S	Jackson	Jackson	Geomap (2009)
RODESSA	Rodessa	Rodessa	https://pubs.usgs.gov/of/2016/1026/ofr20161026.pdf
RODESSA	Rodessa	Rodessa	https://pubs.usgs.gov/of/2016/1026/ofr20161026.pdf
AUSTIN CHALK	Austin Chalk	Austin	Geomap (2009)
FRIO	Frio	Frio	Geomap (2009)
RODESSA	Rodessa	Rodessa	https://pubs.usgs.gov/of/2016/1026/ofr20161026.pdf
MIOCENE	Miocene	Fleming	Geomap (2009)
AUSTIN CHALK	Austin Chalk	Austin	Geomap (2009)
EAGLEFORD	Eagleford	Eagleford	Geomap (2009)
WOODBINE	Woodbine	Woodbine	Geomap (2009)
SUB-CLARKSVILLE	Clarksville	Clarksville	Geomap (2009)
GOLIAD	Goliad	Goliad	https://citeseerx.ist.psu.edu/document?repid=rep1&type=pdf&doi=d91b2c88ce1ae6fadff51afd823dac7829777e29
TRAVIS PEAK	Travis peak	Trinity	https://pubs.usgs.gov/bul/b2184-e/B2184E-508.pdf
FRIO	Frio	Frio	Geomap (2009)
JACKSON (COLE)	Jackson	Jackson	Geomap (2009)

VICKSBURG - DISPOSAL	Vicksburg	Vicksburg	Geomap (2009)
TRAVIS PEAK	Travis peak	Trinity	https://pubs.usgs.gov/bul/b2184-e/B2184E-508.pdf
GLEN ROSE - DISPOSAL	Glen rose	Trinity	Geomap (2009)
EDWARDS - H2S	Edwards	Washita	Geomap (2009)
COLE	Cole	Jackson	Geomap (2009)
VICKSBURG - DISPOSAL	Vicksburg	Vicksburg	Geomap (2009)
WOODBINE	Woodbine	Woodbine	Geomap (2009)
FREDERICKSBURG	Fredericksburg	Fredericksburg	Geomap (2009)
JACKSON SHALE	Jackson	Jackson	Geomap (2009)
MIOCENE C	Miocene	Fleming	Geomap (2009)
GLEN ROSE	Glen rose	Trinity	Geomap (2009)
EDWARDS LIMESTONE - H2S	Edwards	Washita	Geomap (2009)
VICKSBURG	Vicksburg	Vicksburg	Geomap (2009)
T/DUCK CREEK	Duck creek	Washita	https://www.twdb.texas.gov/publications/reports/numbered_reports/doc/R314/Report%20314.pdf
WILCOX - DISPOSAL	Wilcox	Wilcox	Geomap (2009)

CATAHOULA/FRIO	Catahoula	Catahoula	https://pubs.usgs.gov/of/1994/0461/report.pdf
CATAHOULA	Catahoula	Catahoula	https://pubs.usgs.gov/of/1994/0461/report.pdf
HET II	Heterostegina	Catahoula	https://pubs.usgs.gov/of/1994/0461/report.pdf
TOP OF WOODBINE SAND	Woodbine	Woodbine	Geomap (2009)
HACKBERRY - DISPOSAL	Hackberry	Frio	Geomap (2009)
MIOCENE	Miocene	Fleming	Geomap (2009)
FLEMING-CATAHOULA - DISPOSAL	Fleming	Fleming	Geomap (2009)
HOCKLEY	Hockley (Hockleyensis)	Jackson	https://www.twdb.texas.gov/groundwater/models/gam/ygjk/YGJK_Structure_Report.pdf
FRIO - DISPOSAL	Frio	Frio	Geomap (2009)
MIOCENE	Miocene	Fleming	Geomap (2009)
HOCKLEY - DISPOSAL	Hockley (Hockleyensis)	Jackson	https://www.twdb.texas.gov/groundwater/models/gam/ygjk/YGJK_Structure_Report.pdf
MIOCENE-LARGARTO-OAKVILLE-	Miocene	Fleming	Geomap (2009)

INJECTION/ DISPOSAL			
GLEN ROSE - DISPOSAL	Glen rose	Trinity	Geomap (2009)
EDWARDS - H2S	Edwards	Washita	Geomap (2009)
RODESSA	Rodessa	Rodessa	https://pubs.usgs.gov/of/2016/1026/ofr20161026.pdf
MIOCENE - DISPOSAL	Miocene	Fleming	Geomap (2009)
FRIO - DISPOSAL	Frio	Frio	Geomap (2009)
GRETA	Greta	Frio	https://scholarworks.uark.edu/etd/2873/
SAN MIGUEL	San miguel	Taylor	Geomap (2009)
MIOCENE - DISPOSAL	Miocene	Fleming	Geomap (2009)
FRIO - DISPOSAL	Frio	Frio	Geomap (2009)
CATAHOULA - DISPOSAL	Catahoula	Catahoula	https://pubs.usgs.gov/of/1994/0461/report.pdf
CATAHOULA - DISPOSAL	Catahoula	Catahoula	https://pubs.usgs.gov/of/1994/0461/report.pdf
GRETTA	Greta	Frio	https://scholarworks.uark.edu/etd/2873/
RODESSA	Rodessa	Rodessa	https://pubs.usgs.gov/of/2016/1026/ofr20161026.pdf
PETTET	Pettet	Trinity	https://pubs.usgs.gov/of/1994/0461/report.pdf
JAMES LIME	James	Trinity	Geomap (2009)
RODESSA	Rodessa	Rodessa	https://pubs.usgs.gov/of/2016/1026/ofr20161026.pdf

PETTET	Pettet	Trinity	https://pubs.usgs.gov/of/1994/0461/report.pdf
JAMES LIME	James	Trinity	Geomap (2009)
EDWARDS - H2S	Edwards	Washita	Geomap (2009)
GEORGETOWN	Georgetown	Washita	Geomap (2009)
NACATOCH	Nacatoch	Navarro	https://repositories.lib.utexas.edu/bitstream/handle/2152/77501/txu-oclc-10367600.pdf?sequence=1
MIOCENE - DISPOSAL	Miocene	Fleming	Geomap (2009)
CATAHOULA	Catahoula	Catahoula	https://pubs.usgs.gov/of/1994/0461/report.pdf
WOODBINE	Woodbine	Woodbine	Geomap (2009)
1ST YEGUA SAND	Yegua	Claiborne	Geomap (2009)
SLIGO	Sligo	Trinity	Geomap (2009)
MIOCENE/FLEMING	Miocene	Fleming	Geomap (2009)
GRETTA - DISPOSAL	Greta	Frio	https://scholarworks.uark.edu/etd/2873/
PALUXY	Paluxy	Fredericksburg	Geomap (2009)
FRIO 5100	Frio	Frio	Geomap (2009)
WOODBINE	Woodbine	Woodbine	Geomap (2009)
LULING WILCOX	Luling	Wilcox	https://pubs.usgs.gov/of/2017/1111/ofr20171111.pdf
WOODBINE - EAST TEXAS FIELD	Woodbine	Woodbine	Geomap (2009)

(DISTRICT 6E)			
WOODBINE	Woodbine	Woodbine	Geomap (2009)
BUDA	Buda	Washita	Geomap (2009)
MIOCENE, LOWER-FRIO - DISPOSAL	Miocene	Fleming	Geomap (2009)
CATAHOULA-FRIO - INJECTION/ DISPOSAL; H2S	Catahoula	Catahoula	https://pubs.usgs.gov/of/1994/0461/report.pdf
CATAHOULA-ANAHUAC - INJECTION/ DISPOSAL; H2S	Catahoula	Catahoula	https://pubs.usgs.gov/of/1994/0461/report.pdf
GRETA	Greta	Frio	https://scholarworks.uark.edu/etd/2873/
GEORGETOWN	George town	Washita	Geomap (2009)
1ST YEGUA	Yegua	Claiborne	Geomap (2009)
MIOCENE / FLEMING	Miocene	Fleming	Geomap (2009)
WILCOX	Wilcox	Wilcox	Geomap (2009)
GLEN ROSE	Glen rose	Trinity	Geomap (2009)
EDWARDS - DISPOSAL	Edwards	Washita	Geomap (2009)

CATAHOULA - DISPOSAL	Catahoula	Catahoula	https://pubs.usgs.gov/of/1994/0461/report.pdf
RODESSA	Rodessa	Rodessa	https://pubs.usgs.gov/of/2016/1026/ofr20161026.pdf
BMA	Anhydrite	Trinity	https://pubs.geoscienceworld.org/aapg/books/book/1484/chapter-abstract/107178760/Summary-of-Subsurface-Geology-of-Northeast-Texas?redirectedFrom=fulltext
QUEEN CITY - INJECTION/ DISPOSAL; POSSIBLE LOST CIR	Queen city	Claiborne	Geomap (2009)
YEGUA	Yegua	Claiborne	Geomap (2009)
VICKSBURG	Vicksburg	Vicksburg	Geomap (2009)
WOODBINE	Woodbine	Woodbine	Geomap (2009)
WILCOX	Wilcox	Wilcox	Geomap (2009)
WOODBINE	Woodbine	Woodbine	Geomap (2009)
HOCKLEY	Hockley (Hockleyensis)	Jackson	https://www.twdb.texas.gov/groundwater/models/gam/ygjk/YGJK_Structure_Report.pdf
GRETA	Greta	Frio	https://scholarworks.uark.edu/etd/2873/
GRETA	Greta	Frio	https://scholarworks.uark.edu/etd/2873/
YEGUA - DISPOSAL	Yegua	Claiborne	Geomap (2009)
CATAHOULA/FRIO	Catahoula	Catahoula	https://pubs.usgs.gov/of/1994/0461/report.pdf

MID FRIO	Frio	Frio	Geomap (2009)
CATAHOULA	Catahoula	Catahoula	https://pubs.usgs.gov/of/1994/0461/report.pdf
CATAHOULA	Catahoula	Catahoula	https://pubs.usgs.gov/of/1994/0461/report.pdf
MIOCENE - DISPOSAL	Miocene	Fleming	Geomap (2009)
FRIO-DISCORBIS - DISPOSAL	Frio	Frio	Geomap (2009)
OLMOS	Olmos	Navarro	https://pubs.usgs.gov/dds/dds-069/dds-069-h/REPORTS/69_H_CH_2.pdf
CATAHOULA	Catahoula	Catahoula	https://pubs.usgs.gov/of/1994/0461/report.pdf
GRETA	Greta	Frio	https://scholarworks.uark.edu/etd/2873/
GRETA	Greta	Frio	https://scholarworks.uark.edu/etd/2873/
MIOCENE - DISPOSAL	Miocene	Fleming	Geomap (2009)
CATAHOULA-FRIO - INJECTION/ DISPOSAL; H2S	Catahoula	Catahoula	https://pubs.usgs.gov/of/1994/0461/report.pdf
COCKFIELD	Cockfield	Claiborne	Geomap (2009)
SUB-CLARKSVILLE	Clarksville	Clarksville	Geomap (2009)
TRAVIS PEAK	Travis peak	Trinity	https://pubs.usgs.gov/bul/b2184-e/B2184E-508.pdf
PETTET	Pettet	Trinity	https://pubs.usgs.gov/of/1994/0461/report.pdf
COLE SAND	Cole	Jackson	Geomap (2009)

MIOCENE	Miocene	Fleming	Geomap (2009)
CATAHOULA-ANAHUAC - INJECTION/ DISPOSAL; H2S	Catahoula	Catahoula	https://pubs.usgs.gov/of/1994/0461/report.pdf
WOODBINE - EAST TEXAS FIELD (DISTRICT 6E)	Woodbine	Woodbine	Geomap (2009)
SUB-CLARKSVILLE	Clarksville	Clarksville	Geomap (2009)
GRETA	Greta	Frio	https://scholarworks.uark.edu/etd/2873/
FRIO	Frio	Frio	Geomap (2009)
CATAHOULA - DISPOSAL	Catahoula	Catahoula	https://pubs.usgs.gov/of/1994/0461/report.pdf
JACKSON - INJECTION/ DISPOSAL; H2S	Jackson	Jackson	Geomap (2009)
EDWARDS - DISPOSAL	Edwards	Washita	Geomap (2009)
GOVT. WELLS	Government wells	Jackson	https://repositories.lib.utexas.edu/bitstream/handle/2152/77978/txu-oclc-612464.pdf?sequence=1
CATAHOULA - DISPOSAL, H2S (CORDELE,	Catahoula	Catahoula	https://pubs.usgs.gov/of/1994/0461/report.pdf

WEST AREA)			
MIOCENE - DISPOSAL	Miocene	Fleming	Geomap (2009)
WOODBINE-LOLA - PRODUCTION	Woodbine	Woodbine	Geomap (2009)
WOODBINE - PRODUCTION	Woodbine	Woodbine	Geomap (2009)
RODESSA	Rodessa	Rodessa	https://pubs.usgs.gov/of/2016/1026/ofr20161026.pdf
CATAHOULA-FRIO - INJECTION/ DISPOSAL; H2S	Catahoula	Catahoula	https://pubs.usgs.gov/of/1994/0461/report.pdf
MIOCENE - DISPOSAL	Miocene	Fleming	Geomap (2009)
CATAHOULA	Catahoula	Catahoula	https://pubs.usgs.gov/of/1994/0461/report.pdf
BLOSSOM	Blossom	Austin	https://pubs.usgs.gov/of/1994/0461/report.pdf
CATAHOULA	Catahoula	Catahoula	https://pubs.usgs.gov/of/1994/0461/report.pdf
CATAHOULA	Catahoula	Catahoula	https://pubs.usgs.gov/of/1994/0461/report.pdf
CATAHOULA	Catahoula	Catahoula	https://pubs.usgs.gov/of/1994/0461/report.pdf
CATAHOULA	Catahoula	Catahoula	https://pubs.usgs.gov/of/1994/0461/report.pdf
FRIO	Frio	Frio	Geomap (2009)

FRIO - DISPOSAL	Frio	Frio	Geomap (2009)
CATAHOULA	Catahoula	Catahoula	https://pubs.usgs.gov/of/1994/0461/report.pdf
GRETA	Greta	Frio	https://scholarworks.uark.edu/etd/2873/
ANAHUAC	Anahuac	Frio	Geomap (2009)
GRETA	Greta	Frio	https://scholarworks.uark.edu/etd/2873/
YEGUA B	Yegua	Claiborne	Geomap (2009)
JACKSON - INJECTION/ DISPOSAL; H2S	Jackson	Jackson	Geomap (2009)
MCFADDIN (4400)	Mcfaddin	Frio	https://www.osti.gov/servlets/purl/140595
COLE	Cole	Jackson	Geomap (2009)
GRETA	Greta	Frio	https://scholarworks.uark.edu/etd/2873/
GRETTA - DISPOSAL	Greta	Frio	https://scholarworks.uark.edu/etd/2873/
PETTET	Pettet	Trinity	https://pubs.usgs.gov/of/1994/0461/report.pdf
GRETA	Greta	Frio	https://scholarworks.uark.edu/etd/2873/
FRIO - DISPOSAL	Frio	Frio	Geomap (2009)
YEGUA	Yegua	Claiborne	Geomap (2009)
JACKSON	Jackson	Jackson	Geomap (2009)
FRIO	Frio	Frio	Geomap (2009)
AUSTIN CHALK	Austin Chalk	Austin	Geomap (2009)

WOODBINE	Woodbine	Woodbine	Geomap (2009)
WILCOX	Wilcox	Wilcox	Geomap (2009)
GLEN ROSE	Glen rose	Trinity	Geomap (2009)
LOWER WILCOX	Wilcox	Wilcox	Geomap (2009)
EDWARDS - H2S	Edwards	Washita	Geomap (2009)
FRIO - DISPOSAL	Frio	Frio	Geomap (2009)
CATAHOULA - DISPOSAL	Catahoula	Catahoula	https://pubs.usgs.gov/of/1994/0461/report.pdf
PETTET	Pettet	Trinity	https://pubs.usgs.gov/of/1994/0461/report.pdf
WOODBINE	Woodbine	Woodbine	Geomap (2009)
FRIO	Frio	Frio	Geomap (2009)
YEGUA - DISPOSAL	Yegua	Claiborne	Geomap (2009)
GRETTA - DISPOSAL	Greta	Frio	https://scholarworks.uark.edu/etd/2873/
GRETTA - DISPOSAL	Greta	Frio	https://scholarworks.uark.edu/etd/2873/
GRETTA - DISPOSAL	Greta	Frio	https://scholarworks.uark.edu/etd/2873/
GRETTA - DISPOSAL	Greta	Frio	https://scholarworks.uark.edu/etd/2873/
GRETTA - DISPOSAL	Greta	Frio	https://scholarworks.uark.edu/etd/2873/
MIOCENE	Miocene	Fleming	Geomap (2009)

FRIO - DISPOSAL	Frio	Frio	Geomap (2009)
WALES	Not real formation	Wilcox	https://www.gcags.org/Journal/2017.GCAGS.Journal/2017.GCAGS.Journal.v6.10.p150-160.Hamilton.and.Gottardi.pdf
MIDWAY	Midway	Midway	https://pubs.usgs.gov/of/1994/0461/report.pdf
GRETTA - DISPOSAL	Greta	Frio	https://scholarworks.uark.edu/etd/2873/
BUDA	Buda	Washita	Geomap (2009)
TOP WOODBINE	Woodbine	Woodbine	Geomap (2009)
BASE WOODBINE	Woodbine	Woodbine	Geomap (2009)
COLE	Cole	Jackson	Geomap (2009)
GEORGETOWN	Georgetown	Washita	Geomap (2009)
PETTET	Pettet	Trinity	https://pubs.usgs.gov/of/1994/0461/report.pdf
1ST YEGUA	Yegua	Claiborne	Geomap (2009)
VICKSBURG - DISPOSAL	Vicksburg	Vicksburg	Geomap (2009)
TOP SMACKOVER	Smackover	Smackover	Geomap (2009)
TRAVIS PEAK	Travis peak	Trinity	https://pubs.usgs.gov/bul/b2184-e/B2184E-508.pdf
FRIO	Frio	Frio	Geomap (2009)

GLEN ROSE	Glen rose	Trinity	Geomap (2009)
GRETA	Greta	Frio	https://scholarworks.uark.edu/etd/2873/
FRIO	Frio	Frio	Geomap (2009)
WOODBINE	Woodbine	Woodbine	Geomap (2009)
COCKFIELD	Cockfield	Claiborne	Geomap (2009)
RODESSA	Rodessa	Rodessa	https://pubs.usgs.gov/of/2016/1026/ofr20161026.pdf
CATAHOULA	Catahoula	Catahoula	https://pubs.usgs.gov/of/1994/0461/report.pdf
FRIO	Frio	Frio	Geomap (2009)
GRETA	Greta	Frio	https://scholarworks.uark.edu/etd/2873/
GRETTA - DISPOSAL	Greta	Frio	https://scholarworks.uark.edu/etd/2873/
GRETA	Greta	Frio	https://scholarworks.uark.edu/etd/2873/
TOP OF FRIO	Frio	Frio	Geomap (2009)
VICKSBURG	Vicksburg	Vicksburg	Geomap (2009)
RODESSA	Rodessa	Rodessa	https://pubs.usgs.gov/of/2016/1026/ofr20161026.pdf
PETTET	Pettet	Trinity	https://pubs.usgs.gov/of/1994/0461/report.pdf
GLEN ROSE	Glen rose	Trinity	Geomap (2009)
RODESSA	Rodessa	Rodessa	https://pubs.usgs.gov/of/2016/1026/ofr20161026.pdf
FRIO-DISCORBIS - DISPOSAL	Frio	Frio	Geomap (2009)

MIOCENE-LAGARTO-OAKVILLE - INJECTION/ DISPOSAL; H2S	Miocene	Fleming	Geomap (2009)
FRIO-DISCORBIS - DISPOSAL	Frio	Frio	Geomap (2009)
RODESSA	Rodessa	Rodessa	https://pubs.usgs.gov/of/2016/1026/ofr20161026.pdf
CATAHOULA	Catahoula	Catahoula	https://pubs.usgs.gov/of/1994/0461/report.pdf
GRETA	Greta	Frio	https://scholarworks.uark.edu/etd/2873/
MIDCENE	Miocene	Fleming	Geomap (2009)
NAVARO A	Navaro	Navarro	Geomap (2009)
YEGUA - DISPOSAL	Yegua	Claiborne	Geomap (2009)
GLEN ROSE - DISPOSAL	Glen rose	Trinity	Geomap (2009)
EDWARDS - H2S	Edwards	Washita	Geomap (2009)
RODESSA GLOYD	Rodessa	Rodessa	https://pubs.usgs.gov/of/2016/1026/ofr20161026.pdf
CATAHOULA-FRIO - INJECTION/ DISPOSAL	Catahoula	Catahoula	https://pubs.usgs.gov/of/1994/0461/report.pdf
ESCONDIDO	Escondido	Escondido	Geomap (2009)
EDWARDS - DISPOSAL	Edwards	Washita	Geomap (2009)

GRETA STRINGER	Greta	Frio	https://scholarworks.uark.edu/etd/2873/
EDWARDS - DISPOSAL	Edwards	Washita	Geomap (2009)
EDWARDS - H2S, DISPOSAL	Edwards	Washita	Geomap (2009)
PETERS	Peters	Jackson	https://www.osti.gov/servlets/purl/140595
COOK MOUNTAIN	Cook mountain	Claiborne	Geomap (2009)
LOWER MIOCENE	Miocene	Fleming	Geomap (2009)
LOWER MIOCENE	Miocene	Fleming	Geomap (2009)
COLE	Cole	Jackson	Geomap (2009)
FRIO - DISPOSAL	Frio	Frio	Geomap (2009)
CARRIZO	Carrizo	Wilcox	Geomap (2009)
YEGUA - DISPOSAL	Yegua	Claiborne	Geomap (2009)
PETTET	Pettet	Trinity	https://pubs.usgs.gov/of/1994/0461/report.pdf
GRETA	Greta	Frio	https://scholarworks.uark.edu/etd/2873/
SINTON	Sinton	Frio	https://scholarworks.uark.edu/cgi/viewcontent.cgi?article=4380&context=etd
WILCOX - DISPOSAL	Wilcox	Wilcox	Geomap (2009)
DUCK CREEK	Duck creek	Washita	https://www.twdb.texas.gov/publications/reports/numbered_reports/doc/R314/Report%20314.pdf
CATAHOULA	Catahoula	Catahoula	https://pubs.usgs.gov/of/1994/0461/report.pdf

EDWARDS LIME	Edwards	Washita	Geomap (2009)
DUCK CREEK	Duck creek	Washita	https://www.twdb.texas.gov/publications/reports/numbered_reports/doc/R314/Report%20314.pdf
MIOCENE - DISPOSAL	Miocene	Fleming	Geomap (2009)
MIOCENE M10	Miocene	Fleming	Geomap (2009)
AUSTIN CHALK	Austin Chalk	Austin	Geomap (2009)
FLEMING - DISPOSAL	Fleming	Fleming	Geomap (2009)
WILCOX	Wilcox	Wilcox	Geomap (2009)
SAN MIGUEL CREEK (WILCOX CONS.)	San miguel	Taylor	Geomap (2009)
OLMOS	Olmos	Navarro	https://pubs.usgs.gov/dds/dds-069/dds-069-h/REPORTS/69_H_CH_2.pdf
GLEN ROSE	Glen rose	Trinity	Geomap (2009)
PETTIT	Pettet	Trinity	https://pubs.usgs.gov/of/1994/0461/report.pdf
WOODBINE	Woodbine	Woodbine	Geomap (2009)
BUDA	Buda	Washita	Geomap (2009)
WOODBINE	Woodbine	Woodbine	Geomap (2009)
LOWER WILCOX	Wilcox	Wilcox	Geomap (2009)
WILCOX	Wilcox	Wilcox	Geomap (2009)

FRIO - DISPOSAL	Frio	Frio	Geomap (2009)
PETTIT	Pettet	Trinity	https://pubs.usgs.gov/of/1994/0461/report.pdf
TRAVIS PEAK	Travis peak	Trinity	https://pubs.usgs.gov/bul/b2184-e/B2184E-508.pdf
UPPER EDWARDS	Edwards	Washita	Geomap (2009)
T. MASSIVE WILCOX	Wilcox	Wilcox	Geomap (2009)
HETT	Heterostegina	Catahoula	https://pubs.usgs.gov/of/1994/0461/report.pdf
MAIN HOCKLEY	Hockley (Hockleyensis)	Jackson	https://www.twdb.texas.gov/groundwater/models/gam/ygjk/YGJK_Structure_Report.pdf
UPPER HOCKLEY	Hockley (Hockleyensis)	Jackson	https://www.twdb.texas.gov/groundwater/models/gam/ygjk/YGJK_Structure_Report.pdf
MIOCENE MARGINULINA A	Miocene	Fleming	Geomap (2009)
PLACEDO, EAST (4000)	Placedo	Frio	https://www.osti.gov/servlets/purl/140595
MASSIVE ANAHYDRITE	Anhydrite	Trinity	https://pubs.geoscienceworld.org/aapg/books/book/1484/chapter-abstract/107178760/Summary-of-Subsurface-Geology-of-Northeast-Texas?redirectedFrom=fulltext
MIOCENE - DISPOSAL	Miocene	Fleming	Geomap (2009)
MIDWAY	Midway	Midway	https://pubs.usgs.gov/of/1994/0461/report.pdf

KIAMICHI	Kiamichi	Fredericksburg	Geomap (2009)
LOWER EDWARDS	Edwards	Washita	Geomap (2009)
WOODBINE	Woodbine	Woodbine	Geomap (2009)
BASE OF WILCOX	Wilcox	Wilcox	Geomap (2009)
MIOCENE - DISPOSAL	Miocene	Fleming	Geomap (2009)
WILCOX	Wilcox	Wilcox	Geomap (2009)
WILCOX	Wilcox	Wilcox	Geomap (2009)
FRIO	Frio	Frio	Geomap (2009)
TRAVIS PEAK	Travis peak	Trinity	https://pubs.usgs.gov/bul/b2184-e/B2184E-508.pdf
LOWER WILCOX	Wilcox	Wilcox	Geomap (2009)
GOVERNMENT WELLS SAND	Government wells	Jackson	https://repositories.lib.utexas.edu/bitstream/handle/2152/77978/txu-oclc-612464.pdf?sequence=1
EDWARDS - H2S, DISPOSAL	Edwards	Washita	Geomap (2009)
LOWER EDWARDS	Edwards	Washita	Geomap (2009)
EDWARDS	Edwards	Washita	Geomap (2009)
GEORGETOWN	George town	Washita	Geomap (2009)
LOWER WILCOX	Wilcox	Wilcox	Geomap (2009)

WILCOX - DISPOSAL	Wilcox	Wilcox	Geomap (2009)
OLMOS/SAN MIGUEL	Olmos	Navarro	https://pubs.usgs.gov/dds/dds-069/dds-069-h/REPORTS/69_H_CH_2.pdf
QUEEN CITY	Queen city	Claiborne	Geomap (2009)
MASSIVE WILCOX	Wilcox	Wilcox	Geomap (2009)
AUSTIN CHALK	Austin Chalk	Austin	Geomap (2009)
DEXTER	Dexter	Woodbine	https://www.gcags.org/Journal/2016.GCAGS.Journal/2016.GCAGS.Journal.v5.02.p25-46.Vallabhaneni.et.al.pdf
GLEN ROSE - DISPOSAL	Glen rose	Trinity	Geomap (2009)
MIOCENE	Miocene	Fleming	Geomap (2009)
WILCOX	Wilcox	Wilcox	Geomap (2009)
CATAHOULA	Catahoula	Catahoula	https://pubs.usgs.gov/of/1994/0461/report.pdf
DEXTER	Dexter	Woodbine	https://www.gcags.org/Journal/2016.GCAGS.Journal/2016.GCAGS.Journal.v5.02.p25-46.Vallabhaneni.et.al.pdf
LEWISVILLE A	Lewisville	Eagleford	https://carrresources.com/wp-content/uploads/2020/08/Regional-Woodbine.pdf
LEWISVILLE C	Lewisville	Eagleford	https://carrresources.com/wp-content/uploads/2020/08/Regional-Woodbine.pdf
FRIO	Frio	Frio	Geomap (2009)
JACKSON (COLE I)	Jackson	Jackson	Geomap (2009)
GEORGETOWN - H2S	George town	Washita	Geomap (2009)
CATAHOULA	Catahoula	Catahoula	https://pubs.usgs.gov/of/1994/0461/report.pdf

SUB-CLARKSVILLE	Clarksville	Clarksville	Geomap (2009)
FRIO 7200 SAND	Frio	Frio	Geomap (2009)
FRIO 7000 SAND	Frio	Frio	Geomap (2009)
FRIO 7680 SAND	Frio	Frio	Geomap (2009)
PATTIT	Pettet	Trinity	https://pubs.usgs.gov/of/1994/0461/report.pdf
WOODBINE	Woodbine	Woodbine	Geomap (2009)
RODESSA	Rodessa	Rodessa	https://pubs.usgs.gov/of/2016/1026/ofr20161026.pdf
PETTIT	Pettet	Trinity	https://pubs.usgs.gov/of/1994/0461/report.pdf
WILCOX	Wilcox	Wilcox	Geomap (2009)
WILCOX	Wilcox	Wilcox	Geomap (2009)
COLE	Cole	Jackson	Geomap (2009)
UPPER/MIDDLE MIOCENE	Miocene	Fleming	Geomap (2009)
COLE	Cole	Jackson	Geomap (2009)
WILCOX	Wilcox	Wilcox	Geomap (2009)
AUSTIN CHALK	Austin Chalk	Austin	Geomap (2009)
RODESSA	Rodessa	Rodessa	https://pubs.usgs.gov/of/2016/1026/ofr20161026.pdf
LOWER EDWARDS	Edwards	Washita	Geomap (2009)
YEGUA B	Yegua	Claiborne	Geomap (2009)

MIRANDO SAND	Mirando	Jackson	https://repositories.lib.utexas.edu/bitstream/handle/2152/77978/txu-oclc-612464.pdf?sequence=1
YEGUA B	Yegua	Claiborne	Geomap (2009)
WILCOX	Wilcox	Wilcox	Geomap (2009)
OLMOS	Olmos	Navarro	https://pubs.usgs.gov/dds/dds-069/dds-069-h/REPORTS/69_H_CH_2.pdf
EAGLE FORD	Eagleford	Eagleford	Geomap (2009)
MIOCENE	Miocene	Fleming	Geomap (2009)
UPPER WILCOX	Wilcox	Wilcox	Geomap (2009)
WILCOX	Wilcox	Wilcox	Geomap (2009)
AUSTIN CHALK - H2S	Austin Chalk	Austin	Geomap (2009)
EAGLE FORD - H2S	Eagleford	Eagleford	Geomap (2009)
WILCOX	Wilcox	Wilcox	Geomap (2009)
PETTET	Pettet	Trinity	https://pubs.usgs.gov/of/1994/0461/report.pdf
WILCOX - DISPOSAL	Wilcox	Wilcox	Geomap (2009)
FRIO	Frio	Frio	Geomap (2009)
CATAHOULA-FRIO - INJECTION/ DISPOSAL; H2S	Catahoula	Catahoula	https://pubs.usgs.gov/of/1994/0461/report.pdf
LULING 6790	Luling	Wilcox	https://pubs.usgs.gov/of/2017/1111/ofr20171111.pdf
LEWISVILLE	Lewisville	Eagleford	https://carrresources.com/wp-content/uploads/2020/08/Regional-Woodbine.pdf

GRETA SAND	Greta	Frio	https://scholarworks.uark.edu/etd/2873/
TOP LOWER WILCOX	Wilcox	Wilcox	Geomap (2009)
GLEN ROSE	Glen rose	Trinity	Geomap (2009)
RODESSA	Rodessa	Rodessa	https://pubs.usgs.gov/of/2016/1026/ofr20161026.pdf
CARRIZO	Carrizo	Wilcox	Geomap (2009)
YEGUA	Yegua	Claiborne	Geomap (2009)
QUEEN CITY - INJECTION/ DISPOSAL	Queen city	Claiborne	Geomap (2009)
GRETA	Greta	Frio	https://scholarworks.uark.edu/etd/2873/
GRETTA-DISPOSAL	Greta	Frio	https://scholarworks.uark.edu/etd/2873/
OLMOS	Olmos	Navarro	https://pubs.usgs.gov/dds/dds-069/dds-069-h/REPORTS/69_H_CH_2.pdf
EDWARDS	Edwards	Washita	Geomap (2009)
PETTIT	Pettet	Trinity	https://pubs.usgs.gov/of/1994/0461/report.pdf
SAN MIGUEL	San miguel	Taylor	Geomap (2009)
UPPER EDWARDS	Edwards	Washita	Geomap (2009)
LOWER EDWARDS	Edwards	Washita	Geomap (2009)
TOP RODESSA	Rodessa	Rodessa	https://pubs.usgs.gov/of/2016/1026/ofr20161026.pdf

WILCOX - DISPOSAL	Wilcox	Wilcox	Geomap (2009)
WOODBINE	Woodbine	Woodbine	Geomap (2009)
PETTET	Pettet	Trinity	https://pubs.usgs.gov/of/1994/0461/report.pdf
EDWARDS	Edwards	Washita	Geomap (2009)
JACKSON (COLE)	Jackson	Jackson	Geomap (2009)
COLE II (JACKSON FORMATION)	Cole	Jackson	Geomap (2009)
MIOCENE	Miocene	Fleming	Geomap (2009)
MIOCENE	Miocene	Fleming	Geomap (2009)
WILCOX	Wilcox	Wilcox	Geomap (2009)
FRIO	Frio	Frio	Geomap (2009)
WILCOX	Wilcox	Wilcox	Geomap (2009)
OLMOS B	Olmos	Navarro	https://pubs.usgs.gov/dds/dds-069/dds-069-h/REPORTS/69_H_CH_2.pdf
MIOCENE-FLEMING(LAGARTO)-OAKVILLE - INJECTION/DISP	Miocene	Fleming	Geomap (2009)
LOWER MIOCENE	Miocene	Fleming	Geomap (2009)
LEWISVILLE "A"	Lewisville	Eagleford	https://carrresources.com/wp-content/uploads/2020/08/Regional-Woodbine.pdf

MASSIVE LOWER WILCOX	Wilcox	Wilcox	Geomap (2009)
WOODBINE	Woodbine	Woodbine	Geomap (2009)
GLEN ROSE - DISPOSAL	Glen rose	Trinity	Geomap (2009)
EDWARDS - H2S	Edwards	Washita	Geomap (2009)
MIOCENE	Miocene	Fleming	Geomap (2009)
FRIO	Frio	Frio	Geomap (2009)
SAN MIGUEL - H2S	San miguel	Taylor	Geomap (2009)
OLMOS - DISPOSAL	Olmos	Navarro	https://pubs.usgs.gov/dds/dds-069/dds-069-h/REPORTS/69_H_CH_2.pdf
CATAHOULA-FRIO - INJECTION/ DISPOSAL; H2S	Catahoula	Catahoula	https://pubs.usgs.gov/of/1994/0461/report.pdf
EDWARDS - H2S, DISPOSAL	Edwards	Washita	Geomap (2009)
MASSIVE FRIO	Frio	Frio	Geomap (2009)
4070' MIOCENE	Miocene	Fleming	Geomap (2009)
WILCOX - DISPOSAL	Wilcox	Wilcox	Geomap (2009)
FREDRICKSBERG	Fredericksburg	Fredericksburg	Geomap (2009)

GRETA	Greta	Frio	https://scholarworks.uark.edu/etd/2873/
EDWARDS - H2S	Edwards	Washita	Geomap (2009)
MIOCENE - DISPOSAL	Miocene	Fleming	Geomap (2009)
KIAMICHI	Kiamichi	Fredericksburg	Geomap (2009)
LOWER EDWARDS	Edwards	Washita	Geomap (2009)
UPPER EDWARDS	Edwards	Washita	Geomap (2009)
ANAHUAC	Anahuac	Frio	Geomap (2009)
M10 MIOCENE	Miocene	Fleming	Geomap (2009)
OLMOS	Olmos	Navarro	https://pubs.usgs.gov/dds/dds-069/dds-069-h/REPORTS/69_H_CH_2.pdf
RODESSA	Rodessa	Rodessa	https://pubs.usgs.gov/of/2016/1026/ofr20161026.pdf
WILCOX - DISPOSAL	Wilcox	Wilcox	Geomap (2009)
EDWARDS	Edwards	Washita	Geomap (2009)
GLEN ROSE	Glen rose	Trinity	Geomap (2009)
GLEN ROSE - DISPOSAL	Glen rose	Trinity	Geomap (2009)
EDWARDS - H2S	Edwards	Washita	Geomap (2009)
RODESSA	Rodessa	Rodessa	https://pubs.usgs.gov/of/2016/1026/ofr20161026.pdf

RODESSA	Rodessa	Rodessa	https://pubs.usgs.gov/of/2016/1026/ofr20161026.pdf
LOWER EDWARDS	Edwards	Washita	Geomap (2009)
TOP OF MIOCENE	Miocene	Fleming	Geomap (2009)
EDWARDS - H2S	Edwards	Washita	Geomap (2009)
MICOENE 2	Miocene	Fleming	Geomap (2009)
WOLCOX	Wilcox	Wilcox	Geomap (2009)
CATAHOULA	Catahoula	Catahoula	https://pubs.usgs.gov/of/1994/0461/report.pdf
GLEN ROSE - DISPOSAL	Glen rose	Trinity	Geomap (2009)
GEORGTOWN	George town	Washita	Geomap (2009)
GRETA	Greta	Frio	https://scholarworks.uark.edu/etd/2873/
WILCOX	Wilcox	Wilcox	Geomap (2009)
VAN (UPPER RODESSA)	Rodessa	Rodessa	https://pubs.usgs.gov/of/2016/1026/ofr20161026.pdf
B/FRIO	Frio	Frio	Geomap (2009)
WILCOX - INJECTION/ DISPOSAL	Wilcox	Wilcox	Geomap (2009)
MIOCENE M10	Miocene	Fleming	Geomap (2009)
EDWARDS - H2S	Edwards	Washita	Geomap (2009)
MIRANDO SAND	Mirando	Jackson	https://repositories.lib.utexas.edu/bitstream/handle/2152/77978/txu-oclc-612464.pdf?sequence=1

T/YEGUA	Yegua	Claiborne	Geomap (2009)
SINTON	Sinton	Frio	https://scholarworks.uark.edu/cgi/viewcontent.cgi?article=4380&context=etd
WOODBINE	Woodbine	Woodbine	Geomap (2009)
OLMOS	Olmos	Navarro	https://pubs.usgs.gov/dds/dds-069/dds-069-h/REPORTS/69_H_CH_2.pdf
ESCONDIDO	Escondido	Escondido	Geomap (2009)
WOODBINE	Woodbine	Woodbine	Geomap (2009)
SUBCLARKSVILLE	Clarksville	Clarksville	Geomap (2009)
LOWER WILCOX	Wilcox	Wilcox	Geomap (2009)
EDWARDS - H2S	Edwards	Washita	Geomap (2009)
OLMOS	Olmos	Navarro	https://pubs.usgs.gov/dds/dds-069/dds-069-h/REPORTS/69_H_CH_2.pdf
CATAHOULA-FRIO - INJECTION/ DISPOSAL; H2S	Catahoula	Catahoula	https://pubs.usgs.gov/of/1994/0461/report.pdf
WILCOX - DISPOSAL	Wilcox	Wilcox	Geomap (2009)
EDWARDS - DISPOSAL	Edwards	Washita	Geomap (2009)
PETTIT	Pettet	Trinity	https://pubs.usgs.gov/of/1994/0461/report.pdf
VICKSBURG	Vicksburg	Vicksburg	Geomap (2009)
FRIO	Frio	Frio	Geomap (2009)

WILCOX - DISPOSAL	Wilcox	Wilcox	Geomap (2009)
EDWARDS	Edwards	Washita	Geomap (2009)
ELLENBURGER	Ellenburger	Ellenberger	file:///C:/Users/okeziec.old/Downloads/Thesis-1988-A518d%20(2).pdf
GRETA	Greta	Frio	https://scholarworks.uark.edu/etd/2873/
EDWARDS - H2S	Edwards	Washita	Geomap (2009)
CATAHOULA - DISPOSAL	Catahoula	Catahoula	https://pubs.usgs.gov/of/1994/0461/report.pdf
FRIO - DISPOSAL	Frio	Frio	Geomap (2009)
WOODBINE	Woodbine	Woodbine	Geomap (2009)
MIOCENE	Miocene	Fleming	Geomap (2009)
CATAHOULA	Catahoula	Catahoula	https://pubs.usgs.gov/of/1994/0461/report.pdf
EDWARDS - H2S	Edwards	Washita	Geomap (2009)
RODESSA	Rodessa	Rodessa	https://pubs.usgs.gov/of/2016/1026/ofr20161026.pdf
OLMOS	Olmos	Navarro	https://pubs.usgs.gov/dds/dds-069/dds-069-h/REPORTS/69_H_CH_2.pdf
EDWARDS - H2S	Edwards	Washita	Geomap (2009)
CATAHOULA	Catahoula	Catahoula	https://pubs.usgs.gov/of/1994/0461/report.pdf
BASE OF MASSIVE ANHYDRITE	Anhydrite	Trinity	https://pubs.geoscienceworld.org/aapg/books/book/1484/chapter-abstract/107178760/Summary-of-Subsurface-Geology-of-Northeast-Texas?redirectedFrom=fulltext

OLMOS - DISPOSAL	Olmos	Navarro	https://pubs.usgs.gov/dds/dds-069/dds-069-h/REPORTS/69_H_CH_2.pdf
MIOCENE - DISPOSAL	Miocene	Fleming	Geomap (2009)
FRIO - DISPOSAL	Frio	Frio	Geomap (2009)
WOODBINE	Woodbine	Woodbine	Geomap (2009)
FRIO - DISPOSAL	Frio	Frio	Geomap (2009)
CATAHOULA - DISPOSAL, H2S (CORDELE, WEST AREA)	Catahoula	Catahoula	https://pubs.usgs.gov/of/1994/0461/report.pdf
GRETA UPPER	Greta	Frio	https://scholarworks.uark.edu/etd/2873/
CATAHOULA-FRIO - INJECTION/ DISPOSAL	Catahoula	Catahoula	https://pubs.usgs.gov/of/1994/0461/report.pdf
EDWARDS	Edwards	Washita	Geomap (2009)
WILCOX - DISPOSAL	Wilcox	Wilcox	Geomap (2009)
BLOSSOM	Blossom	Austin	https://pubs.usgs.gov/of/1994/0461/report.pdf
NACATOCH - OVER PRESSURED, WATER FLOW	Nacatoch	Navarro	https://repositories.lib.utexas.edu/bitstream/handle/2152/77501/txu-oclc-10367600.pdf?sequence=1
WILCOX - DISPOSAL	Wilcox	Wilcox	Geomap (2009)

WILCOX - DISPOSAL	Wilcox	Wilcox	Geomap (2009)
EDWARDS - H2S, DISPOSAL	Edwards	Washita	Geomap (2009)
WILCOX - DISPOSAL	Wilcox	Wilcox	Geomap (2009)
TRAVIS PEAK	Travis peak	Trinity	https://pubs.usgs.gov/bul/b2184-e/B2184E-508.pdf
FRIO - DISPOSAL	Frio	Frio	Geomap (2009)
EDWARDS - H2S, DISPOSAL	Edwards	Washita	Geomap (2009)
GLEN ROSE - DISPOSAL	Glen rose	Trinity	Geomap (2009)
WOODBINE	Woodbine	Woodbine	Geomap (2009)
GRETA	Greta	Frio	https://scholarworks.uark.edu/etd/2873/
GEORGETOWN	George town	Washita	Geomap (2009)
PETTET	Pettet	Trinity	https://pubs.usgs.gov/of/1994/0461/report.pdf
FRIO	Frio	Frio	Geomap (2009)
TOP FRIO	Frio	Frio	Geomap (2009)
WOODBINE	Woodbine	Woodbine	Geomap (2009)
WILCOX - DISPOSAL	Wilcox	Wilcox	Geomap (2009)
GEORGETOWN - H2S	George town	Washita	Geomap (2009)
FRIO - DISPOSAL	Frio	Frio	Geomap (2009)

GOV'T WELLS	Government wells	Jackson	https://repositories.lib.utexas.edu/bitstream/handle/2152/77978/txu-oclc-612464.pdf?sequence=1
GEORGETOWN	George town	Washita	Geomap (2009)
RODESSA	Rodessa	Rodessa	https://pubs.usgs.gov/of/2016/1026/ofr20161026.pdf
CATAHOULA - DISPOSAL	Catahoula	Catahoula	https://pubs.usgs.gov/of/1994/0461/report.pdf
JACKSON - DISPOSAL	Jackson	Jackson	Geomap (2009)
CATAHOULA-FRIO - INJECTION/ DISPOSAL	Catahoula	Catahoula	https://pubs.usgs.gov/of/1994/0461/report.pdf
WILCOX - DISPOSAL	Wilcox	Wilcox	Geomap (2009)
CARRIZO	Carrizo	Wilcox	Geomap (2009)
4400 SAND	4400	Frio	https://www.osti.gov/servlets/purl/140595
RODESSA	Rodessa	Rodessa	https://pubs.usgs.gov/of/2016/1026/ofr20161026.pdf
MIOCENE - DISPOSAL	Miocene	Fleming	Geomap (2009)
WOODBINE	Woodbine	Woodbine	Geomap (2009)
PETTUS	Pettet	Trinity	https://pubs.usgs.gov/of/1994/0461/report.pdf
FRIO - DISPOSAL	Frio	Frio	Geomap (2009)
MIOCENE	Miocene	Fleming	Geomap (2009)
WOODBINE	Woodbine	Woodbine	Geomap (2009)

EDWARDS	Edwards	Washita	Geomap (2009)
GLEN ROSE	Glen rose	Trinity	Geomap (2009)
RODESSA	Rodessa	Rodessa	https://pubs.usgs.gov/of/2016/1026/ofr20161026.pdf
RODESSA	Rodessa	Rodessa	https://pubs.usgs.gov/of/2016/1026/ofr20161026.pdf
FRIO	Frio	Frio	Geomap (2009)
WOODBINE	Woodbine	Woodbine	Geomap (2009)
PETTET	Pettet	Trinity	https://pubs.usgs.gov/of/1994/0461/report.pdf
ESCONDIDO	Escondido	Escondido	Geomap (2009)
WOODBINE - EAST TEXAS FIELD (DISTRICT 6E)	Woodbine	Woodbine	Geomap (2009)
WOODBINE	Woodbine	Woodbine	Geomap (2009)
OLMOS	Olmos	Navarro	https://pubs.usgs.gov/dds/dds-069/dds-069-h/REPORTS/69_H_CH_2.pdf
CATAHOULA-FRIO	Catahoula	Catahoula	https://pubs.usgs.gov/of/1994/0461/report.pdf
CATAHOULA	Catahoula	Catahoula	https://pubs.usgs.gov/of/1994/0461/report.pdf
TRAVIS PEAK	Travis peak	Trinity	https://pubs.usgs.gov/bul/b2184-e/B2184E-508.pdf
WOODBINE	Woodbine	Woodbine	Geomap (2009)
NACATOCH	Nacatoch	Navarro	https://repositories.lib.utexas.edu/bitstream/handle/2152/77501/txu-oclc-10367600.pdf?sequence=1

RODESSA	Rodessa	Rodessa	https://pubs.usgs.gov/of/2016/1026/ofr20161026.pdf
PETTET	Pettet	Trinity	https://pubs.usgs.gov/of/1994/0461/report.pdf
JAMES LIME	James	Trinity	Geomap (2009)
FRIO	Frio	Frio	Geomap (2009)
PETTET	Pettet	Trinity	https://pubs.usgs.gov/of/1994/0461/report.pdf
PETTET	Pettet	Trinity	https://pubs.usgs.gov/of/1994/0461/report.pdf
FRIO - DISPOSAL	Frio	Frio	Geomap (2009)
MIOCENE - DISPOSAL	Miocene	Fleming	Geomap (2009)
WOODBINE	Woodbine	Woodbine	Geomap (2009)
GRETTA - DISPOSAL	Greta	Frio	https://scholarworks.uark.edu/etd/2873/
FRIO - DISPOSAL	Frio	Frio	Geomap (2009)
PETTET	Pettet	Trinity	https://pubs.usgs.gov/of/1994/0461/report.pdf
RODESSA	Rodessa	Rodessa	https://pubs.usgs.gov/of/2016/1026/ofr20161026.pdf
WOODBINE	Woodbine	Woodbine	Geomap (2009)
JACKSON - INJECTION/ DISPOSAL; H2S	Jackson	Jackson	Geomap (2009)
TRAVIS PEAK	Travis peak	Trinity	https://pubs.usgs.gov/bul/b2184-e/B2184E-508.pdf
RODESSA	Rodessa	Rodessa	https://pubs.usgs.gov/of/2016/1026/ofr20161026.pdf
FRIO	Frio	Frio	Geomap (2009)

FRIO FORMATION	Frio	Frio	Geomap (2009)
PETTIT	Pettet	Trinity	https://pubs.usgs.gov/of/1994/0461/report.pdf
RODESSA	Rodessa	Rodessa	https://pubs.usgs.gov/of/2016/1026/ofr20161026.pdf
OAKVILLE	Oakeville	Fleming	Geomap (2009)
SUB-CLARKSVILLE	Clarksville	Clarksville	Geomap (2009)
WILCOX - DISPOSAL	Wilcox	Wilcox	Geomap (2009)
B/MA	Anhydrite	Trinity	https://pubs.geoscienceworld.org/aapg/books/book/1484/chapter-abstract/107178760/Summary-of-Subsurface-Geology-of-Northeast-Texas?redirectedFrom=fulltext
WILCOX	Wilcox	Wilcox	Geomap (2009)
JACKSON - INJECTION/ DISPOSAL; H2S	Jackson	Jackson	Geomap (2009)
RODESSA	Rodessa	Rodessa	https://pubs.usgs.gov/of/2016/1026/ofr20161026.pdf
COLE SAND	Cole	Jackson	Geomap (2009)
MIOCENE	Miocene	Fleming	Geomap (2009)
WILCOX - DISPOSAL	Wilcox	Wilcox	Geomap (2009)
FRIO	Frio	Frio	Geomap (2009)
WILCOX	Wilcox	Wilcox	Geomap (2009)
EAGLEFORD	Eagleford	Eagleford	Geomap (2009)

YEGUA A	Yegua	Claiborne	Geomap (2009)
YEGUA SD	Yegua	Claiborne	Geomap (2009)
RODESSA	Rodessa	Rodessa	https://pubs.usgs.gov/of/2016/1026/ofr20161026.pdf
FRIO - DISPOSAL	Frio	Frio	Geomap (2009)
GRETA FORMATION, 4523 FT TOP	Greta	Frio	https://scholarworks.uark.edu/etd/2873/
FRIO - DISPOSAL	Frio	Frio	Geomap (2009)
CATAHOULA - DISPOSAL	Catahoula	Catahoula	https://pubs.usgs.gov/of/1994/0461/report.pdf
FRIO - DISPOSAL	Frio	Frio	Geomap (2009)
YEGUA - DISPOSAL	Yegua	Claiborne	Geomap (2009)
CATAHOULA-FRIO - INJECTION/ DISPOSAL	Catahoula	Catahoula	https://pubs.usgs.gov/of/1994/0461/report.pdf
CATAHOULA	Catahoula	Catahoula	https://pubs.usgs.gov/of/1994/0461/report.pdf
TRAVIS PEAK	Travis peak	Trinity	https://pubs.usgs.gov/bul/b2184-e/B2184E-508.pdf
FRIO	Frio	Frio	Geomap (2009)
EAGLE FORD	Eagleford	Eagleford	Geomap (2009)
EAGLE FORD	Eagleford	Eagleford	Geomap (2009)

AUSTIN CHALK - H2S	Austin Chalk	Austin	Geomap (2009)
TOP OF WILCOX	Wilcox	Wilcox	Geomap (2009)
PALUXY	Paluxy	Fredericksburg	Geomap (2009)

Appendix B – Injection Volume and Permitted Volume

The figures below show the monthly injection volume and permitted volume for each saltwater disposal well plotted against year. The red lines represent the permitted volume, while the blue lines represent the monthly injection volume. Out of 4805 wells, only 120 wells have been represented here. To view all the plots, visit https://www.dropbox.com/scl/fi/btto0j065t6s1d56lyws4/Volume-and-Permitted-Volume.pdf?rlkey=x7hq34eizn0ocwu9yu264rzqp&st=skpc75ax&dl=0

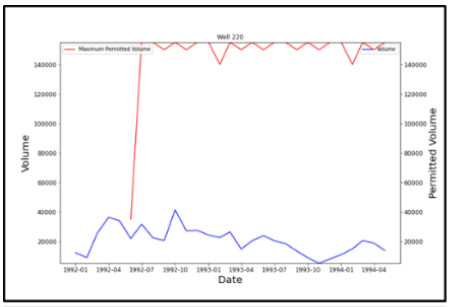
Well 220
Maximum Permitted Volume
Volume
Volume
Permitted Volume
Date

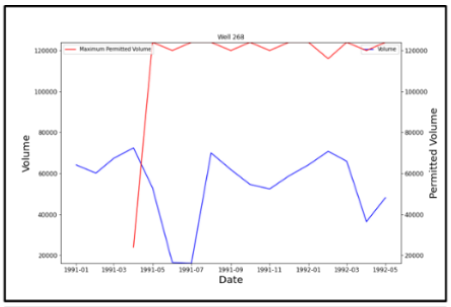
Well 268
Maximum Permitted Volume
Volume
Volume
Permitted Volume
Date

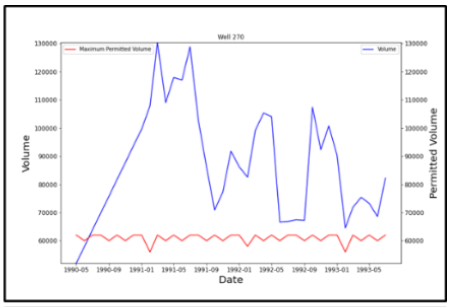
Well 270
Maximum Permitted Volume
Volume
Volume
Permitted Volume
Date

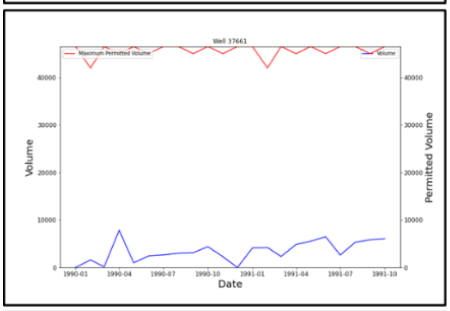
Well 37661
Maximum Permitted Volume
Volume
Volume
Permitted Volume
Date

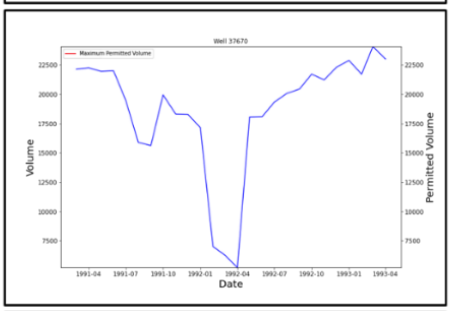
Well 37670
Maximum Permitted Volume
Volume
Volume
Permitted Volume
Date

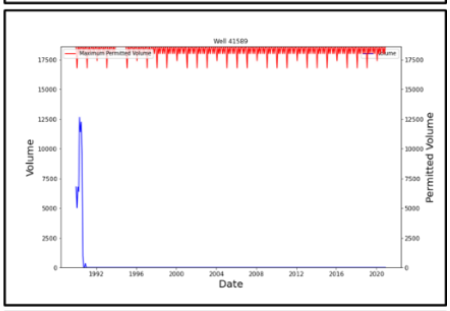
Well 41589
Maximum Permitted Volume
Volume
Volume
Permitted Volume
Date

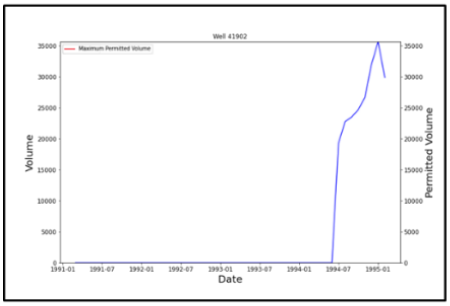
Well 41962
Maximum Permitted Volume
Volume
Volume
Permitted Volume
Date

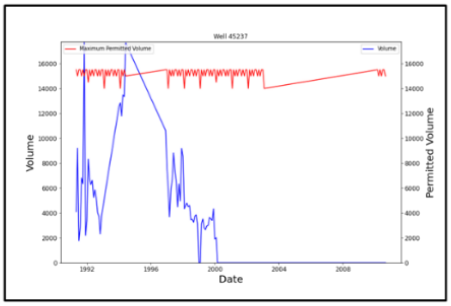
Well 45237
Maximum Permitted Volume
Volume
Volume
Permitted Volume
Date

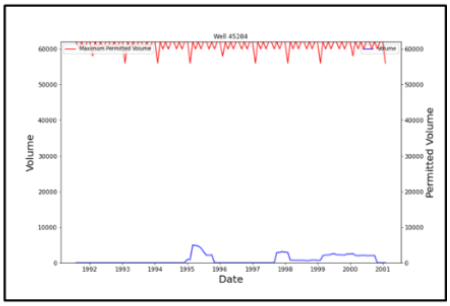
Well 45284
Maximum Permitted Volume
Volume
Volume
Permitted Volume
Date

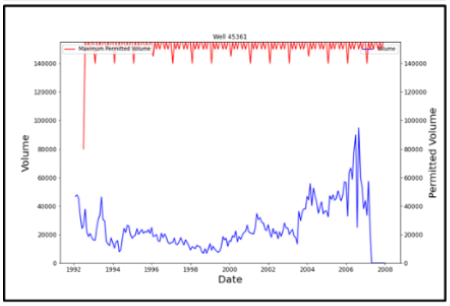
Well 45361
Maximum Permitted Volume
Volume
Volume
Permitted Volume
Date

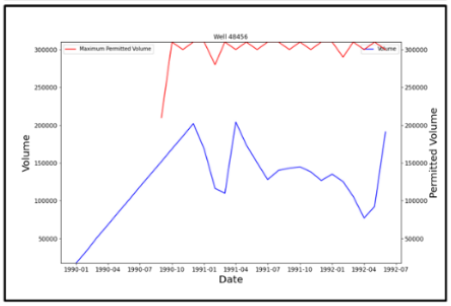
Well 48456
Maximum Permitted Volume
Volume
Volume
Permitted Volume
Date

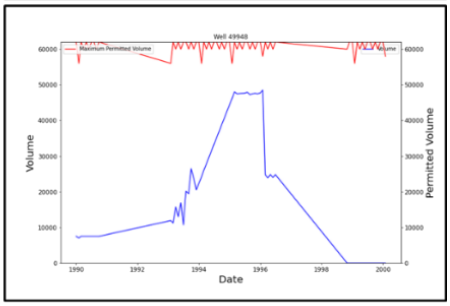
Well 49948
Maximum Permitted Volume
Volume
Volume
Permitted Volume
Date

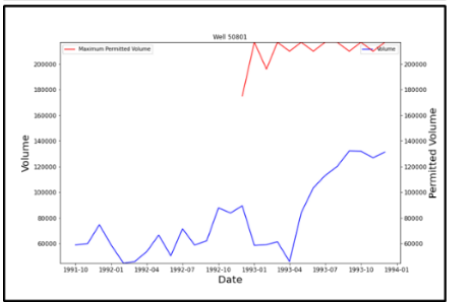
Well 50801
Maximum Permitted Volume
Volume
Volume
Permitted Volume
Date

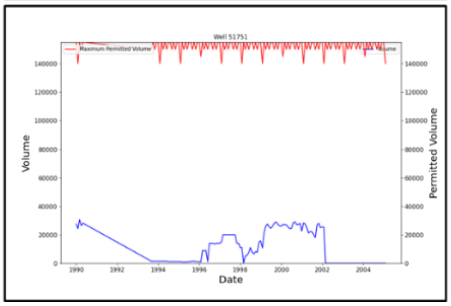
Well 51751
Maximum Permitted Volume
Volume
Volume
Permitted Volume
Date

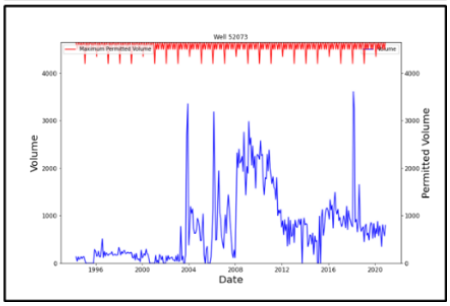
Well 52073
Maximum Permitted Volume
Volume
Volume
Permitted Volume
Date

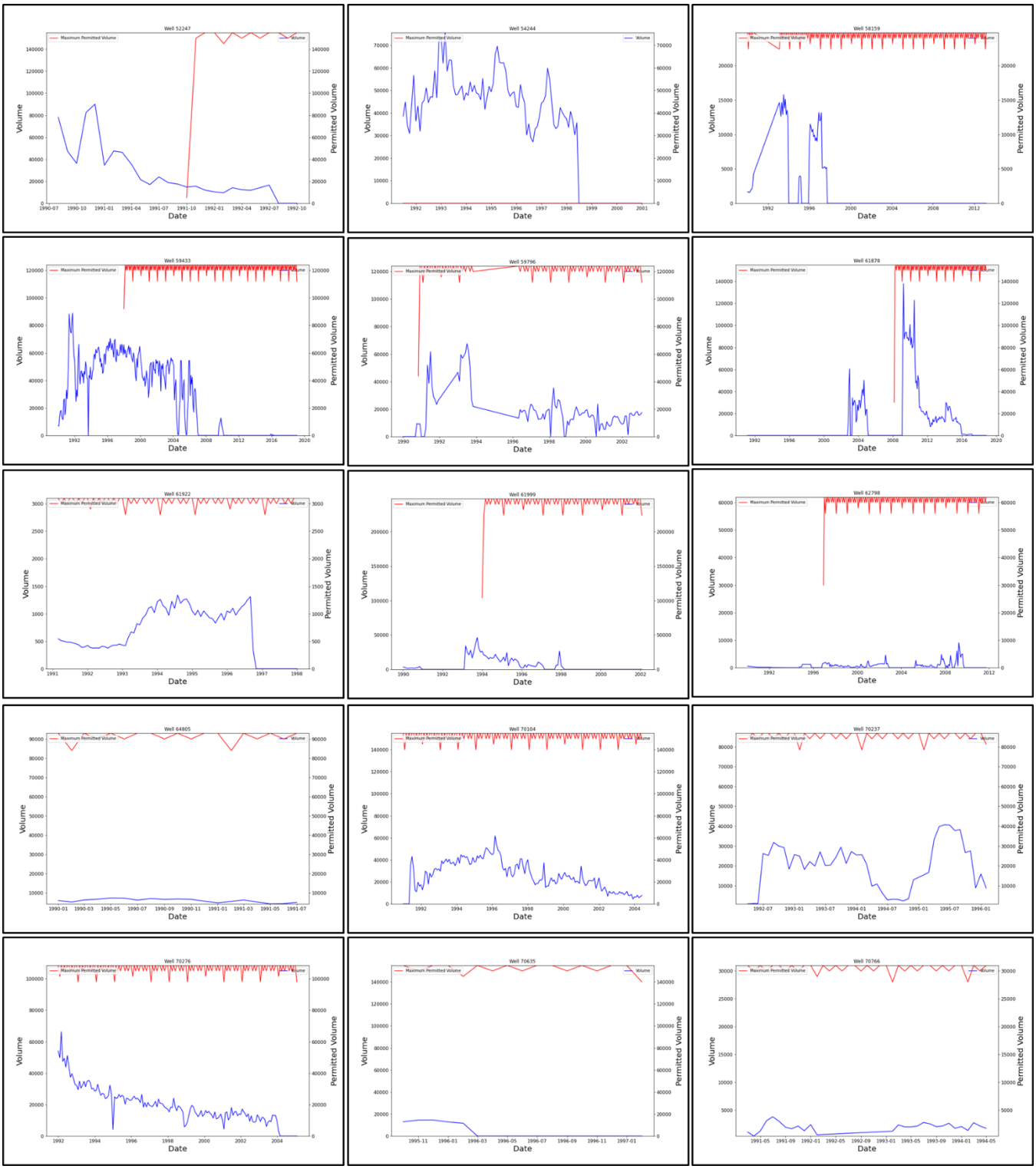
Well 52247
Well 54244
Well 58159
Well 59433
Well 59796
Well 61878
Well 61922
Well 61999
Well 62798
Well 64805
Well 70104
Well 70237
Well 70276
Well 70635
Well 70766
Maximum Permitted Volume
Volume
Volume
Permitted Volume
Date

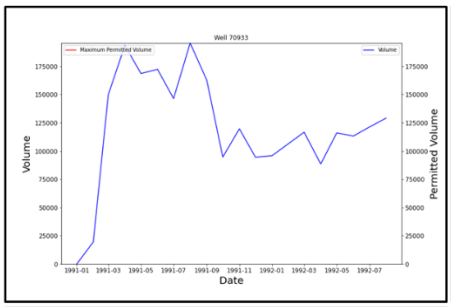
Well 70933
Maximum Permitted Volume
Volume
Volume
Permitted Volume
Date

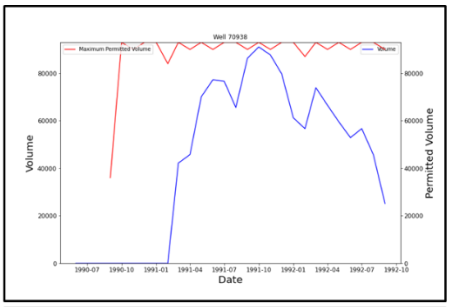
Well 70938
Maximum Permitted Volume
Volume
Volume
Permitted Volume
Date

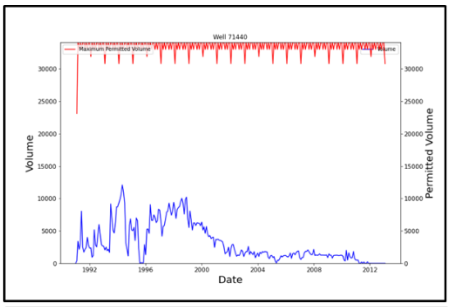
Well 71440
Maximum Permitted Volume
Volume
Volume
Permitted Volume
Date

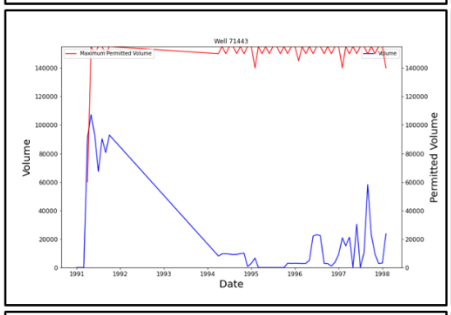
Well 71443
Maximum Permitted Volume
Volume
Volume
Permitted Volume
Date

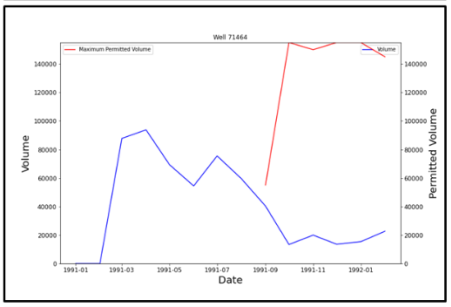
Well 71464
Maximum Permitted Volume
Volume
Volume
Permitted Volume
Date

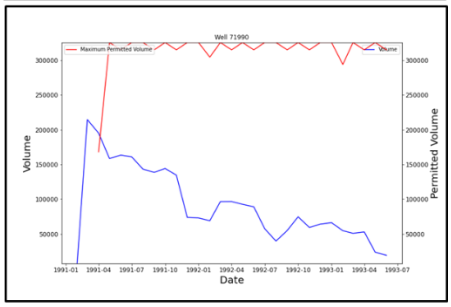
Well 71990
Maximum Permitted Volume
Volume
Volume
Permitted Volume
Date

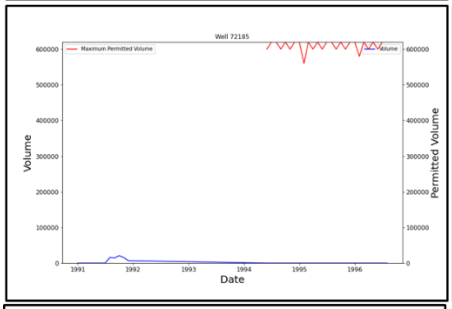
Well 72185
Maximum Permitted Volume
Volume
Volume
Permitted Volume
Date

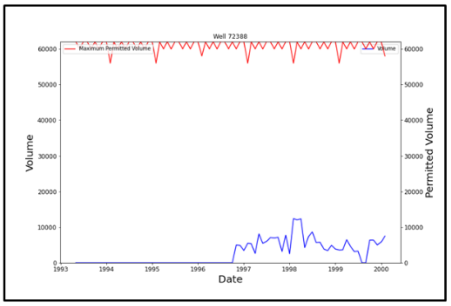
Well 72388
Maximum Permitted Volume
Volume
Volume
Permitted Volume
Date

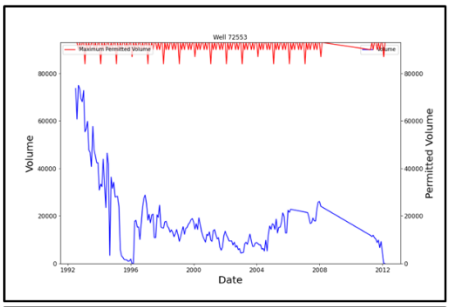
Well 72553
Maximum Permitted Volume
Volume
Volume
Permitted Volume
Date

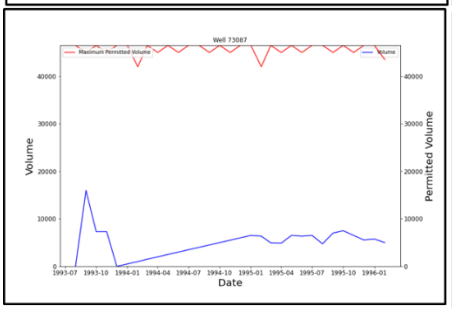
Well 73087
Maximum Permitted Volume
Volume
Volume
Permitted Volume
Date

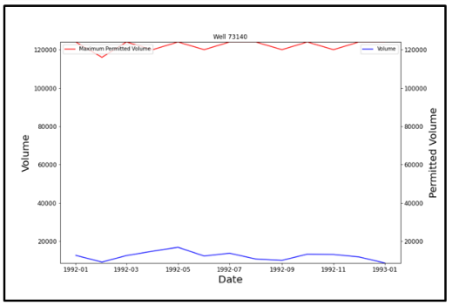
Well 73140
Maximum Permitted Volume
Volume
Volume
Permitted Volume
Date

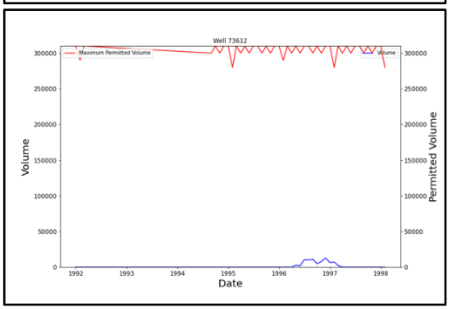
Well 73612
Maximum Permitted Volume
Volume
Volume
Permitted Volume
Date

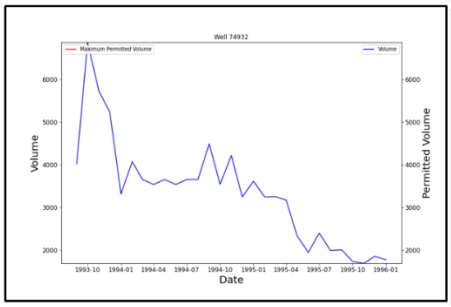
Well 74932
Maximum Permitted Volume
Volume
Volume
Permitted Volume
Date

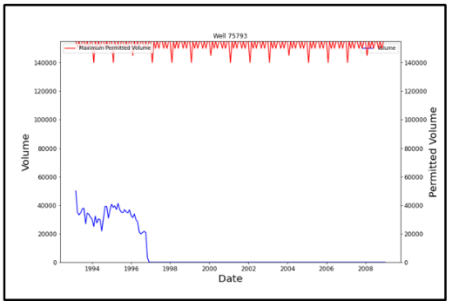
Well 75793
Maximum Permitted Volume
Volume
Volume
Permitted Volume
Date

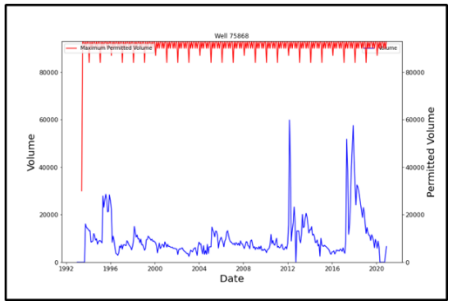
Well 75868
Maximum Permitted Volume
Volume
Volume
Permitted Volume
Date

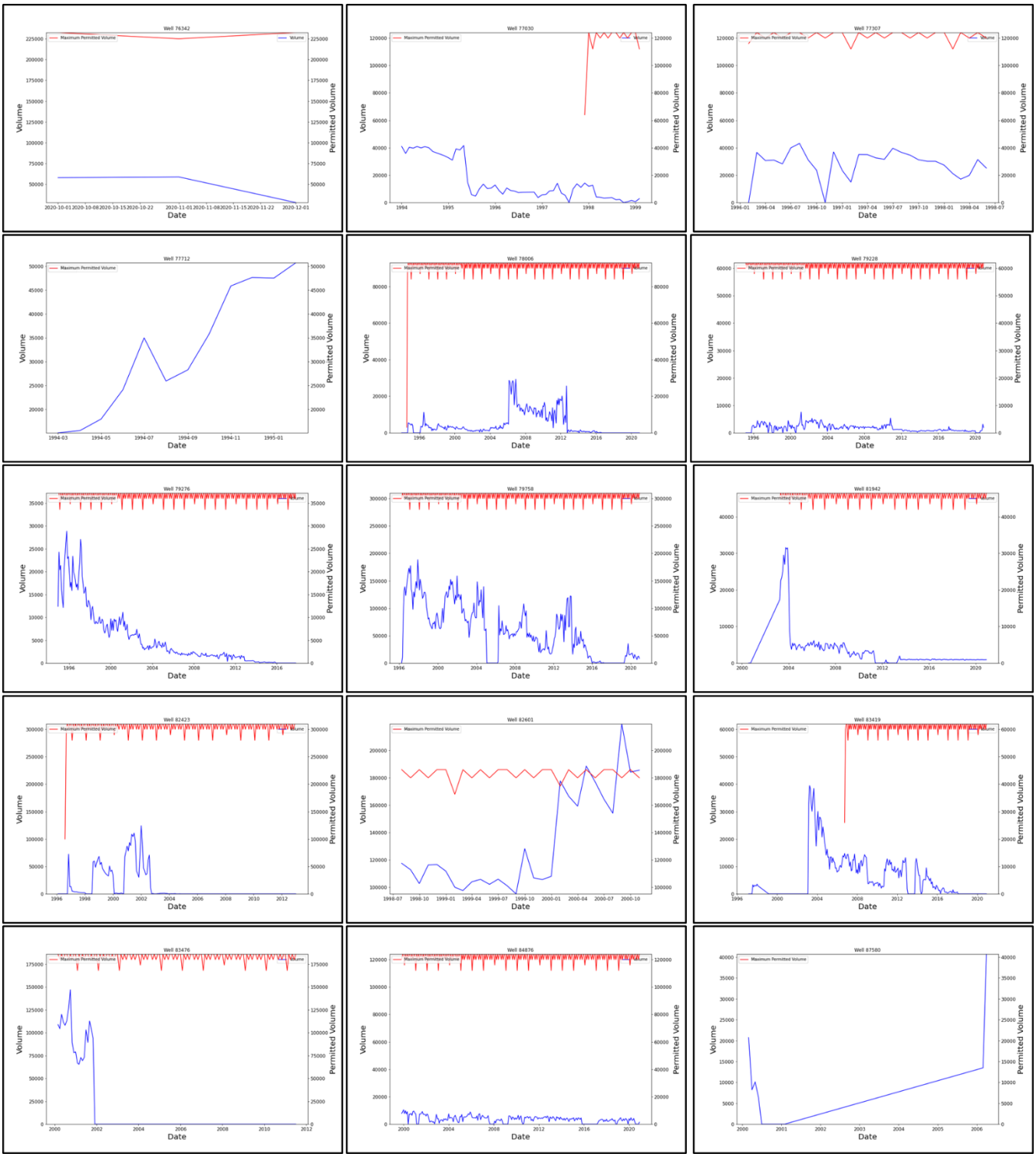
Well 76342
Well 77030
Well 77307
Well 77712
Well 78006
Well 79228
Well 79276
Well 79758
Well 81942
Well 82423
Well 82601
Well 83419
Well 83476
Well 84876
Well 87580
Maximum Permitted Volume
Volume
Date
Permitted Volume

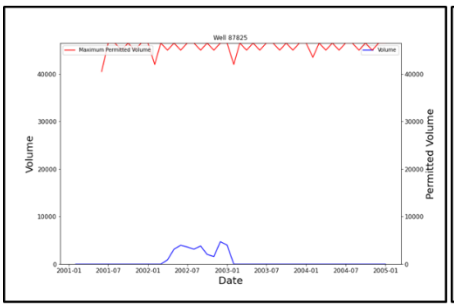
Well 87825
Maximum Permitted Volume
Volume
Volume
Permitted Volume
Date

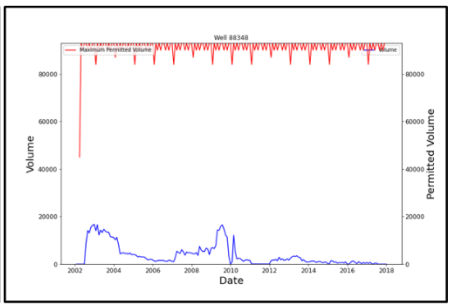
Well 88348
Maximum Permitted Volume
Volume
Volume
Permitted Volume
Date

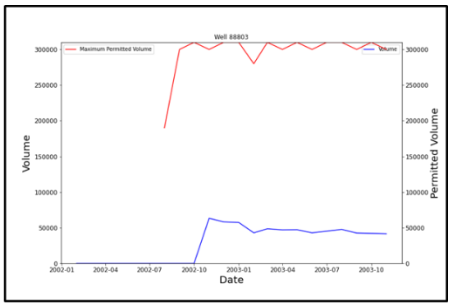
Well 88803
Maximum Permitted Volume
Volume
Volume
Permitted Volume
Date

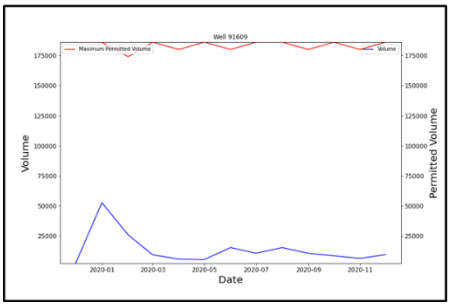
Well 91609
Maximum Permitted Volume
Volume
Volume
Permitted Volume
Date

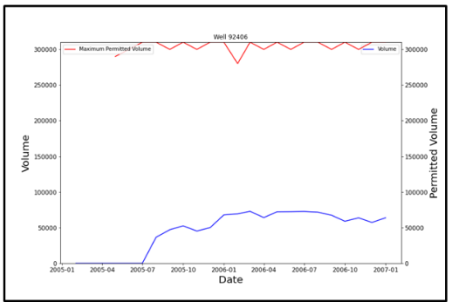
Well 92406
Maximum Permitted Volume
Volume
Volume
Permitted Volume
Date

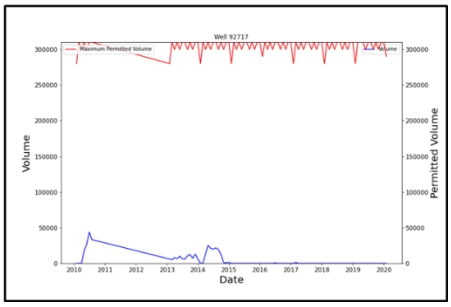
Well 92717
Maximum Permitted Volume
Volume
Volume
Permitted Volume
Date

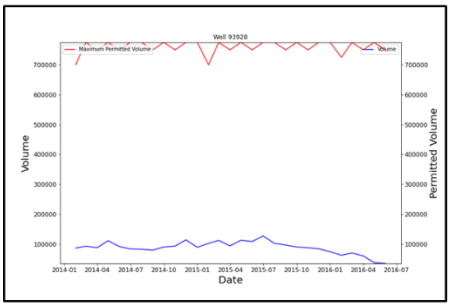
Well 93928
Maximum Permitted Volume
Volume
Volume
Permitted Volume
Date

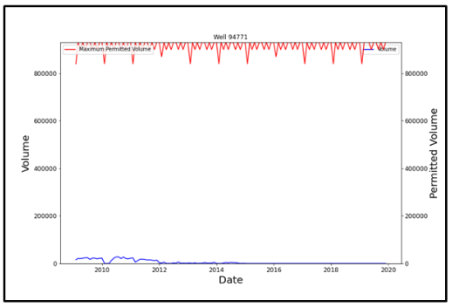
Well 94771
Maximum Permitted Volume
Volume
Volume
Permitted Volume
Date

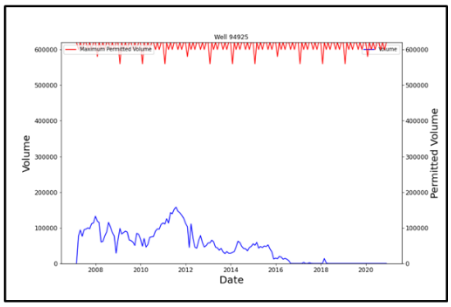
Well 94925
Maximum Permitted Volume
Volume
Volume
Permitted Volume
Date

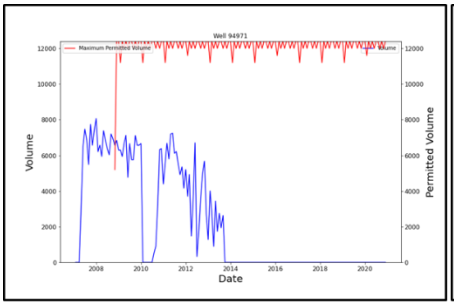
Well 94971
Maximum Permitted Volume
Volume
Volume
Permitted Volume
Date

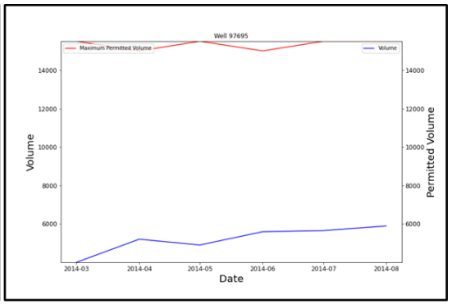
Well 97695
Maximum Permitted Volume
Volume
Volume
Permitted Volume
Date

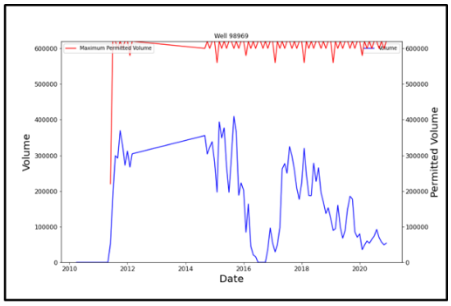
Well 98969
Maximum Permitted Volume
Volume
Volume
Permitted Volume
Date

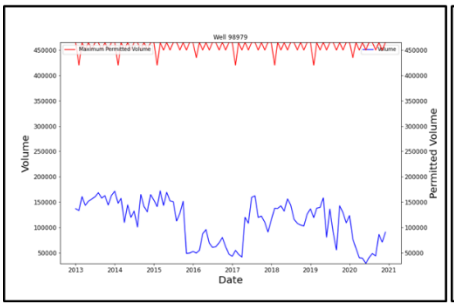
Well 98979
Maximum Permitted Volume
Volume
Volume
Permitted Volume
Date

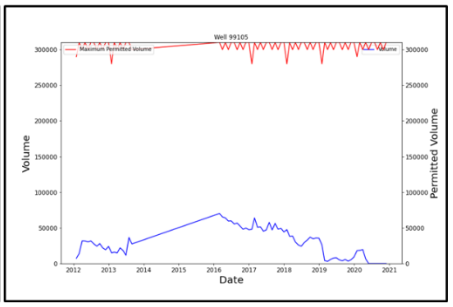
Well 99105
Maximum Permitted Volume
Volume
Volume
Permitted Volume
Date

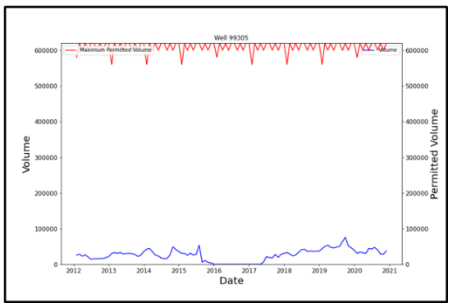
Well 99305
Maximum Permitted Volume
Volume
Volume
Permitted Volume
Date

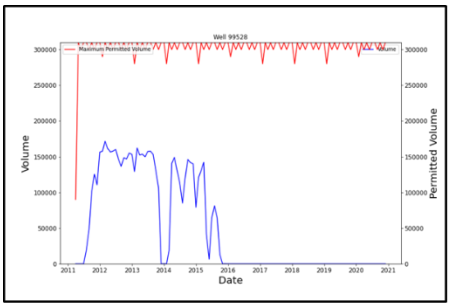
Well 99528
Maximum Permitted Volume
Volume
Volume
Permitted Volume
Date

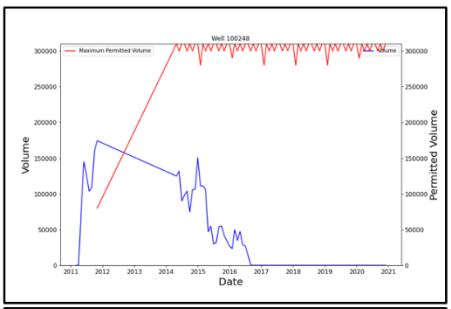
Well 100248
Maximum Permitted Volume
Volume
Volume
Permitted Volume
Date

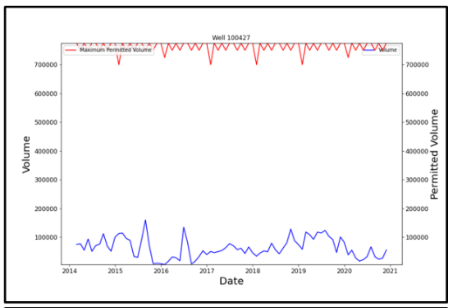
Well 100427
Maximum Permitted Volume
Volume
Volume
Permitted Volume
Date

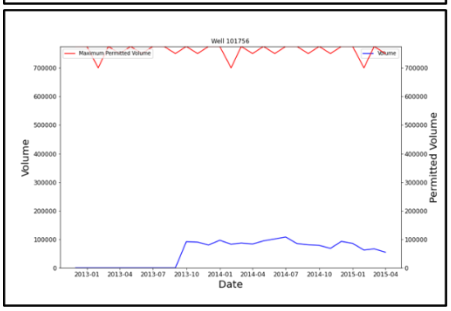
Well 101756
Maximum Permitted Volume
Volume
Volume
Permitted Volume
Date

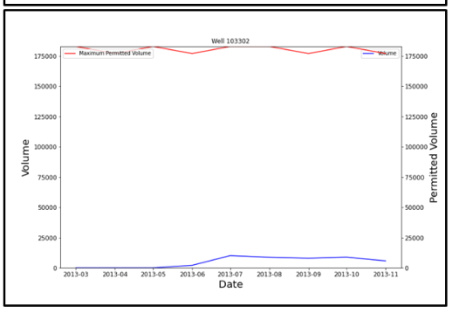
Well 103302
Maximum Permitted Volume
Volume
Volume
Permitted Volume
Date

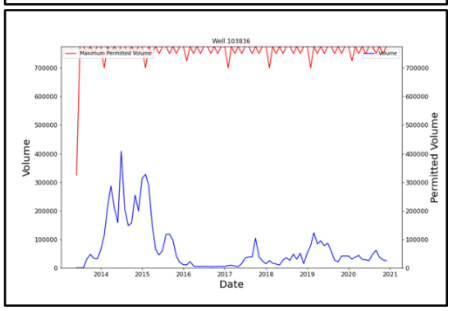
Well 103836
Maximum Permitted Volume
Volume
Volume
Permitted Volume
Date

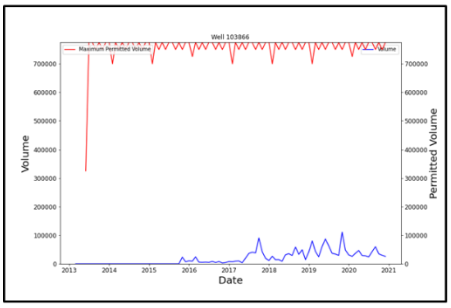
Well 103866
Maximum Permitted Volume
Volume
Volume
Permitted Volume
Date

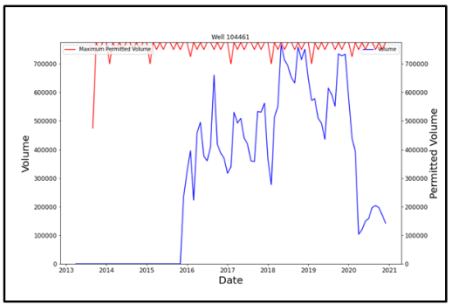
Well 104461
Maximum Permitted Volume
Volume
Volume
Permitted Volume
Date

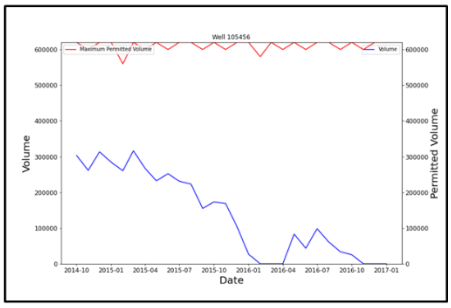
Well 105456
Maximum Permitted Volume
Volume
Volume
Permitted Volume
Date

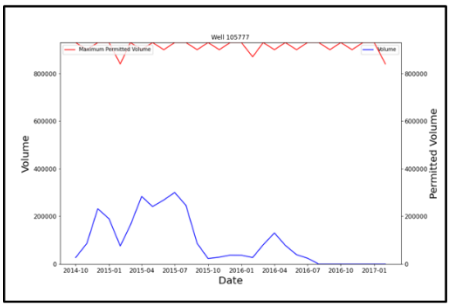
Well 105777
Maximum Permitted Volume
Volume
Volume
Permitted Volume
Date

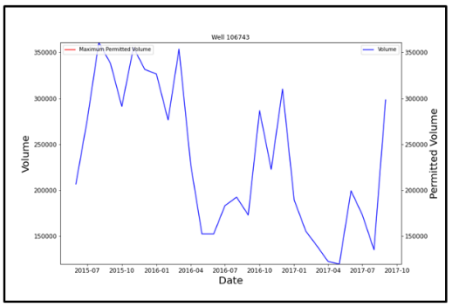
Well 106743
Maximum Permitted Volume
Volume
Volume
Permitted Volume
Date

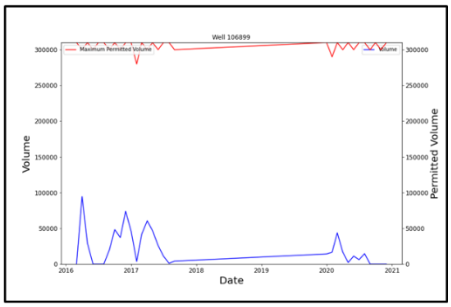
Well 106899
Maximum Permitted Volume
Volume
Volume
Permitted Volume
Date

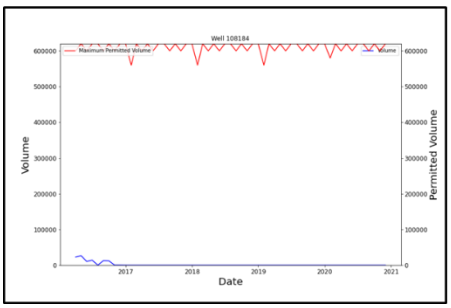
Well 108184
Maximum Permitted Volume
Volume
Volume
Permitted Volume
Date

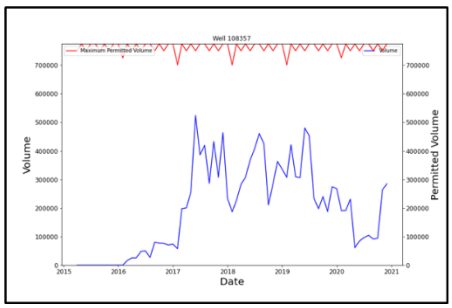
Well 108357
Maximum Permitted Volume
Volume
Volume
Permitted Volume
Date

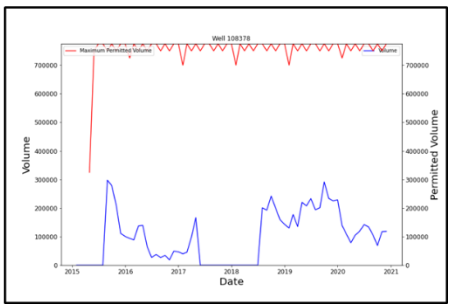
Well 108378
Maximum Permitted Volume
Volume
Volume
Permitted Volume
Date

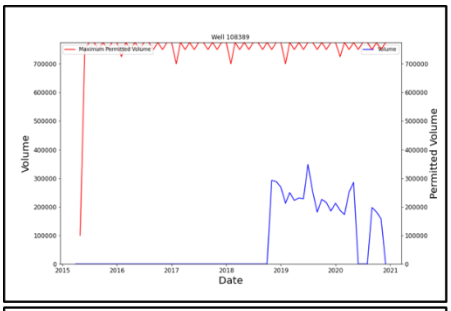
Well 108389
Maximum Permitted Volume
Volume
Volume
Permitted Volume
Date

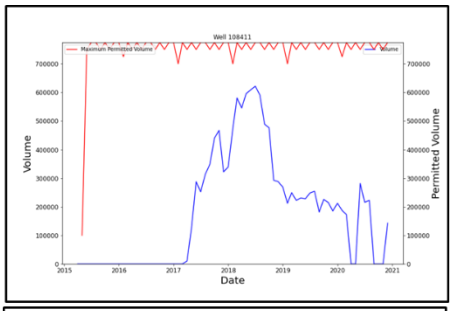
Well 108411
Maximum Permitted Volume
Volume
Volume
Permitted Volume
Date

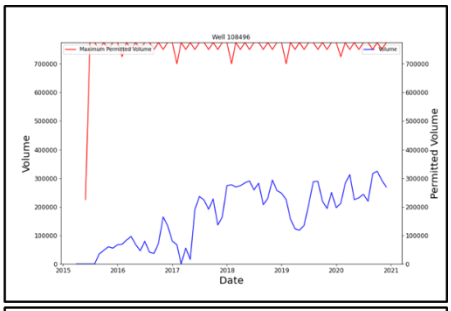
Well 108496
Maximum Permitted Volume
Volume
Volume
Permitted Volume
Date

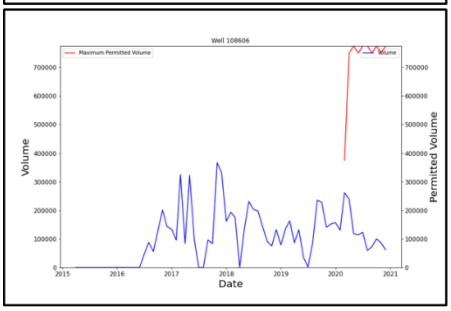
Well 108606
Maximum Permitted Volume
Volume
Volume
Permitted Volume
Date

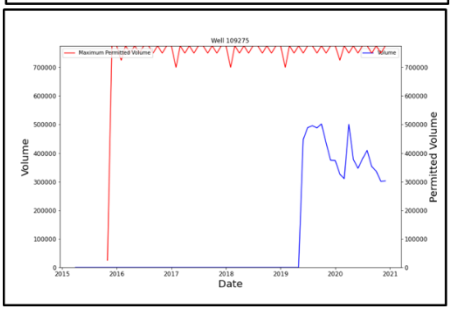
Well 109275
Maximum Permitted Volume
Volume
Volume
Permitted Volume
Date

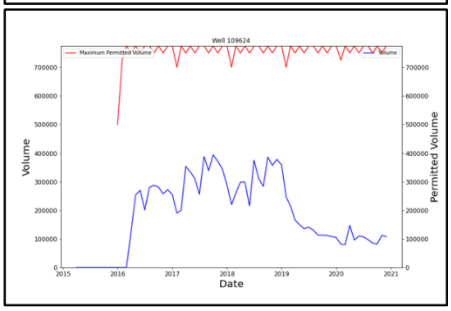
Well 109624
Maximum Permitted Volume
Volume
Volume
Permitted Volume
Date

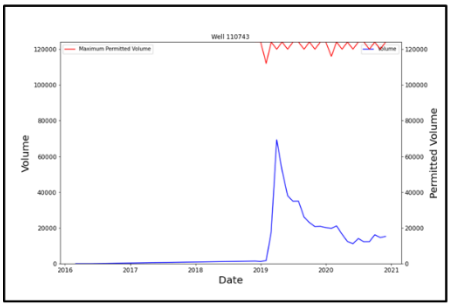
Well 110743
Maximum Permitted Volume
Volume
Volume
Permitted Volume
Date

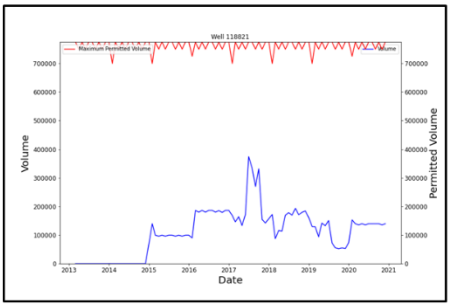
Well 118821
Maximum Permitted Volume
Volume
Volume
Permitted Volume
Date

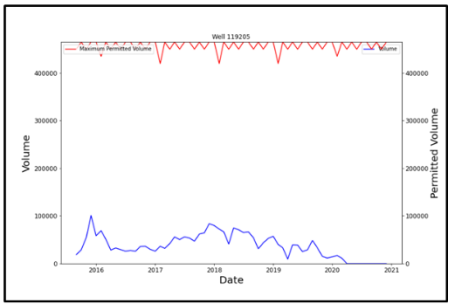
Well 119205
Maximum Permitted Volume
Volume
Volume
Permitted Volume
Date

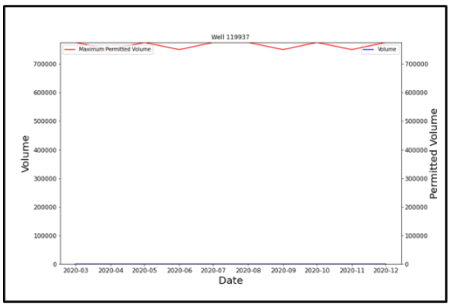
Well 119937
Maximum Permitted Volume
Volume
Volume
Permitted Volume
Date

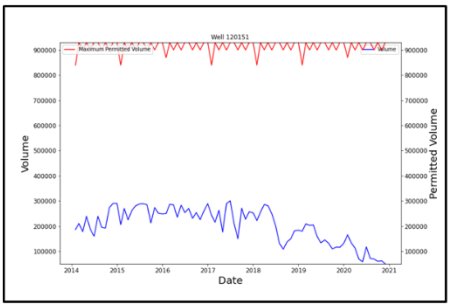
Well 120151
Maximum Permitted Volume
Volume
Volume
Permitted Volume
Date

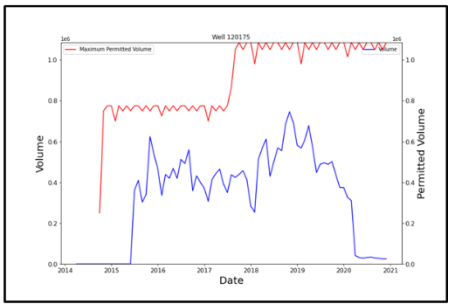
Well 120175
Maximum Permitted Volume
Volume
Volume
Permitted Volume
Date

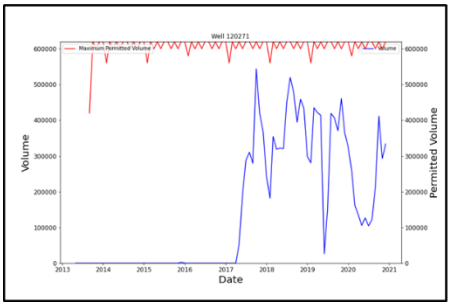
Well 120271
Maximum Permitted Volume
Volume
Volume
Permitted Volume
Date

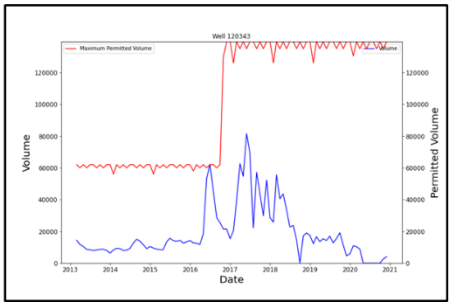
Well 120343
Maximum Permitted Volume
Volume
Volume
Permitted Volume
Date

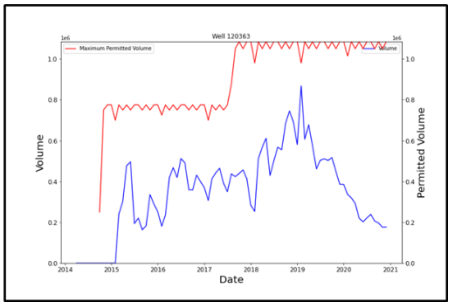
Well 120363
Maximum Permitted Volume
Volume
Volume
Permitted Volume
Date

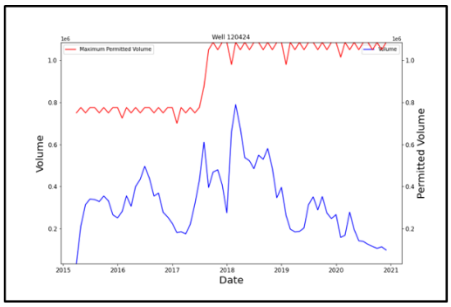
Well 120424
Maximum Permitted Volume
Volume
Volume
Permitted Volume
Date

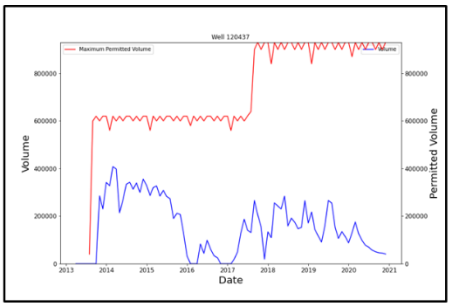
Well 120437
Maximum Permitted Volume
Volume
Volume
Permitted Volume
Date

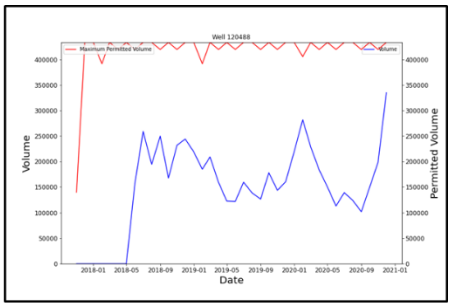
Well 120488
Maximum Permitted Volume
Volume
Volume
Permitted Volume
Date

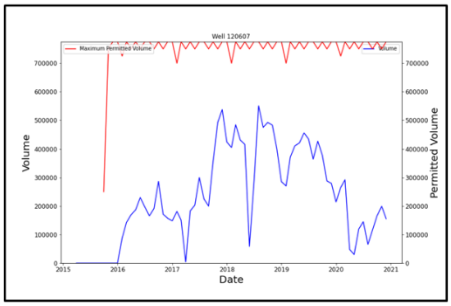
Well 120607
Maximum Permitted Volume
Volume
Volume
Permitted Volume
Date

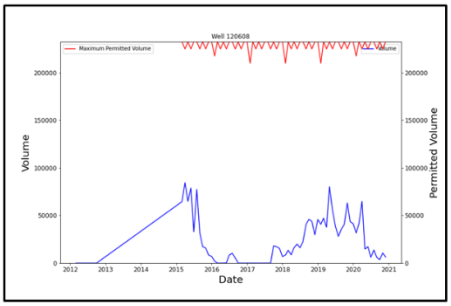
Well 120608
Maximum Permitted Volume
Volume
Volume
Permitted Volume
Date

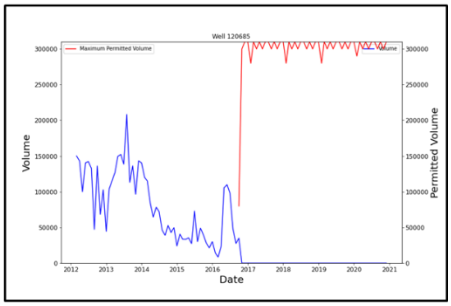
Well 120685
Maximum Permitted Volume
Volume
Volume
Permitted Volume
Date

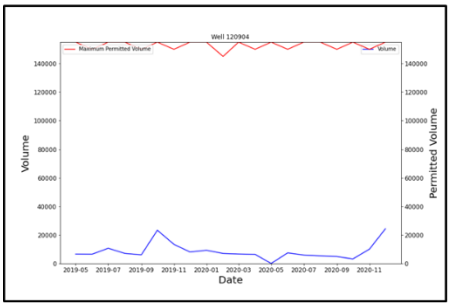
Well 120904
Maximum Permitted Volume
Volume
Volume
Permitted Volume
Date

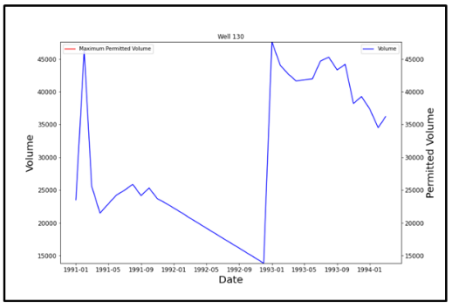
Well 130
Maximum Permitted Volume
Volume
Volume
Permitted Volume
Date

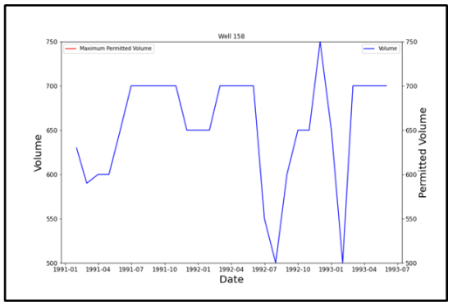
Well 158
Maximum Permitted Volume
Volume
Volume
Permitted Volume
Date

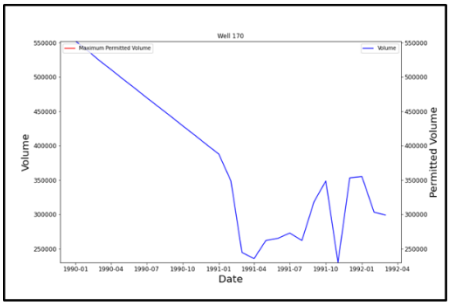
Well 170
Maximum Permitted Volume
Volume
Volume
Permitted Volume
Date

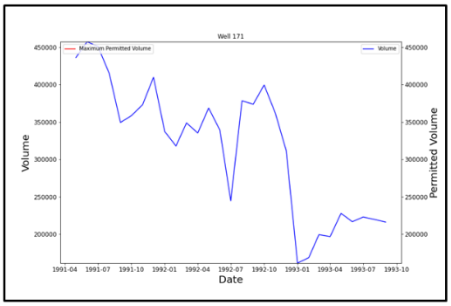
Well 171
Maximum Permitted Volume
Volume
Volume
Permitted Volume
Date

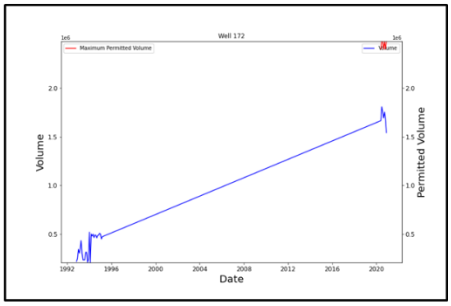
Well 172
Maximum Permitted Volume
Volume
Volume
Permitted Volume
Date

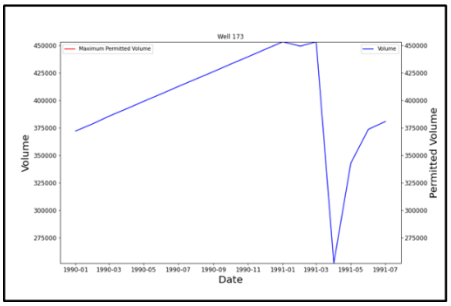
Well 173
Maximum Permitted Volume
Volume
Volume
Permitted Volume
Date

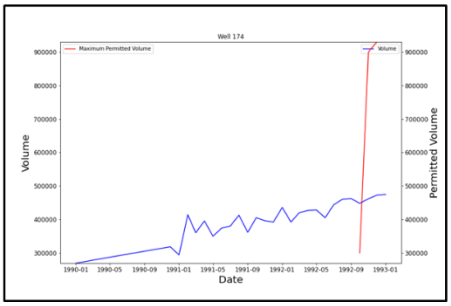
Well 174
Maximum Permitted Volume
Volume
Volume
Permitted Volume
Date

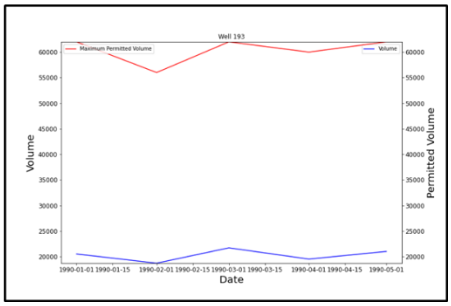
Well 193
Maximum Permitted Volume
Volume
Volume
Permitted Volume
Date

Appendix C - Injection Pressure, Permitted Pressure, and Injection Rate

The figures below show the monthly injection pressure, maximum monthly pressure, permitted pressure and rates for each saltwater disposal well plotted against year. The red lines represent the monthly injection pressure, the green line represent the maximum monthly pressure, the yellow line represent the permitted pressure, while the blue lines represent the monthly injection rate. Some of the wells do not have their monthly permitted pressures reported. Out of 592 wells, only 120 wells have been represented here. Kindly note that only wells verified to be injecting into the same formation should be compared. To view all the plots, visit https://www.dropbox.com/scl/fi/jm07sy3dzsgzsgm6c0ns1/Pressures-and-Rate.docx?rlkey=7h8qpc3a8uwjo8lb31g1pe11b&st=kb0ym3h9&dl=0

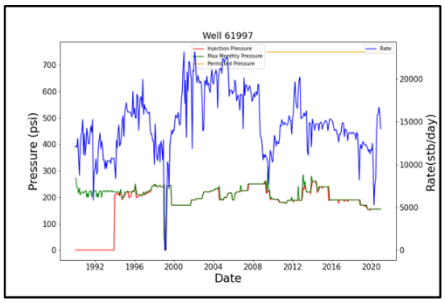
Well 61997
Injection Pressure
Max Monthly Pressure
Permitted Pressure
Rate
Pressure (psi)
Rate(stb/day)
Date

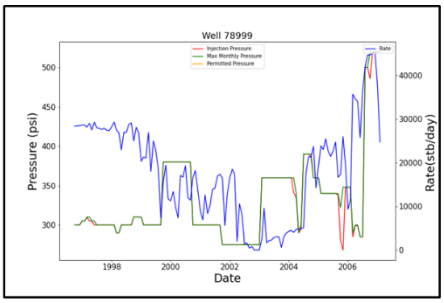
Well 78999
Injection Pressure
Max Monthly Pressure
Permitted Pressure
Rate
Pressure (psi)
Rate(stb/day)
Date

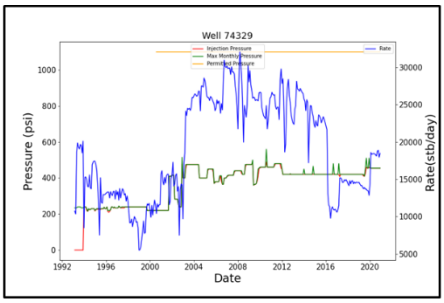
Well 74329
Injection Pressure
Max Monthly Pressure
Permitted Pressure
Rate
Pressure (psi)
Rate(stb/day)
Date

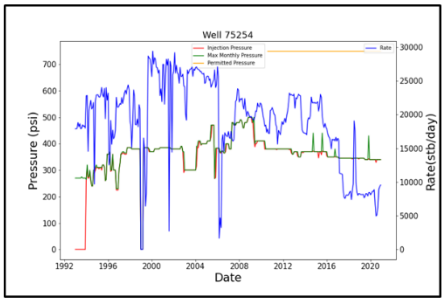
Well 75254
Injection Pressure
Max Monthly Pressure
Permitted Pressure
Rate
Pressure (psi)
Rate(stb/day)
Date

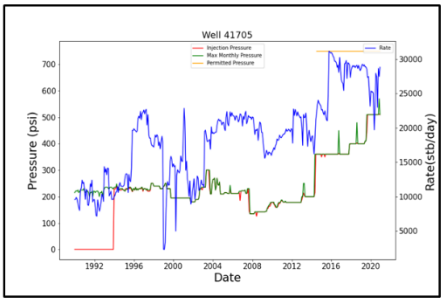
Well 41705
Injection Pressure
Max Monthly Pressure
Permitted Pressure
Rate
Pressure (psi)
Rate(stb/day)
Date

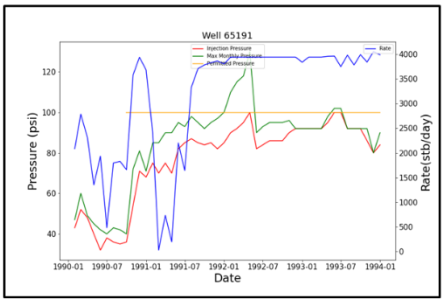
Well 65191
Injection Pressure
Max Monthly Pressure
Permitted Pressure
Rate
Pressure (psi)
Rate(stb/day)
Date

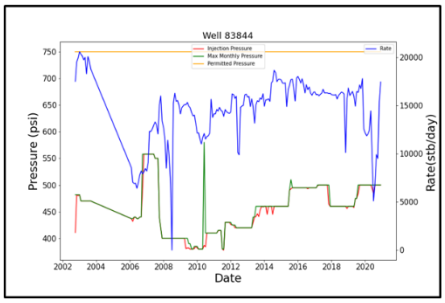
Well 83844
Injection Pressure
Max Monthly Pressure
Permitted Pressure
Rate
Pressure (psi)
Rate(stb/day)
Date

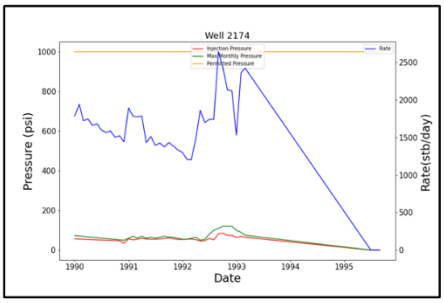
Well 2174
Injection Pressure
Max Monthly Pressure
Permitted Pressure
Rate
Pressure (psi)
Rate(stb/day)
Date

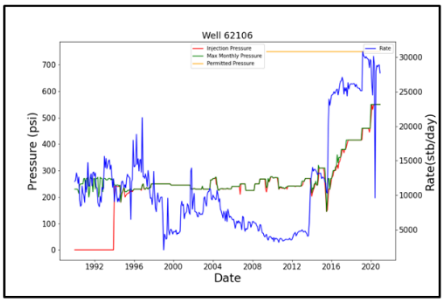
Well 62106
Injection Pressure
Max Monthly Pressure
Permitted Pressure
Rate
Pressure (psi)
Rate(stb/day)
Date

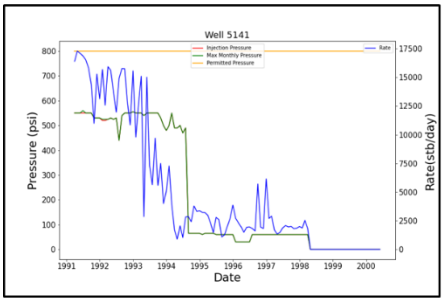
Well 5141
Injection Pressure
Max Monthly Pressure
Permitted Pressure
Rate
Pressure (psi)
Rate(stb/day)
Date

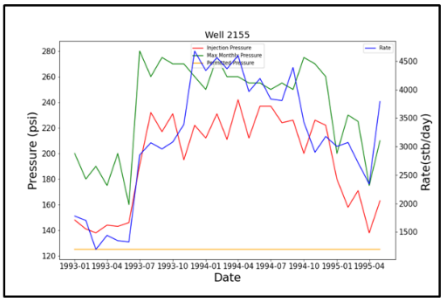
Well 2155
Injection Pressure
Max Monthly Pressure
Permitted Pressure
Rate
Pressure (psi)
Rate(stb/day)
Date

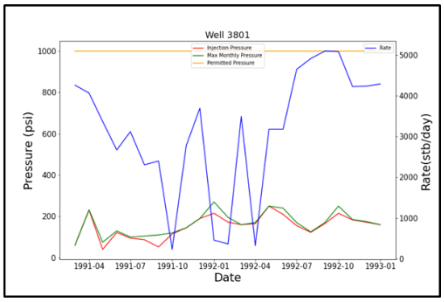
Well 3801
Injection Pressure
Max Monthly Pressure
Permitted Pressure
Rate
Pressure (psi)
Rate(stb/day)
Date

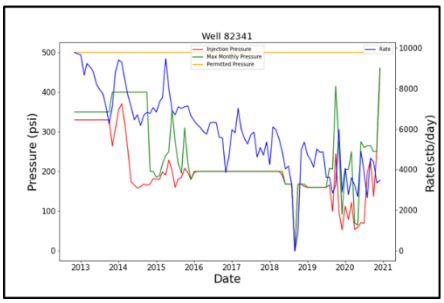
Well 82341
Injection Pressure
Max Monthly Pressure
Permitted Pressure
Rate
Pressure (psi)
Rate(stb/day)
Date

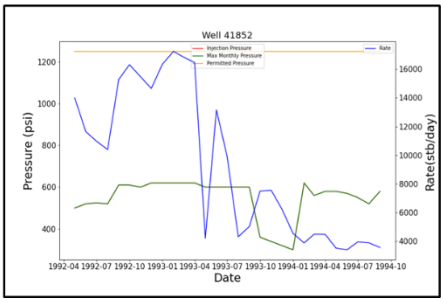
Well 41852
Injection Pressure
Max Monthly Pressure
Permitted Pressure
Rate
Pressure (psi)
Rate(stb/day)
Date

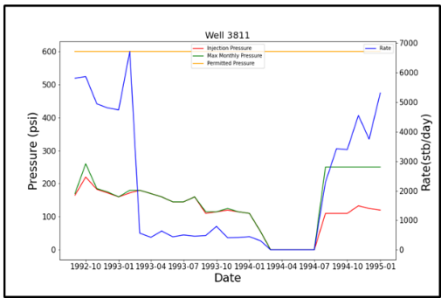
Well 3811
Injection Pressure
Max Monthly Pressure
Permitted Pressure
Rate
Pressure (psi)
Rate(stb/day)
Date

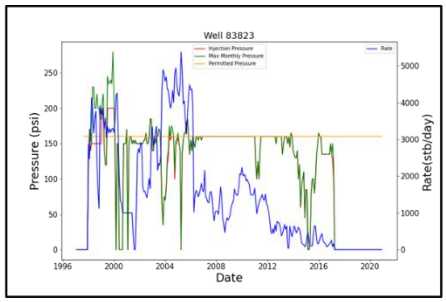
Well 83823
Injection Pressure
Max Monthly Pressure
Permitted Pressure
Rate
Pressure (psi)
Rate(stb/day)
Date

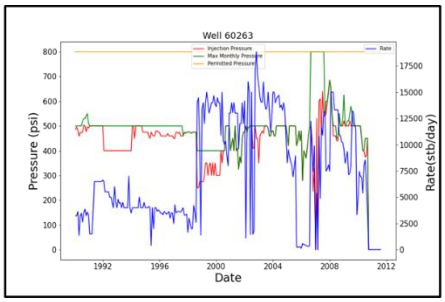
Well 60263
Injection Pressure
Max Monthly Pressure
Permitted Pressure
Rate
Pressure (psi)
Rate(stb/day)
Date

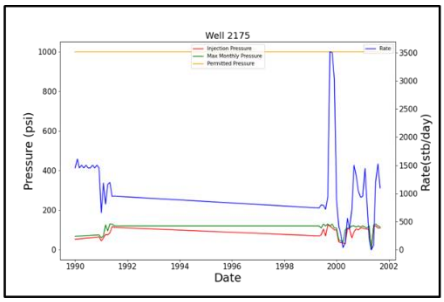
Well 2175
Injection Pressure
Max Monthly Pressure
Permitted Pressure
Rate
Pressure (psi)
Rate(stb/day)
Date

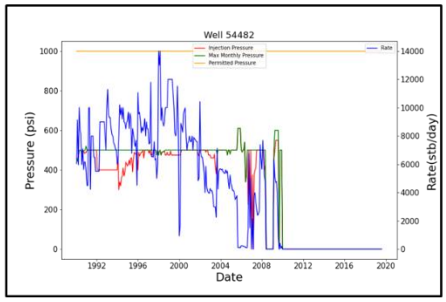
Well 54482
Injection Pressure
Max Monthly Pressure
Permitted Pressure
Rate
Pressure (psi)
Rate(stb/day)
Date

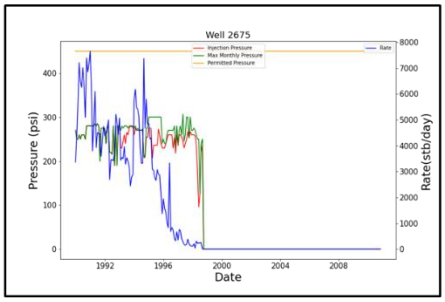
Well 2675
Injection Pressure
Max Monthly Pressure
Permitted Pressure
Rate
Pressure (psi)
Rate(stb/day)
Date

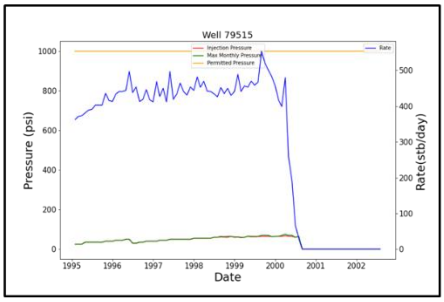
Well 79515
Injection Pressure
Max Monthly Pressure
Permitted Pressure
Rate
Pressure (psi)
Rate(stb/day)
Date

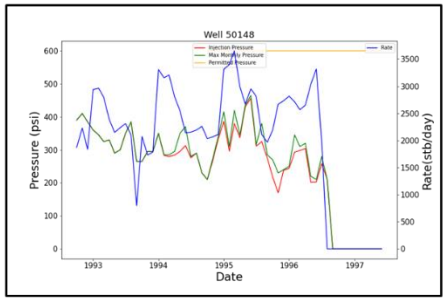
Well 50148
Injection Pressure
Max Monthly Pressure
Permitted Pressure
Rate
Pressure (psi)
Rate(stb/day)
Date

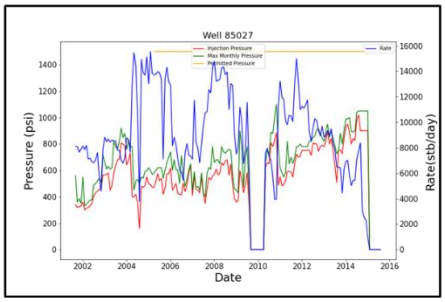
Well 85027
Injection Pressure
Max Monthly Pressure
Permitted Pressure
Rate
Pressure (psi)
Rate(stb/day)
Date

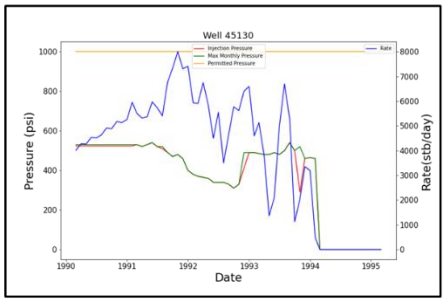
Well 45130
Injection Pressure
Max Monthly Pressure
Permitted Pressure
Rate
Pressure (psi)
Rate(stb/day)
Date

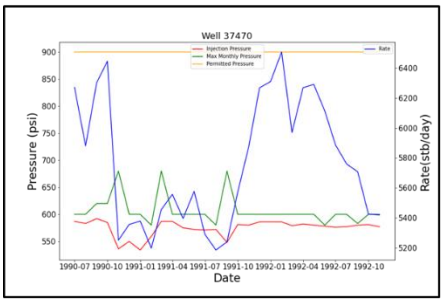
Well 37470
Injection Pressure
Max Monthly Pressure
Permitted Pressure
Rate
Pressure (psi)
Rate(stb/day)
Date

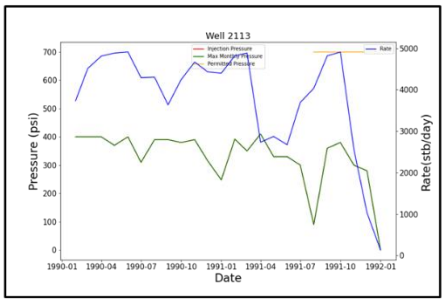
Well 2113
Injection Pressure
Max Monthly Pressure
Permitted Pressure
Rate
Pressure (psi)
Rate(stb/day)
Date

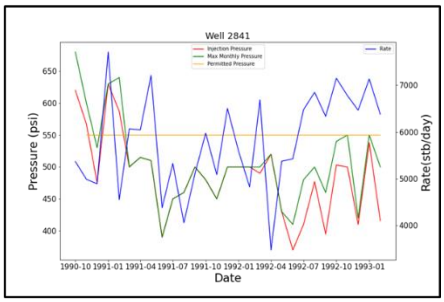
Well 2841
Injection Pressure
Max Monthly Pressure
Permitted Pressure
Rate
Pressure (psi)
Rate(stb/day)
Date

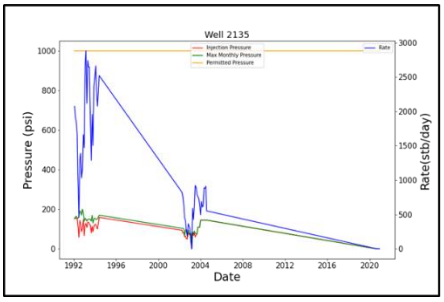
Well 2135
Injection Pressure
Max Monthly Pressure
Permitted Pressure
Rate
Pressure (psi)
Rate(stb/day)
Date

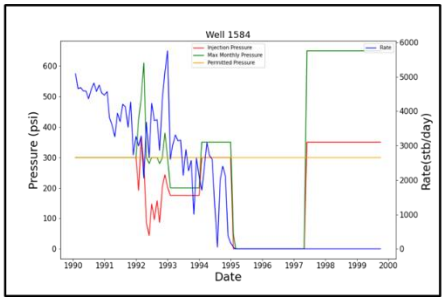
Well 1584
Injection Pressure
Max Monthly Pressure
Permitted Pressure
Rate
Pressure (psi)
Rate(stb/day)
Date

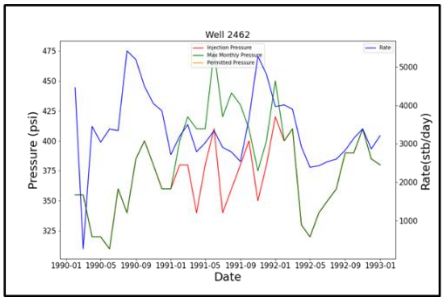
Well 2462
Injection Pressure
Max Monthly Pressure
Permitted Pressure
Rate
Pressure (psi)
Rate(stb/day)
Date

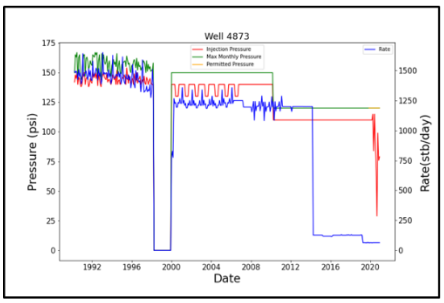
Well 4873
Injection Pressure
Max Monthly Pressure
Permitted Pressure
Rate
Pressure (psi)
Rate(stb/day)
Date

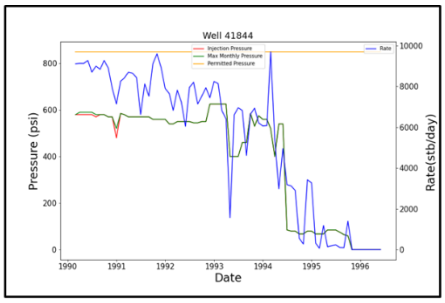
Well 41844
Injection Pressure
Max Monthly Pressure
Permitted Pressure
Rate
Pressure (psi)
Rate(stb/day)
Date

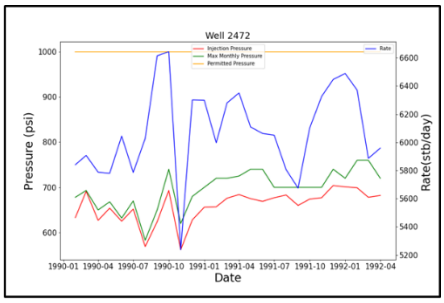
Well 2472
Injection Pressure
Max Monthly Pressure
Permitted Pressure
Rate
Pressure (psi)
Rate(stb/day)
Date

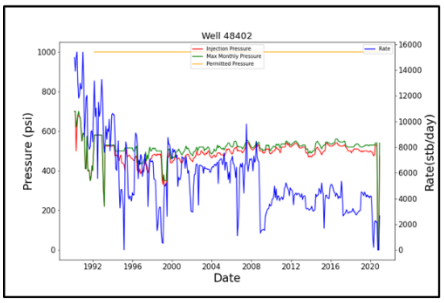
Well 48402
Injection Pressure
Max Monthly Pressure
Permitted Pressure
Rate
Pressure (psi)
Rate(stb/day)
Date

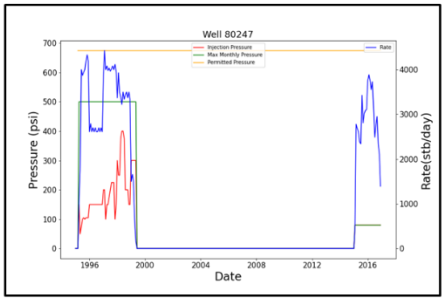
Well 80247
Injection Pressure
Max Monthly Pressure
Permitted Pressure
Rate
Pressure (psi)
Rate(stb/day)
Date

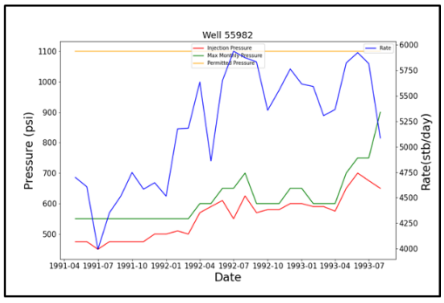
Well 55982
Injection Pressure
Max Monthly Pressure
Permitted Pressure
Rate
Pressure (psi)
Rate(stb/day)
Date

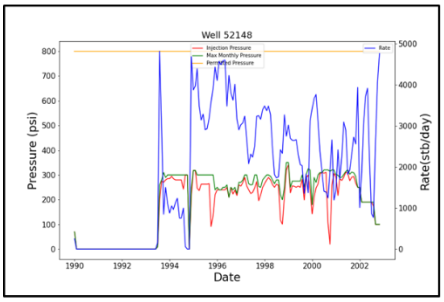
Well 52148
Injection Pressure
Max Monthly Pressure
Permitted Pressure
Rate
Pressure (psi)
Rate(stb/day)
Date

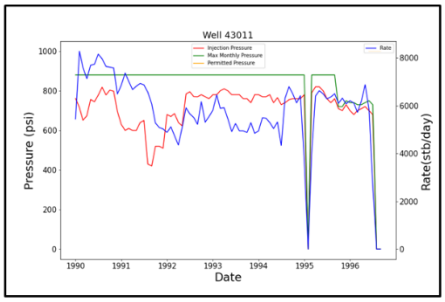
Well 43011
Injection Pressure
Max Monthly Pressure
Permitted Pressure
Rate
Pressure (psi)
Rate(stb/day)
Date

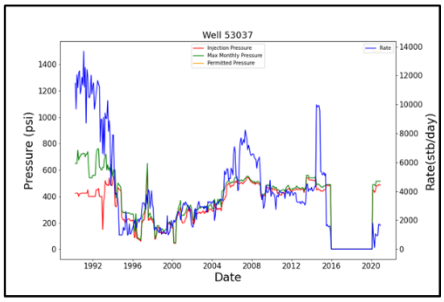
Well 53037
Injection Pressure
Max Monthly Pressure
Permitted Pressure
Rate
Pressure (psi)
Rate(stb/day)
Date

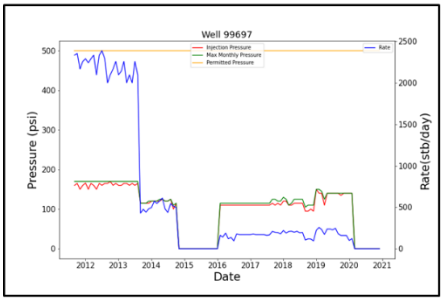
Well 99697
Injection Pressure
Max Monthly Pressure
Permitted Pressure
Rate
Pressure (psi)
Rate(stb/day)
Date

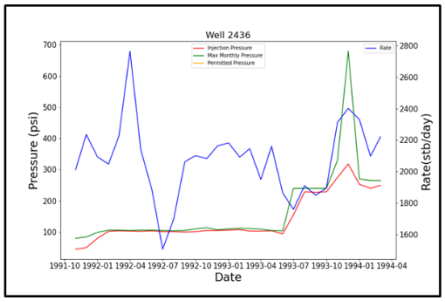
Well 2436
Injection Pressure
Max Monthly Pressure
Permitted Pressure
Rate
Pressure (psi)
Rate(stb/day)
Date

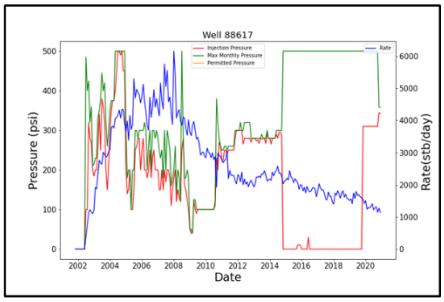
Well 88617
Injection Pressure
Max Monthly Pressure
Permitted Pressure
Rate
Pressure (psi)
Rate(stb/day)
Date

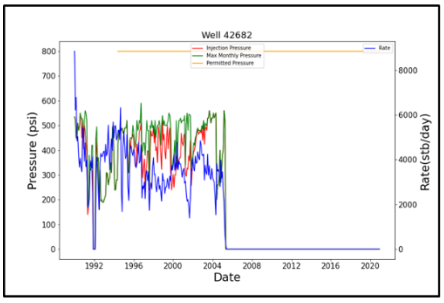
Well 42682
Injection Pressure
Max Monthly Pressure
Permitted Pressure
Rate
Pressure (psi)
Rate(stb/day)
Date

Well 56143
Injection Pressure
Max Monthly Pressure
Permitted Pressure
Rate
Pressure (psi)
Rate(stb/day)
Date

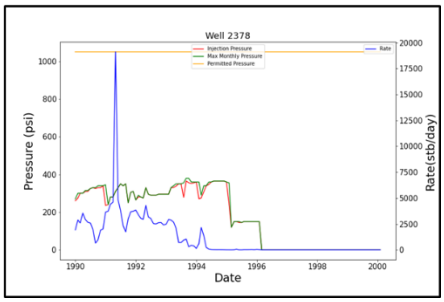
Well 2378
Injection Pressure
Max Monthly Pressure
Permitted Pressure
Rate
Pressure (psi)
Rate(stb/day)
Date

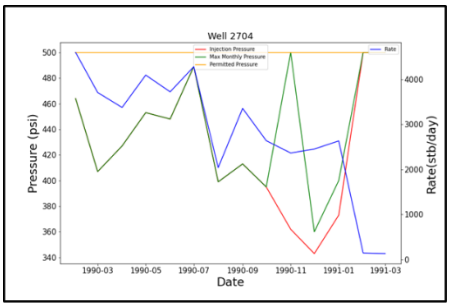
Well 2704
Injection Pressure
Max Monthly Pressure
Permitted Pressure
Rate
Pressure (psi)
Rate(stb/day)
Date

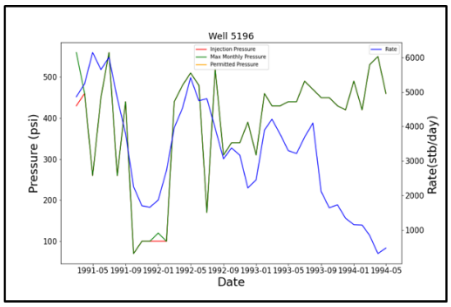
Well 5196
Injection Pressure
Max Monthly Pressure
Permitted Pressure
Rate
Pressure (psi)
Rate(stb/day)
Date

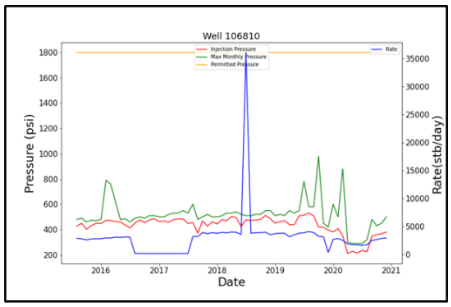
Well 106810
Injection Pressure
Max Monthly Pressure
Permitted Pressure
Rate
Pressure (psi)
Rate(stb/day)
Date

Well 93712
Injection Pressure
Max Monthly Pressure
Permitted Pressure
Rate
Pressure (psi)
Rate(stb/day)
Date

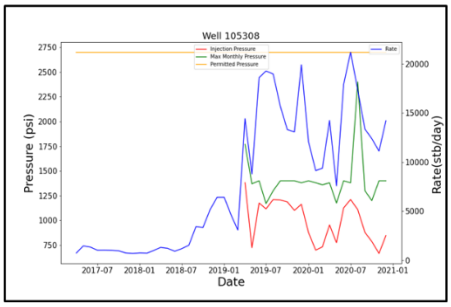
Well 105308
Injection Pressure
Max Monthly Pressure
Permitted Pressure
Rate
Pressure (psi)
Rate(stb/day)
Date

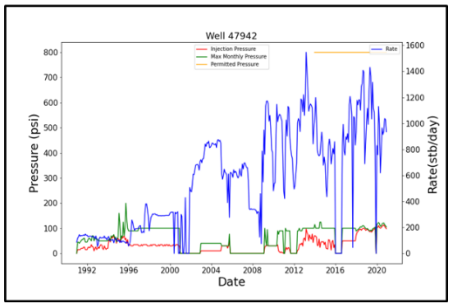
Well 47942
Injection Pressure
Max Monthly Pressure
Permitted Pressure
Rate
Pressure (psi)
Rate(stb/day)
Date

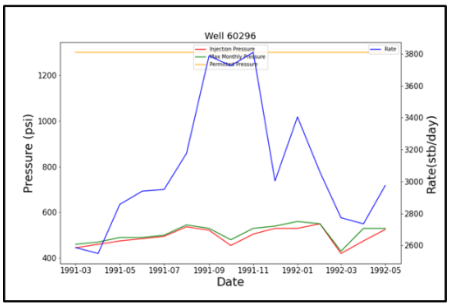
Well 60296
Injection Pressure
Max Monthly Pressure
Permitted Pressure
Rate
Pressure (psi)
Rate(stb/day)
Date

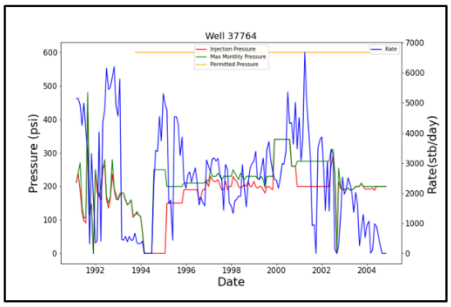
Well 37764
Injection Pressure
Max Monthly Pressure
Permitted Pressure
Rate
Pressure (psi)
Rate(stb/day)
Date

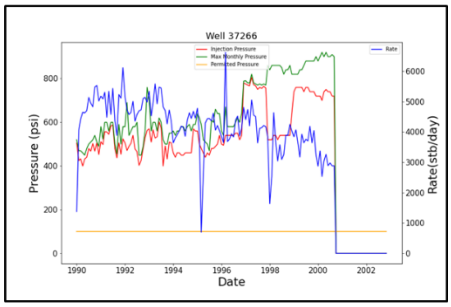
Well 37266
Injection Pressure
Max Monthly Pressure
Permitted Pressure
Rate
Pressure (psi)
Rate(stb/day)
Date

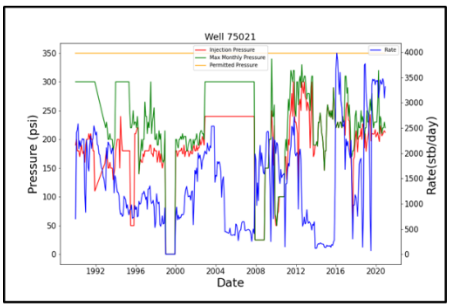
Well 75021
Injection Pressure
Max Monthly Pressure
Permitted Pressure
Rate
Pressure (psi)
Rate(stb/day)
Date

Well 95453
Injection Pressure
Max Monthly Pressure
Permitted Pressure
Rate
Pressure (psi)
Rate(stb/day)
Date

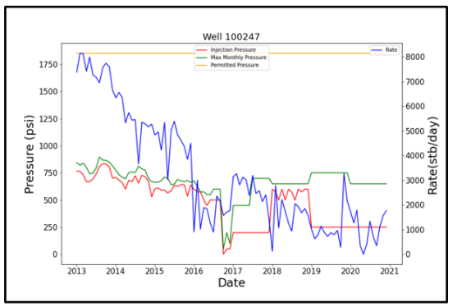
Well 100247
Injection Pressure
Max Monthly Pressure
Permitted Pressure
Rate
Pressure (psi)
Rate(stb/day)
Date

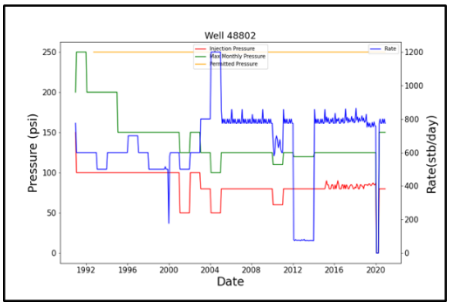
Well 48802
Injection Pressure
Max Monthly Pressure
Permitted Pressure
Rate
Pressure (psi)
Rate(stb/day)
Date

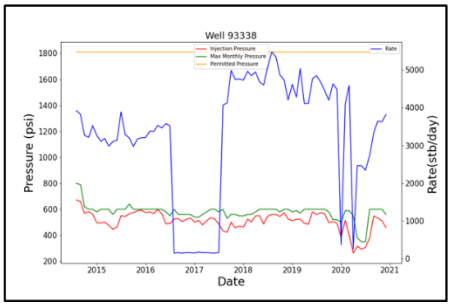
Well 93338
Injection Pressure
Max Monthly Pressure
Permitted Pressure
Rate
Pressure (psi)
Rate(stb/day)
Date

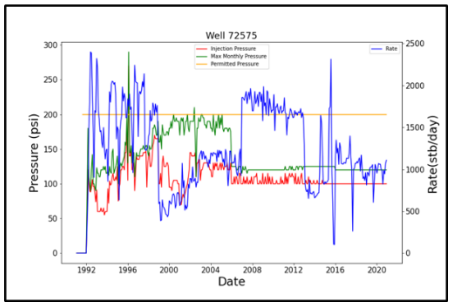
Well 72575
Injection Pressure
Max Monthly Pressure
Permitted Pressure
Rate
Pressure (psi)
Rate(stb/day)
Date

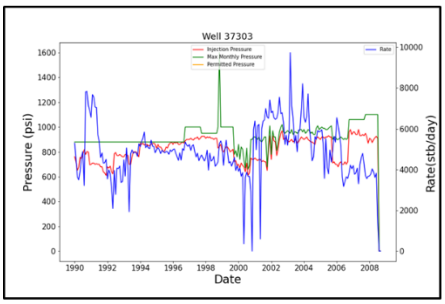
Well 37303
Injection Pressure
Max Monthly Pressure
Permitted Pressure
Rate
Pressure (psi)
Rate(stb/day)
Date

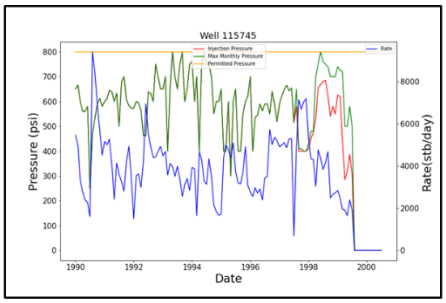
Well 115745
Injection Pressure
Max Monthly Pressure
Permitted Pressure
Rate
Pressure (psi)
Rate(stb/day)
Date

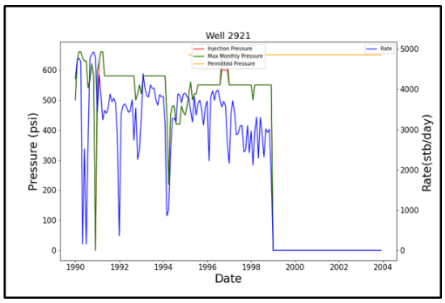
Well 2921
Injection Pressure
Max Monthly Pressure
Permitted Pressure
Rate
Pressure (psi)
Rate(stb/day)
Date

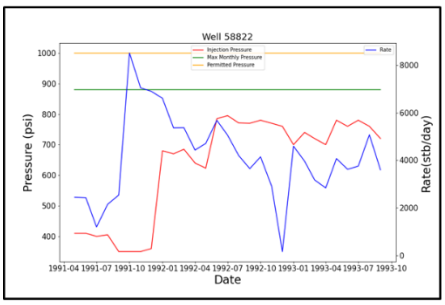
Well 58822
Injection Pressure
Max Monthly Pressure
Permitted Pressure
Rate
Pressure (psi)
Rate(stb/day)
Date

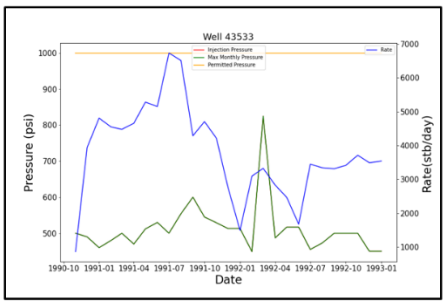
Well 43533
Injection Pressure
Max Monthly Pressure
Permitted Pressure
Rate
Pressure (psi)
Rate(stb/day)
Date

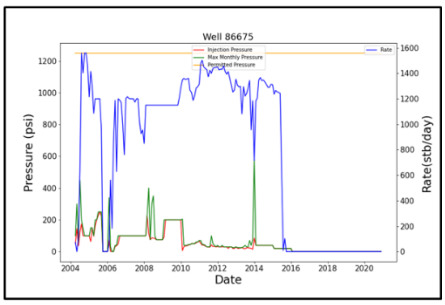
Well 86675
Injection Pressure
Max Monthly Pressure
Permitted Pressure
Rate
Pressure (psi)
Rate(stb/day)
Date

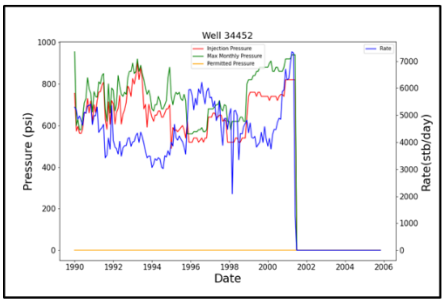
Well 34452
Injection Pressure
Max Monthly Pressure
Permitted Pressure
Rate
Pressure (psi)
Rate(stb/day)
Date

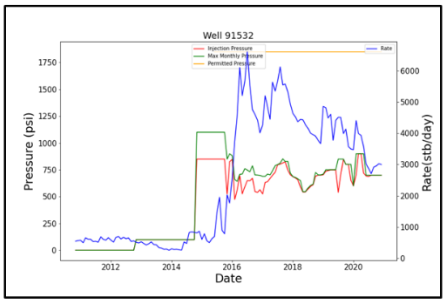
Well 91532
Injection Pressure
Max Monthly Pressure
Permitted Pressure
Rate
Pressure (psi)
Rate(stb/day)
Date

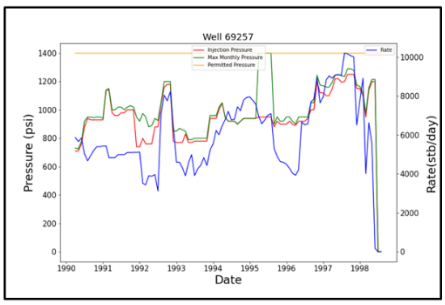
Well 69257
Injection Pressure
Max Monthly Pressure
Permitted Pressure
Rate
Pressure (psi)
Rate(stb/day)
Date

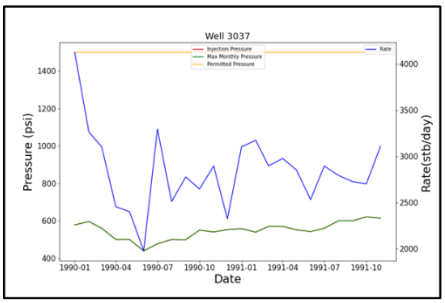
Well 3037
Injection Pressure
Max Monthly Pressure
Permitted Pressure
Rate
Pressure (psi)
Rate(stb/day)
Date

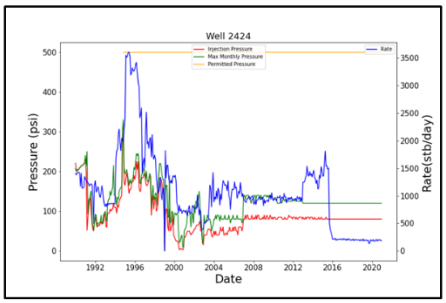
Well 2424
Injection Pressure
Max Monthly Pressure
Permitted Pressure
Rate
Pressure (psi)
Rate(stb/day)
Date

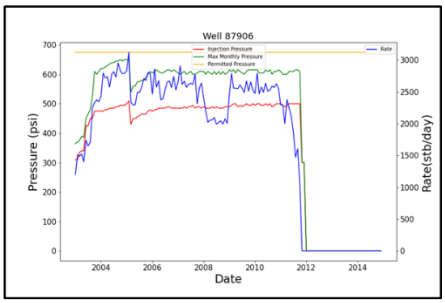
Well 87906
Injection Pressure
Max Monthly Pressure
Permitted Pressure
Rate
Pressure (psi)
Rate(stb/day)
Date

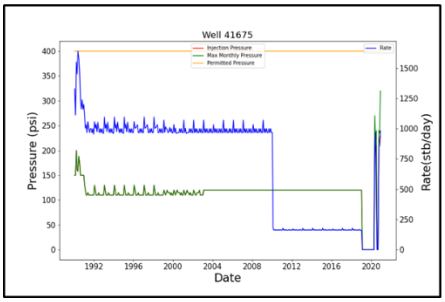
Well 41675
Injection Pressure
Max Monthly Pressure
Permitted Pressure
Rate
Pressure (psi)
Rate(stb/day)
Date

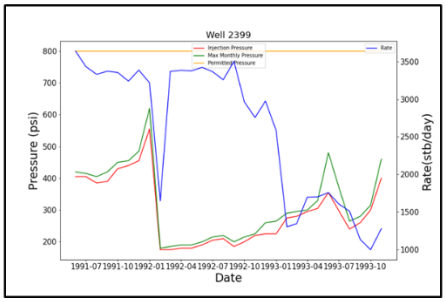
Well 2399
Injection Pressure
Max Monthly Pressure
Permitted Pressure
Rate
Pressure (psi)
Rate(stb/day)
Date

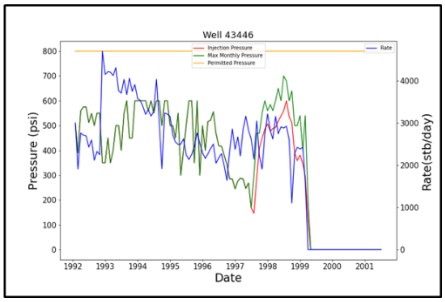
Well 43446
Injection Pressure
Max Monthly Pressure
Permitted Pressure
Rate
Pressure (psi)
Rate(stb/day)
Date

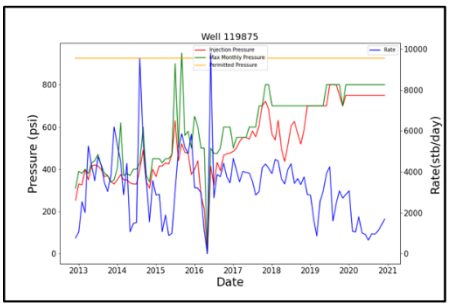
Well 119875
Injection Pressure
Max Monthly Pressure
Permitted Pressure
Rate
Pressure (psi)
Rate(stb/day)
Date

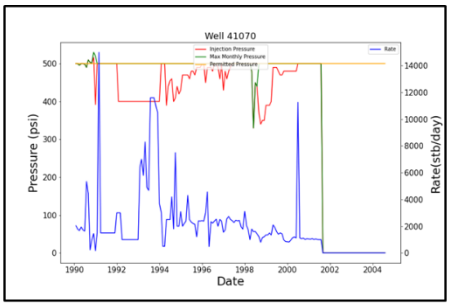
Well 41070
Injection Pressure
Max Monthly Pressure
Permitted Pressure
Rate
Pressure (psi)
Rate(stb/day)
Date

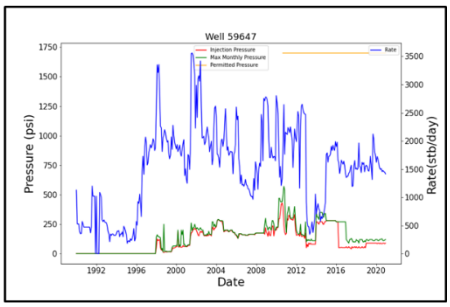
Well 59647
Injection Pressure
Max Monthly Pressure
Permitted Pressure
Rate
Pressure (psi)
Rate(stb/day)
Date

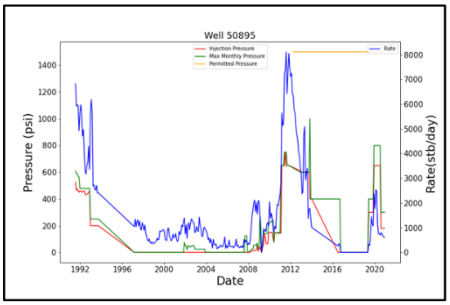
Well 50895
Injection Pressure
Max Monthly Pressure
Permitted Pressure
Rate
Pressure (psi)
Rate(stb/day)
Date

Well 53162
Injection Pressure
Max Monthly Pressure
Permitted Pressure
Rate
Pressure (psi)
Rate(stb/day)
Date

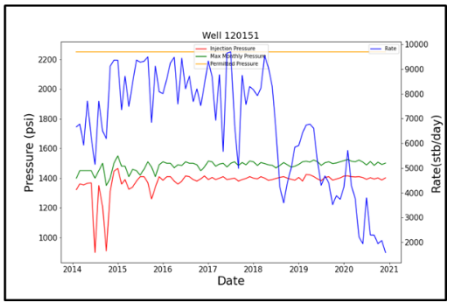
Well 120151
Injection Pressure
Max Monthly Pressure
Permitted Pressure
Rate
Pressure (psi)
Rate(stb/day)
Date

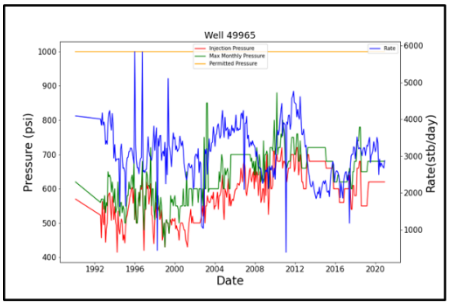
Well 49965
Injection Pressure
Max Monthly Pressure
Permitted Pressure
Rate
Pressure (psi)
Rate(stb/day)
Date

Well 92660
Injection Pressure
Max Monthly Pressure
Permitted Pressure
Rate
Pressure (psi)
Rate(stb/day)
Date

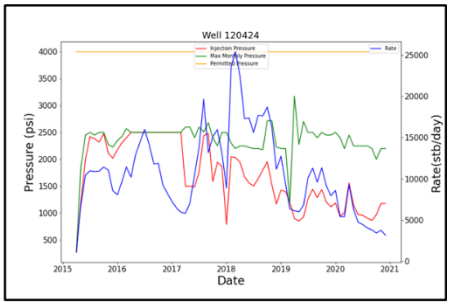
Well 120424
Injection Pressure
Max Monthly Pressure
Permitted Pressure
Rate
Pressure (psi)
Rate(stb/day)
Date

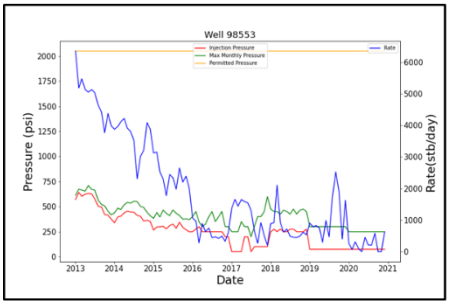
Well 98553
Injection Pressure
Max Monthly Pressure
Permitted Pressure
Rate
Pressure (psi)
Rate(stb/day)
Date

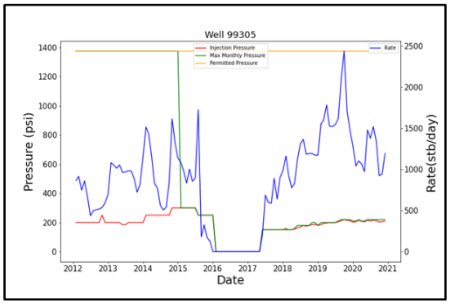
Well 99305
Injection Pressure
Max Monthly Pressure
Permitted Pressure
Rate
Pressure (psi)
Rate(stb/day)
Date

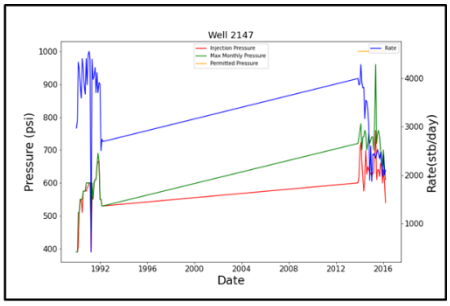
Well 2147
Injection Pressure
Max Monthly Pressure
Permitted Pressure
Rate
Pressure (psi)
Rate(stb/day)
Date

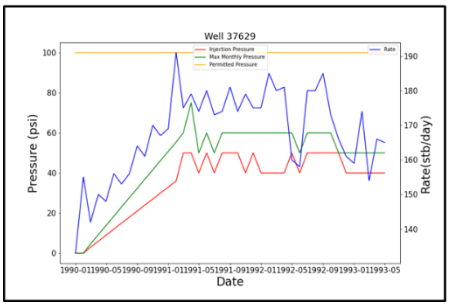
Well 37629
Injection Pressure
Max Monthly Pressure
Permitted Pressure
Rate
Pressure (psi)
Rate(stb/day)
Date

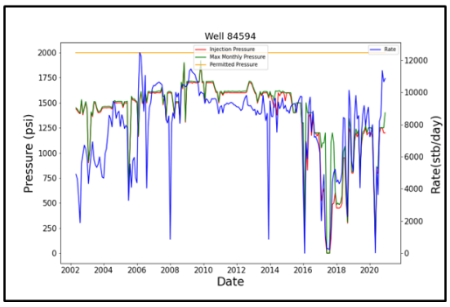
Well 84594
Injection Pressure
Max Monthly Pressure
Permitted Pressure
Rate
Pressure (psi)
Rate(stb/day)
Date

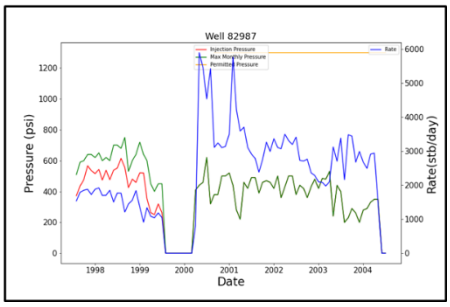
Well 82987
Injection Pressure
Max Monthly Pressure
Permitted Pressure
Rate
Pressure (psi)
Rate(stb/day)
Date

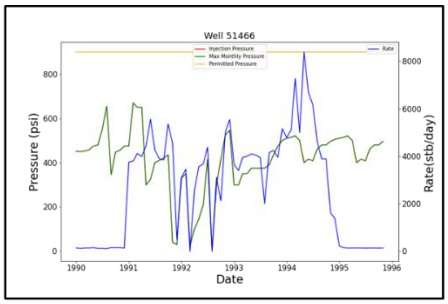
Well 51466
Injection Pressure
Max Monthly Pressure
Permitted Pressure
Rate
Pressure (psi)
Rate(stb/day)
Date

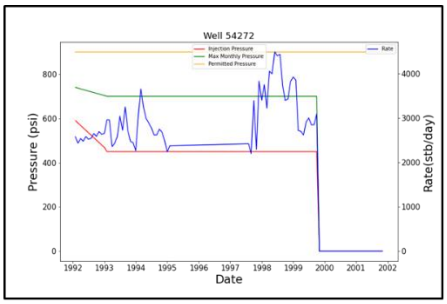
Well 54272
Injection Pressure
Max Monthly Pressure
Permitted Pressure
Rate
Pressure (psi)
Rate(stb/day)
Date

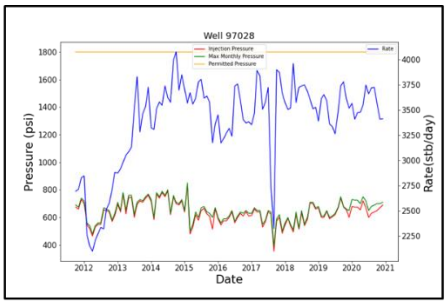
Well 97028
Injection Pressure
Max Monthly Pressure
Permitted Pressure
Rate
Pressure (psi)
Rate(stb/day)
Date

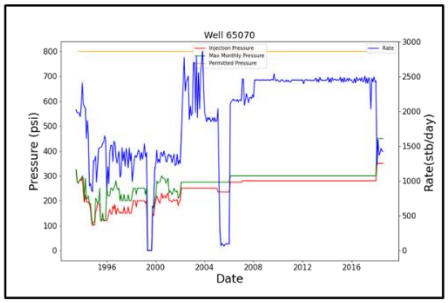
Well 65070
Injection Pressure
Max Monthly Pressure
Permitted Pressure
Rate
Pressure (psi)
Rate(stb/day)
Date

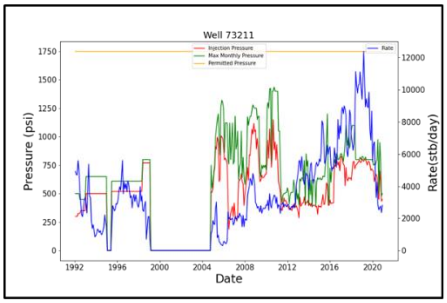
Well 73211
Injection Pressure
Max Monthly Pressure
Permitted Pressure
Rate
Pressure (psi)
Rate(stb/day)
Date

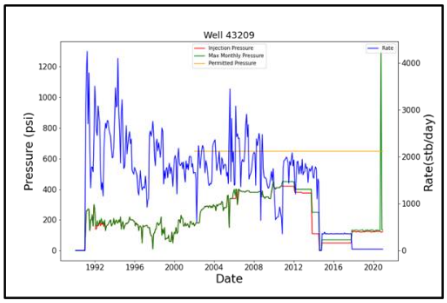
Well 43209
Injection Pressure
Max Monthly Pressure
Permitted Pressure
Rate
Pressure (psi)
Rate(stb/day)
Date

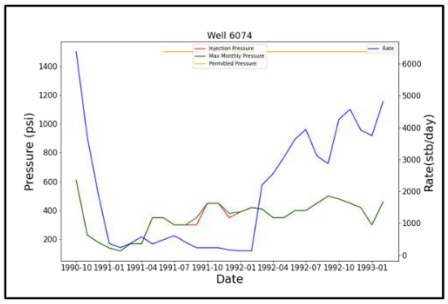
Well 6074
Injection Pressure
Max Monthly Pressure
Permitted Pressure
Rate
Pressure (psi)
Rate(stb/day)
Date

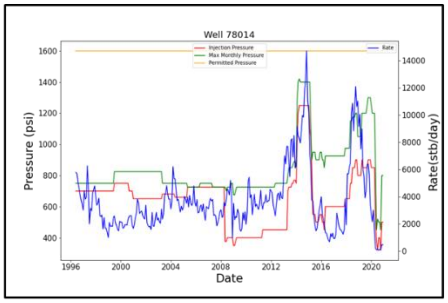
Well 78014
Injection Pressure
Max Monthly Pressure
Permitted Pressure
Rate
Pressure (psi)
Rate(stb/day)
Date

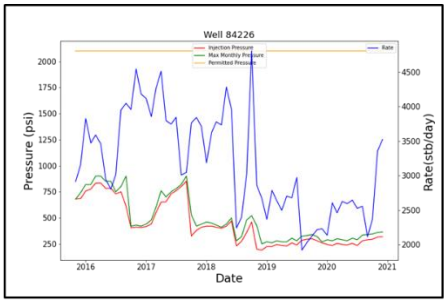
Well 84226
Injection Pressure
Max Monthly Pressure
Permitted Pressure
Rate
Pressure (psi)
Rate(stb/day)
Date

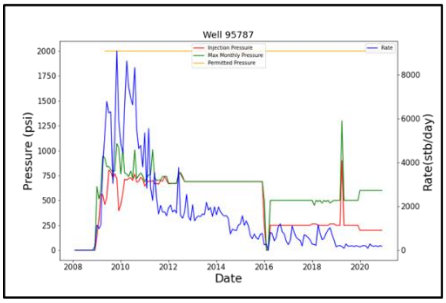
Well 95787
Injection Pressure
Max Monthly Pressure
Permitted Pressure
Rate
Pressure (psi)
Rate(stb/day)
Date

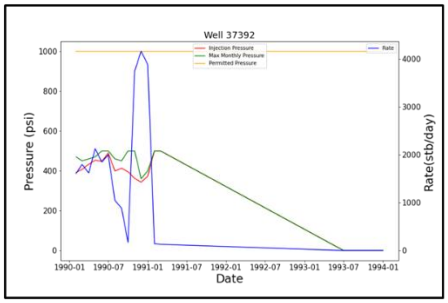
Well 37392
Injection Pressure
Max Monthly Pressure
Permitted Pressure
Rate
Pressure (psi)
Rate(stb/day)
Date

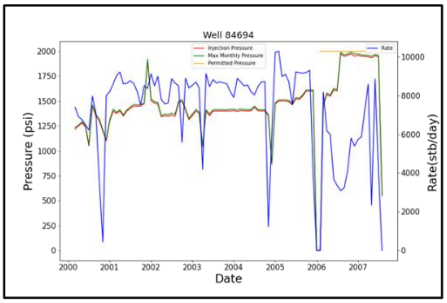
Well 84694
Injection Pressure
Max Monthly Pressure
Permitted Pressure
Rate
Pressure (psi)
Rate(stb/day)
Date

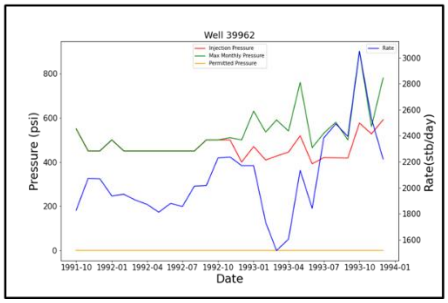
Well 39962
Injection Pressure
Max Monthly Pressure
Permitted Pressure
Rate
Pressure (psi)
Rate(stb/day)
Date

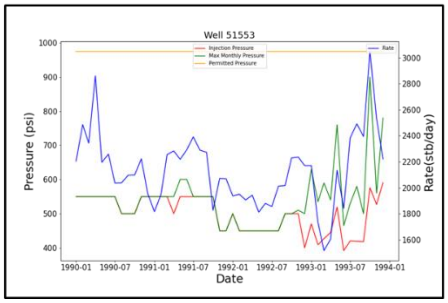
Well 51553
Injection Pressure
Max Monthly Pressure
Permitted Pressure
Rate
Pressure (psi)
Rate(stb/day)
Date

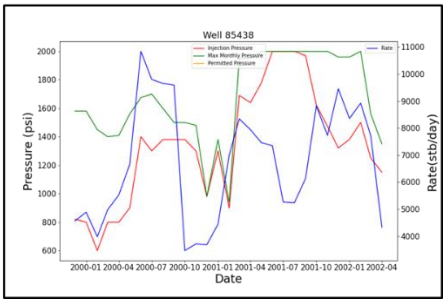
Well 85438
Injection Pressure
Max Monthly Pressure
Permitted Pressure
Rate
Pressure (psi)
Rate(stb/day)
Date

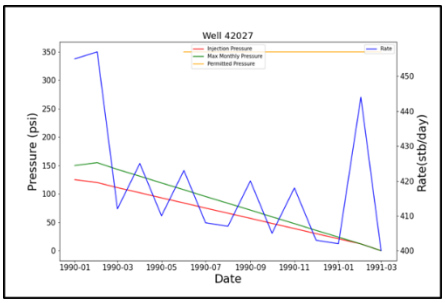
Well 42027
Injection Pressure
Max Monthly Pressure
Permitted Pressure
Rate
Pressure (psi)
Rate(stb/day)
Date

Well 49528
Injection Pressure
Max Monthly Pressure
Permitted Pressure
Rate
Pressure (psi)
Rate(stb/day)
Date

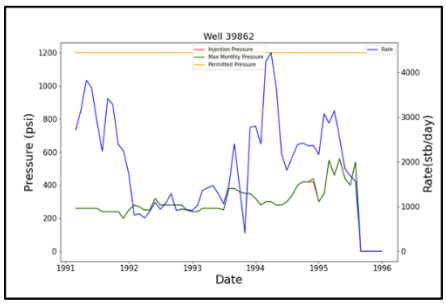
Well 39862
Injection Pressure
Max Monthly Pressure
Permitted Pressure
Rate
Pressure (psi)
Rate(stb/day)
Date

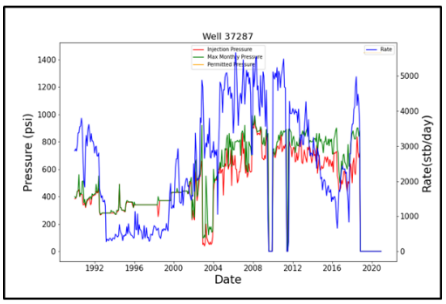
Well 37287
Injection Pressure
Max Monthly Pressure
Permitted Pressure
Rate
Pressure (psi)
Rate(stb/day)
Date

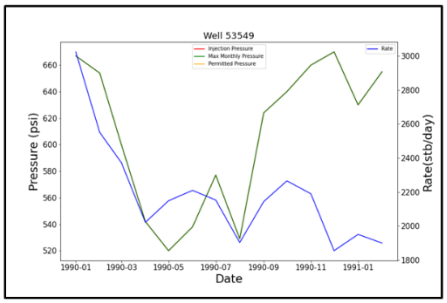
Well 53549
Injection Pressure
Max Monthly Pressure
Permitted Pressure
Rate
Pressure (psi)
Rate(stb/day)
Date

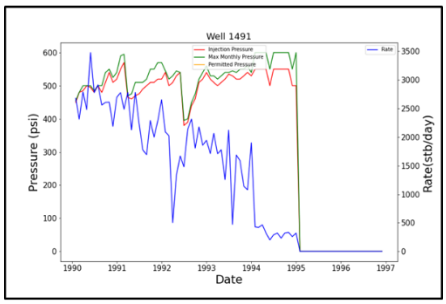
Well 1491
Injection Pressure
Max Monthly Pressure
Permitted Pressure
Rate
Pressure (psi)
Rate(stb/day)
Date

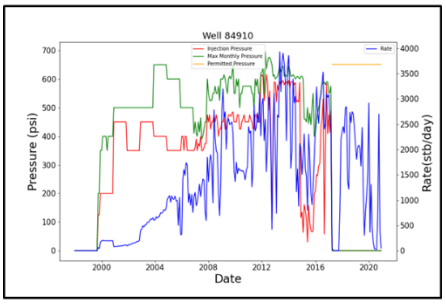
Well 84910
Injection Pressure
Max Monthly Pressure
Permitted Pressure
Rate
Pressure (psi)
Rate(stb/day)
Date

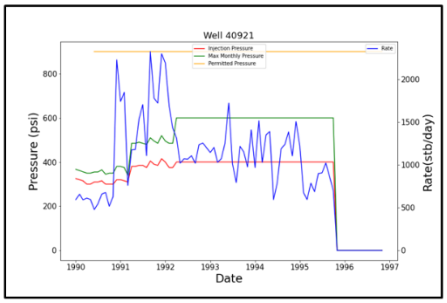
Well 40921
Injection Pressure
Max Monthly Pressure
Permitted Pressure
Rate
Pressure (psi)
Rate(stb/day)
Date

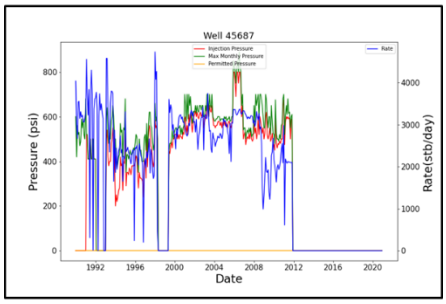
Well 45687
Injection Pressure
Max Monthly Pressure
Permitted Pressure
Rate
Pressure (psi)
Rate(stb/day)
Date

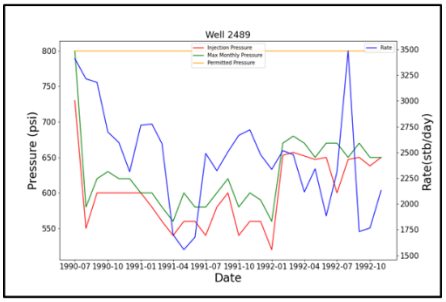
Well 2489
Injection Pressure
Max Monthly Pressure
Permitted Pressure
Rate
Pressure (psi)
Rate(stb/day)
Date

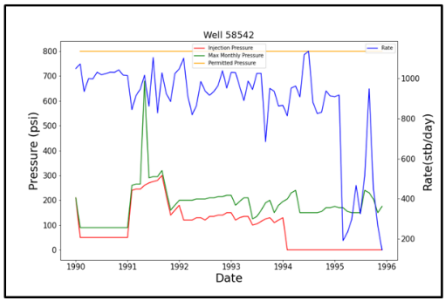
Well 58542
Injection Pressure
Max Monthly Pressure
Permitted Pressure
Rate
Pressure (psi)
Rate(stb/day)
Date

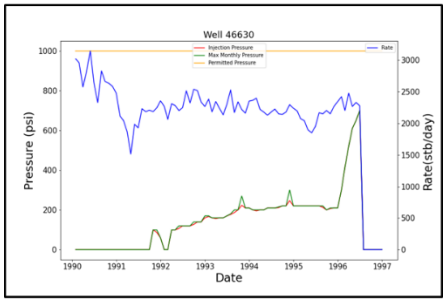
Well 46630
Injection Pressure
Max Monthly Pressure
Permitted Pressure
Rate
Pressure (psi)
Rate(stb/day)
Date

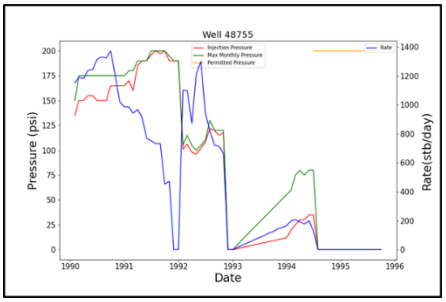
Well 48755
Injection Pressure
Max Monthly Pressure
Permitted Pressure
Rate
Pressure (psi)
Rate(stb/day)
Date

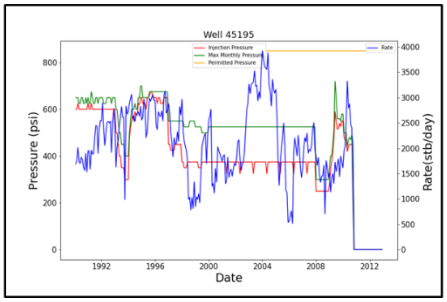
Well 45195
Injection Pressure
Max Monthly Pressure
Permitted Pressure
Rate
Pressure (psi)
Rate(stb/day)
Date

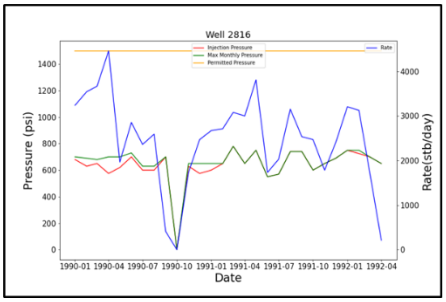
Well 2816
Injection Pressure
Max Monthly Pressure
Permitted Pressure
Rate
Pressure (psi)
Rate(stb/day)
Date

References

Adams, R.L., & Carr, J.P. (2010). *Regional depositional systems of the Woodbine, Eagle Ford, and Tuscaloosa of the U.S. Gulf Coast* [PDF]. Gulf Coast Association of Geological Societies Transactions, 60, 3-27. Retrieved from https://carrresources.com/wp-content/uploads/2020/08/Regional-Woodbine.pdf

Ammentop, A.D. (1988). *Depositional systems, petrography, and petroleum geology of a Caddo conglomerate (Atokan) wave-reworked braid Delta in North-Central Texas* [Master's Thesis, Oklahoma State University].

Babcock, C. (1969). *Geology of the upper Cretaceous clastic section Northern peninsular Florida* [PDF]. Retrieved from http://ufdcimages.uflib.ufl.edu/UF/00/00/11/20/00001/UF00001120.pdf

Baker, E.T. (1978*). Stratigraphic and hydrogeologic framework of part of the coastal plain of Texas (Report 77-712)* [PDF]. United States Geological Survey. Retrieved from https://transboundary.tamu.edu/media/1169/1979_baker.pdf

Baker, E.T. (1979). *Stratigraphic and hydrogeologic framework of part of the Coastal plain of Texas (Report 236)* [PDF]. Texas Department of Water Resources. Retrieved from https://www.twdb.texas.gov/publications/reports/numbered_reports/doc/R236/R236.pdf

Baker, E.T. (1995*). Stratigraphic nomenclature and geologic sections of the Gulf Coastal plain of Texas (Report 94-461)* [PDF]. United States Geological Survey. Retrieved from https://pubs.usgs.gov/of/1994/0461/report.pdf

Baker, R.A., & Ardis, A.F. (1992). *Configuration of the base of the Edwards-Trinity aquifer system and hydrogeology of the underlying pre-Cretaceous rocks, West-Central Texas (Report 91-4071)* [PDF]. United States Geological Survey. Retrieved from https://pubs.usgs.gov/wri/wri91-4071/pdf/wri91-4071.pdf

Bartberger, C.E., Dyman, T.S., Condon, S.M. (2003). *Potential for a basin-centered gas accumulation in Travis Peak (Houston) formation, Gulf Coast basin, U.S.A* [PDF] (Bulletin 2184-E). United States Geological Survey. Retrieved from https://pubs.usgs.gov/bul/b2184-e/B2184E-508.pdf

Bennion, D.B., & Bachu, S. (2010). *Drainage and imbibition* CO_2*/brine relative permeability curves at reservoir conditions for carbonate formations*. Paper Presented at the SPE Annual Technical Conference and Exhibition, Florence, Italy. https://doi.org/10.2118/134028-MS

Bradshaw, J., Bachu, S., Bonijoly, D., Burruss, D., Holloway, S., Christensen, N.P., & Mathiassen, O.M. (2007). CO_2 storage capacity estimation: issues and development of standards. *International Journal of Greenhouse Gas Control*, 1(1), 62-68. https://doi.org/10.1016/S1750-5836(07)00027-8

Brasier, F., & Kobelski, B. (1996). Injection of industrial wastes in the United States. In J.A. Apps and Chin-Fu Tsang (Eds.), *Deep injection of disposal of hazardous industrial waste: scientific and engineering aspects* (pp. 1-8). Academic Press.

Bump, A.P., Hovorka, S.D., & Meckel, T.A. (2021). Common risk segment mapping: streamlining exploration for carbon storage sites, with application to coastal Texas and Louisiana. *International Journal of Greenhouse Gas Control*, 111. https://doi.org/10.1016/j.ijggc.2021.103457

Bump, A.P., & Hovorka, S.D. (2024). Pressure space: the key subsurface commodity for CCS. *International Journal of Greenhouse Gas Control,* 136. https://doi.org/10.1016/j.ijggc.2024.104174

Burnside, N.M., & Naylor, M. (2014). Review and implications of relative permeability of CO_2/brine systems and residual trapping of CO_2. *International Journal of Greenhouse Gas Control*, 23, 1-11. https://doi.org/10.1016/j.ijggc.2014.01.013

Carsey, J.B. (1950). Geology of gulf coastal area and continental shelf. *AAPG Bulletin*, 34(3), 361-385. https://doi.org/10.1306/3D933EEA-16B1-11D7-8645000102C1865D

Chenault, D.S., & Lambert, L.L. (2005). Sequence of the mid-Comanche series, South Texas region. *Gulf Coast Association of Geological Societies Transactions*, 55, 71-88. Retrieved from https://archives.datapages.com/data/gcags/data/055/055001/71_gcags550071.htm

Chowdhury, A.H., & Turco, M.J. (2006. February). *Geology of the Gulf Coast aquifer, Texas (Report 365, Chapter 2)* [PDF]. Texas Water Development Board. Retrieved from https://www.twdb.texas.gov/publications/reports/numbered_reports/doc/R365/R365_Composite.pdf

Clark, J.E., Bonura, D.K., & Van Voorhees, R.F. (2005). An overview of injection history in the United States of America. *Developments in Water Science*, 52, 3-12. https://doi.org/10.1016/S0167- 5648(05)52001-X

Clean Air task Force. (2024). *Global carbon capture activity and project map*. Retrieved from https://www.catf.us/ccsmapglobal/

Condon, S.M., & Dyman, T.S. (2006). *2003 geological assessment of undiscovered conventional oil and gas resources in the upper Cretaceous Navarro and Taylor groups, Western Gulf Province, Texas. United States Geological Survey (Chapter 2)* [PDF]. Retrieved from https://pubs.usgs.gov/dds/dds-069/dds-069-h/REPORTS/69_H_CH_2.pdf

Cook, T.D. (1979). Exploration history of South Texas Lower Cretaceous Carbonate platform. *AAPG Bulletin*, 63(1), 32-49. https://doi-org.ezproxy.lib.utexas.edu/10.1306/C1EA55B2-16C9-11D7-8645000102C1865D

Corpus Christi Geological Society. (1968). Natural gas in post-Eocene Formations of the South. *AAPG Special Volumes.* 1, 233-263. Retrieved from https://archives.datapages.com/data/specpubs/fieldst1/data/a007/a007/0001/0200/0233.htm

Davis, M.E. (1987). *Stratigraphic and hydrogeologic framework of the Alabama coastal plain (Report 87-4112)* [PDF]. United States Geologic Survey. Retrieved from https://pubs.usgs.gov/wri/1987/4112/report.pdf

Davis, P., & Goode, O.N. (1957). *A report on the old Luling (Edwards Limestone) Field, Caldwell and Guadalupe Counties, Texas*. Paper presented at the Fall Meeting of the Society of Petroleum Engineers of AIME, Dallas, Texas. https://doi.org/10.2118/882-G

Depaz, M.J.H. (2004). *Reservoir characterization and development opportunities in Jacob field, South-Central Texas* [Master's thesis, Texas A&M University]. Retrieved from https://core.ac.uk/download/pdf/4268365.pdf

De Silva, P.N.K., & Ranjith, P.G. (2012). A study of methodologies for CO_2 storage capacity estimation of saline aquifers. *Fuel*, 93, 13-27. https://doi.org/10.1016/j.fuel.2011.07.004

Esri. (n.d.). *What is ArcMap?* Retrieved July 17, 2024, from https://desktop.arcgis.com/en/arcmap/latest/map/main/what-is-arcmap-.htm#ESRI_SECTION1_B088FC4AC7194A55B10799B6A2C0FC8C

Ewing, T.E., Budnik, R.T., Jackson, M.P.A., Ruppel, S.C., Garrison, J.R., Lovell, S.E., Sandstrom, M.A., Goldstein, A.G., Muehlberger, W.R., Woodruff, C.M., Henry, C.D., & Nicholas, R.L. (1990). *Tectonic map of Texas*. Bureau of Economic Geology.

Fallin, J.A.T. (1989). *Hydrogeology of Lower Cretaceous strata under the Southern high plains of Texas and New Mexico (Report No. 314)* [PDF]. Texas Water Development Board. Retrieved from https://www.twdb.texas.gov/publications/reports/numbered_reports/doc/R314/Report%20314.pdf

Fanchi, J.R. (2002). Chapter 6 – Fluid properties. In J.R. Fanchi (Ed.), *Shared Earth Modeling* (pp. 87-107). Butterworth-Heinemann. https://doi.org/10.1016/B978-075067522-2/50006-9

Fang, Y., Baojun, B., Dazhen, T., Dunn-Norman, S., & Wronkiewicz, D. (2010). Characteristics of CO_2 sequestration in saline aquifers. *Petroleum Science*, 7, 83-92. Retrieved from https://link.springer.com/article/10.1007/s12182-010-0010-3

Fisher, W.L., Proctor, C.V., Galloway, W.E., & Nagle, J.S. (1970). *Depositional systems in the Jackson group of Texas – their relationship to oil, gas, and uranium (Geological Circular 70-4)* [PDF]. Gulf Coast Geological Societies. Retrieved from https://repositories.lib.utexas.edu/server/api/core/bitstreams/e3812a16-65ca-4c67-a4ec-398fc14bd4ee/content

Fisher, W.L., & Rodda, P.U. (1969). Edwards formation (Lower Cretaceous), Texas: dolomitization in a carbonate platform system. *AAPG Bulletin*, 53(1), 55-72. https://doi-org.ezproxy.lib.utexas.edu/10.1306/5D25C593-16C1-11D7-8645000102C1865D

Foote, R.Q., Massingill, L.M., & Wells, R.H. (1988). *Petroleum geology and the distribution of conventional crude oil, natural gas, and natural gas liquids, East Texas basin (Report 88-450K)* [PDF]. United States Geological Survey. Retrieved from https://pubs.usgs.gov/of/1988/0450k/report.pdf

Galloway, W.E. (1977). *Catahoula formation of the Texas Coastal plain: depositional systems, composition, structural development, ground-water flow history, and uranium distribution*. United States. https://doi.org/10.2172/7301167

Galloway, W.E., & Kaiser, W.E. (1980). *Catahoula formation of Texas Coastal Plain: origin, geochemical evolution, and characteristics of uranium deposit (Report of Investigations No. 100).* The University of Texas at Austin, Bureau of Economic Geology. https://doi.org/10.23867/RI0100D

Galloway, W.E., Ewing, T.E., Garrett, C.M., Tyler, N., & Bebout, D.G. (1983). *Atlas of major Texas oil reservoirs*. The University of Texas at Austin, Bureau of Economic *Geology*. Retrieved from https://store.beg.utexas.edu/atlases-of-major-oil-and-gas-reservoirs/1779-at0002.html

Ganat, T., Hrairi, M., Badawy, A., Khosravi, V., & Abdalla, M. (2024). Advancing sandstone reservoir compressibility prediction: a correlation-driven methodology. *Petroleum Research*, 9(2), 273-279. https://doi.org/10.1016/j.ptlrs.2024.01.006

Ganjdanesh, R., & Hosseini, S.A. (2017). Geologic carbon storage capacity estimation using Enhanced Analytical Simulation Tool (EASiTool). *Energy Procedia*, 114, 4690-4696. https://doi.org/10.1016/j.egypro.2017.03.1601

Gao, Z. (2018). *Temporal evolution of the sediment routing pathway into the Delaware basin, West Texas* [Master's Thesis, Texas A&M University]. Retrieved from https://oaktrust.library.tamu.edu/bitstream/handle/1969.1/173304/GAO-THESIS-2018.pdf?sequence=1

Geomap. (2009). *Extended area reference map 380 Gulf Coast* (2009 Edition).

Global CCS Institute. (2023, November). *Global status of ccs 2023: scaling up through 2030* [PDF]. Retrieved from https://res.cloudinary.com/dbtfcnfij/images/v1700717007/Global-Status-of-CCS-Report-Update-23-Nov/Global-Status-of-CCS-Report-Update-23-Nov.pdf?_i=AA

Gupta, S. (2018, May 10). *Data Visualization for beginners - part 1.* Hackerearth. Retrieved from https://www.hackerearth.com/blog/developers/data-visualization-techniques/

Hamilton, S., & Gottardi, R. (2017). A re-evaluation of the Northern A.W.P. field, McMullen county, Texas. *Gulf Coast Association of Geological Societies*, 6, 150-160. Retrieved from https://www.gcags.org/Journal/2017.GCAGS.Journal/2017.GCAGS.Journal.v6.10.p150-160.Hamilton.and.Gottardi.pdf

Harris, C.R., Millman, K.J., van der Walt, S.J., Gommers, R., Virtanen, P., Cournapeau, D., Wieser, E., Taylor, J., Berg, S., Smith, N., Kern, R., Picus, M., Hoyer, S., van Kerkwijk, M.H., Brett, M., Haldane, A., Del Río, J.F., Wiebe, M., Peterson, P., Gérard-Marchan, P., Sheppard, K., Reddy, T., Weckesser, W., Abbasi, H., Gohlke, C., Oliphant, T. (2020). Array programming with NumPy. *Nature*, 585, 357-362. https://doi.org/10.1038/s41586-020-2649-2

Hosseini, S.A., Reza, G., & Seunghee K. (2018). *Enhanced Analytical Simulation Tool (EASiTool) for* CO_2 *storage capacity estimation and uncertainty quantification*. United States. https://doi.org/10.2172/1463329

Hosseini, S.A., & Nicot, J. (2012). Numerical modeling of a multiphase water-oil-CO_2 system using a water-CO_2 system: application to thr far field of a U.S. Gulf Coast reservoir. *International Journal of Greenhouse Gas Control,* 10, 88-99. https://doi.org/10.1016/j.ijggc.2012.06.001

Hovorka, S.D., mace, R.E., & Collins, E.W. (1998). *Permeability structure of the Edwards Aquifer, South Texas – implications of Aquifer management (Report of Investigations No. 250).* The University of Texas at Austin, Bureau of Economic Geology.

IHS Markit (2021). *Petra: integrated software and delivery tools to advance E&P workflow* [PDF]. Retrieved from https://cdn.ihsmarkit.com/www/pdf/0921/Petra-Upstream-Rebrand-Brochure-U1-Final-HiRes.pdf

International Energy Agency. (2016, November). *20 years of carbon capture and storage: accelerating future deployment* [PDF]. Retrieved from https://iea.blob.core.windows.net/assets/24c3d26b-aa44-4b54-b9c0-5201d4d86a04/20YearsofCarbonCaptureandStorage_WEB.pdf

International Energy Agency GHG (2018, November). *Well Engineering and Injection Regularity in CO_2 Storage Wells (Report 2018-08)* [PDF]. Retrieved from https://ieaghg-publications.s3.eu-north-1.amazonaws.com/Technical+Reports/2018-08+Well+Engineering+and+Injection+Regularity+in+CO2+Storage+Wells.pdf

Kincade, S.C. (2018). *The occurrence of the Greta sandstone, Frio formation (late Oligocene), Texas Gulf Coastal plain* [Master's Thesis, University of Arkansas]. Retrieved from https://scholarworks.uark.edu/cgi/viewcontent.cgi?article=4380&context=etd

Knox, P.R., Kelley, V.A., Vreugdenhil, A., Deeds, N., & Seni, S. (2007). *Structure of the Yegua Jackson aquifer of the Texas Gulf Coastal plain* [PDF]. Texas Water Development Board. Retrieved from https://www.twdb.texas.gov/groundwater/models/gam/ygjk/YGJK_Structure_Report.pdf

Krevor, S.C.M., Pini, R., Zuo, L., & Benson, S.M. (2012). Relative permeability and trapping of CO_2 and water in sandstone reservoir conditions. *Water Resources Research*, 48 (2) https://doi.org/10.1029/2011WR010859

Lau, P.K. (2022). *Carbon Capture, Utilization, and Storage: class vi wells and US state primacy*. Mayer Brown. Retrieved from https://www.mayerbrown.com/en/insights/publications/2022/06/carbon-capture-utilization-and-storage-class-vi-wells-and-us-state-primacy

Lindsey, R. (2024, April 9). *Climate change: atmospheric carbon dioxide.* National Oceanic and Atmospheric Administration Climate. Retrieved from https://www.climate.gov/news-features/understanding-climate/climate-change-atmospheric-carbon-dioxide

Martin, A.T. (2014). *Depositional; History and stratigraphic Framework of upper Cretaceous (Campanian to Maastrichtian) strata in the Minerva-Rockdale oil field of Milam county and adjacent counties, Texas* [Master's Thesis, University of Arkansas]. Retrieved from https://scholarworks.uark.edu/cgi/viewcontent.cgi?article=3849&context=etd

McCurdy, R. (2011). *Underground injection wells for produced water disposal* [PDF]. United States Environmental Protection Agency. Retrieved from https://www.epa.gov/sites/default/files/documents/21_McCurdy_-_UIC_Disposal_508.pdf

McGowen, M.K., & Lopez, C.M. (1983). *Depositional systems in the Nacatoch formation (upper Cretaceous), Northeast Texas and Southwest Arkansas (Report No. 137)* [PDF]. Bureau of Economic Geology, The University of Texas at Austin. Retrieved from https://repositories.lib.utexas.edu/bitstream/handle/2152/77501/txu-oclc-10367600.pdf?sequence=1

Merrill, M.D. (2016). *Geologic assessment of undiscovered conventional oil and gas resources in Albian clastic and updip Albian clastic assessment units, U.S. Gulf Coast region (Report 2016-1026)* [PDF]. United States Geological Survey. Retrieved from https://pubs.usgs.gov/of/2016/1026/ofr20161026.pdf

Moody chart. (2023, March 13). In Wikipedia. https://en.wikipedia.org/wiki/Moody_chart

NASA Earth Observatory. (n.d.). *World of change: global temperatures.* Retrieved July 24, 2024, from https://earthobservatory.nasa.gov/world-of-change/global-temperatures

NASA Goddard Institute for Space Studies. (2023). *GISS surface temperature analysis (GISTEMP)*. https://data.giss.nasa.gov/gistemp/

National Petroleum Council. (2019, December). *Meeting the dual challenge: A roadmap to at scale deployment of carbon capture, use, and storage* [PDF]. United States Department of Energy. Retrieved from https://www.energy.gov/sites/default/files/2021-06/2019%20-%20Meeting%20the%20Dual%20Challenge%20Vol%20II%20Appendix%20C.pdf

Newman, G.H. (1973). Pore-volume compressibility of consolidated, friable, and unconsolidated reservoir rocks under hydraulic loading. *Journal of Petroleum Technology.* 25 (2), 139 -134. https://doi.org/10.2118/3835-PA

Nichols, P.H., Peterson, G.E., & Wuestner, C.E. (1968). *Summary of subsurface geology of Northeast Texas*, 1. https://doi.org/10.1306/M9363C69

Nicot, J., Costley, R.A., & Huang, Y. (2013*). Geographical, geological, and hydrogeological attributes of formations in the footprint of the Eagle Ford shale* [PDF]. Bureau of Economic Geology, University of Texas at Austin. Retrieved from https://www.beg.utexas.edu/files/publications/contract-reports/CR2013-Nicot-1.pdf

Ni, H., Dasari, G., Teletzke, G., & Saris, A. (2021, April 6). *Evaluating technical feasibility of gigaton scale* CO_2 *storage using produced water disposal data in US Gulf Coast*. Paper Presented at the 15th GHGT Conference. Retrieved from https://papers.ssrn.com/sol3/papers.cfm?abstract_id=3903753#

Pedregosa, F., Varoquax, G., Gramfort, A., Michel, V., Thirion, B., Grisel, O., Blondel, M., Muller, A., Nothman, J., Louppe, G., Prettenhofer, P., Weiss, R., Dubourg, V., Vanderplas, J., Passos, A., Cournapeau, D., Brucher, M., Perrot, M., & Edouard, D. (2012). Scikit -learn: machine learning in python. *arXiv.* https://doi.org/10.48550/arXiv.1201.0490

Peterson, J.A. (1985). *Petroleum geology and resources of Northeastern Mexico* [PDF]. United States Geological Survey. Retrieved from https://pubs.usgs.gov/circ/1985/0943/report.pdf

Phelps, R. M., Kerans, C., Loucks, R. G., Da Gama, R. O., Jeremiah, J., & Hull, D. (2014). Oceanographic and eustatic control of carbonate platform evolution and sequence stratigraphy on the Cretaceous (Valanginian-Campanian) passive margin, Northern Gulf of Mexico. *Sedimentology*, 61(2), 461-496. https://doi.org/10.1111/sed.12062

Rose P.R. (1972). *Edwards group, surface and subsurface, central Texas.* University of Texas a Austin, Bureau of Economic Geology. http://dx.doi.org/10.26153/tsw/5060

Schultz, A.L. (1993). *Defining the Edwards aquifer freshwater/saline-water with geophysical logs and measured data (San Antonio to Kyle, Texas)* (Report No. 93-06). Edwards Underground Water District. Retrieved from

https://www.edwardsaquifer.org/science_docs/defining-the-edwards-aquifer-freshwater-saline-water-interface-with-geophysical-logs-and-measured-data-san-antonio-to-kyle-texas/

Smith, R.E. (1996). EPA mission research in support of hazardous waste injection 1986-1994. In J.A. Apps and Chin-Fu Tsang (Eds.), *Deep Injection Disposal of Hazardous and Industrial Waste* (pp. 9-24). Academic Press.

Swanson, S.M., Enomoto C.B., Dennen, K.O., Valentine, B.J., & Cahan, S.M. (2017). *Geologic assessment of undiscovered oil and gas resources – Lower Cretaceous Albian to Upper Cretaceous Cenomanian carbonate rocks of the Fredericksburg and Washita Groups, United States Gulf of Mexico Coastal Plain and state waters* (United States Geological Survey Open-File Report 2016-1199). United States Geological Survey. https://doi.org/10.3133/ofr20161199

The Intergovernmental Panel on Climate Change. (2018). *Global warming of 1.5°C*. Retrieved from https://www.ipcc.ch/sr15/

The Intergovernmental Panel on Climate Change. (2014). *Fifth assessment report*. Retrieved from https://www.ipcc.ch/assessment-report/ar5/

The Intergovernmental Panel on Climate Change. (2007). AR4 Climate Change 2007: Synthesis Report. https://www.ipcc.ch/report/ar4/syr/

Tiab, D., & Donaldson, E.C. (2012). Chapter 9 – Effect of stress on reservoir rock properties. In D. Tiab & E.C. Donaldson (Eds.), *Petrophysics* (3rd ed., pp. 553-666). Gulf Professional Publishing. https://doi.org/10.1016/B978-0-12-383848-3.00009-8

Tsar, M., Ghasemiziarhani, M., Ofori, K., Bahrami, H., & Iglauer, S. (2013). The effect of well orientation (vertical and horizontal) on CO_2 sequestration in a water saturated formation saline aquifer in Western Australia. *European Association of Geoscientists & Engineers*. https://doi.org/10.3997/2214-4609.20130502

United States Environmental Protection Agency. (1980, May 19). *Federal Register*, 45(98), 33290-33418.

United States Environmental Protection Agency. (2024, July 10). *General information about injection wells*. Retrieved from https://www.epa.gov/uic/general-information-about-injection-wells

United States Environmental Protection Agency. (2024, July 10). *Class II oil and gas related injection wells*. Retrieved from https://www.epa.gov/uic/class-ii-oil-and-gas-related-injection-wells

United States Environmental Protection Agency. (2024, July 12). *Class VI – wells used for geologic sequestration of carbon dioxide*. Retrieved from https://www.epa.gov/uic/class-vi-wells-used-geologic-sequestration-carbon-dioxide

United States Environmental Protection Agency. (2024). *Current class vi projects under review at EPA*. Retrieved from https://www.epa.gov/uic/current-class-vi-projects-under-review-epa

United States Geological Survey. (2021, May 24). *Faults in the Gulf of Mexico [gcfaultsg]*. Retrieved from https://www.sciencebase.gov/catalog/item/imap/60abc3f9d34ea221ce51e45f

van der Meer, L.G.H., & Yavuz, F. (2009). CO_2 Storage capacity calculations for the Dutch subsurface. *Energy Procedia*, 1(1), 2615-2622. https://doi.org/10.1016/j.egypro.2009.02.028

Virtanen, P., Gommers, R., Oliphant, T., Haberland, M., Reddy, T., Cournapeau, D., Burovski, E., Peterson, P., Weckesser, W., Bright, J., van der Walt, S.J., Brett, M., Wilson, J., Millman, J., Mayorov, N., Nelson, A.R., Jones, E., Kern, R., Larson, E., Carey, C.J., Polat, I., Feng, Y., Moore, E.W., VanderPlas, J., Laxalde, D., Perktold J., Cimrman R., Henriksen I., Quintero E.A., Harris C.R., Archibald A.M., Ribeiro A.H., Pedregosa, F., & van Mulbregt, P. (2020). SciPy 1.0: fundamental algorithms for scientific computing in Python. *Nature*, 17, 261-272. https://doi.org/10.1038/s41592-019-0686-2

Vallabhaneni, S., Olszewski, T.D., Pope, M.C., & Heidari, Z. (2016). Facies and stratigraphic interpretation of the Eaglebine Play in Central Texas. *Gulf Coast Association of Geological Societies*, 5, 25-46. Retrieved from https://archives.datapages.com/data/gcags-journal/data/005/005001/pdfs/25.htm

Walter, T.G., & Seni, S.J. (1994). *Geothermal and heavy-oil resources in Texas*. United States. https://doi.org/10.2172/140595

Warner, D.L., & Orcutt, D.H. (1973). Industrial wastewater-injection wells in United States -status of use and regulation, 1973. In *Underground Waste Management and Artificial Recharge* (2, 687-697). Preprints of papers presented at the Second International Symposium on Underground Waste Management and Artificial Recharge, New Orleans, LA, September 26–30, 1973, American Association of Petroleum Geologists, United States Geological Survey, and International Association of Hydrological Sciences.

Warwick, P.D. (2017). *Geological assessment of undiscovered conventional oil and gas resources in the lower Paleogene Midway and Wilcox groups, and the Carrizo sand of the Claiborne group, of the Northern Gulf Coast region (Report 2017-1111)* [PDF]. United States Geological Survey. Retrieved from https://pubs.usgs.gov/of/2017/1111/ofr20171111.pdf

Worrell, M.R. (2017). *Structural and stratigraphic reconstruction of the whiting dome salt structure in Viosca Knoll-Mississippi Canyon, GOM, using 3D seismic data* [Master's Thesis, Stephen F. Austin University]. Retrieved from https://scholarworks.sfasu.edu/cgi/viewcontent.cgi?article=1106&context=etds

Wilmarth, M.G. (1938). *Lexicon of geologic names of the United States (including Alaska)* (Bulletin 896). United States Geological Survey. Retrieved from https://ngmdb.usgs.gov/Prodesc/proddesc_94681.htm

Young, S.C., Knox, P.R., Baker, E., Budge, T., Hamlin, S., Galloway, B., Kalbouss, R., & Deeds, N. (2010). *Hydrostratigraphy of the Gulf Coast aquifer from the Brazos river to Rio Grande* [PDF]. Texas Water Development Board. Retrieved from https://citeseerx.ist.psu.edu/document?repid=rep1&type=pdf&doi=d91b2c88ce1ae6fadff51afd823dac7829777e29